Titre: Title:	Acid and alkali doped PBI electrolyte in electrochemical system
Auteur: Author:	Baozhong Xing
Date:	2001
Type:	Mémoire ou thèse / Dissertation or Thesis
Référence: Citation:	Xing, B. (2001). Acid and alkali doped PBI electrolyte in electrochemical system [Ph.D. thesis, École Polytechnique de Montréal]. PolyPublie. https://publications.polymtl.ca/7069/

UNIVERSITÉ DE MONTRÉAL

ACID AND ALKALI DOPED PBI ELECTROLYTE IN ELECTROCHEMICAL SYSTEM

BAOZHONG XING

DÉPARTEMENT DE GÉNIE PHYSIQUE ET DE GÉNIE DES MATÉRIAUX

ÉCOLE POLYTECHNIQUE DE MONTRÉAL

THÈSE PRÉSENTÉE EN VUE DE L'OBTENTION DU DIPLÔME DE PHILOSOPHIAE DOCTOR (Ph.D.)

(GÉNIE MÉTALLURGIQUE)

AVRIL 2001

UNIVERSITÉ DE MONTRÉAL

ÉCOLE POLYTECHNIQUE DE MONTRÉAL

Cette thèse intitulée:

ACID AND ALKALI DOPED PBI ELECTROLYTE IN ELECTROCHEMICAL SYSTEM

présentée par: XING Baozhong

en vue de l'obtention du diplôme de: Philosophiae Doctor

a été dûment acceptée par le jury d'examen constitué de:

M. AJERSCH Frank, Ph.D., président

M. SVADAGO Oumarou, Ph.D., membre et directeur de recherche

M. BOUKHILI Rachid, Ph.D., membre

M. CIUREANU Mariana, Ph.D., membre

To my parents, my wife and my son

Acknowledgements

I would not have been able to achieve as well and as much as what I have achieved without the invaluable support and encouragement of the people around me.

Most of all, I am grateful to Dr. O. Savadogo for his invaluable guidance, support and encouragement through my Ph. D. program, nurturing my professional and personal growth.

Finally, I would like to thank my parents, my wife Yongqin Zhang and my son Ruimeng Xing for being the home of my soul and their unconditional love and support.

Résumé

Dans ce travail, la conductivité de la membrane du PBI pur, dopé d'acide et d'alcalin a été étudiée d'une façon systématique. Une nouvelle méthodologie pour étudier la cinétique de l'absorption dans la solution d'électrolyte a été établie en surveillant le changement de la conductivité pendant le processus de l'absorption. Un modèle sur le processus de dope et le mécanisme de conductivité est proposé. La performance de PBI (dopé sous conditions optimale) dans la cellule du combustible comme PEM a été évaluée.

Les résultats expérimentaux montrent que le Polybenzimidazole (PBI) vierge dans une solution acide est un isolant ionique. Cela a permis d'avoir clarifié la confusion qui a duré depuis longtemps dans ce domaine.

La membrane PBI dopée d'acide est un conductreur ionique. La conductivité augmente avec la concentration de la solution acide. Dans une solution acide de haute concentration, la conductivité augmente avec le type d'acide dans l'ordre: H_2SO_4 > H_3PO_4 > $HClO_4$ > HNO_3>HCl. La cinétique du processus de dope a été étudiée par une méthode de mesures continue. Le mécanisme de la conductivité ionique a été établi. Les membranes PBI dopées avec H_2SO_4 et H_3PO_4 exposent une meilleure performance que Nafion®. Le PBI dopé a plus de résistance contre la poison de CO. 3% CO dans H_2 a peu d'effet sur la membrane PBI dopée de H_3PO_4 à 185°C.

La conductivité de la membrane PBI dopé d'alcali change avec la concentration de la solution alcaline et le type des alcalis. La conductivité a un maximum dans les solutions de KOH et de NaOH. La conductivité maximale dans KOH est plus haute que dans NaOH et LiOH. Elle est à-peu-près 5 fois de celle de Nafion® dans une solution alcaline. Le processus d'absorption de deux phases dans une solution alcaline a été observé. La première phase est le processus d'infiltration des alcalis dans la membrane PBI. Dans le processus d'infiltration, il y a deux processus : celui de la diffusion et celui d'interaction.

Il est conclu que le processus d'infiltration est contrôlé par le taux de l'interaction entre l'alcali et les molécules de PBI. La deuxième phase est le processus de relaxation dans la membrane. Cette phase contribue plus sur la conductivité pour la membrane que la première. Le mécanisme de la conductivité ionique a été établi. Dans une solution, les cations et OH^- participent tous les deux au transport de courant. C'est l'OH qui brise les liens entre les molécules de PBI et permet aux cations de traverser la membrane. La performance de la membrane PBI dopé d'alcaliu (dopé sous conditions optimales) dans la cellule du combustible comme PEM est aussi bonne que le Nafion®.

Abstract

In this work the conductivity of blank PBI membrane, acid doped PBI and alkaline doped PBI was systematically studied. A new methodology for sorption kinetics study in electrolyte solution has been established by monitoring the conductivity change during the sorption process. The model of the doping process and mechanism of conductivity are proposed. The performance of PBI (doped under optimum conditions) in fuel cell as PEM was evaluated.

The experimental results show that the blank PBI in acid solution is an ionic insulator. It clarified the long time confusion in this area.

The acid doped PBI membrane is an ionic conductor. The conductivity increases with the concentration of the acid solution. In high concentration acid solution, the conductivity increases with the type of acid in the order: $H_2SO_4 > H_3PO_4 > HClO_4 > HNO_3 > HCl$. The kinetics of the doping process was studied, by a continuous method. The ionic conductivity mechanism was established. The PBI membranes doped with H_2SO_4 and H_3PO_4 exhibit better performance than Nafion®. The doped PBI has more resistance to CO poison. 3% CO in H_2 has little effect on the H_3PO_4 doped PBI membrane at 185°C.

The conductivity of the alkali doped PBI membrane changes with the concentration of the alkaline solution and the type of the alkalis. The conductivity has a maximum in KOH and NaOH solution. The maximum conductivity in KOH is higher than in NaOH and LiOH. It is about 5 times of that of Nafion® in alkaline solution. The two-step sorption process in alkaline solution was observed. The first step is the permeation process of the alkalis in the PBI membrane. The permeation is the results of diffusion and interaction. It is concluded that the permeation process is controlled by the rate of interaction between the alkali and PBI molecule. The second step is the relaxation process in the membrane. This step contributes more to the conductivity for the membrane than the first step. The

ionic conductivity mechanism was established. In solution the cations and OH^- all participate in the transport of current. It is the OH^- that breaks the bonds between PBI molecules and enables the cations pass through the membrane. The performance of alkali doped PBI (doped under optimum conditions) in fuel cell as PEM is as good as Nafion®.

Condensé de la thèse

1. Introduction

Pour diminuer l'effet toxique de CO et d'augmenter l'usage de la chaleur gaspillée de cellules du combustible de la membrane de l'électrolyte des polymère solides (SPEMFCs), il est nécessaire de travailler à haute température (>100°C). Afin d'augmenter l'efficacité, le processus d'lectrolyse avec de l'eau vaporisée est utilisé à haute température et à pression élevée. Par conséquent, une membrane de l'électrolyte du polymère solide qui peut travailler à haute température est exigée. La famille la plus populaire de la membrane acide de sulfonique du perfluorinated, tel que Nafion, membrane Dow, et Aciplx-S, ne peut pas travailler à température > 100°C. Il est nécessaire de développer une nouvelle membrane de l'électrolyte du polymère solide. Polybenzimidazole (PBI) a une très bonne stabilité thermique et chimique. Après avoir été dopé de l'acide, il a une conductivité ionique et peut travailler à haute température comme des membranes de l'électrolyte du polymère solide. C'est un candidat potentiel.

Quelques systèmes électrochimiques travaillent en condition de la solution alcaline, tel que la cellule de combustible alcalin, l'électrolyse de l'eau et des batteries alcalines. Dans la solution alcaline, la polarisation d'activitée de l'électrode est beaucoup moins que sous autres conditions, même sans catalyseurs d'éléments nobles, tel que Pt ou Ru, etc. Cependant, l'utilisation la solution alcaline comme électrolyte augmente la complexité des systèmes. La substitution de la solution alcaline avec électrolyte du polymère du type de base peut simplifier les systèmes. PBI a été utilisé comme matrice dans les batteries alcalines et bonne performance a été observé. Cela est une potentiel d'utiliser PBI comme un type de base polymère électrolyte.

2. Revue de la littérature

2.1. PBI pur:

- Le PBI pur est presque amorphe. La plastification et recuite affectent la structure morphologique et ses propriétés physique du PBI.
- Le PBI pur a des propriétés mécaniques excellentes et une bonne stabilité, qui sont affectées par le poids moléculaire, la plastification et le recuit.
- Le PBI pur est un isolant électronique.

La conductivité ionique du PBI pur est très importante pour comprendre le mécanisme de la conduction ionique dans le PBI - dopée d'acide. Les résultats rapportés de dans la littérature sont en conflit. Cela devrait être étudié systématiquement.

2.2. PBI dopé de l'acide

- Le dope avec l'acide augmente la cristallinitée du PBI. La cristallinitée du PBI atteindra un maximum avec l'augmentation du niveau de dope. Le maximum est atteint à bas niveau de dope. Le changement sur la cristallinien a une tendance similaire que celui de modules avec le niveau de dope. Les recuites augmentent la cristallinité.
- La membrane de PBI dopée de l'acide a une conductivité ionique.
    - Les acides utilisés sont HCl, HCOOH, H_2SO_4, et H_3PO_4.
    - Le sel de PBI avec HCOOH et HCl ont une conductivité ionique faible (10^{-6} S/cm et 10^{-8} S/cm, respectivement).
    - Le PBI dopé avec H_3PO_4 a une conductivité ionique de 0.02~0.04 S/cm à la température de 130~190°C.
    - La conductivité de PBI dopé avec H_2SO_4 et H_3PO_4 augmente avec le niveau de dope, la température et l'activité de la vapeur d'eau.
- La pellicule de PBI fondue de la solution PBI/TFA/H_3PO_4 a la même composition que celle de DMAc séché. Cependant, la pellicule de PBI fondue de la solution PBI/TFA/H_3PO_4 a une conductivité ionique deux fois plus haute et une cristallinité plus élevée que celui fondu de DMAc.

- Le PBI dopé de H_3PO_4 a une perméabilité de gaz, un coefficient de la traînée électro - osmotique, et un nombre de transmission de H_3PO_4 plus faibles que Nafion.
- L'acide, l'eau et la sorptions de méthanol suivent le modèle de sorption de duel-mode. H_2SO_4 a une tendance plus haute de combiner avec le PBI qu'avec H_3PO_4. Chaque molécule de H_3PO_4 neutralise 1 groupe de base dans le PBI, et chaque molécule de H_2SO_4 neutralise 1.5 groupes de base dans le PBI. Par conséquent, le PBI absorbe plus de H_3PO_4 que la H_2SO4.

La conductivité ionique du PBI pur est incertaine. Différents auteurs ont donné des résultats différents. Hoel et Grunwald ont obtenu $2 \sim 8\times10^{-4}$ S/cm pour PBI dans une humidité variant de 0 à 100% avec électrolyse de l'hydrogène. Cette valeur est beaucoup plus haute celle obtenue par Ahoroni et al. ($\sim10^{-12}$ S/cm), qui n'ont pas donnés de détaille de leur condition de travail. Gilipa et al. ont obtenu 6.3×10^{-3} S/cm dans une solution acide.

Il semble que les structures morphologiques de PBI dopé de H_3PO_4 affecte la conductivité ionique. Cependant, le rapport entre la structure morphologique et la conductivité ionique n'est pas claire. Il serait possible d'augmenter la conductivité ionique de PBI dopé de H_3PO_4 en optimisant la structure de la morphologie.

Le type d'acide affecte considérablement la conductivité ionique du PBI dopé. Le H_3PO_4 augmente le plus considérablement la conductivité d'après la littérature. Nouvel acide et conditions de dope peuvent augmenter la conductivité ionique de PBI dopé d'acide. Un modèle fondamental sur le mécanisme de la conductivité ionique faciliterait la future recherche et les applications, qui n'est pas disponible de la littérature. Pour identifier la structure de la morphologie optimale du PBI dopé d'acide et trouver un meilleur acide et les conditions de dope convenables, il est nécessaire d'effectuer des études sur le mécanisme de la conductivité ionique de PBI dopé d'acide.

2.2. PBI dopé d'alcali

Selon la structure moléculaire de PBI, l'alcalin peut aussi lier avec le PBI. Il devrait avoir un effet similaire sur la conductivité ionique que l'acide. Il n'existe aucune recherche disponible dans la littérature sur le dope d'alcali, bien qu'il y eût des études de l'application de PBI hybride avec des matériaux de structure poreuse dans une solution alcaline.

3. Essais

La pellicule de PBI avec une épaisseur de 40 μm a été acheté à Hoechest Celanese. La pellicule a été coupée en petits échantillons de carré de 3×3 cm^2. Les échantillons ont été lavés dans l'eau bouillante dé- ionée pour plus de 6 heures afin d'éliminer les impudicités LiCl. Ces échantillons pures ont été gardés dans l'eau. Les échantillons ont été dopés en les immergeant dans la solution acide ou alcaline dans la cellule de la mesure de la conductivité. La conductivité a périodiquement été mesurée pendant le processus de dope. La mesure a été accomplie dans la solution de dope en utilisant une sonde (probe) de deux-points classique avec une cellule de mesure de la conductivité de la maison. La perméabilité, le nombre de transmission, et le coefficient de la traînée électro - osmotique ont été mesurés dans une cellule de deux-chambres.

La performance de la cellule de combustible a été testée dans une station de cellule de combustible BC-50 de Globe Teck Inc. Une anode, une cathode et un électrode de référence ont été pressés à chaud sur chaque membrane de PBI à 80°C sous pression de 4.8103 Pa pour 4 minutes. La charge totale de Pt catalyseur était de 0.4 $mg.cm^{-2}$. La surface de l'électrode (anode et cathode) était de 6.25 cm^2. L'assemblée de l'électrode de la membrane résultante (MEA - membrane electrode assembly) a été incorporé dans un seul appareil d'essais. L'essai d'une seule cellule a été effectuée à un ratio de pression de H_2/O_2 de 1/1 atm à plusieurs températures cellulaires. Aucune hydratation spécifique des membranes a été faite avant la polarisation.

4. Résultats

4.1. PBI pur

Ce travail a permis d'avoir clarifié que le PBI pur est isolant ionique et électronique. La conductivité du PBI pur est de l'ordre de ~10^{-9} S/cm dans les solutions de HCl, HNO_3, $HClO_4$, H_2SO_4 et de H_3PO_4 à différentes concentrations.

La valeur de la conductivité ionique rapportée par Galip est celle de PBI après avoir dopé avec HCl. L'effet de dope sur la conductivité n'a pas été considéré, ce qui a été confirmé par les auteurs. La conductivité ionique de PBI pur a été mesurée dans une cellule de combustible de H_2/O_2 avec les électrodes de Pt. Il est alentour de 10^{-13} ~ 10^{-12} S/cm. La valeur rapportée par Hoel ne pourrait pas être atteinte. Les résultats dans la présente thèse indiquent que le PBI pur est isolant ionique dans une solution ou dans un environnement gazeux.

4.2. PBI dopé d'acide

Le processus de dope d'acide peut augmenter la conductivité ionique de PBI aussi haut jusqu'à ~10^{-2} S/cm. La courbe du changement de la conductivité contre le temps pendant le processus de dope a deux phases, ce qui montre que le dope acide de PBI est un processus de absorption en deux-étapes. C'est la première fois que le deux étapes d'absorption dans PBI ont été observé. Le résultat de Galip et al. avec une méthode de deux étapes a confirmé l'absorption de deux phases proposée, bien que cela ne soit pas aussi clair que la méthode continue utilisée dans ce travail. L'augmentation de la conductivité est principalement dans la deuxième phase, le processus de relaxation des molécules de PBI pendant le processus de dope. La structure du cristal liquide du PBI pur est cassée par les molécules acides, et la nouvelle structure est formée.

La conductivité de PBI dopé avec des acides de concentration élevée (≥ 8M) augmente considérablement avec le type d'acides de dope dans l'ordre: H_2SO_4>H_3PO_4>$HClO_4$>

HNO_3>HCl. La conductivité protonique de PBI dopé avec H_2SO_4 de 16 M ou H_3PO_4 de 14.6 M sont près de la conductivité de Nafion® 117.

Quand la concentration des acides de dope est basse (≤ 2M), la conductivité de PBI dopé augmente avec le type des acides dans l'ordre: H_3PO_4>H_2SO_4>HCl >HNO_3>$HClO_4$. Dans ce cas, le PBI dopé avec H_3PO_4 a montré une conductivité protonique la plus élevée. Cela indique que le PBI dopé avec l'acide du multiproton a la plus haute conductivité. Cela peut impliquer que il est plus facile pour l'acide de multiproton de former un groupe de conduite ionique. Le proton plus faible dans l'acide de multiproton est vaguement lié avec PBI et plus libre de conduire des ions. C'est pourquoi PBI dopé de H_3PO_4 a la haute conductivité, même à basse concentration. La conductivité augmente avec la concentration de l'acide, d'une façon monotone. Il n'y a pas de maximum sur la courbe de conductivité contre concentration. Cela montre que la conductivité ne lie pas directement avec le cristallinité du PBI. Elle est liée avec la quantité de acides absorbés dans PBI. Le taux d'augmentation de la conductivité avec la concentration est beaucoup plus haut à haute concentration qu'à basse concentration. Cela indique que l'acide surplus absorbé à haute concentration contribue plus à la conductivité. Cela peut être attribué à la combinaison plus faible aux molécules de PBI.

La morphologie du PBI dopé d'acide affecte considérablement la conductivité à haute concentration de H_2SO_4. La conductivité de PBI dopé de H_2SO_4 est de 0.06 S/cm. Après séché dans l'air pour plus de sept jours, elle est de 0.1 S/cm dans la même solution d'essais.

La performance de la membrane PBI dopé avec haute concentration de H_2SO_4 ou de H_3PO_4 comme électrolyte du polymère solide dans la cellule du combustible de H_2/O_2 a été étudiée. Pour la membrane PBI dopée avec H_2SO_4 et séchée dans l'air pour une journée, la performance est améliorée avec l'augmentation de la concentration de la solution de H_2SO_4 de 8-12 M. Pour la membrane PBI dopée de H_2SO_4 de 16 M, la

polarisation ne peut même pas être obtenue. Cependant, après avoir été séché pour sept jours, la performance de la membrane est améliorée bien que ce ne soit pas encore aussi bon que celle dopées en basse concentration. Après avoir séché pour plus de sept jours, la performance est meilleure que la membrane Nafion.

La performance augmente avec la température dans l'ordre 70°C < 50°C < 30°C. Cela montre l'effet du processus de la déshydratation dans la membrane.

La membrane PBI dopée avec 85% H3PO4 a été testée dans une cellule de combustible de H_2/O_2 à 185°C. Sa performance s'améliore avec la température. Il peut avoir encore bonne performance en utilisant H_2 avec 3% CO à 185°C.

4.3. PBI dopé de alcali

La membrane PBI devient conductrice ionique à partir d'un isolant après avoir dopé dans une solution alcaline. La conductivité du PBI dopé alcaline change avec le type et la concentration de l'électrolyte alcaline. La conductivité augmente avec l'intensité de l'agent alcalin, KOH>NaOH>LiOH.

Le changement de conductivité avec les concentrations d'électrolyte dépend aussi du type alcalin. La plus haute conductivité a été obtenue à 6 M pour KOH et à 8 M pour NaOH. Pour LiOH, la plus haute conductivité est obtenue à une concentration de 4 M.

La plus haute conductivité de PBI dopé de KOH (9.5×10^{-2} S/cm) à 25°C est plus élevée que les valeurs optimales obtenue avec PBI dopé de H_2SO_4 (6×10^{-2} S/cm à 25°C), PBI dopé de H_3PO_4 (2×10^{-3} S/cm à 25°C) et Nafion® 117 (0.012 S/cm dans NaOH de 1 M à 25°C).

La présence de carbonate dans la solution alcaline diminue la conductivité de la membrane PBI dopé. La conductivité de PBI dopé dans la solution binaire de KOH et

K_2CO_3 diminue à partir de 0.095 S/cm jusqu'à 0.016 S/cm lorsque la concentration de K_2CO3 augmente de 0 à 3 M.

La conductivité du PBI (dopé dans la solution de KOH de 8 M) augmente de 0.02 à 0.095 S/cm quand la température augmente de 25 à 70°C.

L'amélioration de la conductivité du PBI dopé alcalin peut être attribuée à la modification spécifique de PBI par la molécule alcaline et OH^-, au lieu des cations de l'électrolyte alcaline. Cela est supporté par la conductivité de PBI dopée dans NaCl (10^{-9} S/cm) et Na_2CO_3 (10^{-6} S/m). Pour la même concentration de dope d'électrolyte, la conductivité de NaOH est plus haute que celle de NaCl. Ce point de vue est aussi supporté par les valeurs de transmission ionique de K^+, Na^+ et Li^+ et leur perméabilité dans PBI dopé de alcaline. La différence entre les nombres de transmission du cation n'est pas aussi grande que celle entre les conductivités de PBI dopé dans la solution alcaline correspondante, ce qui montre que l'OH brise les liens de l'hydrogène entre les molécules de PBI.

La perméabilité de KOH, NaOH, et LiOH dans la membrane PBI dépend de la concentration. Il y a une gamme de concentration optimale où la perméabilité a un maximum. La perméabilité de membrane PBI dopé dans différents types d'alcali est dans l'ordre KOH > NaOH > LiOH. La différence entre eux, surtout entre KOH (ou NaOH) et LiOH, n'est pas aussi grande que celle de la conductivité. Cela indique que la conductivité du PBI dopé d'alcali dépend de l'intensité de la solution alcaline et de la structure de PBI dopé d'alcali, et non simplement de la perméabilité.

La perméabilité hydraulique dans la membrane PBI dopé d'alcali dépend de la concentration de la solution alcaline. Elle diminue avec la concentration de la solution de KOH ou de NaOH. Cependant, la perméabilité hydraulique augmente légèrement avec la concentration de solution de LiOH. La perméabilité hydraulique dans la KOH ou la NaOH est au même niveau (~10^{-10} m^2/S). Dans la solution de LiOH, elle est dans l'ordre

de 10^{-12} m^2/S qui sont 100 fois plus petites que dans KOH et NaOH. Ces résultats indiquent que la structure de la membrane PBI dopé d'alcaline dépend du type et de l'intensité des alcalis.

Les nombres de transmission ionique de K^+, Na^+ et Li^+ dans une membrane PBI dopé d'alcali mesurés dans la solution dope alcaline respectivement, varient entre 0.6 et 0.3. Ils diminuent lorsque que la concentration de la solution alcalines augmente. Cela indique que le cation et OH^- tous les deux participent au transport de courant et contribuent à la conductivité ionique.

Similaire au processus de dope dans une solution acide, le processus de dope dans une solution alcaline est un processus d'absorption de deux phases. La première phase est le processus d'infiltration d'alcali dans le PBI pur. Cela comprend deux composants, le processus de la diffusion conduite par la différence de la concentration et le processus d'interaction entre les molécules PBI et alcali. Ce processus est contrôlé par l'interaction entre les molécules PBI et les alcali, et non par le processus de la diffusion alcalin. La deuxième phase est le processus de la relaxation de la membrane PBI qui rend les molécules de PBI plus faciles de se déplacer et permet à l'alcali de filtrer plus facilement. C'est le principal contributaire pour la conductivité ionique de la membrane PBI. Cela indique que la conductivité de la membrane PBI est déterminée par la morphologie de PBI dopé. À partir du premier phase, la perméabilité de l'alcali dans PBI pur peut être calculée. Le temps de relaxation d'une membrane PBI dans la solution alcaline peut être calculé à partir du deuxième phase. La perméabilité alcaline augmente dans l'ordre KOH > NaOH > LiOH. Lee temps de relaxation dans alcali diminue dans l'ordre KOH < NaOH < LiOH. La perméabilité et le taux de relaxation ont un maximum dans la solution de NaOH à ~8 M (KOH, 6 M). À cette concentration, l'épaisseur de la membrane après avoir dopé a un maximum aussi. Cela est aussi coïncident avec le maximum de la conductivité. CO_3^{2-} à une basse concentration dans KOH de 6 M n'affecte ni la perméabilité ni le temps de la relaxation. À une haute concentration de carbonate, la perméabilité se baisse. Ces

faits indiquent que la concentration détermine la structure de la membrane dopée, qui détermine la conductivité.

La cellule du combustible de H_2/O_2 PEMFC basée sur la membrane PBI dopé de KOH a un courant de 0.62A/cm à 0.6V, ce qui montrent que la membrane PBI dopée de KOH se comporte aussi bien que Nafion® 117 membranes dans H_2/O_2 PEMFC. La membrane PBI a dopé dans la solution de KOH et celle de KOH + K_2CO_3 a une performance aussi bonne que Nafion® 117 dans la cellule du combustible de H_2/O_2 à 50°C. Elle peut être une candidate potentielle pour un nouveau type de PEM.

5. Conclusions

Le PBI pur est un isolant électronique et ionique. Après avoir dopé avec un acide ou un alcali, il devient un conducteur ionique. Le PBI dopé reste encore électroniquement isolant.

Le processus de dope est un processus d'absorption de deux phases: celui de diffusion et celui de relaxation. Le processus de relaxation est contributaire principal au changement de la conductivité ionique. Il détermine la structure de la morphologie de la membrane PBI et sa conductivité ionique.

Une membrane PBI dopé de H_2SO_4 et H_3PO_4 et une dopé de KOH ont une très bonne performance dans la cellule du combustible de H_2/O_2. Elle est meilleur qu'une membrane Nafion. Avec une membrane PBI dopé de H_3PO_4, 3% CO dans H_2 n'affecte pas la performance de la cellule du combustible. Avec une membrane PBI dopé de KOH, le CO_3^{2-} ne montre pas grand effet sur la performance.

Pour la première fois, une nouvelle méthodologie d'étudier la cinétique de l'absorption dans une solution d'électrolyte a été établie avec une surveillance du changement de la conductivité pendant le processus d'absorption.

Table of contents

List of figures

List of tables

Nomenclature

aq	Aqueous solution
b	Affinity constant (the ratio of adsorption rate constant to desorption rate constant)
C	Concentration of acid (or alkali) in aqueous phase
C_A	Concentration of acid in liquid phase
C_{eq}	Concentration of acid (or alkali) in polymer at equilibrium
C'_H	Hole or site saturation constant
C_L	Concentration of acid in solution phase
C_P	Concentration of acid in polymer phase
D	Diffusion coefficient
E_r	The reversible potential of the reaction
F	Farad constant
Δg, ΔG	The total free energyΔG is the total free energy
Δh, ΔH	The total energy change of this reaction
J	The flux of transport current
k_D	Distribution constant or Nernst partition coefficient
K_D	Distribution or partition coefficient of the acid between the two phases
K_D	Nernst partition coefficient
L	The thickness of the membrane
n	The number of electrons involved in this reaction
P	Pressure
P	Permeability coefficient
S	Conductivity
Δs, ΔS	The entropy change
$\Delta S_{universe}$	The entropy change of the universe of the reversible process in fuel cell

$\Delta S_{thermal\ surroundings}$	The entropy change of the thermal surroundings of the reversible process in fuel cell
t	Time
T	Temperature
T_g	The glass transition temperature
t_+	The transference number of the positive ion
U_+	The mobility of cations in electrical field
U_-	The mobility of anions in electrical field
V	The terminal voltage of the fuel cell
z_+	Charge numbers of the cations
z_-	Charge numbers of the anions
ϕ_{rev}	The theoretical maximum "thermal" efficiency of the fuel cell
ϕ	The thermal efficiency of the practical fuel cell
ϕ_E	The voltage efficiency of the fuel cell
ϕ	The thermal efficiency of the practical fuel cell
ϕ_E	The voltage efficiency of the fuel cell
ϕ_i	The current efficiency of the practical fuel cell
ϕ_s	The system efficiency
η_{inh}	The inherent viscosity
η_{act}	Activation overpotential (potential drop) from the reaction
η_{ohm}	Ohmic overpotential from ohmic resistance
η_{mass}	Concentration overpotential from mass transport resistance
θ	Diffraction angle
ν	Molar change (volume)

Foreword

Fuel cells can decrease pollution and increase efficiency of the energy conversion. The solid polymer electrolyte membrane fuel cell is more compact and has higher power density than other type fuel cell. In order to use reformed hydrogen or hydrocarbon directly and to increase the thermal efficiency of the whole system, fuel cells need to run at high temperature. Solid polymer electrolyte membranes, having high conductivity, high chemical and thermal stability, low gas permeability, able to withstand high temperature and of low cost, are the key factors that determine the development of the fuel cell and other electrochemical systems. Up to now the most successful membrane is Nafion®. It has high stability and high conductivity. However Nafion® cannot meet other requirements of the electrochemical systems. The development of new membranes is vital to the development and application of electrochemical systems.

PBI (polybenzimidazole) has excellent stability and mechanical properties. After doping with acid it exhibits ionic conductivity and can work at high temperature (~ 200°C). It is less expensive than Nafion®. The fundamental studies on the doping process, the conductivity mechanism and especially the behavior of PBI in alkaline solution are essential to optimize the doping conditions and direct the developments of new solid polymer membrane electrolyte.

CHAPTER 1

INTRODUCTION AND LITERATURE REVIEW

Introduction

More and more energy is needed in industry and people's daily life. The main energy source is fossil fuel. The energy in the fossil fuel is in the form of chemical energy. The energy most needed is mechanical energy and electricity. The heat engine (steam engine and internal combustion engine) converts the fossil fuel into mechanical energy or electricity through combustion. The direct combustion causes pollution, the CO_2 released causes global warming. The impurities in the fossil fuel containing N and S produce harmful substances, such as NO_x, and SO_x, during the combustion at high temperature. The incomplete oxidation produces multicycle aromatic substances that cause cancer and other serious diseases. To solve the problems mentioned above, new technologies are needed. The efficiency of the new technology must be higher than the conventional ones and must be able to work at low temperature. One of the new energy technologies is fuel cell.

Literature Review

1. Fuel cell working principle and classification

Fuel cell is an electrochemical device that directly transforms chemical energy to electricity. The working principle of a fuel cell is shown in Figure 1.1. The fuel cell is composed of an anode and a cathode. The fuel (H_2) is oxidized at the anode compartment and gives out electrons and protons. The electrons then transfer to the cathode through an external circuit. The protons migrate to the cathode compartment through the electrolyte between the two electrodes. The oxygen is reduced at the cathode, and combines with the protons to form water. During this process, electricity is produced. Because pure water is the only product the reaction does not involve any pollution emission.

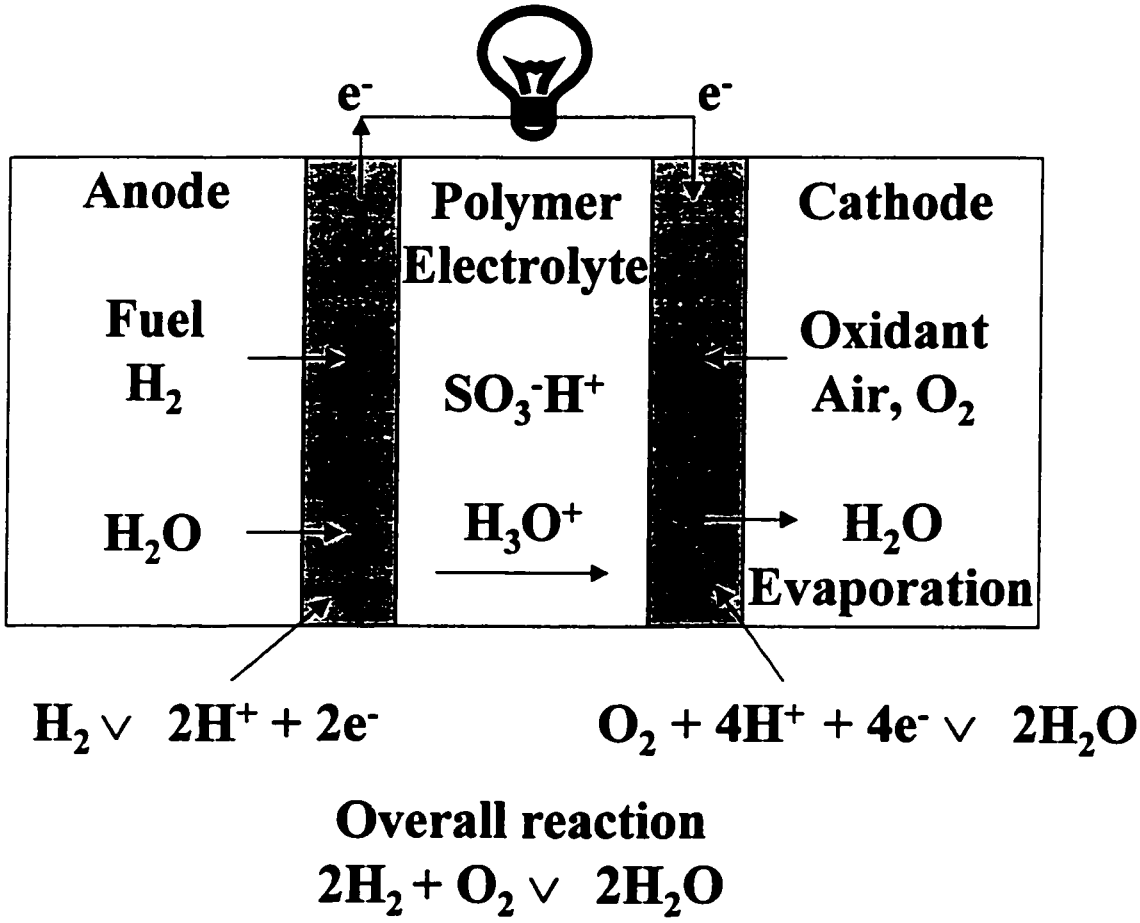

Figure 1.1. The working principle of H_2/O_2 fuel cell

Fuel cells can be classified according to the electrolyte, working temperature, the application and the fuel used. The fuel cell classification is shown in Table 1.1.

Table 1.1. The fuel cell classifications and applications

Fuel cell Types	Operating T (°C)	Electrolyte	Fuels	Output	Potential Markets
Alkaline	60-90	35-50% KOH	Hydrogen (without CO_2)	1,5-15kW	Space stations, vehicles
Polymer	50-80	Proton Exchange Membrane	Hydrogen, natural gas, methanol, gasoline	100W-250kW	Vehicles, distributed production on main electrical networks and independent networks, portable power units, space stations, submarine propulsion
Phosphoric Acid	160-220	Concentrated liquid phosphoric acid	Hydrogen, natural gas, liquid mineral gas, light petroleum distillates	50 kW-200 kW	Vehicles, distributed production
Molten Carbonate Salt	620-660	Molten carbonate salts Li_2CO_3/ Na_2CO_3	Hydrogen, natural gas, coal gas, diesel, kerosene, propane Methanol	250kW-2MW	Distributed production on main electrical networks and independent networks, centralized production
Solid Oxide	800-1000	Zirconium oxide stabilized with yttrium oxide.	Hydrogen, coal gas, diesel fuel, kerosene	1kW-100kW	Distributed production, centralized production
Direct Methanol	60-90	Proton exchange membrane	Diluted methanol (about 3%)	No system developed yet	Vehicles

According to the electrolyte of the fuel cell the classification is: alkaline fuel cells (AFCs), phosphoric acid fuel cells (PAFCs), molten carbonate fuel cells (MCFCs), solid oxide fuel cells (SOFCs), and solid polymer electrolyte membrane fuel cells (SPEFCs).

According to the working temperature, the fuel cells can be classified as low temperature fuel cells, middle temperature fuel cells, and high temperature fuel cells. According to the application, the fuel cells can be classified as portable fuel cells, movable fuel cells, and

stationary fuel cells. According to the fuel, the fuel cells can be classified as hydrogen fuel cells, methanol fuel cells, and hydrocarbon fuel cells.

SPEFCs have many advantages over the others. For example, SPEFC is compact and simple. It can provide high current density and run at low temperature (< - 40 °C). These advantages make it suitable for portable power source and for electrical vehicles.

2. Comparison of fuel cell with battery

In comparison with battery, fuel cell can continually produce electricity. Battery can only work periodically. After all the reactants consumed it cannot work any more. Before it can work again it must recharged. Fuel cell can also give higher energy density than battery because it can use fuels with higher energy density (Tables 1.2 and 1.3). The specific energy and energy density are expressed as watt-hours per kg or per L reactant, i.e., Wh/kg and Wh/L, respectively.

Table 1.2. The energy density of anodes

Material	Mass density g/ml	Equivalent weight g/faraday	Specific energy Ah/kg
Pb	11.3	104	238
Cd	8.7	56	480
Zn	7.1	33	812
Fe	7.9	28	960
Mg	1.7	12	2230
Na	0.97	23	1170
Li	0.53	7	3830
H_2	Gas	1	26802
CH_4	Gas	2	13401
CH_3OH		5.34	5019

Table 1.3. The energy density of cathodes

Material	Mass density g/ml	Equivalent weight g/faraday	Specific energy Ah/kg
MnO_2	5.0	43.5	616
HgO	11.0	108	248
CuO	6.0	72	312
AgCl	5.6	144	156
$CuCl_2$	3.0	67	400
PbO_2	9.4	120	223
NiOOH	7.0	91	295
Ag_2O	7.0	62	432
Sulphur	2.0	16	1675
Oxygen	Gas	8	3350
Chlorine	Gas	35.5	755
Bromine	3.1	80	355
Fluorine	Gas	19	1410

Other related parameters are specific power and power density that are expressed as watts/kg and watts/L respectively. These two factors involved are the capacity in ampere-hours (Ah) per kg or per L reactant and mean voltage during the discharge. The ampere-hours (Ah) per kg or per L reactant, as shown in Table 1.2 and 1.3, are obtained from the coulombs (faraday) per kg or per L reactant.

The gas or liquid state of reactants and products provides advantages of easy feeding and exhausting for fuel cell. For battery, the reactants and products must be sealed in it. Therefore battery cannot use gas reactants or the reaction that produces gas state products in order to increase the energy and power density. In battery the concentration of liquid reactants and their activities will decrease as the reactants are consumed. Therefore the voltage of the battery will drop. The best state of reactants for battery is solid state. The activity of the reactants will keep constant (~1) during the discharge (working). Therefore the battery usually uses metal anode and solid-state oxidant as cathode reactant. It limits the specific energy of battery.

On the other hand, in fuel cell the products are exhausted out of the system. Accordingly fuel cell exhibits higher energy and power density.

3. Thermal efficiency

Fuel cell has higher efficiency than internal combustion engine. This is related to the absence of classical Carnot-cycle limit for fuel cell.

The overall reaction occurring in H_2/O_2 fuel cell is:

$$H_2 + 1/2O_2 = H_2O \quad (1)$$

The total energy change (ΔH) of this reaction is given by:

$$\Delta H = \Delta G + T\Delta S \quad (2)$$

where ΔG is the total free energy and ΔS is the entropy change. The free-energy change ΔG is the maximum energy that can be converted to mechanical energy [1]. The free-energy change of the electrochemical reaction is related to the reversible potential (E_r) of the cell by the relation,

$$\Delta G = -nFE_r \quad (3)$$

For H_2/O_2 fuel cell, the free energy change under standard conditions of temperature and pressure (T=25 °C, $P_{H_2} = P_{O_2} = 1$ atm, H_2O in liquid state) is -56.32 kcal·mol^{-1}. The number of electrons involved in this reaction is 2. Thus, the reversible potential is 1.229 V. For methanol fuel cell, the reaction is

$$CH_3OH\ (aq) + 3/2O_2 = CO_2 + 2H_2O \quad (4)$$

The free energy change under standard conditions of temperature and pressure is -166.96 kcal·mol^{-1}. The number of electrons involved in this reaction is 6. Thus, the reversible potential is 1.199 V. Thermodynamic data of the most important fuel cell reactions at standard conditions are listed in Table 1.4.

The reversible potential (E_r) changes with temperature and pressure as expressed by the following equations [2].

Table 1.4. Thermodynamic data of the most important fuel cell reactions (per mole)

Reaction	T (K; °C)	Δg° (kJ)	Δh° (kJ)	Δs° J/K	n	ν^a (°)	E_r (V)	ϕ_{rev}
$H_2 + 1/2O_2 \rightarrow H_2O$ (l)	298; 25	-237	-285	-162	2	-1.5	1.23	0.83
$H_2 + 1/2O_2 \rightarrow H_2O$ (g)	298; 25	-229	-242	-44	2	-0.5	1.18	0.95
$NH_3 + 3/4O_2 \rightarrow 1/2N_2 + H_2O$ (l)	298; 25	-226	-225	-97	3	-1.25	1.17	0.89
$N_2H_4 + O_2 \rightarrow N_2 + 2H_2O$ (l)	298; 25	-312	-311	+2	4	-1.0	1.61	1.00
$C + 1/2O_2 \rightarrow CO$	298; 25	-137	-110	+89	2	+0.5	0.71	1.24
$C + 1/2O_2 \rightarrow CO$	773; 500	-180	-110	+90	2	+0.5	0.93	1.63
$C + 1/2O_2 \rightarrow CO$	1,273; 1,000	-224	-113	-87	2	+0.5	1.16	1.97
$C + O_2 \rightarrow CO_2$	298; 25	-394	-384	+33	4	0	1.02	1.00
$C + O_2 \rightarrow CO_2$	773; 500	-396	-394	+2	4	0	1.03	1.00
$C + O_2 \rightarrow CO_2$	1,273; 1,000	-396	-395	+1	4	0	1.03	1.00
$CO + 1/2O_2 \rightarrow CO_2$	298; 25	-257	-283	-86	2	-0.5	1.33	0.91
$CO + 1/2O_2 \rightarrow CO_2$	923; 650				2	-0.5	1.00	
$CO + 1/2O_2 \rightarrow CO_2$	1,273; 1,000	-172	-281	-86	2	-0.5	0.89	0.61
CH_3OH (l) $+ 3/2O_2 \rightarrow CO_2 + 2H_2O$ (l)	298; 25	-704	-727	-77	6	-0.5	1.21	0.97
$CH_4 + 2O_2 \rightarrow CO_2 + 2H_2O$ (l)	298; 25	-802	-804	-6	8	-2.0	1.04	1.00

ν^a = molar change (volume)

$$E_r = E_r^0 + (\frac{\partial E}{\partial T})_p (T - 298) = E_r^0 + \frac{\Delta S}{nF}(T - 298) \quad (5)$$

$$E_r = E_r^0 - \frac{(\Delta n)RT}{nF} \ln P \quad (6)$$

where Δn is the change in the number of gas molecules during the reaction, ΔS is the entropy change for the reaction. For H_2/O_2 fuel cell, E_r decreases with temperature because ΔS is negative[3]. The entropy change ΔS is related to the Δn. As a rough rule of thumb, if Δn is positive, the entropy change is positive (due to increasing disorder), while

if Δn is negative (increasing order), ΔS is negative, and if Δn is zero ΔS is also zero [4]. When the water produced is in liquid state the $|\Delta S|$ is larger than that when water is in vapor (Δn=-3/2 in the former and −1/2 in the later case). Therefore the effect of temperature with liquid water forming, $\partial E/\partial T = -0.54mV/°C$, is larger than that with vapor, $\partial E/\partial T = -0.25mV/°C$. For methanol fuel cell, when methanol and water are all in liquid state, Δn=-1/2, ΔS is negative as shown in Table 1.4 [5]. Therefore the reversible potential (E_r) decreases with the temperature. When methanol and water are all in vapor state, Δn=3/2, ΔS is positive. The reversible potential (E_r) increases with the temperature. In conclusion, higher reversible potential of H_2/O_2 fuel cell will be obtained when water is in liquid form than in vapor form; and higher reversible potential of methanol fuel cell will be obtained when methanol and water are in vapor form than in liquid form.

The second item in equation (2), TΔS, is from the entropy change. This part of energy is the minimum heat exchange of fuel cell with the thermal surroundings. Therefore the theoretical maximum "thermal" efficiency of the fuel cell is [6]

$$\phi_{rev} = \frac{\Delta G}{\Delta H} = \frac{\Delta G}{\Delta G + T\Delta S} \tag{7}$$

When ΔS is negative, ϕ_{rev} is less than 100% because ΔG and ΔH are always negative for fuel cell reaction (spontaneous reaction). There must be some energy, TΔS, transferred to thermal surroundings as heat to keep the entropy change of the universe of the reversible process in fuel cell $\Delta S_{universe} = \Delta S + \Delta S_{thermal\ surroundings} = 0$ according to the second law of thermodynamics [39]. This part of the energy cannot be converted to mechanical energy by any means. When ΔS is positive, ϕ_{rev} is larger than 100%. The fuel cell will absorb heat, TΔS, from the thermal surroundings to keep the entropy change of the universe of the reversible process in fuel cell $\Delta S_{universe} = 0$. The theoretical maximum "thermal" efficiency η_{rev} and other thermodynamic data are shown in Table 1.4.

In practical SPEFCs working process, mass transport, adsorption and desorption, and reaction are included. For each step there is resistance, therefore, overpotential. Therefore, the voltage output of the fuel cell is

$$V = E_r - \eta_{act} - \eta_{ohm} - \eta_{mass} \tag{8}$$

where η_{act}, η_{ohm}, and η_{mass} are the activation overpotential (potential drop) from the reaction, ohmic overpotential from ohmic resistance, and concentration overpotential from mass transport resistance respectively, as shown in Figure 1.2. When a net current is drawn from a practical fuel cell, the terminal voltage of the cell, V, drops from the open circuit potential, E_r, by an amount which increases with the increasing cell current output, as shown in Figure 1.2. The cell is said to exhibit polarization, of which there are mainly three types: activation polarization, concentration polarization, and ohmic polarization.

The thermal efficiency of the practical fuel cell at working condition is

$$\phi = \phi_{rev}\phi_E \tag{9}$$

and

$$\phi_E = \frac{V}{E_r} \tag{10}$$

where ϕ_E is the voltage efficiency of the fuel cell. It is always <1. If the reaction has side reaction, e.g.,

$$H_2 + O_2 = H_2O_2 \tag{11}$$

In this process the number of electrons involved is 2 instead of 4 for producing H_2O. With the same consumption of O_2, the current output of the fuel cell will be lower than that with no side reaction, i.e., just producing H_2O. The side reaction causes current loss and decreases the current efficiency, ϕ_i. For the whole fuel cell system, the pretreatment of fuel gas, cooling of the system, and recycling or reprocessing of the reaction gases etc., will cause energy loss. The efficiency of these processes is the system efficiency, ϕ_s.

Therefore the total efficiency of the practical fuel cell system is

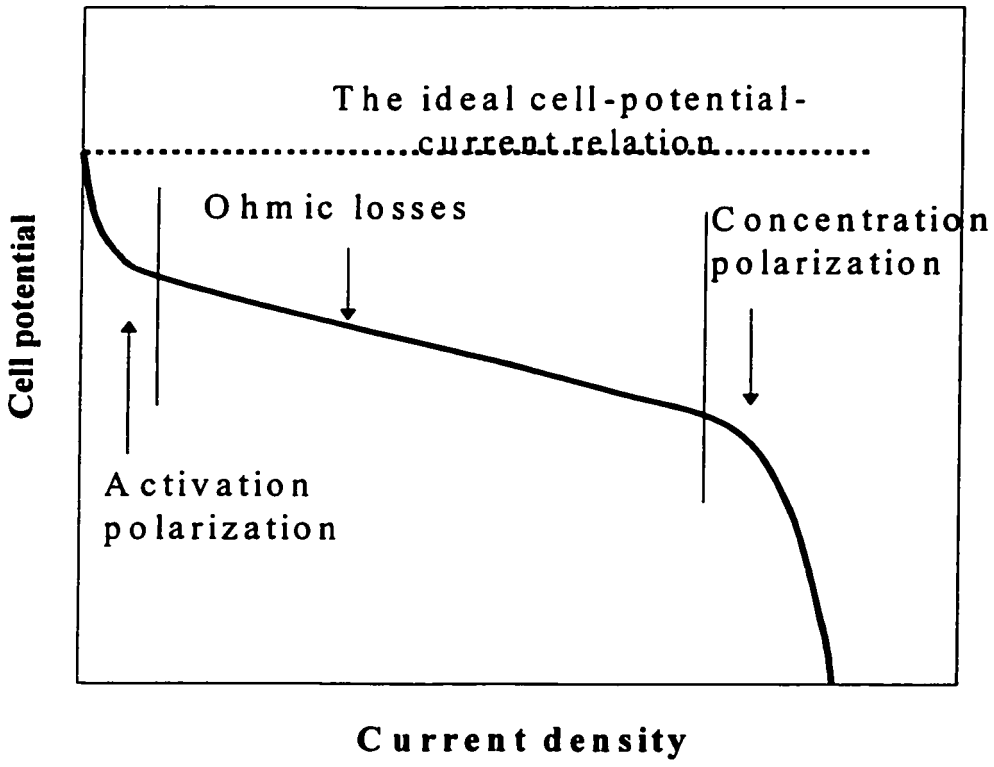

Figure 1.2. Fuel cell polarization curve

$$\phi = \phi_{rev}\phi_E\phi_i\phi_s \quad (12)$$

It is obvious that to increase the total efficiency of the fuel cell, the work must concentrate on increasing ϕ_E (electrocatalyst, electrolyte, and cell design), ϕ_i (electrocatalyst, in the case selectivity), and ϕ_s (total system and stack design). It is clear that the fuel cell system produces both electrical energy and heat. All of the energy loss converts to heat. Generally, it is important to strive for a low ratio of heat versus electrical energy. In practical fuel cell, heat losses (i.e., waste or by-product heat) often can be utilized for other processes such as the gasification of a fossil fuel, reactant preheating, the maintenance of the cell operating temperature in the case of a high temperature fuel cell, or simply for on-site heat requirements. This increases total efficiency of the fuel cell.

To increase ϕ_E and ϕ_i the efforts have been made on electrocatalyst, electrolyte, and cell design. The best catalysts are still Pt, Pd, Ru or their alloys, even though they are very expensive and of limited supply. Decreasing the loading of the catalyst can reduce the cost. The loading can be as low as 0.1 mg/cm^2 [7, 18, 19]. With the nano technology the electrodes can still have good performance at low loading [8]. The use of ink electrode with diffusion layer decreases the resistance of gas mass transport [9]. The Teflon in the ink helps the transport of water and avoids the electrode flood [10-12]. It improves the performance of the electrode. The impregnate of polymer electrolyte decreases the proton transport resistance in the electrode and improves the performance of the electrode [13-15]. The polymer electrolyte development provides the possibility of using thin electrolyte layer between the two electrodes [16]. It decreases the ohmic overpotential in the electrolyte.

4. Solid polymer electrolyte

As a solid polymer electrolyte membrane used in SPEMFCs, it must have certain outstanding properties [17]: good ionic conductivity; good mechanical properties; enough thermo and chemical stability; low gas permeability; low cost and electronic insulator.

Nafion® membrane is widely used in SPEFCs. It has high ionic conductivity, good stability and mechanical properties. However it has relatively high permeability for hydrogen in fuel cell and the price of Nafion® membrane is too high (~780 US $/m^2$). Another drawback of Nafion® membrane is that it cannot work at high temperature. The maximum working temperature for Nafion® membrane is ~100°C. When fuel cell operating at this low temperature, the waste heat from fuel cell cannot be used efficiently. If the fuel is pure hydrogen the fuel cell with Pt catalyst loading as low as 0.05~0.1 mg/cm^2 can still have satisfactory performance, with 0.7~1.2 A/cm^2 current density output at voltage of 0.5V [18, 19]. If there is trace amount of CO in hydrogen as impurity the performance of the fuel cell drops significantly even at high Pt (or Pt/Ru) catalyst loading. The CO poisons the Pt (or Pt/Ru) catalyst. For example, when the concentration of CO is 10 ppm in hydrogen, the fuel cell with 4 mg/cm^2 Pt loading can only have ~0.3 A/cm^2 current density output at 0.5V [7]. The hydrogen fuel for fuel cell is mainly from hydrocarbon reforming or cracking. CO is one of the main by-product [20, 21] and it is not easy to be removed completely [22]. If the fuel cell uses methanol or hydrocarbon directly as fuel, CO forms in the reaction and poisons the catalyst. The best way to solve the CO poison problem is to increase the SPEMFCs' working temperature [7]. When the fuel cell works above 200°C the effect of CO poison can be neglected. However Nafion cannot work properly at high temperature. New polymer membrane for SPEMFCs working at ~200°C with low cost and low fuel permeability is needed.

5. Polybenzimidazole (PBI)

An aromatic heterocyclic polymer, polybenzimidazole (PBI), is a good candidate for the new polymer membrane for SPEMFCs. It has excellent thermal and chemical stability [23-28], and superior mechanical properties. PBI (70 US $/bl, ~7 US $/m^2$) is much cheaper than Nafion®. PBI has lower permeability for hydrogen than Nafion® [29-30]. But blank PBI has no electronic and ionic conductibility [31-34]. Fortunately after doping

with acid, especially doping with Phosphoric acid (H_3PO_4) and sulphuric acid (H_2SO_4), PBI becomes a good ionic conductor [29, 35-44], still being good electron insulator. It has superior stability and good mechanical properties. Phosphoric acid-doped PBI has been developed as polymer electrolyte for methanol fuel cells [29, 35-33].

5.1 Chemical structure and preparation of PBI

Polybenzimidazoles (PBI) are a class of thermally stable polymers, which are condensed from aromatic bis-o-diamines and dicarboxylates, as shown in Figure 1.3. The groups R_1 and R_2 can be aromatic, aliphatic, or may contain other groups as ether, ketone, sulfone, etc.

The polymer repeat unit is benzimidazole that contains a 1, 3-dinitrogen heterocycle. Benzimidazole, as a monomer, has high melting and boiling points of 170 and >360°C, respectively. As a comparison indene (structure shown in Figure 1.4), a hydrocarbon analog of benzimidazole, has melting and boiling points of -2 and 183°C. The unusual thermal properties of polybenzimidazoles can be attributed to their molecular structure. Benzimidazoles and indene have the similar structures. The molecular weight difference is only 2. The difference is that there are two nitrogen atoms in benzimidazole instead of two carbons in indene.

PBI has been discovered for more than 40 years. In the polybenzimidazole family a lot of polymers are synthesized and studied. However, most studies have been focused on poly[2-, 2'-(m-phenylene)-5, 5'-bibenzimidazole] for many years (Figure 1.4). Nowadays when referring to polybenzimidazole (PBI), it means poly[2-, 2'-(m-phenylene)-5, 5'-bibenzimidazole].

5.2 Solubility of PBI and the cast of PBI film

PBI can dissolve in concentrated H_2SO_4, H_3PO_4, and some polar aprotic solvents, such as N,N-dimethylacetamide (DMAc), N,N-dimethylfomamide (DMF), dimethylsulfoxide

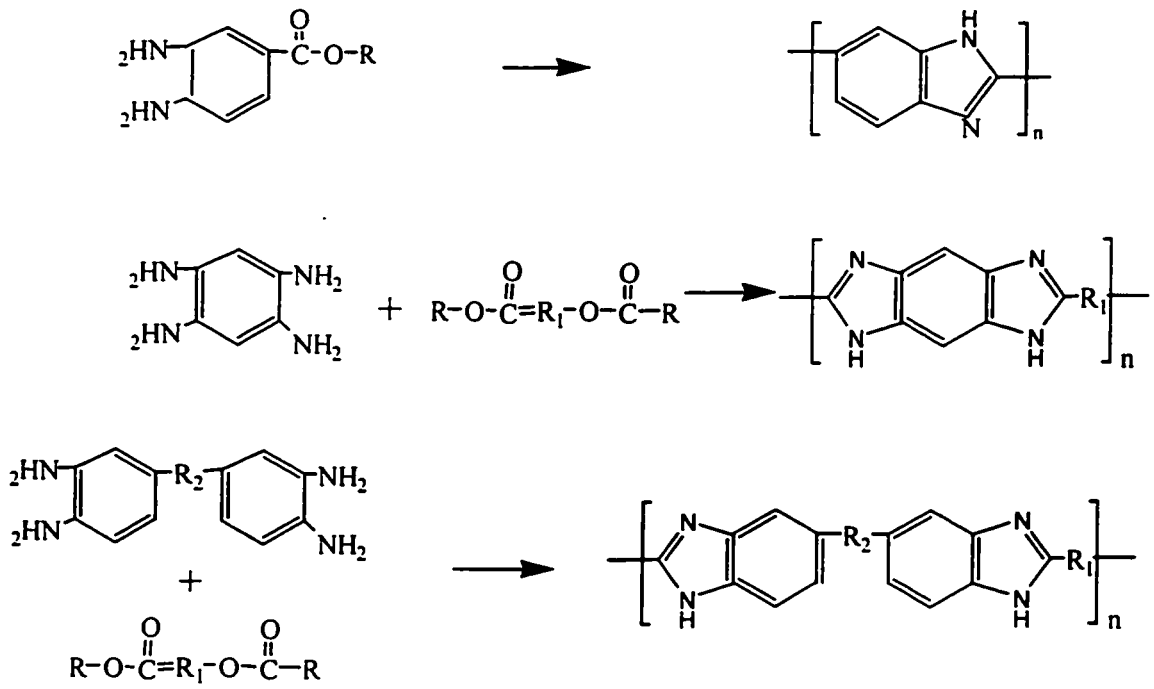

Figure 1.3. Monomer types and polybenzimidazole structures

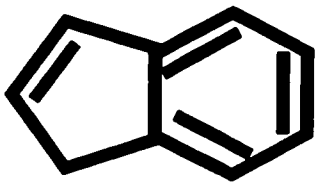

The chemical structure of indene

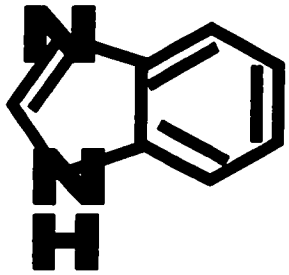

The chemical structure of benzimidazole

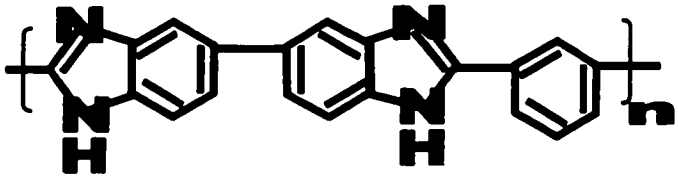

The chemical structure of
Poly[2, 2'-(m-phenylene)-5, 5'-bibenzimidazole]
(Polybenzimidazole) (PBI)

Figure 1.4. Chemical structure of benzimidazole, indene, and PBI

(DMSO) and N-methylpyrrolidone (NMP), normally at high temperature [33, 74, 75]. It can partially dissolve in butyl alcohol, 2-(2ethoxyethoxy)ethanol, and acetic acid [31]. In DMAc PBI dissolves 10% at 70°C, 65% at 140°C, and 75% at 165°C (the boiling point of DMAc). The unsolved content is high molecular weight polymer [34]. The solubility exceeds 98% at 240°C and 80 psi. Oxygen and water must be excluded from the system to prevent oxidative cross-linking and gel formation. The solution can be stabilized by adding 2% LiCl [45]. The film casting technique from N, N-dimethylacetamide (DMAc) solution of PBI was developed by Hoechst Celanese Corp. [45]. The PBI film was cast from DMAc solution at 110°C for ~15 min.

Ameri [62] developed a new method to directly cast H_3PO_4 doped PBI film from a solvent mixture of trifluoroacetic acid (TFA), H_3PO_4 and water. With suitable ratio PBI can dissolve in the solvent mixture at room temperature. The best ratio was PBI: 5g, TFA: 134.25g, H_3PO_4: 4.8g, and H_2O: 0.32g. To prepare the PBI/TFA/H_3PO_4 solution, PBI and TFA were refluxed in a flask in an oil bath overnight (or at least 4-5 hours) and H_3PO_4 was added the next day. Film can be cast from this solution after filtration, and the solvent was evaporated under vacuum at room temperature. The film was doped with H_3PO_4 during cast process. Other acid mixture solutions were studied, such as, PBI/TFA/Hexafluoroglutaric acid (HFGA)/ H_3PO_4, PBI/TFA/Squaric acid (SA)/ H_3PO_4. The work has been covered in patent [55].

The film cast from DMAc has good mechanical properties. The mechanical properties of the film cast from TFA/H_3PO_4/water solution at room temperature are not as good as cast from DMAc [62]. However, the conductivity of PBI film cast from PBI/TFA/ H_3PO_4 mixture solution is about twice of that cast from DMAc. There is no improvement in the conductivity of PBI film cast from PBI/TFA/SA/H_3PO_4 solution. The element analysis indicates that no TFA or SA remains in the dried film. This implies that the morphology structure may affect the conductivity of the H_3PO_4 doped PBI membrane. For PBI film cast from PBI/TFA/HFGA/ H_3PO_4 solution, there is one mole of HFGA for each mole of

PBI, because of the high boiling point of HFGA (134-138°C). It has poor conductivity and mechanical properties.

The film has also been cast from sulfuric acid at 250°C [30, 54].

To get a good film that has good conductivity, suitable mechanical properties and stability, the relationship between the properties and structure needs to be established and new casting methods should be developed.

5.3 The properties of PBI film

The study on the film hadn't been active until a few years ago. The PBI film is still not commercially available now. The properties of the film at many conditions have not been studied. With the bloom of the application study on the film in electrochemical process, especially in fuel cell, the fundamental study on PBI film increases. The properties of the PBI film and modified film are discussed below.

5.3.1 Physical properties

The physical properties of the PBI film cast from DMAc and after different treatments are summarized in Table 1.5 and 1.6 [45, 46, 67, 77]. PBI has much higher modulus than normal plastics. Plasticization, molecular weight, annealing and cast method affect the physical properties.

5.3.1.1 Molecular weight effect

The molecular weight significantly affects the modulus and toughness of PBI films. By using higher molecular weight (HI MW) polymer the breaking extensions increase by a factor of 5 with only a 0.2 increase in the polymer's inherent viscosity [67, 77]. Therefore, the membrane used for SPEMFCs is cast with higher molecular weight PBI.

Table 1.5. PBI film physical property summary [45, 77]

Property	Cast PBI	Annealed PBI	Plasticized PBI	HI MW* PBI	Plasticized HI MW PBI	Poly-propylene
Break strength (PSI)	17K#	27K	15K	14K	14K	3.48-5.51K
Break elongation (%)	14	24	20	97	97	200-600
Modulus (PSI)	400K	550K	330K	460K	410K	145-232K
Moisture content (%)	10	5	12	10	12	
Density (g/cm^3)	1.2	1.3	1.4			
LOI (PCT. Oxygen)	>40		>70			
TMA shrinkage (%)						
100°C	0.9		0.8			
200°C	2.0		1.7			
300°C	2.7		2.5			
400°C	3.0		2.7			
500°C	3.1		2.9			

*HI MW: high molecular weight

#K, ×1000

5.3.1.2 Plasticization effect

5.3.1.2.1 Water plasticization

Water plasticizes PBI. It reduces the modulus and toughness, as shown in Table 1.6.

5.3.1.2.2 Acid plasticization

5.3.1.2.2.1 H_3PO_4 doped PBI

Powers [45] mentioned that the plasticization of the film by making it absorb phosphoric acid from a dilute solution did not significantly affect the physical properties except that the handling characteristics of film had a dampened characteristics. Moaddel [67] and Ameri [77] reported results from dynamic mechanical analysis (DMA). The modulus of PBI increases when the doping level is < 100% mole phosphoric acid, and decreases when the doping level is >100% mole phosphoric acid, as shown Table 1.7 and 1.8. The

dynamic mechanical analysis of blank PBI film in air shows that the glass transition temperature (T_g) is about 420°C [78]. The storage modulus first decreases at the T_g, and then increases due to oxidation. There is a broad sub-T_g transition at 280°C. The DMAs of PBI films doped with 100, 200, and 300 mole% H_3PO_4 show two plateau regions and a transition temperature for all samples [67]. At doping level of 50~100%, the modulus has a maximum [67,77]. The modulus decreases with the increase of doping level when the doping level is >100 mole% (Table 1.7). With less than 300 mole% H_3PO_4, the modulus is higher than that of blank PBI; it is lower than that of blank PBI when doping level >300%.

Table 1.6. Tensile properties of PBI: dry, wet, and annealed at 250°C for 1 h; 100%, 200%, 320% PBI H_3PO_4 doped; doped and then heated at 250°C for 1 h

Sample	Modulus 10^9 Pa	Toughness 10^6 Pa	Yield stress 10^8 Pa	Yield strain %	Stress at break 10^8 Pa	Strain at break %
PBI, dry	1.94	105.00	1.22	11.6	1.09	105.0
PBI, wet (20% water)	1.38	82.70	0.79	12.6	1.10	94.0
PBI, annealed	3.74	13.32	-	-	2.04	9.75
PBI 100% H_3PO_4	3.53	48.53	1.45	20.6	1.46	38.0
PBI 200% H_3PO_4	3.16	46.16	1.35	20.7	1.35	38.0
PBI 320% H_3PO_4	1.35	48.41	0.61	21.7	0.68	82.0
PBI 100% H_3PO_4 250°C, 1h	6.21	10.48			2.99	6.1
PBI 200% H_3PO_4 250°C, 1h	6.00	6.64			2.66	4.8
PBI 320% H_3PO_4 250°C, 1h	7.1	4.56			2.33	3.5

At high temperature close to T_g the moduli of H_3PO_4 doped PBI are lower than those at room temperature. The storage moduli in the second run are higher than those in the first run, which is due to the crystallization [67] (Table 1.8). In second run the storage moduli are not significantly affected by the temperature and doping level.

Table 1.7. Storage moduli and transition temperatures of PBI and acid doped PBI measured by DMA (first run)

H_3PO_4/ PBI, mole %	First run, E' (10^9) Pa		Transition range °C
	30°C	150°C	
0	1.45	1.37	-
100	3.8	1.83	175 – 205
200	3.17	1.7	170 – 205
320	1.45	0.65	150 – 200

Table 1.8. Storage moduli and transition temperatures of PBI and acid doped PBI measured by DMA (second run)

H_3PO_4/ PBI, mole %	Second run, E' (10^9) Pa		Transition range °C	High temperature plateau region E' (10^9) Pa
	30°C	150°C		
0	-	-	420	-
100	6.1	5.4	302	1.5
200	5.7	5.4	280	1.12
320	5.5	3.6	203	0.46

5.3.1.2.2.2 H_2SO_4 doped PBI

After doped with H_2SO_4, the modulus and toughness decrease, as shown in Table 1.9. The physical properties of H_2SO_4 doped PBI are worse than those of H_3PO_4 doped PBI.

Table 1.9. Tensile properties of PBI: dry, wet, doped (80, 105, 230, 340 mole% H_2SO_4)

Sample	Modulus 10^9 Pa	Toughness 10^6 Pa	Yield stress 10^6 Pa	Yield strain %	Stress at break 10^6 Pa	Strain at break %
PBI, dry	1.94	105.00	122	6.5	109	105.0
PBI, wet 20%* water	1.38	82.70	79	6.2	110	94.0
PBI, 80 % H_2SO_4	1.86	26.4	70	5.9	68.9	41.5
PBI, 105 % H_2SO_4	1.15	26.1	54	4.8	54.8	51.6
PBI, 240 % H_2SO_4	0.54	20.3	28	5.0	30.6	76.6
PBI, 340 % H_2SO_4	0.36	4.7	15	2.5	15.0	33.6

*Molar percentage

5.3.1.3 Annealing effect

Annealing the PBI can increase the molecular weight and cause cross-linking, which results in the presence of insolubles, moisture regain reduction, and increases of inherent viscosity, strength, density, as shown in Table 1.5 and 1.6 [45, 46, 67]. DMA result indicates that there is a sub-Tg transition at 150-350°C [67]. Annealing in this temperature range allows the PBI film to relax and densify. After PBI cast from DMAc was annealed at 250°C for 1 h, the density increased 2.4% from 1.274 to 1.305 [45, 67]. Annealing decreases the toughness of PBI film. For H_3PO_4 doped PBI, annealing increases the modulus, as shown in Table 1.6. The tendency of modulus change with doping level is opposite to blank PBI. The modulus increases with doping level after annealing. Annealing decreases the toughness for H_3PO_4 doped PBI.

Annealing affects the free volume. PALS is a powerful technique to study vacancies in metals and semiconductors [50], and to study polymer free volume hole size and distribution [51-57]. The effects of thermal expansion and corresponding transition temperatures, molecular weight [58], pressure [55], mechanical stress [60-62], chemical structure [63-65] and degree of crystallinity [57] on free volume have been studied by

positron annihilation lifetime spectroscopy (PALS). Sodaye et al. studied the microstructure of Nafion 117 using PALS [66]. The results show the effect of water uptake on cluster size and the free volume structure. The incorporation of water leads to the expansion of the cluster size, and systematically decreases the mean free volume hole size. Moaddel studied the effect of annealing on free volume of PBI film using PALS. Moaddel's PALS results show the free volume fraction of the PBI film cast from DMAc solution significantly decreases at temperature from 140 to 250°C [67]. The density increase of annealed PBI is due to the decrease of the number of free volume holes, rather than a decrease of hole size. The changes of free volume may lead to significant changes in mechanical properties. This may explain the annealing effects. The annealing of cast PBI film increases its modulus and densification four times compared to any other glass polymer.

5.3.1.4 PBI film cast from PBI/TFA/H_3PO_4 solution

The PBI film cast from PBI/TFA/H_3PO_4 solution has lower modulus and toughness than H_3PO_4 doped PBI film cast from DMAc solution, as shown in Table 1.10 [77].

5.3.2 Thermal and chemical stability

5.3.2.1 Blank PBI

PBI has high transition temperature. Three distinct transition regions are observed for PBI by torsional braid analysis [47]: a relaxation process at about –70°C, a transition without modulus change at about 310°C and a Tg at 430°C. The annealing of PBI film in nitrogen at 500°C for 200 minute can increase the glass transition temperature to 500°C.

PBI has high chemical stability compared to polyethylene because of its higher limiting oxygen index (LOI). For blank PBI the LOI is 41% [79]. This compares favorably with the value of 23% for nylon 66, 20% for cotton, and 21% for polyester. Plasticization can increase the chemical stability [45]. The phosphoric acid plasticized PBI has a significantly higher limiting oxygen index (70%) than blank PBI (41%). The PBI phosphate disassociates above 850°C. The sulfonated PBI is less likely to convert to

carbonaceous material than blank PBI. For PBI sulfate the disassociation temperature is above 350°C.

Table 1.10. Comparison of tensile test results of 510 mole % conventional H_3PO_4 doped PBI (DMAc) films and PBI/TFA/H_3PO_4 film

Sample	Modulus 10^6 Pa	Toughness 10^6 Pa	Yield stress 10^6 Pa	Yield strain %	Stress at break 10^6 Pa	Strain at break %
510 mole% H_3PO_4 doped PBI η_{inh}=0.91	192.5	7.85	24	8.8	35.9	32.2
510 mole % H_3PO_4 doped PBI η_{inh}=1.42	220.5	76.03	22	21.6	42.1	310.8
PBI/TFA/H_3PO_4 600 mole % η_{inh}=1.25	78.3	7.63	—	—	11.6	80.2

The thermogravimetric analysis (TGA) study on blank PBI in nitrogen or 5% hydrogen shows that there is ~10% weight loss between 50 and 250°C. A further 10 to 15% is lost between 550 and 900°C, and the derivative shows two peaks (at ~ 600°C and ~ 750°C, respectively) in this temperature interval. The tow peaks possibly indicates two distinct thermal decomposition processes [80]. Additionally, the derivative shows a small shoulder between 400 and 550°C suggesting minor thermal decomposition in this temperature range. The material remaining after the sample has been heated to 900°C, (~75%) appears similar to glassy carbon. The mass spectroscopy (MS) experiment shows that the initial weight loss from 50 to 250°C mainly corresponds to the desorption of residual water out of PBI, and CO_2 formation between 150 and 250°C [80]. A second maximum between 400 and 550°C, which corresponds to the shoulder observed in the weight loss derivative in the same temperature interval. Weight loss derivative increases above 550°C with a maximum at 600°C, which corresponds to benzene formation. The weight loss derivative maximum at 750°C corresponds to hydrogen cyanide formation. If

allowance is made for the moisture in blank PBI, the conversion of PBI polymer mass to carbon is ~80% in nitrogen or hydrogen [45].

The results of thermogravimetric analysis (TGA) on blank PBI in air are similar to that in nitrogen or hydrogen below 500°C [80]. From 500 to 800°C, decomposition of membrane commences, losing nearly all mass. PBI in air is less stable than that in nitrogen or hydrogen.

PBI shows good stability at elevated temperature. TGA experiments show that PBI begins to lose weight above 500°C in air, and 600°C in nitrogen [45, 80]. When PBI is heated at 500°C in air for 3 hours, it loses about 50% of its weight.

5.3.2.2 Acid doped PBI

The thermal and chemical stability improvement of the acid doped PBI is due to the formation of PBI salts. The early work [48] showed significantly better oxidative stability of PBI film cast from sulfuric acid than that cast from organic solvent. However, the data from other studies failed to support the observation [49]. The discrepancies may be due to a combined effect of the thermal stability of the PBI salt and the oxidative stability of the PBI cation [45].

Phosphoric acid doped PBI (preconditioned in 2% aqueous phosphoric acid) loses 2% less than blank PBI by weight in three hour at 500°C [45].

The thermostability of H_3PO_4 doped PBI is different from that of blank PBI [80]. For H_3PO_4 doped PBI, there are two maximums in the weight loss derivative below 400°C. The second maximum in the weight loss derivative below 400°C corresponds to the water formation from the dehydration of H_3PO_4, i.e.,

$$2\ H_3PO_4 \rightarrow H_4P_2O_7 + H_2O.$$

This is confirmed by Wasmus et al. [81] with solid-state nuclear magnetic resonance (NMR). Above 600°C an additional peak of water was observed which was not present in blank PBI. It is from the water forming in the following reaction, $H_4P_2O_7 \rightarrow 2\ HPO_3 + H_2O$. The decomposition above 600°C is faster than that of blank PBI.

For H_3PO_4 doped PBI with 10 – 15 w/o platinum on it, the weight loss derivative curve in nitrogen or hydrogen is similar to the film without Pt [80]. The difference is that the peaks from the phosphoric acid decomposition are smaller than those without Pt, and they shift to higher temperatures. These results indicate that the thermal stability of phosphoric acid doped PBI is suitable for high temperature SPEMFCs.

The dehydration of H_3PO_4 in PBI, i.e., $2\ H_3PO_4 \rightarrow H_4P_2O_7 + H_2O$, is confirmed by Moaddel [67] and Ameri [77] with differential scanning calorimetry (DSC). The DSC of H_3PO_4 doped PBI was run at both atmospheric pressure and high pressure. DSC of PBI with 300 mole% H_3PO_4 (49 wt% acid) shows an exothermic peak at 150°C followed by an endothermic peak at 175°C. The exotherm is due to crystallization and the endotherm is due to water evaporation. In order to eliminate the effect of water evaporation in the experiment, a DSC of doped PBI was run under 200 psi N_2 pressure. High pressure DSC of PBI containing 320 mole% H_3PO_4 shows only an exothermic peak from 100°C to 220°C with a maximum at 150°C due to crystallization. DSC measurement in a closed system under pressure eliminated water evaporation.

The sulfuric acid doping increases the stability of PBI [45, 68].

5.3.3 Sorption and transport of acid in PBI film

5.3.3.1 Sorption equilibrium and kinetics

PBI film can absorb phosphoric and sulfuric acids from their dilute solutions (Plasticization), which makes the film more stable and less strong [45]. Moaddel [67] studied the sorption equilibrium and proposed a dual-mode sorption model. The sorption

of acid in PBI film can be divided into two stages, the Langmuir type sorption and Nernst distribution law sorption. In the first stage, Langmuir sorption mode, acid is absorbed into the PBI film by either chemical bond (hydrogen bond or ionic bond) at some specific sites or by filling the free volume in the film. After those special sites or free volume in the film are saturated, the acid will further dissolves into the film, which has the characteristics of Nernst distribution law sorption.

The Langmuir sorption is represented by:

$$C_{eq} = \frac{C'_H bC}{1+bC}$$

The Nernst distribution law is characterized as:

$$\frac{C_P}{C_L} = k_D$$

Therefore the dual mode sorption can be presented as:

$$C_{eq} = k_D C + \frac{C'_H bC}{1+bC}$$

where

C_P: Concentration of acid in polymer phase

C_A: Concentration of acid in liquid phase

K_D: Distribution or partition coefficient of the acid between the two phases

C'_H: Hole or site saturation constant

b: Affinity constant (the ratio of adsorption rate constant to desorption rate constant)

k_D: Nernst partition coefficient

C: Concentration of acid in aqueous phase

C_{eq}: Concentration of acid in polymer

For phosphoric acid the hole saturation constant, C'_H, is 2 moles of H_3PO_4/mole of PBI repeat unit. It means that each PBI repeat unit can absorb two phosphoric acid molecules on the adsorption sites, the two basic groups. For sulfuric acid, C'_H is 1.3 moles of

H_2SO_4/mole of PBI repeat unit. The less H_2SO_4 taken by each PBI repeat unit implies that H_2SO_4 molecules may bond with the basic groups in different ionic states, some as SO_4^{2-} and some as HSO_4^-.

The affinity constant is 1784 for H_2SO_4, and 137 for H_3PO_4, respectively. This indicates that H_2SO_4 has higher tendency to form a complex (or salt) and be absorbed into the film. The distribution or partition coefficient of the acid between the two phases is 6.55 for H_2SO_4, and 8.79 for H_3PO_4. This shows that H_3PO_4 has a higher tendency to dissolve in the film.

The kinetic study of the acid sorption in PBI film shows that the absorption is a fast process and it has two steps [44].

5.3.3.2 Transport of acid

The permeability of PBI film to acids was measured in a two-chamber cell with PBI film set between the two chambers [67]. The results show that the acid permeation in the swollen film is the Fickian diffusion. The permeability coefficient of PBI films is the same for the films with different thickness (0.0078 or 0.013 cm) respectively. This indicates that there are no obvious boundary layer (surface layer of the film) effects on the permeability measurement. The permeability is acid concentration dependent. The permeability of 1.4 M H_2SO_4 in PBI is lower than that of 0.1 M H_2SO_4. The partial mobility of bonded H_2SO_4 is small due to the strong interaction between polymer and acid.

Another transport property is the permeability of gas (fuel or oxygen) in the film. The application in fuel cells requires that the film has high conductivity and low gas permeability. The permeability of gas in PBI is ten times less than Nafion [29].

5.3.4 Electrical properties

Blank PBI is an electrical insulator with a resistivity of about 10^{12} ohm·cm [71, 72, 31-34]. Doping PBI with acid can lower down the resistivity. However, the resistivity of the doped products is still high enough to be qualified for insulator as shown in Table 1.11. It is also indicated that its salts with acids and complexes with metal ions are also insulators [34]. The high electrical resistivity of PBI film and its salt after modification makes it suitable for polymer electrolyte.

Table 1.11. The electrical properties of PBI

PBI	Resistivity, ohm·cm	Reference
Blank PBI	10^{12}	[56, 57, 16-19]
HCl salt of PBI	10^{6}	[19]
27% H_3PO_4 doped PBI	10^{8}	[56, 57]
HCOOH salt	10^{8}	[19]

5.3.5 Ionic conductivity

5.3.5.1 Conventional acid doped PBI (cast from DMAc)

The ionic conductivity of PBI is shown in Table 1.12. Pure PBI film is a poor ionic conductor. Griswald et al. [72] reported that the conductivity is 2.85×10^{-7} for PBI with nominal moisture, 2.67×10^{-6} for water swollen PBI film, 9.13×10^{-3} for water swollen acidified PBI, and 1.63×10^{-3} S/cm for sodium salt of sulfonated PBI. Hoel et al. reported that PBI had a high protonic conductivity (e.g. $2 \sim 8\times10^{-4}$ S · cm^{-1}) in the humidity ranging from 0 to 100% [33]. Conductivity of 350% H_3PO_4 doped PBI is ~0.02 S/cm at 190°C [35]. The conductivity of 500% H_3PO_4 doped PBI is about twice that of 338% doped PBI. For H_2SO_4 doped PBI when the concentration of H_2SO_4 increased from 40% to 205% the conductivity increased. However for sulfonated PBI when concentration changed in the same range (heating at 350°C for 5 min.) the conductivity reduced [35].

Table 1.12. The ionic conductivity of PBI

PBI	Conductivity, S/cm	Reference
Blank PBI, nominal moisture	2.85×10^{-7}	[57]
water swollen PBI film	2.67×10^{-6}	
water swollen acidified PBI film	9.13×10^{-3}	
sodium salted sulfonated PBI	1.63×10^{-3}	
humidity 0 to 100% with electrodes	$2\sim8\times10^{-4}$	[18]
350% H_3PO_4 doped PBI, 190°C	0.02	[20]
500% H_3PO_4 doped PBI, 190°C	0.039	

5.3.5.1.1 In acid solution with different concentrations

The ionic conductivity of HCl, HNO_3, HClO4, H_2SO_4 and H_3PO_4 doped PBI has not been systematically studied in solution before. Xing and Savadogo [44] found that the conductivity of blank PBI film in different kind of acid solution with different concentration changes slightly with the test media electrolyte solutions. The ionic conductivity of blank PBI is in the range of about 10^{-10} S/cm, as shown in Table 1.13. After doped with acids the conductivity significantly increases. The higher the concentration of the acid solution is, the higher the conductivity is. The conductivity changes in the order H_2SO_4 > H_3PO_4 > $HClO_4$> HNO_3>HCl for high concentrations (11-16 mol/L) of the doping acid. The PBI film doped with 16 M H_2SO_4 has the highest conductivity, about 0.06 S/cm. The conductivity of PBI film doped with 11 M H_3PO_4 is about 4.3×10^{-3} S/cm, and 1.9×10^{-2} S/cm with 14.6 M H_3PO_4. The conductivity of PBI film doped with H_3PO_4 has very high conductivity at low concentration. It does not change very with the acid concentration from 1 to 11 M. So the H_2SO_4 and H_3PO_4 doped PBI films at high level are hopeful candidates for polymer electrolyte, especially applicable in fuel cells.

Table 1.13. The conductivity of blank PBI in various acid solutions with various concentrations (S/cm $\times 10^{10}$)

Concentration of the doping electrolyte, (mol/L)	1	2	4	6	8	10	11
$HClO_4$	7.15	12.6	26.2	67.3	70.1	96.3	
HNO_3		10.3	9.7		9.9		
H_2SO_4	39.4	24.9	12.4	4.32	3.41		
HCl		14.9	13.3		4.24		
H_3PO_4	18.4			9.0			3.0

5.3.5.1.2 H_3PO_4 doped PBI in water vapor

Temperature and water vapor activity affect the ionic conductivity of acid doped PBI. The conductivity increases with temperature and water vapor activity [67, 77], as shown in Table 1.14.

Table 1.14. Temperature and water vapor activity effect on conductivity of PBI doped with 500 mole% phosphoric acid

Temperature, °C	Water vapor activity	Conductivity, S/cm
130	0.03	0.005
190	0.03	0.022
130	0.1	0.011
150	0.1	0.017
190	0.1	0.038

5.3.5.2 PBI film cast from PBI/TFA/H_3PO_4 and PBI/TFA/SA/H_3PO_4 solutions

The PBI film cast from PBI/TFA/H_3PO_4 mixture solution has higher conductivity than that cast from DMAc at the same doping level (Table 1.15) [77]. The conductivity increases with temperature and water vapor activity. The annealing effect on its conductivity is listed in Table 1.16 [77]. During the annealing, the sample was placed in the oven and the temperature was ramped to 190°C, held at 190°C for 5 minutes, then cooled to room temperature. After annealing, the conductivity does not change obviously at high temperature. At low temperature the conductivity increases after annealing. The different effects of temperature on conductivity may be caused by the automatic

annealing effect for the non-annealing sample during the conductivity measurement at high temperature. After annealing, the temperature effect on conductivity is declined.

Table 1.15. The conductivity of PBI film cast from PBI/TFA/ H_3PO_4 solution (580 mole% H_3PO_4)

Thickness mil	Temperature °C	P_{water} torr	Water activity	K S/cm	Equilibration time, h
1.2	130	283	0.135	0.055	1
1.2	130	403	0.193	0.072	0.75
1.1	131	362	0.173	0.05-0.052	1
1.1	150	190	0.053	0.052	1.5
1.2	150	276	0.077	0.056	0.75
1.1	150	351	0.098	0.048	1
1.2	150	583	0.163	0.083	0.75
1.1	151	93	0.026	0.043	13
1.1	171	330	0.055	0.053	1
1.1	190	145	0.015	0.060	2

For the PBI film cast from PBI/TFA/SA/H_3PO_4 mixture solution the conductivity is of the same order with the PBI film cast from DMAc at the same doping level as shown in Table 1.17 [77]. The conductivity is lower than that of PBI film cast from PBI/TFA/SA/H_3PO_4 mixture solution.

5.4 Morphology Structure

Polymer structure has a direct impact on polymer properties. Orientation, degree of crystallization, crystallite size and perfection are all parameters that have significant effects on the physical properties of a polymer. A certain combination of polymer structural characteristics is required to produce the optimum balance of physical properties for a given polymer end application.

Table 1.16. The conductivity of PBI film cast from PBI/TFA / H_3PO_4 solution, after annealing (580 mole% H_3PO_4)

Temperature °C	P_{water} torr	Water activity	K S/cm	Equilibration time, h
134	341	0.149	0.075	2
172	265	0.04	0.074	3.5
195	251	0.024	0.078	1.5
195	177	0.017	0.068	1
195	461	0.044	0.083	1
195	262	0.025	0.049	16
195	756	0.072	0.068	2

Table 1.17. The conductivity of PBI film cast from PBI/TFA/SA/ H_3PO_4 solution (470 mole% H_3PO_4)

Temperature °C	P_{water} torr	Water activity	K S/cm	Equilibration time, h
152	188	0.050	0.025	0.25
152	254	0.067	0.028	1
152	337	0.089	0.028	16.3
152	353	0.094	0.03	2
152	538	0.143	0.034	1
152	163	0.017	0.021	19.6
190	318	0.034	0.035	2
190	334	0.035	0.035	2
190				

Several studies were made to determine the structure and morphology of PBI. In spite of the efforts, mostly from Celanese Research Company and Case Western Reserve University (CWRU), very little was accomplished.

5.4.1 Blank PBI

PBI by itself is almost amorphous. Crystallinity can be induced only under certain conditions. In most of the cases, it functions as an amorphous polymer with high T_g. It has been reported that extraction of PBI powder with hot DMAc gives a residue which shows some Crystallinity [82]. The reprecipitated portion of the soluble extract is completely amorphous. Treatment of this amorphous PBI with phenol at 290 – 350°C for

two hours (under pressure) induces crystalline structure in PBI. The x-ray picture shows five sharp rings implying at least five reflections. In another experiment, crystalline PBI structure formed when PBI fiber was treated with phenol and water under pressure. The study indicated that solvent might be included in the crystal structure. Crystallization can also takes place on immersion of PBI fiber into formic acid solution in the concentration range of 20 – 90%, with the best crystallinity at about 85 – 90% formic acid concentration [83]. The sample treated by immersing PBI in formic acid solution has the two strongest reflections in x-ray pictures on the meridian, probably on the 2^{nd} and 4^{th} layer lines. This fiber pattern also shows some of meridian reflections at 1^{st}, 2^{nd}, and 4^{th} layer lines. Unfortunately, there was no calculation on unit cell dimension. The phenol-water treated PBI fiber was not characterized further because it had poor physical properties. This group concluded that there was no improvement in properties by either increasing the orientation or crystallization compared to original PBI fiber for application at elevated temperature. The only improvement that was seen by increasing the molecular orientation of PBI fiber was the improvement in the strength and stiffness of the material at high strain rate.

Blank PBI film cast from DMAc is an amorphous polymer. The wide angle x-ray diffractometer (WAXD) scan of pure PBI film has a broad halo with small bumps, which is a demonstration of a small amount of crystallinity in a predominantly amorphous phase.

5.4.2 H_3PO_4 doped PBI

5.4.2.1 Conventional acid doped PBI cast from DMAc

5.4.2.1.1 WAXD data

Acid doping and annealing affect the structure of PBI. PBI films were doped with 110, 220, 290, 400, and 480 mole% H_3PO_4, then these films were heated for two hours at 130°C, 160°C, and 190°C, stepwise [77]. WAXD were run on these films before heat treatment and after each heating step.

In WAXD graphs, three peaks can be recognized at about 2θ = 9, 19, and 24° which are equivalent to d-spacings of 9.8, 4.6, and 3.6 A. At each acid concentration, as the heat treatment temperature increases, the first and second peaks become more intense and sharper. This phenomenon becomes more distinct, especially at higher acid concentration when the second peak (2θ = 19°) becomes very sharp after heat treatment.

In order to illustrate the effect of temperature and acid concentration on these films, the WAXD spectrum of phosphoric acid has been deconvoluted. All WAXD spectra show four peaks. One of these peaks is amorphous background at about 2θ = 20°. Two others, because of narrower half width, were assigned to crystalline domains, 2θ = 9, 19°. The fourth peak, 2θ = 24°, which is not part of crystalline structure because it decreases with annealing, has been assigned to be a paracrystalline-like peak. The peak at 24° does not sharpen by annealing. Thus the organization reflected by this peak is not the initial stage, or part of crystalline structure that will grow by annealing of the sample.

As can be seen for higher concentrations of phosphoric acid (higher than 220M%), the difference in behavior of crystalline peak at 2θ=9 and 19° and the paracrystalline peak are more detectable, especially for the 400 and 480M% conventional phosphoric acid doped PBI (DMAc) films.

The intensity and sharpness of the crystalline peaks increase by annealing while the intensity and sharpness of paracrystalline film decreases. Tables 1.18 and 1.19 show the relative area of each reflection based on the deconvolution of WAXD spectrum of doped PBI films with different concentrations of phosphoric acid, before and after heat treatment at 190°C (A% is percentage of area assigned to certain d-spacing compared to the total area).

Table 1.18. Data based on calculation of deconvoluted WAXD spectrum of different concentration of conventional phosphoric acid doped PBI (DMAc) films without heat treatment

Doping level, M%	110	220	290	400	480
d-spaceing, Å	9.5	9.6	9.7	9.4	7.6
Domain size, Å	24.8	24.4	26.2	20.8	20.8
A%	3.4	2.6	2.4	3.8	5.2
d-spaceing, Å	4.6	4.6	4.6	4.6	4.7
Domain size, Å	20.7	19.7	21.5	27.0	39.9
A%	9.8	12.0	9.0	3.4	1.7
$A_{paracrystalline}$%	21.8	28.7	34.3	46.0	62.5
$A_{Amorphous}$%	65.0	56.6	54.3	46.8	30.6
Total $A_{not\ crystalline}$%	87.8	85.5	88.6	92.8	93.1
$A_{crystallinity}$%	12.2	14.5	11.4	7.2	6.9

Increase in the acid concentration in doped PBI films lowers the initial degree of crystallinity (from 12 to 7%, horizontal lines). Annealing the samples at 190°C for two hours increases crystallinity. The increase in crystallinity at low concentration (110 M%) is about 20%. However the increase in crystallinity at high concentration (480M%) is about 400%. It means annealing increases crystallinity of PBI film with higher acid concentration more than PBI film doped with low acid concentration. After annealing PBI film with higher acid concentration is more crystalline than film with lower acid concentration.

Table 1.19. Data based on calculation of deconvoluted WAXD spectrum of different concentration of conventional phosphoric acid doped PBI (DMAc) films heated for 2 hrs at 190°C

Doping level, M%	110	220	290	400	480
d-spaceing, Å	9.1	9.8	9.7	9.7	9.9
Domain size, Å	26	26	28	27	22
A%	4.4	4.8	3.5	2.4	19.7
d-spaceing, Å	4.8	4.7	4.8	4.7	4.8
Domain size, Å	21	20	20	20	46
A%	10.7	15.6	12.7	21.3	10.1
$A_{paracrystalline}$%	23	31.2	20.4	19.6	54.2
$A_{Amorphous}$%	62.0	48.4	64.0	56.7	16.0
Total $A_{not\ crystalline}$%	85	79.6	84.4	76.3	70.2
$A_{crystallinity}$%	15	20.4	16.2	23.7	29.8

The Dynamic Mechanical Thermal analysis results of PBI films doped with different concentrations of phosphoric acid indicate that as the concentration of phosphoric acid in PBI films increases, glass transition temperature declines. For 500M% phosphoric acid concentration, the glass transition temperature is around 150°C. Polymer above its glass transition temperature has high mobility so it can arrange and pack better than it could if the Tg is higher. Therefore, when this film (~500M% acid) was heated to 190°C, there was a more pronounced increase in peak sharpness; this implies an increase in crystal domain size and crystallinity.

Ameri [77] concluded that conventional phosphoric acid doped PBI (DMAc) film has paracrystalline structures in the molecular level. As the film anneals, some crystalline domains grow but this paracrystalline reflection lessens.

5.4.2.1.2 X-RAY pattern [77]

For the past three decades, researchers have looked for ways to study PBI structure. PBI by itself does not give a useful x-ray pattern for investigation. In CWRU, oriented phosphoric acid doped PBI fibers were used. There are two preparation methods. The first approach was PBI fibers doped with 1.4 mole phosphoric acid solution (yields 210M% conventional phosphoric acid doped PBI (fiber) and then stretched about 50%. This fiber was then dried in a vacuum oven at 60°C and later heated at 190°C for half an hour. In the second approach, PBI fibers were first stretched and then doped using 4 molar phosphoric acid solution (yields 270M% acid). After gentle drying of this fiber with paper towel, it was stretched as much as possible. Then the fiber was held on the frame and dried in a vacuum oven overnight at 70°C. Table 1.20 and 1.21 show the results of x-ray patterns of these two fibers respectively. Three reflections in addition to the reflection for calcium fluoride, can be seen in the X-Ray patterns.

Within experimental error, these two x-ray patterns are in the same range. The first and second reflections show the *001* planes and third one is for *hko* plane. There are two possibilities for the first two reflections: either planes of 002 and 004 with c = 19.5 ± 0.4 Å, or 003 and 006 planes with c = 29.4 ± 0.5 Å. With regard to the fact that the length of a PBI repeat unit is in the order of about 15 to 16 Å, the second case is much more likely. Unfortunately, the number of reflections is limited, which make it impossible to find out more about its morphology.

Table 1.20. X-ray pattern data of 210M% H_3PO_4 doped PBI

Reflection No.	Situation	d-spacing, Å
1	ring more toward meridian	9.89
2	ring	4.82
3	equator	3.55

Table 1.21. X-ray pattern data of 270M% H_3PO_4 doped PBI

Reflection No.	Situation	d-spacing, Å
1	meridian	9.87
2	meridian	4.80
3	equator	3.52

5.4.2.2 PBI film cast from PBI/TFA/H_3PO_4 solution

PBI film cast from PBI/TFA/H_3PO_4 (580M%) solution was not stretched (for orientation) because of low strength and elongation at break. Table 1.22 was based on the deconvoluted WAXD spectrum (Gaussian peaks) of this film and on more probable and realistic peaks. This film shows three times more reflections and it has higher crystallinity than conventional phosphoric acid doped PBI (DMAc) film. The calculated area of narrower peaks (crystalline area), was about 47% in comparison to about 7% for 480 M% conventional phosphoric acid doped PBI (DMAc) film before heat treatment.

X-ray pattern of this film (parallel and perpendicular) is shown in Table 1.23. The film diagrams contain the total of 15 reflections which are indexed by eight planes. The cell indexed by a monoclinic unit cell, according to the following equation, which had the best fit for the observed data:

$$1/(d_{hkl})^2 = \frac{h^2/a^2 + k^2/b^2 - 2hkCos\gamma/ab}{Sin^2\gamma} + l^2/c^2 \qquad (4)$$

Table 1.22. Reflections PBI film cast from PBI/TFA/H_3PO_4 (580 M%) solution

Peak No.	Intensity	2θ	d-spacing, Å
1	w	6.9	12.81
2	w	10.03	9.82
3	m	14.27	6.21
4	s-m	16.09	5.51
5	vs	18.63	4.76
6	m-s	22.1	4.02
7	s	25.26	3.53
8	w	28.82	3.10
9	w	37.3	2.41

Table 1.23. Comparison of observed and calculated d-spacings for PBI film cast from PBI/TFA/H_3PO_4 solution parallel and perpendicular to the film

d(obs), Å	d(cal), Å	Intensity	h	k	l	% mismatch
Parallel, ∥						
16.77	16.83	m	0	0	1	-0.35
13.09	12.99	vm	0	1	0	0.75
8.46	8.41	vvm	0	0	2	0.53
6.82	6.69	vm	2	1	1	1.86
4.65	4.61	m	2	2	2	0.73
3.95	3.93	s-m	1	1	4	0.46
3.95	3.92		4	1	0	0.61
3.95	3.93		2	2	3	0.38
3.6	3.55	s	4	1	2	1.17
Perpendicular, ⊥						
1.88	12.99	vw	0	1	0	-0.86
9.25	9.23	vvw	1	1	1	0.19
4.61	4.61	m	2	2	2	-0.12
3.89	3.93	m	1	1	4	-1.07
3.89	3.92		4	1	0	-0.91
3.89	3.93		2	2	3	-1.15
3.50	3.55	m	4	1	2	-1.65

vs=very strong, s=strong, m=medium, w=weak, vw=very weak

A monoclinic unit cell was assigned with dimensions of: a=15.8 Å, b=13.23 Å, c=16.83 Å, and γ=79.1° in which c is almost equivalent to the length of a PBI repeat. With measured density of 1.65 g/cm^3, it seems reasonable to consider 6 PBI repeats and 18

H_3PO_4 molecules in each cell which gives the calculated density of 1.73 g/cm^3 for crystalline area. Therefore, there will be 3 H_3PO_4 for each PBI repeat in crystalline area and 9 H_3PO_4 molecules for each PBI repeat in amorphous area. If the above mentioned calculations is acceptable, it can be concluded that these phosphoric acid rich amorphous area consequently causes higher conductivity.

5.4.3 PBI fibers and films doped with TFA

The WAXD spectra of PBI film cast from PBI/TFA/H_2O solution has a sharp peak. All the films that were prepared from this type of solution were extremely brittle. Possibly high crystallinity could explain their brittleness. X-ray pictures were taken of the same film, in parallel and perpendicular directions. Table 1.24 shows the x-ray reflections of this film. A total of 15 reflections have been observed which could belong to nine planes. Having these reflections in ring form instead of arc implies that polymer domains in this film were randomly oriented. A monoclinic unit cell was assigned, using equation 4, with dimensions of: a=15.65 Å, b=12.2 Å, c=20.83 Å, and γ=80.4°.

Treating PBI fibers with trifluoroacetic acid vapor for two hours at 200°C in high pressure, gave a good fiber pattern. Table 1.25 shows the observed and calculated d-spacings which seems to be in good agreement, with the maximum mismatch of less than 2%. The equatorial reflections at d equal to 7.9 and 3.97 Å appear to be the orders of common repeat, and are indexed with 200 and 400 planes. Also, equatorial reflection of 6.45 and 3.20 Å seems to be in the same way. Therefore, they are indexed with 020 and 040 planes. By indexing these four reflections, two dimensions of unit cell can be determined, a and b. The fiber diagram contains 19 reflections which are indexed by a monoclinic unit cell, which gave the best fit with dimensions of: a=16.03 Å, b=13.05 Å, c=15.2 Å, and γ=80.4°.

Table 1.24. Comparison of observed and calculated d-spacings for PBI film cast from PBI/TFA/H_3PO_4 solution parallel and perpendicular to the film

d(obs), Å	d(cal), Å	Intensity	h	k	l	% mismatch
Parallel, ||						
20.83	20.83	vs	0	1	1	0
11.98	12.03	m	0	1	0	-0.41
7.72	7.71	vw	2	0	0	0.06
6.99	7.05	w	2	1	0	-0.87
5.98	5.95	w	1	2	0	0.51
4.87	4.90	s-m	3	1	1	-0.65
3.96	3.97	vw	1	3	1	-0.36
3.57	3.59	w	2	3	2	-0.66
Perpendicular, ⊥						
20.60	20.83	s	0	0	1	-1.12
11.97	12.03	m	0	1	0	-0.49
10.49	10.42	w	0	1	1	0.69
7.75	7.72	vw	2	1	0	0.45
6.92	7.05	vw	2	1	0	-1.88
4.90	4.90	m	3	1	1	-0.03
3.56	3.59	s	2	3	2	-0.94

vs=very strong, s=strong, m=medium, w=weak, vw=very weak

Density of trifluoroacetic acid treated PBI was calculated based on monoclinic unit cell and according to:

$$\rho_{Calculated} = \frac{(N_{PBI} \times M_{PBI}) + (N_{TFA} \times M_{TFA})}{(a \times b \times c \sin\gamma) \times 6.023 \times 10^{23}} \quad (5)$$

where N is the number of repeat unit of PBI or TFA in a unit cell, M is the molecular weight of either PBI or TFA, *a*, *b*, and c are unit cell dimensions and γ is the angle between *a* and *b*. Considering density measurement, $\rho_{calculated}$ = 1.407 g/cm^3, the cell density reasonably matched with a cell contains four PBI units and three and half trifluoroacetic acid molecules for each PBI repeat ($\rho_{calculated}$ = 1.483 g/cm^3).

Table 1.25. Comparison of observed and calculated d-spacings for PBI fibers exposed to TFA vapor under high pressure

d(obs), Å	d(cal), Å	Intensity	h	k	l	% mismatch
7.9	7.903	s	2	0	0	-0.03
6.54	6.434	vw	0	2	0	0.25
5.45	5.454	s	2	2	0	-0.08
4.66	4.626	w	2	-2	0	0.73
4.35	4.326	vw	1	3	0	-0.56
3.97	3.951	s	4	0	0	0.47
3.20	3.217	vs	0	4	0	-0.53
11.02	10.96	vw	1	0	1	0.58
8.71	8.86	vw	1	1	1	-1.75
5.96	5.92	vw	0	2	1	0.59
5.39	5.287	vw	1	-2	1	1.91
4.085	4.128	w	0	3	1	-1.05
3.96	3.927	w	2	3	1	0.84
6.83	6.85	m	1	0	2	0.28
5.57	5.48	vw	2	0	2	1.65
4.80	4.84	vw	2	-1	2	-0.88
4.33	4.33	vw	1	-2	2	0.003
3.97	3.94	vw	2	-2	2	0.46
4.83	4.82	w	1	0	3	0.11

vs=very strong, s=strong, m=medium, w=weak, vw=very weak

Comparing the d-spacings of treated fibers and PBI film cast from PBI/TFA/H_2O solution, both were assigned as monoclinic unit cells with different dimensions. It means that crystalline structure of PBI with trifluoroacetic acid can be different in unit cell dimension by mean of preparation procedure.

5.4.4 Summary of morphology structure

X-ray methods were used to investigate the structure of PBI. Treating PBI fibers with trifluoroacetic acid vapor at high pressure for two hours gave a good fiber diagram. This diagram contains 19 reflections which were indexed using a monoclinic unit cell with dimensions of: a=16.03 A, b=13.05 A, c=15.2 A, and y=80.4°. Unit cell density reasonably matched with a cell contains four PBI units and 3.5 trifluoroacetic acid molecules for each PBI repeat.

X-ray patterns of PBI film cast from PBI/TFA/H_2O solution show a crystalline structure that has been indexed using a monoclinic unit with dimensions of: a=15.65 Å, b=12.2 Å, c=20.83 Å, and γ=80.4°. Comparing the unit cell assigned to PBI fiber treated with trifluoroacetic acid under high pressure and PBI film cast from PBI/TFA/H_2O solution, indicates that these two PBI films might have the same molecular structure but with different dimensions of monoclinic unit cell.

Study on phosphoric acid doped PBI (DMAc) films showed that heat treatment increased the crystallinity (up to 30%) in the doped PBI films. However, as the concentration of acid in the unheated film increased, the amount of crystallinity decreased.

Polybenzimidazole can cocrystallize with complexing agents like trifluoroacetic acid, phosphoric acid, TFA/H_3PO_4, and phenol-water to form different crystal structures. The crstalline structure can change depending on the doping procedure.

Conventional phosphoric acid doped PBI (DMAc) film cast from DMAc shows very low crystallinity. After annealing, crystal growth was observed. In the other hand, PBI film cast from PBI/TFA/H_3PO_4 solution has a highly crystalline structure. Comparison of these two films indicates that there are two different levels of crystal structure with different texture.

5.5 PBI in alkaline solution

PBI has also been used in other applications. PBI-impregnated zirconium separator was used in Ni-Cd battery for geosynchronous orbit applications [85]. This cell was capable of being operated at 80% depth of discharge (DOD), and it was about 30% lighter in weight. It would be capable of supporting a geosynchronous mission for ten to fifteen years. In all test regimes, at any DOD and temperature, the cell demonstrated three times the life cycle of the state-of-the-art Ni-Cd cell. PBI fiber has been used as the matrix

materials in alkaline fuel cells [86, 87] performed well (> 0.9 V at i = 1 A/cm^2) after over 13 000 h of operations. However, the level of corrosion of the system was high in 42% KOH. PBI was also used in the alkaline cadmium battery to increase the capacity and life cycle of cadmium anode [88].

Even though PBI has been added to the alkaline solutions in some applications, in none of these cases was a PEMFC based on an alkali-doped PBI film membrane involved. Furthermore, the fundamental studies on the doping of PBI films (pure PBI) in alkaline solution are not available in the literature.

6. Application in fuel cell

H_3PO_4 or H_2SO_4 doped PBI has high ionic conductivity, thermal stability and chemical stability. It can be used in H_2/O_2 and CH_3OH/O_2 fuel cell at high temperature [84, 38]. In CH_3OH/O_2 fuel cell, the 500 M% H_3PO_4 doped PBI membrane cast from PBI/TFA/H_3PO_4 solution (Type II) performs better than the PBI membrane cast from DMAc solution at the same doping level (Type I). This confirms the conductivity measurement result. In H_2/O_2 fuel cell at 150°C, the effect of 1% CO poison is negligible, [38]. 300 h running has been conducted in H_2/O_2 fuel cell [84]. Xing and Savadogo [69] conducted experiments in H_2/O_2 fuel cell at >100°C with 85% H_3PO_4 (14.7 M) doped PBI membrane and at ~ 50°C with 16 M H_2SO_4 doped PBI membrane. It indicated that acid doped PBI can work properly in high temperature SPEMFCs. However, the low open circuit potential of the performance indicated that there may be some fuel permeation through the membrane. Wang in CWRU found that in CH_3OH/O_2 fuel cell the catalyst loading of cathode couldn't be as low as in H_2/O_2 fuel cell, which also indicates the existence of CH_3OH permeation.

Conclusions

PBI has good mechanical and thermal properties. After doping with acid it has high conductivity and low gas permeability. It can be used in full cell as polymer electrolyte membrane. To improve its conductivity, the conductivity mechanism of acid doped PBI should be studied. The relationship between the conductivity and morphology structure needs to be established to optimize the preparation conditions of PBI film suitable to use in fuel cells. Method to decrease the permeability of the membrane is in demand.

The ionic conductive behavior of PBI in alkaline solution needs to be systemically studied.

Reference

[1] G. M. Barrow, *Physical chemistry,* McGraw-Hill Inc., New York, p217, 1988.

[2] L. J. M. J. Blomen and M. N. Mugerwa, *Fuel Cell Systems*, Plenum Press, New York and London, p37, 1993.

[3] G. H. J. Broers and J. A. A. Ketelaar, *Fuel cells,* ed. G. J. Young, Reinhold Pub. Corp., New York, 1960.

[4] L. J. M. J. Blomen and M. N. Mugerwa, *Fuel Cell Systems*, Plenum Press, New York and London, p38, 1993.

[5] L. J. M. J. Blomen and M. N. Mugerwa, *Fuel Cell Systems*, Plenum Press, New York and London, p75, 1993.

[6] L. J. M. J. Blomen and M. N. Mugerwa, *Fuel Cell Systems*, Plenum Press, New York and London, p76, 1993.

[7] D. P. Wilkinson and D. Thompsett, in *"Proceeding of the second International Symposium on New Materials for Fuel Cell and Modern Battery system"*, Eds. O. Savadogo and P. R. Roberge, Montreal, Canada, July 6-7, (1997), p. 266.

[8] H. Wendt, in *"Proceeding of the second International Symposium on New Materials for Fuel Cell and Modern Battery system"*, Eds. O. Savadogo and P. R. Roberge, Montreal, Canada, July 9-13, (1995), p. 532.

[9] L. Giorgi, E. Antolini, A. Pozio and E. Passalacqua, *Proceedings of Fuel Cell Seminar,* November 17-20, 1996, Orlando.

[10] V. A. Paganin, E. A. Ticianelli and E. R. Gonzalez, *J. Appl. Electrochem.* **23,** 1107 (1993)

[11] O. Savadogo and M. Lacroix, in *"Proceeding of the second International Symposium on New Materials for Fuel Cell and Modern Battery system"*, Eds. O. Savadogo and P. R. Roberge, Montreal, Canada, July 6-7, (1997), p873.

[12] L. Giorgi, E. Antolini, A. Pozio and E. Passalacqua, *Electrochimica Acta,* **43** (24), 3675 (1998).

[13] I. D. Raistrick, U.S. Patent No. 4876115 (1989).

[14] M. S. Wilson and S. Gottesfeld, *J. of Appl. Electrochem.*, **22,** 1 (1992).

[15] Z. Poltarzewski; P. Staiti; V. Alderucci; W. Wieczorek; N. Giordano, *J. Electrochem. Soc.* **139**(3), 761 (1992).

[16] A. J. Appleby, *Fuel Cell Handbook*, New York: Van Nostrand Reinhold, 1989.

[17] O. Savadogo, *Journal of New Materials for Electrochemical Systems*, **1**(1), 47 (1998).

[18] S. Escribano, S. Miachon and P. Aldebert, in *"Proceeding of the first International Symposium on New Materials for Fuel Cell and Modern Battery system"*, Eds. O. Savadogo, P. R. Roberge, and T. N. Veziroglu, Montreal, Canada, July 9-13, (1995), p. 135.

[19] S. Besse, G. Bronoel, N. Tassin, Y. Naimi, A. Tounsi, in *"Proceeding of the first International Symposium on New Materials for Fuel Cell and Modern Battery system"*, Eds. O. Savadogo, P. R. Roberge, and T. N. Veziroglu, Montreal, Canada, July 9-13, (1995), p. 144.

[20] M. S. Wilson, C. R. Derouin, J. A. Valerio and S. Gottesfeld, in *"28th intersociety Energy Conversion Engineering Conference Proceedings Atlanta, August, (1993) (American Institue of Aeronautics and Astronautics, Washington, DC (USA), 1994),* p. 1.1203.

[21] R. Kumer and S. Ahmed, in *"Proceeding of the first International Symposium on New Materials for Fuel Cell and Modern Battery system"*, Eds. O. Savadogo, P. R. Roberge, and T. N. Veziroglu, Montreal, Canada, July 9-13, (1995), p. 224.

[22] M. Kahlich, M. M. Schubert, M. Huttner, M. Noeske, H. A. Gasteiger and R. J. Behm, in *"Proceeding of the second International Symposium on New Materials for Fuel Cell and Modern Battery system"*, Eds. O. Savadogo and P. R. Roberge, Montreal, Canada, July 6-10, (1997), p. 642.

[23] G. P. Schulman and W. Lochte, *J. Macromol. Sci. Chem.*, **1**, 413 (1967).

[24] Y. Tsur, Y. L. Freilich, and M. Levy, *J. Polym. Sci.*, **12**, 1531 (1974).

[25] D. N. Gray, G. P. Schulman, and R. T. Conley, *J Macromol. Sci. Chem.*, **1**, 395 (1967).

[26] Dale A. Chatfieleld, *J. Polym. Sci. Chem.*, **19**, 601 (1981).

[27] M. B. Gieselman, and J. R. Reynolds, *Macromolecules*, **26**, 5633 (1993).

[28] P. Musto, F. E. Karasz and W. J. Macknight, *polymer*, **34**, 2934 (1993).

[29] D. Weng, J. S. Wainright, U. Landau, and R. F. Savinell, *J. Electrochem. Soc.*, **143**, 1260 (1996).

[30] D. Weng, J. S. Wainright, U. Landau, and R. F. Savinell, p. 201, in *Electrode Materials and Processes for Energy Conversion and Storage*, S. Srinivasan, D. D. Macdonald, and A. C. Khandkar, Editors, PV 94-23, p. 201 *The Electrochemical Society Proceedings Series*, Pennington, NJ (1994)

[31] H. A. Pohl and R. P. Chartoff, *J. Polym. Sci. Part A*, **2**, 2787 (1964).

[32] S. M. Aharoni and M. H. Litt, *J. Polym. Sci. Polym. Chem. Ed.*, **12**, 639 (1974).

[33] D. Hoel and E. Grunwald, *J. Phys. Chem.*, **81**, 2135 (1977).

[34] S. M. Aharoni and A. J. Signoreli, *J. Appl. Polym. Sci.*, **23**, 2653 (1979).

[35] J. S. Wainright, J. T. Wang, D. Weng, R.F. Savinell and M. Litt, *J. Electrochem. Soc.*, **142**, L121 (1995).

[36] S. R. Samms, S. Wasums, and R. F. Savinell, *J. Electrochem. Soc.*, **143**, 1225 (1996).

[37] W. F. Lin, J. T. Wang, and R. F. Savinell, *J. Electrochem. Soc.*, **144**, 1917 (1997).

[38] J. S. Wainright, R. F. Savinell and M. H. Litt, in *"Proceeding of the second International Symposium on New Materials for Fuel Cell and Modern Battery system"*, Eds. O. Savadogo and P. R. Roberge, Montreal, Canada, July 6-7, (1997), p. 808.

[39] J. T. Wang, J. S. Wainright, R. F. Savinell and M. Litt, *J. Appl. Electrochem.*, **26,** 751 (1996).

[40] J. T. Wang, S. Wasmus, and R. F. Savinell, *J. Electrochem. Soc.*, **143,** 1233 (1996).

[41] S. Wasmus, J. T. Wang, and R. F. Savinell, *J. Electrochem. Soc.*, **142,** 3825 (1995).

[42] Jiangtao Wang, S. Wasmus, and R. F. Savinell, *J. Electrochem. Soc.*, **142,** 4218 (1995).

[43] J. T. Wang, R. F. Savinell, J. Wainright, M. Litt, and H. Yu, *Electrochimica Acta,* **41,** 193 (1996).

[44] B. Xing, and O. Savadogo, *J. New Mat. Electrochem. Syst.*, **2** (1999) 95.

[45] E. J. Powers and G. A. Serad, *Proceedings of the Symposium on the History of High Performance Polymer* at the American Chemical Society Meeting, April 15-18, New York, 1986.

[46] A. K. Engel, T. Yoden, K.Sanui and N. Ogata, *Polymeric Materials Science and Engineering, Proceedings of the ACS Division of Polymeric Materials: Science and Engineering,* Vol. 54, p. 119, ACS, New York, Spring 1986.

[47] J. K. Gillham, *Critical Review of Macromolecular Science*, Vol. 1, p. 83, 1972.

[48] R. T. Conley, J. J. Kane and S. Ghosh, *Hoechst Celanese Corp. Technical Report AFML-TR-71-219 (November 1971)*

[49] J. R. Bron and N. Mc M. Browne, *Australian Def. Scient. Serv. Mtl. Res. Lab. Report MRL-R-674, Maribyrnong Victoria (August 1976)*, p. 4

[50] P. Hautojarvi, ed., "Positrons in Solids", Springer-Verlag, Berlin, Heidelerg (1979).

[51] Y. Kobayashi, W. Zheng, E. F. Meyer, J. D. McGervey, A. M. Jamieson, and R. Simha *Macromolecules,* **22,** 2302 (1989).

[52] S. Tao *J. Chem. Phys.* **56**, 5499 (1972).

[53] J. R.Steven, *Methods of Experimental Physics*, **16A**, 371 (1980).

[54] D. M. Schrader and Y. C. Jean, eds., *Positron and Positronium Chemistry,* Elssevier, New York (1988).

[55] Q. Deng, F. Zandiehndem and Y. C. Jean, *Macromolecules*. **25,** 1090 (1992).

[56] Q. Deng and Y. C. Jean, *Macromolecules*. 26, 30 (1993).

[57] H. Nakanishi, Y. C. Jean, E. G. Smith and T. C. Sandreczki, *J. Polym. Sci., B:* 27, 1419 (1989)

[58] Z. Yu, U. Yahsi, J. D. McGervey, A. M. Jamieson and R. Simha, *J. Polym. Sci., B: Polymer Physic,* **32**, 2637 (1994).

[59] M. Y. Ruan, H. Moaddel, A. M. Jamieson, R. Simha and J. D. McGervey, *Macromolecules*. **25,** 2407 (1992).

[60] O. A. Hasan, M. C. Boyce, X. S. Li and S. Berko, *J. Polym. Sci., B: Polymer Physic,* **31**, 185 (1993).

[61] L. Xie, D. W. Gidley, H. A. Hristov and A. F. Yee, *J. Polym. Sci., B: Polymer Physic,* **33**, 77 (1995).

[62] L. B. Liu, D. Gidley and A. F. Yee, *J. Polym. Sci., B: Polymer Physic,* **30**, 231 (1992).

[63] J. E. Kluin, Z. Yu, S. S. Cleeshouwers, J. D. McGervey, A. M. Jamieson, R. Simha and K. Sommer, *Macromolecules*. **26,** 1853 (1993).

[64] T. Suzuki, Y. Oki, M. Numajiri, T. Miura, K. Kondo and Y. Ito, *Polymer*, **34,** 1361 (1993).

[65] J. A. Hinkley, A. Efrekhari, R. A. Crook, B. J. Jensen and J. J. Singh, *J. Polym. Sci., B: Polymer Physic,* **30**, 1195 (1992).

[66] H. S. Sodaye, P. K. Pujari, A. Goswami and S. B. Manohar, *J. Polym. Sci., B: Polymer Physic,* **35**, 771 (1997).

[67] H. Moaddel *Ph. D. thesis*, "Development and Characterization of Polybenzimidazole as a Solid Polymer Electrolyte", CWRU, (1996).

[68] B. Xing and O. Savadogo, to be published.

[69] B. Xing and O. Savadogo, to be published

[70] R. F. Savinell and M. H. Litt, United States Patent, 5,716,727, (1998).

[71] H. A. Vogel and C. S. Marvel, *J. Polym. Sci.*, **50**, 511 (1961).

[72] D. P. Griswald Jr., A. E. Casey, E. K. Weisberger and J. H. Weisburger, *Cancer Research*, **28**, 924 (May 1968)

[73] K. C. B.Dangayach, K. A. Karim and D. C. Bonner, *J. Appl. Polym. Sci.*, **26**, 559 (1981)

[74] M. Hu, E. M. Pearce and T. K. Kwei, *J. Polym. Sci., A: Polymer Chemistry*, **31**, 553 (1993).

[75] Y. Iwakura, K. Uno and Y. Imai, *J. Polym. Sci., Part A*, **2**, 2605 (1964).

[76] A. B. Conciatori, E. C. Chenevey, T. C. Bohrer and A. E. Prince, Jr., *J. Polym. Sci., C: Polymer Symposia*, **19**, 49 (1967).

[77] R. Ameri, *Ph. D. thesis*, "Polybenzimidazole film containing phosphoric acid as proton exchange membrane (PEM)", CWRU, 1997.

[78] J. K. Gillham, *Crit. Rev. Macromol. SCI*, **1**, 83 (1972)

[79] D. E. Steutz, A. E. DiEdwards, F. Zitomer and B. P. Barnes, *J. Polymer Science, Polymer Chemistry Edition*, **18**, 987 (1980).

[80] S. Samms, S. Wasmus, and R. F. Savinell, *J. Electrochem. Soc.*, **143**, 1225 (1996).

[81] S., Wasmus, B. A. Daunch, H. Moaddel, P. L. Rinaldi, M. H. Litt, C. Rogers, A. Veleriu, G. D. Mateescu, D. A. Tryk, and R. F. Savinell, *Abstract 466, p. 716, The Electrochemical Society Extended Abstracts*, **95-1**, Reno, NV, May 21-26 (1995).

[82] A. B. Conciatori, E. C.Chenevy, C. Bohrer and A. E.Prince, Jr., *J. Polymer Science, Part C*, **19**, 49 (1967).

[83] R. W. Singleton, H. D. Noether and J. F. Tracy, *J. Polymer Science, Part C*, **19**, 65 (1967).

[84] J. T. Wang, *Ph. D. thesis*, "*High temperature proton conducting polymer fuel cell*)", CWRU, 1996.

[85] R.S. Bogner, Electron Dyn. Div., Hughes Aicr. Co., Proc. Intersoc.

[86] CT, USA, Avail.NTIS, Nada [Contract. Rep.] CR (1978), NASA-CR-159653, FCR-1017, 73 pp. From: Sci. Tech. Aerosp. Rep. 1979, 17(24), Abstr. No. N79-33581. CODEN: NSCRAQ ISSN: 0565-7059.

[87] R.E. Martin, Power Syst. Div., United Technol. Corp., South Windsor, CT, USA, Avail. NTIS, NASA [Contract. Rep,] CR (1979), (NASA-CR-159807, FCR-1657), 52 pp. From: Sci. Tech. Aerosp. Rep. 1980, 18(10), Abstr. No. N80-19615. CODEN: NSCRAQ ISSN: 0565-7059.

[88] U.S. Pat. 5,71,038, B. Vyas, (Bell Telephone Laboratories) (Sept. 11, 1984).

CHAPTER 2

THE EFFECT OF ACID DOPING ON THE CONDUCTIVITY OF POLYBENZIMIDAZOLE (PBI)

Baozhong Xing and O. Savadogo

Laboratoire d'Électrochimie et de Matériaux Énergétiques

École Polytechnique de Montréal

C.P. 6079, succ. Centre-Ville

Montréal, Québec, H3C 3A7

Canada

(Published in *J. New Mat. Electrochem. Syst.*, 2 (1999) 95)

Abstract

The protonic conductivity of polybenzimidazole (PBI) in various electrolytes was systemically studied. It was shown that blank PBI is a protonic insulator. Its conductivity in acid electrolyte is at around 10^{-10} to 10^{-9} S · cm^{-1}. After doping it in H_2SO_4, HCl, HNO_3, $HClO_4$ or H_3PO_4 it exhibited high protonic conductivity. The conductivity depends on the type of the doping acid agent and its concentration. The highest conductivity (e.g. 0.0601 S · cm^{-1} for PBI doped with 16 mol/L H_2SO_4) obtained was as good as Nafion® 117. The conductivity increases in the order H_2SO_4 > H_3PO_4 > $HClO_4$> HNO_3>HCl for high concentrations (11-16 mol/L) of the doping acid. It was shown that the high conductivities of PBI films were obtained after doping them with H_2SO_4, H_3PO_4 or $HClO_4$. These high conductivities make them suitable candidates for fuel cell applications. From these results it was shown that the measurement of the conductivity of blank PBI in acid media must be done before a deadline time where the film was not doped with acid.

1. Introduction

Polybenzimidazole (PBI) is an aromatic heterocyclic polymer. It exhibits high thermo and thermo-oxidative stability [1-6], superior mechanical properties and excellent chemical stability. It is an electrical insulator [7-10]. The resistivity of pure blank PBI is 10^{12} ohm·cm [7-10]. It was indicated that its salts with acids and complexes with metal ions are also insulators [10]. It has been shown that the resistivities of the salts were 10^{6} ohm·cm for HCl salt; and 10^{8} ohm·cm for HCOOH salt. A high protonic conductivity (e.g. $2 \sim 8\times10^{-4}$ S · cm^{-1}) has also been shown for PBI in the humidity range from 0 to 100% [9]. This value is much higher than that obtained by Ahoroni et al. [10] ($\sim10^{-12}$ S/ cm). The difference between these values may be attributed to the fact that no difference was made between the electronic conductivity and protonic conductivity. The former one may be a protonic conductivity and the later an electronic conductivity.

Gilipa et al. [11] studied blank PBI protonic conductivity in 4-6 mol/L acid solution. This study did not take into account the possibility of modification of PBI contacting acid due to the reaction between PBI and acids with time. In other words the variation of PBI ionic conductivity with time in acid media has never been studied.

Phosphoric acid-doped polybenzimidazole has been developed as polymer electrolyte for methanol fuel cell [12-21]. It was shown that the polymer cast from a PBI solution and then doped with H_3PO_4 by immersing it into 11 mol/L H_3PO_4 solution exhibited lower conductivity than the polymer directly doped with H_3PO_4 when cast from the solution of PBI polymer and H_3PO_4. The methanol crossover rate through the H_3PO_4 doped PBI film was lowered by one order of magnitude compared to the Nafion® 117 membrane in a solid polymer electrolyte fuel cell. However the methanol crossover is still very high which can particularly affect the cathode performance for the oxygen reduction at low platinum loading [22]. It has been shown that $HClO_4$ is an interesting supporting electrolyte for methanol oxidation [23] due to the lack of adsorption of its anions. No literature is available on the studies of the conductivity of PBI doped with other kinds of

acids including $HClO_4$. Thus it is of considerable importance to study the conductivity of PBI doped in various acids at different concentrations. The aim of this work is to study the conductivity of PBI doped with H_2SO_4, $HClO_4$, HCl, HNO_3 and H_3PO_4 in the concentration range of 1-16 mol/L. The variation of the conductivity with time for different concentrations of acids used for PBI doping was also studied in $HClO_4$ and other various acids. The concentration of the dopant and the doping time that allow the highest conductivity were evaluated.

These results can be used to determine the appropriate electrolyte for the methanol oxidation.

2. Experimental

The PBI film with a thickness of 40 μm was purchased from Hoechest Celanese. The film was cut into small square samples of 3 ×3 cm^2. The samples were washed in boiling deioned water for more than 6 hours to remove the impurities of LiCl. These blank samples were kept in water. The samples were doped by immersing them into the acid solution in a glass cell for a controlled period of time. The conductivity of each doped or undoped sample was measured at different times. The measurement was achieved in acid solution using classical two-point probe with home made conductivity measurement cell as shown in Figure 2.1 [24].

The cell consists of two chambers with 1 cm diameter. The platinum disks were used as working electrodes and connected to a power supply with an amperemeter. The electrolyte was filled into the chambers with a pump from input holes. The electrolyte gets out of the chambers from output holes. The PBI film was installed between the two half measurement cells that were bolted together tightly. A calomel reference electrode with a long capillary connected to the cell near the film was used in each compartment for the potential measurement. The calomel electrodes were connected to a potentiometer. The potential drop across the PBI film was obtained by taking off the

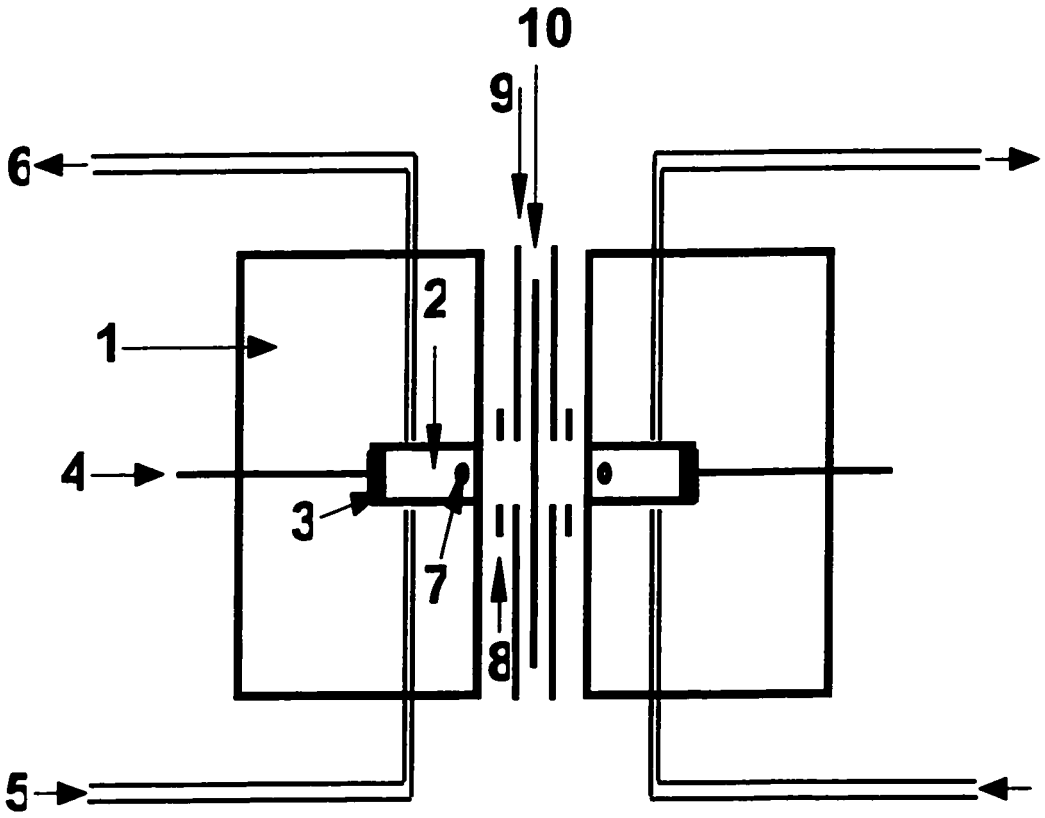

Figure 2.1. The structure of measurement cell

1. Cell body
2. Measurement Chamber
3. Pt electrode
4. Pt electrode
5. Measurement medium solution input from pump
6. Measurement medium solution output
7. Measurement hole connected with calomel measurement electrode
8. Teflon O ring gasket
9. Teflon film gasket
10. PBI membrane

solution's potential drop from total potential drop. To measure the conductivity of the PBI film, the potential drop between the two half cells was taken at different currents. Then a straight line of potential vs. current was plotted. From the slops the total resistance was determined. The potential drop in the electrolyte was measured after resetting the measurement cell without the PBI film. The resistance of the PBI film was obtained by subtracting that of the solution from the total resistance. The conductivity of the PBI film could be calculated from its resistance, thickness and surface area.

For the short time doped samples, the doping process was conducted in situ. The undoped sample was introduced into the measurement cell where the doping acid solution was introduced. The doping time was started when the blank PBI is put in contact with acid solution. The conductivity of PBI film was measured at different times for various electrolytes. For each of these electrolytes, the conductivity of PBI measured immediately after it was put in contact with the electrolyte. The value of this conductivity which does not change with time was taken as the conductivity of the blank PBI. This value varies of course with the acid type of the electrolyte. During the doping process, the conductivity of the films was measured with time. The doping time was deduced when the recorded conductivity was constant again. Then the doped film was kept in the doping electrolyte for 10 days before conductivity measurement in various electrolytes.

The conductivity of all PBI samples doped with different acid at different concentrations for 10 days was measured in 2 mol/L $HClO_4$ solution.

3. Results and discussion

3.1. The conductivity of blank PBI

The variation of the conductivity of PBI film with time is shown in Figure 2.2 for various acid solutions (H_2SO_4, $HClO_4$ HCl, HNO_3 and H_3PO_4). For each concentration – time curve, three regions are observed. In the first region the conductivity does not change very much with time. The value of the conductivity and the time range of this region

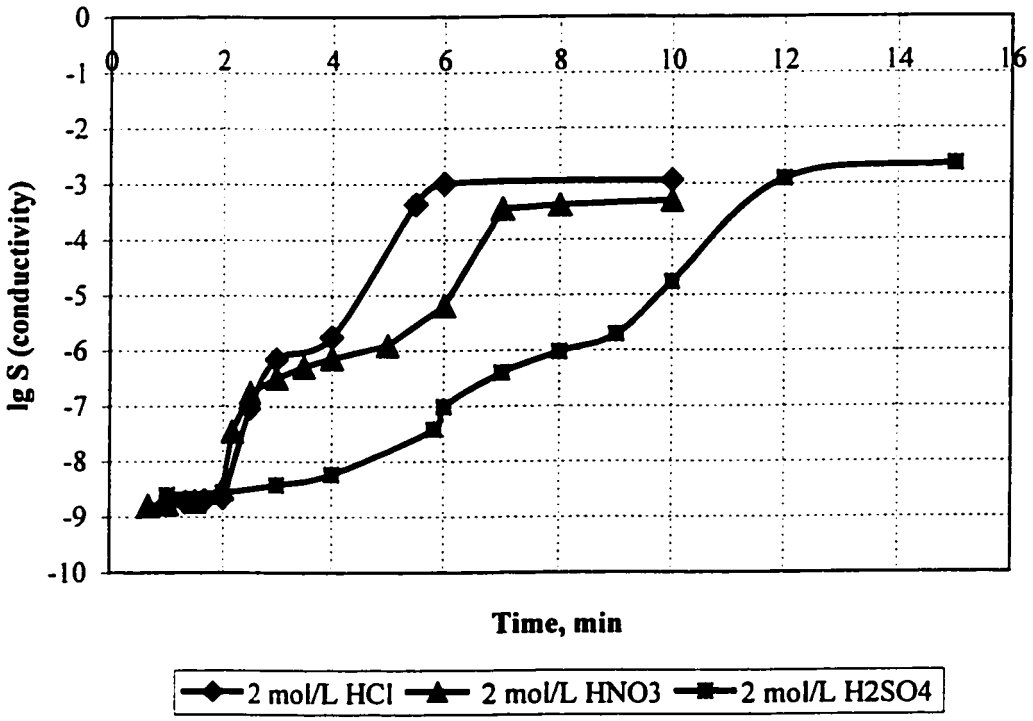

Figure 2.2a. Conductivity – time relationship of PBI in acids

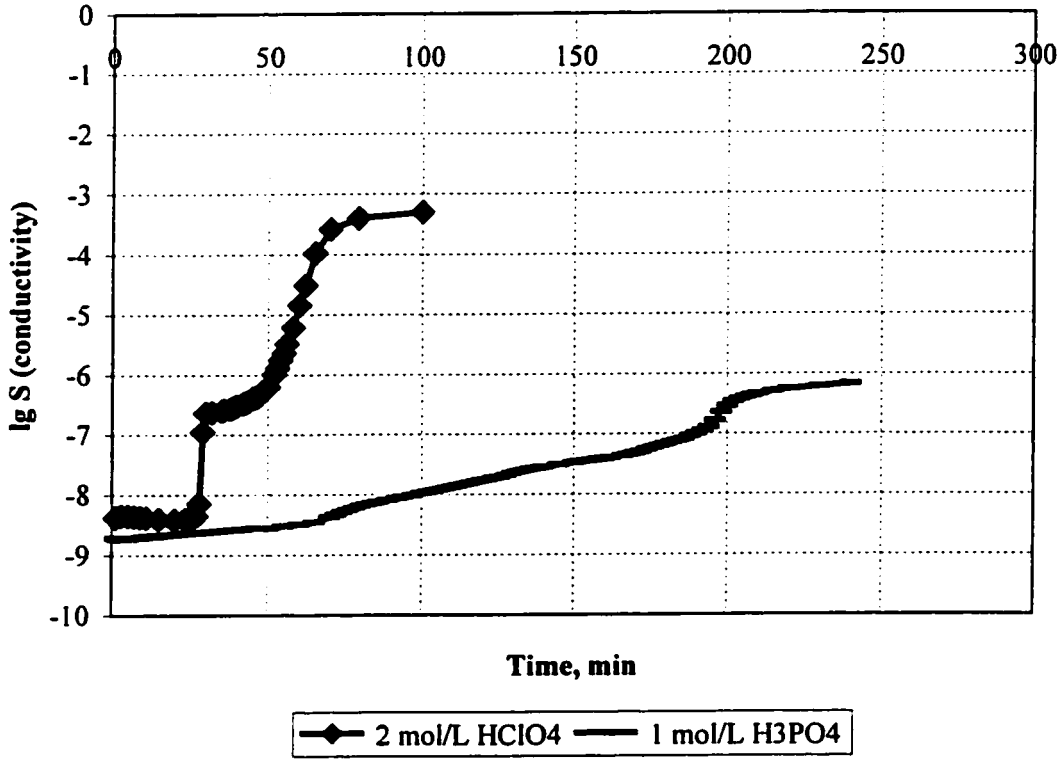

Figure 2.2b. Conductivity – time relationship of PBI in acids

depend on the acid solution. The conductivity of blank PBI in each medium is shown in Table 2.1 for various electrolytes.

Table 2.1. The conductivity of blank PBI in various acid solutions with various concentrations (S/cm $\times 10^{10}$)

Concentration of the doping electrolyte, (mol/L)	1	2	4	6	8	10	11
$HClO_4$	7.2	12.6	26.2	67.3	70.1	96.3	
HNO_3		10.3	9.7		9.9		
H_2SO_4	39.4	24.9	12.4	4.3	3.4		
HCl		14.9	13.3		4.2		
H_3PO_4	18.4			9.0			3.0

For the time longer than the range of the first region, the conductivity increases sharply with time and finally reaches the first plateau. After, the second and the third plateau are respectively observed. The variation of the conductivity with time can be attributed to a doping process of PBI with acid. This doping process is achieved when the conductivity value reaches the third plateau. The occurrence of the "plateau" is related to the mechanism of the doping process. The first plateau is related to the blank PBI. The second plateau is related to reaction of the first nitrogen site of the PBI with the acid. The third plateau is related to the reaction of second nitrogen site of the PBI with the acid. These two "nitrogen sites" may be observed on the PBI structure as shown in Figure 2.3. Thus as a basic polymer, PBI, which has a pK_b of about 6, reacts with acid connecting with it. This is an indication that the conductivity of PBI film will change with time when it is placed in acid solution as shown in Figure 2.2. The time necessary to have the third plateau may be related to the reaction rates between PBI and the acids. It changes with the type of the acid. The shorter the time is, the higher the reaction rate is. The rate changes in the order HCl> HNO_3>H_2SO_4>$HClO_4$ >H_3PO_4. The determination of such exact mechanism is under active investigation.

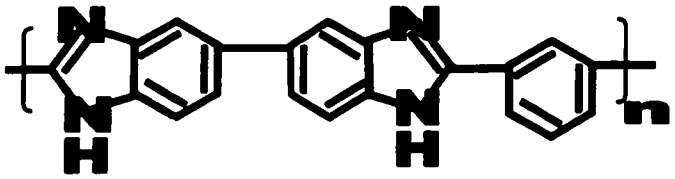

Figure 2.3. A schematic chemical structure of polybenzimidazole

The conductivity values measured before their first changes with time are that of the blank PBI. For example in 4 mol/L HCl the blank conductivity (e.g. 1.33×10^{-9} S/cm) must be measured before 1 minute following it contacts with the electrolyte. For the measurements done in the same solution after 10 minutes (e.g. the time that the PBI film was put in contact with acid solution), the conductivity increases to 3.22×10^{-3} S/cm. It is very close to the value in reference [11] (e.g. 6.3×10^{-3} S/cm). The results obtained in this work show that the conductivity of blank PBI must be determined in specific experimental conditions. In particular the conductivity of blank PBI must be measured in each electrolyte before a certain period of time depending on the electrolyte. For measurements done at time longer than this specific time the conductivity is that of PBI doped with the electrolyte that it is contacting. This indicates that the conductivity obtained in reference [11] may not be considered as the conductivity of blank PBI. The results obtained here (see Table 2.1) indicate that the blank PBI without modification in acid solution exhibit very low protonic conductivity. The conductivity of blank PBI decreases when the concentration of the acid solution increases for H_2SO_4, HCl and H_3PO_4. No obvious change of the conductivity with the acid concentration is observed in the case of HNO_3. In the case of $HClO_4$ the opposite tendency is observed; the conductivity of blank PBI increases with the concentration of $HClO_4$. This conductivity changes also with the acid type for every concentration. These results may be related to a synergetic effect of proton and anion mobility in the corresponding acid solution and the strength of the acid. However the variation of the conductivity of blank PBI in different acid solutions (type and concentration) is not significant (no more than one order of magnitude from an initial value of $\sim10^{-10}$ S/cm). In conclusion, the conductivity of blank PBI in acid media is very small. This conductivity can be increased after doping PBI with the acid.

3.2. The conductivity of PBI doped with acids

3.2.1. Case of PBI doped with H2SO4

Figure 2.4 shows the variation of PBI conductivity measured in 2 mol/L $HClO_4$ with the concentration of the doping acid e.g. H_2SO_4 after doping during 10 days. The conductivity was measured after the doping time was reached e.g. the time range where the conductivity does not change significantly with time. As may be seen the conductivity varies in the range $9.7 \times 10^{-4} \sim 10^{-2}$ S/cm in a very large range of H_2SO_4 concentration e.g. 1 to 14 mol/L. In contrast the conductivity of PBI doped in 16 mol/L H_2SO_4 is 0.060 S/cm. It is close to that of Nafion® 117 in 2 mol/L $HClO_4$ (e.g. 0.064 S/cm). The conductivity of Nafion® 117 obtained here is similar to that obtained elsewhere in H_2SO_4 [11, 25, 26].

Table 2.2. Conductivity of PBI doped with H_2SO_4 and measured in the same solution

Concentration of doping electrolyte, (mol/L)	1	2	4	5	6	7	8
Doping time, min	35	27	30	30	45	60	80
Conductivity, S/cm $\times 10^3$	1.15	3.25	3.96	3.72	3.34	3.65	3.55

Table 2.3. Conductivity of PBI doped in $HClO_4$ and measured in same doping solution

Concentration of the doping electrolyte, (mol/L)	1	2	4	6	8	10
Doping time, min	92	90	100	157	215	213
Conductivity, S/cm $\times 10^4$	6.28	4.37	2.35	2.10	3.30	5.51

The conductivity of PBI doped with different concentrations of H_2SO_4 and measured in the same concentration H_2SO_4 solution is shown in Table 2.3 for different "doping times". The doping time is long for PBI doped in more concentrated H_2SO_4. The conductivity changes slightly from 1.15×10^{-3} to 3.55×10^{-3} S/cm. The highest conductivity is obtained for PBI doped in 4 mol/L H_2SO_4 for 30 minutes. These values at high H_2SO_4

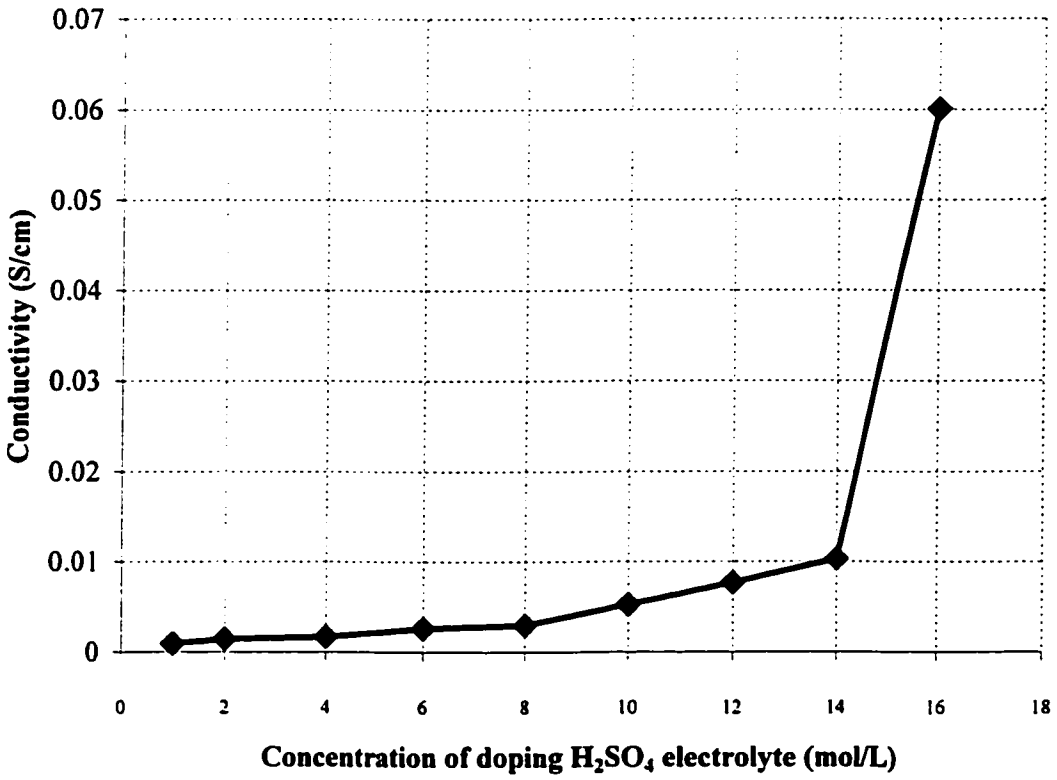

Figure 2.4. Conductivity of PBI doped in H_2SO_4 for 10 days and measured in 2 mol/L $HClO_4$

concentration are higher than those obtained elsewhere on PBI treated with 10% H_2SO_4 (e.g. low concentrated acid, about 1.09 mol/L) [27]. For the same doping agent e.g. H_2SO_4 the conductivity measured in 2 mol/L $HClO_4$ and in different concentrations of H_2SO_4 does not change for PBI doped in H_2SO_4 from 1 to 8 mol/L (Table 2.2). This may be an indication that the doping agent is the key parameter in the conductivity change. This is supported by the result obtained on conductivity of PBI doped with $HClO_4$ and measured in 2 mol/L $HClO_4$. As it may be seen in Figure 2.4 and 2.5, this conductivity is lower than that obtained on PBI doped with H_2SO_4 and measured in 2 mol/L $HClO_4$. The following results support also this interpretation.

3.2.2. Case of PBI doped with $HClO_4$

Figure 2.5 shows the variation of the conductivity of PBI doped with different concentrations of $HClO_4$ and measured in 2 mol/L $HClO_4$.The same trend as Figure 2.4 is observed but for every concentration the conductivity obtained on PBI doped in $HClO_4$ is lower than that in H_2SO_4.

The results in Figure 2.5 are similar to those of PBI doped with H_2SO_4. The difference is that the conductivity of PBI doped with $HClO_4$ is lower than that with H_2SO_4. In Table 2.3 the conductivity has a minimum point at 6 mol/L when concentration increases. This tendency is different with that in Figure 2.5. The conductivity is lower than that doped and measured in H_2SO_4.

3.2.3. Case of PBI doped with HCl

The conductivity of PBI doped in HCl at different concentrations and measured in 2 mol/L $HClO_4$ is shown in Figure 2.6. As it may be seen, the conductivity measured in 2 mol/L $HClO_4$ increases steadily with the HCl concentration. The increase is not as much as in H_2SO_4 for high concentrations of the doping electrolyte. The conductivity of doped PBI in H_2SO_4 or in $HClO_4$ is higher than that in HCl. In Table 1.4 the conductivity of

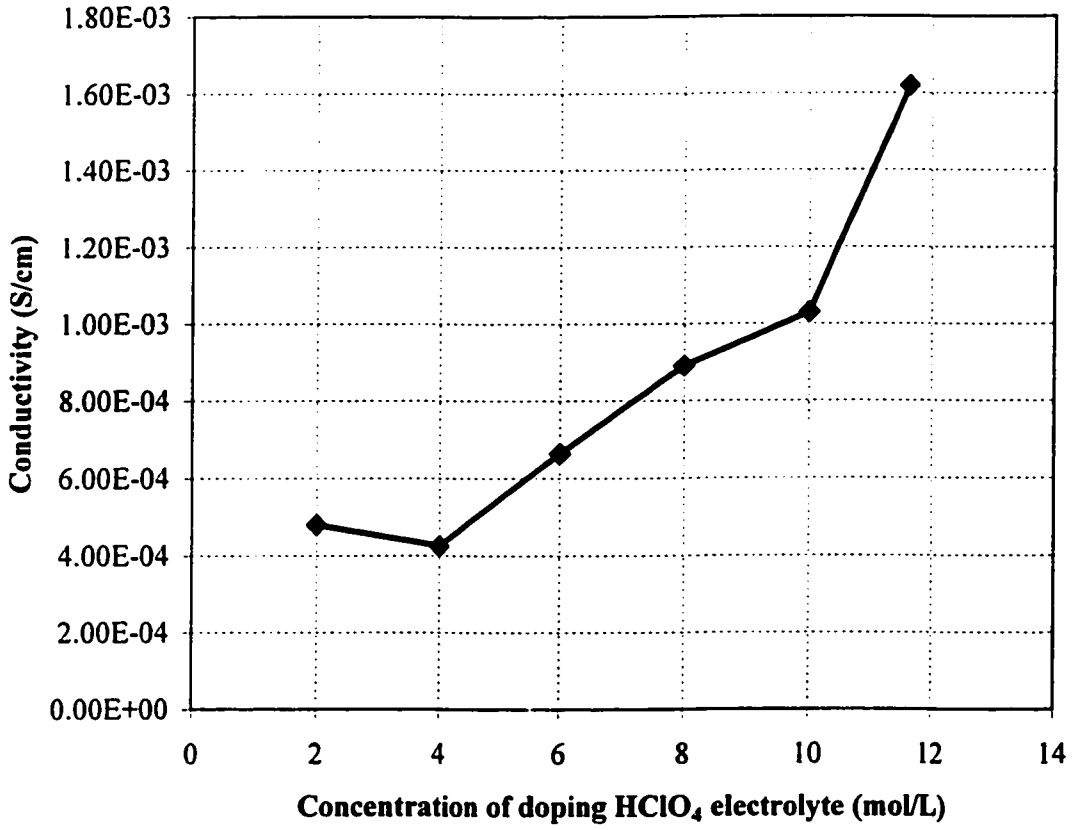

Figure 2.5. Conductivity of PBI doped in $HClO_4$ for 10 days and measured in 2 mol/L $HClO_4$

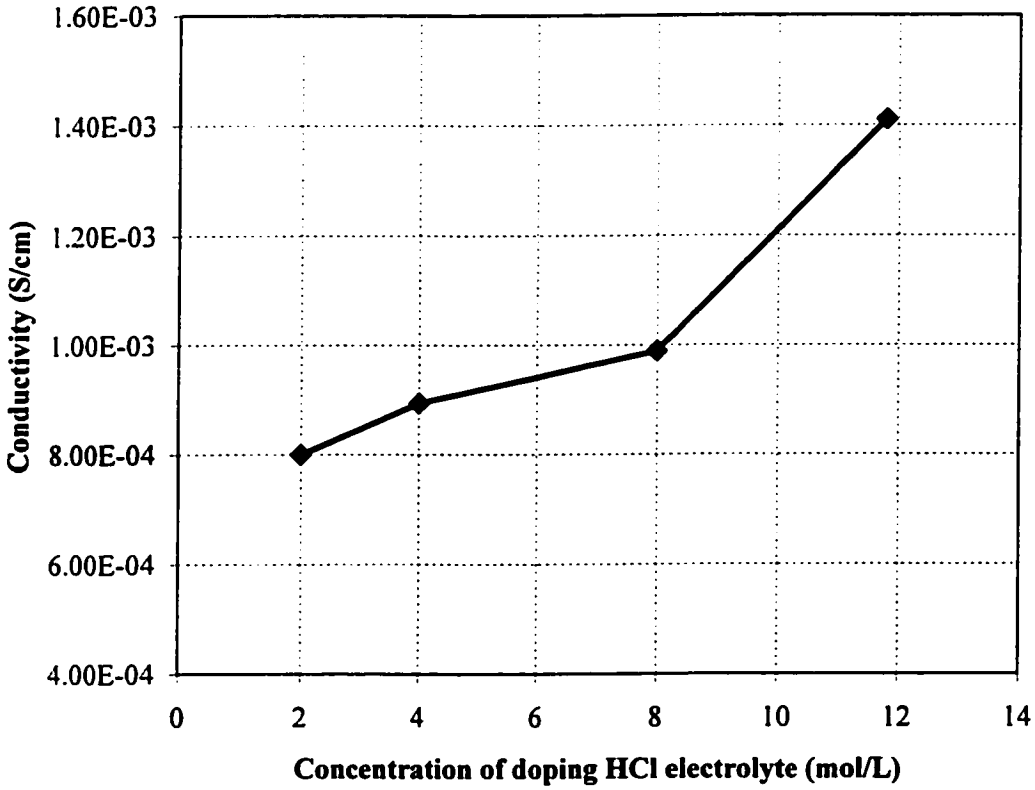

Figure 2.6. Conductivity of PBI doped in HCl for 10 days and measured in 2 mol/L $HClO_4$

PBI doped in HCl and measured in the same electrolyte increases with the doping electrolyte concentration. The conductivity also increases about 2 times from 2 to 8 mol/L while in Figure 2.6 it increases less than 2 times. It shows that the conductivity of one sample measured in HCl increases with the concentration of HCl doping electrolyte. The conductivity measured in HCl is much higher than that measured in $HClO_4$. But the conductivity measured in HCl is similar to that measured in H_2SO_4.

Table 2.4. Conductivity of PBI doped in HCl and measured in the same doping solution

Concentration of doping electrolyte, (mol/L)	2	4	8
Doping time, min	10	10	10
Conductivity, S/cm $\times 10^3$	1.94	3.22	4.04

3.2.4. Effect of doping with HNO_3

The conductivity of PBI doped with HNO_3 at different concentrations is shown in Figure 2.7 and Table 2.5. The conductivity increases with the HNO_3 concentration. At high concentrations the change is not as large as that obtained for PBI doped with H_2SO_4; but it is similar to that obtained for PBI doped in $HClO_4$ and is larger than that obtained for PBI doped in HCl. The conductivity of PBI doped in HNO_3 and measured in HNO_3 is higher than that measured in 2 mol/L $HClO_4$. The conductivity of PBI doped in HNO_3 and measured in HNO_3 is almost the same to that doped in HCl.

Table 2.5. Conductivity of PBI doped in HNO_3 and measured in the same doping solution

Concentration of doping electrolyte, (mol/L)	2	4	8
Doping time, min	30	10	10
Conductivity, S/cm $\times 10^3$	1.36	3.22	4.04

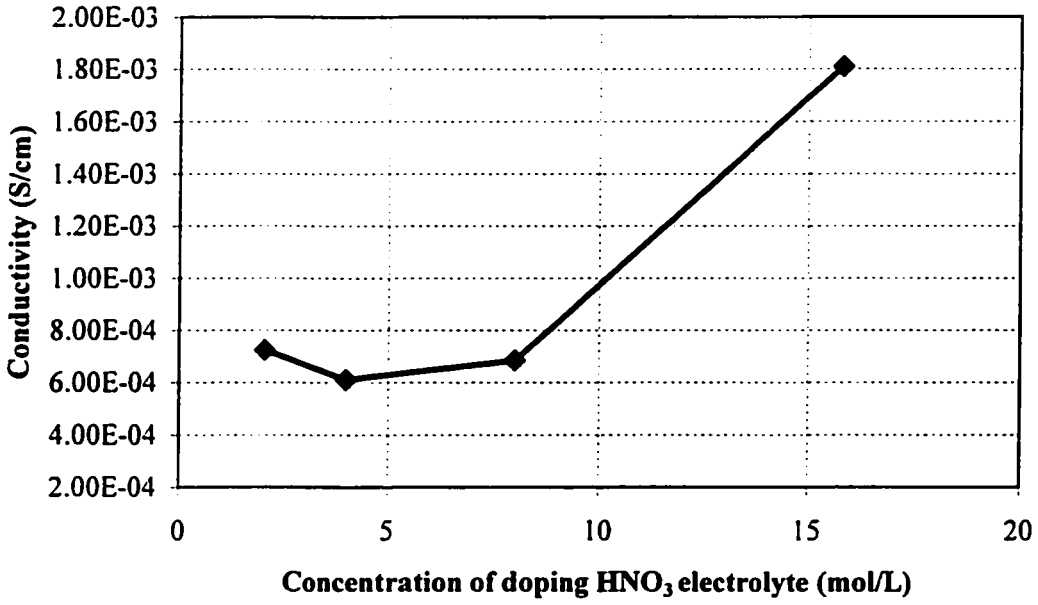

Figure 2.7. Conductivity of PBI doped in HNO_3 for 10 days and measured in 2 mol/L $HClO_4$

3.2.5. Effect of doping with H_3PO_4

The conductivity of PBI doped in different concentrations of H_3PO_4 and measured in 2 mol/L $HClO_4$ is shown in Figure 2.8. In Figure 2.8 the conductivity does not change significantly when the doping electrolyte concentration (H_3PO_4) increases. However, the conductivity at low concentrations is much higher than that of PBI doped in HCl, HNO_3 or $HClO_4$. Even the conductivity of the PBI doped in 1 mol/L H_3PO_4 is higher than that of PBI doped in 15.8 mol/L HNO_3, 11.8 mol/L HCl, 11.6 mol/L $HClO_4$ or 8 mol/L H_2SO_4. The conductivity of PBI doped in 16 mol/L H_3PO_4 solution is very high, but much less than that of PBI doped in 16 mol/L H_2SO_4. The conductivity of PBI doped in H_3PO_4 and measured in the same H_3PO_4 increases with the acid concentration (Table 2.6). But this change is not as significant as that measured in 2 mol/L $HClO_4$ (Figure 2.6).

Table 1.6. Conductivity of PBI doped in H_3PO_4 and measured in the same solution

Concentration of doping electrolyte, mol/L	1	6	11
Doping time, min	950	150	785
Conductivity, S/cm $\times 10^4$	1.33	13.2	24.0

3.2.6. Effect of PBI doped with phosphotungstic acid (PTA)

The variation of the conductivity of PBI doped with PTA at different concentrations and measured in various electrolytes is shown in Tables 2.7-2.13. From these tables many comments may be addressed. The conductivity of PBI doped in PTA is almost the same with that of blank PBI in NaCl solution. From these tables, it can also be seen that the conductivity does not change with time and the measurement medium solutions. This indicates that PTA may not be an efficient dopant for PBI if we want to increase its conductivity in solution. This is an indication that PBI cannot easily form salt with acid like PTA [10]. However, the PBI film that has been immersed in PTA solution exhibits different behaviors as comparing it with the blank PBI when doping it successively in 2 mol/L HCl without immersion in PTA solution. Furthermore, the reaction characteristics of PBI film with acids are changed after immersed in PTA solution. The reaction rate of

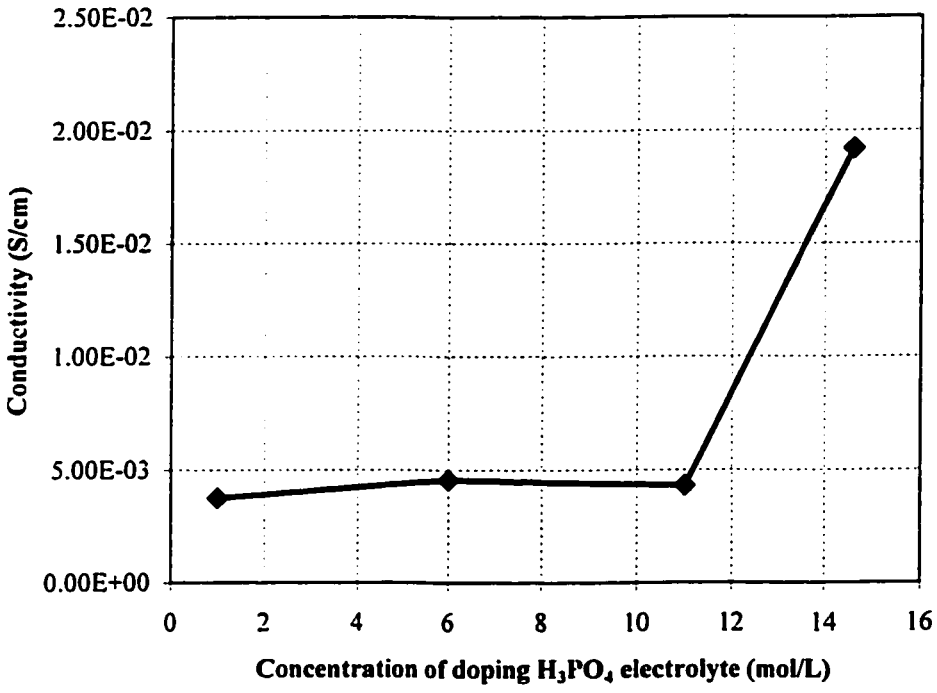

Figure 2.8. Conductivity of PBI doped in H_3PO_4 for 10 days and measured in 2 mol/L $HClO_4$

this kind of PBI film with HCl is 14 times slow as compared with that of blank PBI without immersion in PTA solution with HCl. After it is doped in 2 mol/L HCl successively, the conductivity of PBI immersed in PTA solution is much lower than that of blank PBI directly at the beginning.

Table 2.7. Conductivity of PBI in 2 mol/L NaCl after doping PTA

PTA concentration, %	5	10	20	40	60
Doping time, h	456	456	456	456	456
Conductivity, S/cm×10^8	2.45	1.42	1.05	2.00	2.88
Doping time, h	624	624	624	624	
Conductivity S/cm×10^8	4.24	9.21	1.11	8.76	
Doping time, h	768	768	768	768	
Conductivity S/cm×10^8	73.0	10.9	2.79	2.55	
Doping time, h	888	888	888	888	
Conductivity S/cm×10^8	6.04	7.76	7.78	8.79	

Table 2.8. Conductivity of PBI in 10% PTA after doping PTA

PTA concentration, %	5	10	20	40	60*
Doping time, h	648	648	648	648	648
Conductivity, S/cm×10^8	1.29	5.84	4.36	3.28	158

* The film was heated in 60% PTA for 26.5 hour.

Table 2.9. Conductivity of PBI in 0.1 mol/L NaCl after doping PTA

PTA concentration, %	5	10	20	40	60*
Doping time, h	768	768	768	768	768
Conductivity, S/cm×10^8	0.731	1.50	1.49	2.55	128

Table 2.10. Conductivity of PBI in 1 mol/L Na_2SO_4 after doping PTA

PTA concentration, %	5	10	20	40	60*
Doping time, h	768	768	768	768	768
Conductivity, S/cm×10^8	9.94	10.8	22.9	7.86	124

Table 2.11. Conductivity of PBI in 2 mol/L HCl after doping PTA

PTA concentration, %	5	10	20	40	60*
Doping time, h	888	888	888	888	888
Conductivity, S/cm×10^8	24.9	29.0	30.0	0.887	1100

Table 2.12. Conductivity of PBI film immersed in PTA solution for 888 hours before and after doping 2 mol/L HCl successively, measured in 2 mol/L NaCl

PTA concentration, %	5	10	20	40	60*
Conductivity $B^{\#}$, S/cm×10^8	6.04	7.76	7.78	8.79	7.78
Conductivity $A^{\#}$, S/cm×10^8	1280	524	2510	2060	2660

$B^{\#}$ Before doping, $A^{\#}$ After doping.

Table 2.13. Conductivity (S/cm×10^8) change of PBI after being heated in 60% PTA at boiling point

Before heating	After heating 2.5 h	After heating 26.5 h
28.8	74.8	381

The conductivity of PBI immersed in PTA solution increases with the PTA electrolyte temperature (Table 2.13). The longer the heating time is, the more the increase is. The conductivity is still small compared to the conductivity values obtained in other doping acids.

The conductivity of PBI doped in $HClO_4$, HNO_3, H_2SO_4, HCl or H_3PO_4 and measured in 10% PTA solution is smaller than that of PBI doped in $HClO_4$, HNO_3, H_2SO_4, HCl or H_3PO_4 and measured in these acids.

The results obtained here indicate that PTA is not a good dopant for PBI if we want to increase its protonic conductivity in solution. But it does not mean that PTA could not have an effect on the conductivity of PBI under the fuel cell conditions. The membrane of Nafion® 117 doped with PTA gives out a better performance than without doping [28]. It shows that the doping of PTA improves the protonic conductive of Nafion® 117 in fuel cell. The effect of PTA on the conductivity of PBI under fuel cell conditions is under active investigation.

4. Conclusion

The blank PBI film is a protonic and an ionic insulator in NaCl or acid electrolyte. The conductivity of blank PBI in acid electrolyte changes with the concentration of the electrolyte. For a given acid electrolyte, the conductivity of blank PBI decreases slightly when the acid concentration increases in the case of HCl or H_3PO_4. It increases with the acid concentration in $HClO_4$. For HNO_3 or H_2SO_4 there is no effect of the acid of concentration on the blank PBI conductivity. Thus the conductivity of blank PBI changes slightly with the type of the acid electrolytes and its concentration. It changes with 2 mol/L acid electrolytes in the order: H_3PO_4>HCl>$HClO_4$>HNO_3>H_2SO_4. For higher concentrations (≥8M), the conductivity of blank PBI changes in the order $HClO_4$> HNO_3> H_2SO_4>HCl>H_3PO_4.

The conductivity of PBI doped with high concentration of acids (≥8M) changes significantly with the type of the doping acids in the order: H_2SO_4 > H_3PO_4 > $HClO_4$> HNO_3>HCl. The conductivity of PBI doped with H_2SO_4 or H_3PO_4 exhibited the two first highest values. These values are similar to that of Nafion® 117. Thus PBI doped with high concentrations of H_2SO_4 or H_3PO_4 exhibited a protonic conductivity similar to that of Nafion® 117. When the concentration of doping acids is low (≤2M), the conductivity of doped PBI changes with the type of acids in the order: H_3PO_4> H_2SO_4>HCl >HNO_3>$HClO_4$. In this case PBI doped with H_3PO_4 exhibited the highest protonic conductivity. It was also shown that the PBI doped with concentrated $HClO_4$ exhibited an

interesting conductivity. As an example, the value of the conductivity of PBI doped with 11.6 mol/L $HClO_4$ and measured in 2 mol/L $HClO_4$ is 2×10^{-3} S/cm at room temperature. It is relatively high and may be interesting for methanol oxidation in $HClO_4$. Therefore, $HClO_4$ doped PBI is a very promising candidate for methanol fuel cell. This study is under active investigation.

5. Reference

[1] G. P. Schulman and W. Lochte, *J. Macromol. Sci. Chem.*, **1**, 413 (1967).

[2] Y. Tsur, Y. L. Freilich, and M. Levy, *J. Polym. Sci.*, **12**, 1531 (1974).

[3] D. N. Gray, G. P. Schulman, and R. T. Conley, *J. Macromol. Sci. Chem.*, **1**, 395 (1967).

[4] Dale A. Chatfieleld, *J. Polym. Sci. Chem.*, **19**, 601 (1981).

[5] M. B. Gieselman, and J. R. Reynolds, *Macromolecules*, **26**, 5633 (1993).

[6] P. Musto, F. E. Karasz and W. J. Macknight, *polymer*, **34**, 2934 (1993).

[7] H. A. Pohl and R. P. Chartoff, *J. Polym. Sci. Part A*, **2**, 2787 (1964).

[8] S. M. Aharoni and M. H. Litt, *J. Polym. Sci. Polym. Chem. Ed.*, **12**, 639 (1974).

[9] D. Hoel and E. Grunwald, *J. Phys. Chem.*, **81**, 2135 (1977).

[10] S. M. Aharoni and A. J. Signoreli, *J. Appl. Polym. Sci.*, **23**, 2653 (1979).

[11] X. Glipa, M. E. Haddad, D. J. Jones, J. Roziere, *Solid State Ionics*, **97**, 323 (1997).

[12] J. S. Wainright, J. T. Wang, D. Weng, R.F. Savinell, M. Litt, *J. Electrochem. Soc.*, **142**, L121 (1995).

[13] S. R. Samms, S. Wasums, and R. F. Savinell, *J. Electrochem. Soc.*, **143**, 1225 (1996).

[14] D. Weng, J. S. Wainright, U. Landau, and R. F. Savinell, *J. Electrochem. Soc.*, **143**, 1260 (1996).

[15] W. F. Lin, J. T. Wang, and R. F. Savinell, *J. Electrochem. Soc.*, **144**, 1917 (1997).

[16] J. S. Wainright, R. F. Savinell and M. H. Litt, in *"Proceeding of the second International Symposium on New Materials for Fuel Cell and Modern Battery*

system", Eds. O. Savadogo and P. R. Roberge, Montreal, Canada, July 6-7, (1997), p. 808.

[17] J. T. Wang, J. S. Wainright, R. F. Savinell, M. Litt, *J. Appl. Electrochem.*, **26,** 751 (1996).

[18] J. T. Wang, S. Wasmus, and R. F. Savinell, *J. Electrochem. Soc.*, **143,** 1233 (1996).

[19] S. Wasmus, J. T. Wang, and R. F. Savinell, *J. Electrochem. Soc.*, **142,** 3825 (1995).

[20] Jiangtao Wang, S. Wasmus, and R. F. Savinell, *J. Electrochem. Soc.*, **142,** 4218 (1995).

[21] J. T. Wang, R. F. Savinell, J. Wainright, M. Litt, and H. Yu, *Electrochimica Acta,* **41,** 193 (1996).

[22] O. Savadogo, *J. New Mat. Electrochem. Syst.* **1,** 47 (1998).

[23] S. Mukerjee, and J. McBreen, *in "Proceedings of the Second International Symposium on New Materials for Fuel Cell and Modern Battery Systems" Eds, O. Savadogo and P. R. Roberge, Montreal Canada,* July 6-10, 1997, p. 548.

[24] B. Tazi and O. Savadogo, *in "Proceedings of the Second International Symposium on New Materials for Fuel Cell and Modern Battery Systems" Eds, O. Savadogo and P. R. Roberge, Montreal Canada,* July 6-10, 1997, p864.

[25] B. Tazi, and O. Savadogo, *J. New Mat. Electrochem. Syst.* (submitted).

[26] Hong Wang and G. A. Capuano, *J. Electrochem. Soc.*, **145,** 780 (1998).

[27] C. A. Linkous and D. K. Slattery, *Frontiers Science (New Eeergy system and Conversions)*, **7,** 257 (1993).

[28] Malhotra Sanjiv, Datta Ravindra, *J. Electrochem. Soc.*, **144,** L23 (1997).

CHAPTER 3

HYDROGEN/OXYGEN POLYMER ELECTROLYTE MEMBRANE FUEL CELLS (PEMFCS) BASED ON ALKALINE-DOPED POLYBENZIMIDAZOLE (PBI)

Baozhong Xing and O. Savadogo

Laboratoire d'Électrochimie et de Matériaux Énergétiques

École Polytechnique de Montréal

C.P. 6079, Succ. Centre-Ville

Montréal, Québec, H3C 3A7, Canada

(Published in *Electrochemistry Communications*, 2, 2000, p697-702)

Abstract

When complexed with alkaline such as potassium hydroxide, sodium hydroxide or lithium hydroxide, films (40 μm thick) of polybenzimidazole (PBI) show conductivity in the 5×10^{-5}-10^{-1} S/cm range, depending on the type of alkali, the time of immersion in the corresponding base bath and the temperature of immersion. It has been shown that PBI has a remarkable capacity to concentrate KOH, even in an alkaline bath of concentration 3 M. The highest conductivity of KOH-doped PBI (9×10^{-2} S/cm) at 25°C obtained in this work is higher than we had obtained previously as optimum values for H_2SO_4-doped PBI (5×10^{-2} S/cm at 25°C) and H_3PO_4-doped PBI (2×10^{-3} S/cm at 25°C). PEMFCs based on an alkali-doped PBI membrane were demonstrated, and their characteristics exhibited the same performance as those of PEMFCs based on Nafion® 117. Their development is currently under active investigation.

Key words: Alkaline doped PBI, improved hydrogen/oxygen PEMFC Fuel Cell based on KOH-doped PBI.

1. Introduction

Polybenzimidazole (PBI) exhibited excellent thermo-chemical stability and mechanical properties [1-6]. It is much cheaper and has much lower permeability for hydrogen than Nafion® [7-8]. Blank PBI is an electronic and ionic insulator [9-12], which becomes a very good ionic conductor when it is doped with acids in proper conditions [13-24]. It remains an electronic insulator after doping. Phosphoric-acid-doped polybenzimidazole has been used as a polymer electrolyte for the methanol fuel cell [14-23]. The phosphoric acid concentration used was less than 11 M. Recently, we have shown that PBI doped with high concentrations (>11 M) of H_3PO_4 or H_2SO_4 exhibited high ionic conductivity at 25°C e.g. 2×10^{-3} and 5×10^{-2} S/cm respectively [24]. It has been shown that H_2/O_2 PEMFCs based on H_2SO_4 doped PBI exhibited better characteristics (i_{600} = 810 mV) than H_2/O_2 PEMFC based on Nafion® 117 (i_{600} = 540 mV) [25].

PBI has also been also used in various other applications. PBI-impregnated zirconium separator had been used in Ni-Cd battery for geosynchronous orbit applications [26]. This cell was capable of being operated at 80% depth of discharge (DOD), and it was about 30% lighter. As well it would be capable of supporting a geosynchronous mission for ten to fifteen years. In all test regimes, at any DOD and temperature, the cell demonstrated three times the life cycle of the state-of-the-art Ni-Cd cell. PBI fibre has been used as the matrix materials in alkaline fuel cells [27, 28] performing well (> 0.9 V at i = 1 A/cm^2) after over 13 000 h of operations. However, the level of corrosion of the system was high in 42% KOH. PBI was also used in the alkaline cadmium battery to increase the capacity and life cycle of cadmium anode [29].

Even though PBI has been added to the alkaline solutions in some applications, in none of these cases was a PEMFC based on an alkali-doped PBI film membrane involved. Furthermore, the fundamental studies on the doping of PBI films (net PBI 100%) in alkaline solution are lacking in the literature. Our work here investigated the effects of the type and concentration of the alkaline solution on the conductivity of PBI and the mechanism of diffusion of alkaline species in PBI.

2. Experimental

2.1. Conductivity measurements

PBI film (purchased from Hoechst Celanese, 40 μm thick) was cut into 3×3 cm^2 samples. They were washed in boiling DI water for more than 6 hours to remove the impurity, LiCl. The water was changed several times during washing. The samples were then kept in DI water. The PBI was doped by immersing the sample in an alkaline solution for a certain period of time. The conductivity of the PBI membrane doped with the alkaline solution was measured in the doping solutions and in a 1 M alkaline solution. The conductivity was measured with a homemade four-electrode conductivity cell using direct current after the samples has been doped for 10 days. The conductivity cell is shown in Figure 3.1.

2.2. Fuel cell performance evaluation

For the PEMFC performance evaluation, an anode, a cathode and a dynamic hydrogen electrode (DHE) reference electrode of 20% Pt/C (catalyst loading of 0.35 mg Pt cm^{-2}) from E-Tek were hot pressed onto each KOH doped PBI membrane at 145°C under 110 MPa for 4 minutes. The hydrogen reference electrode was incorporated on the anode side. The electrode (anode and cathode) surface area was 6.25 cm^2. The resulting membrane electrode assembly (MEA) was incorporated into a single test fixture. The cell was then installed in a Globe Tek (Model BC-60) fuel-cell station. The single-cell test was carried out at an optimum pressure ratio for H_2/O_2 of 1/1 atmosphere. The cell

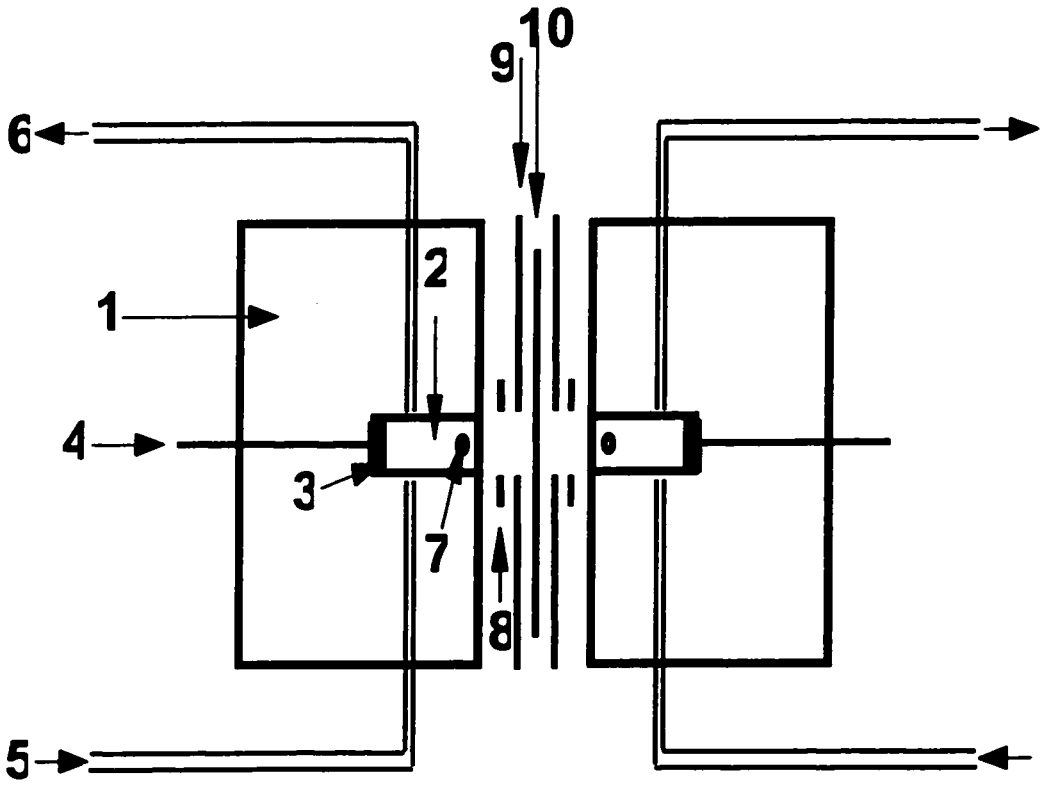

Figure 3.1. The structure of measurement cell

1. Cell body
2. Measurement chamber
3. Pt electrode
4. Pt electrode
5. Measurement medium solution input from pump
6. Measurement medium solution output
7. Measurement hole connected with calomel measurement electrode
8. Teflon O ring gasket
9. Teflon film gasket
10. PBI membrane

voltage versus current density curves of the fuel-cell-based KOH PBI membrane was recorded at 50°C.

3. Results and discussion

3.1. Conductivity measured in the electrolyte

Figures 3.2 and 3.3 show the variation of PBI conductivity with the type and concentration of the alkaline doping electrolytes. As may be seen, the alkaline-doped-PBI conductivity changes with the type and concentration of the alkaline electrolyte, increasing with the strength of the alkaline agent; the highest conductivity is obtained with PBI doped with KOH and the lowest conductivity is obtained with PBI doped with LiOH. The conductivity of PBI doped with LiOH is 1500 times lower than that of PBI doped with NaOH and 3,000 times lower than that doped with KOH. This is an indication that the alkaline strength may have an effect on this conductivity. The change in conductivity with electrolyte concentrations also depends on the alkali type. The highest conductivity was obtained at 6 M for potassium hydroxide and at 8 M for sodium hydroxide. For lithium hydroxide, the highest conductivity is obtained at a concentration of 4 M.

The optimum alkaline concentration, which gives the highest conductivity, increases with the doping time. As can be seen in Table 3.1, the optimum concentration of sodium hydroxide is 8 M for 0.1 day of doping and 12 M for 100 days of doping. The optimum conductivity corresponding to the optimum concentration of NaOH increases with the doping time. For doping time longer than ten days the conductivity is stable. This is related to the increase of the alkaline species in the membrane with time. After 10 days, the membrane is saturated with the alkaline species and the conductivity becomes stable.

In the case of LiOH, the conductivity of PBI doped with LiOH increases with LiOH concentration up to 4 M (the electrolyte is almost saturated with LiOH at this

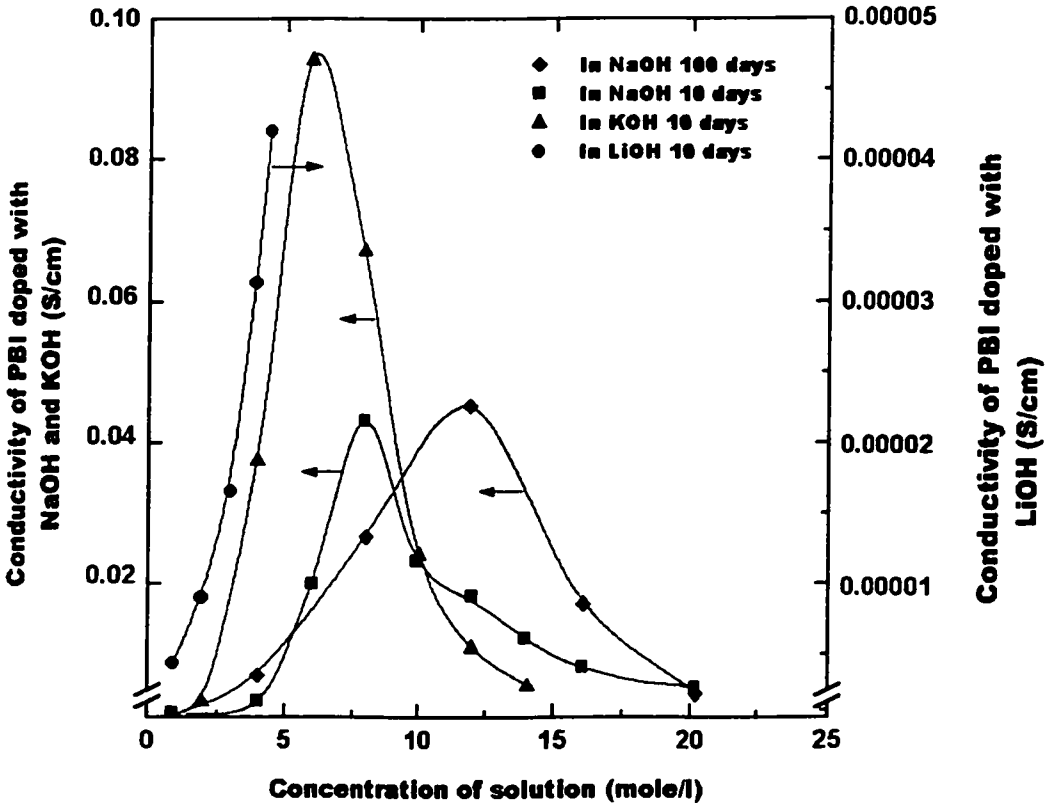

Figure 3.2. Variation of the alkaline doped PBI conductivity with the doping electrolyte concentration for various alkali electrolytes. The conductivity was measured in the doping electrolyte.

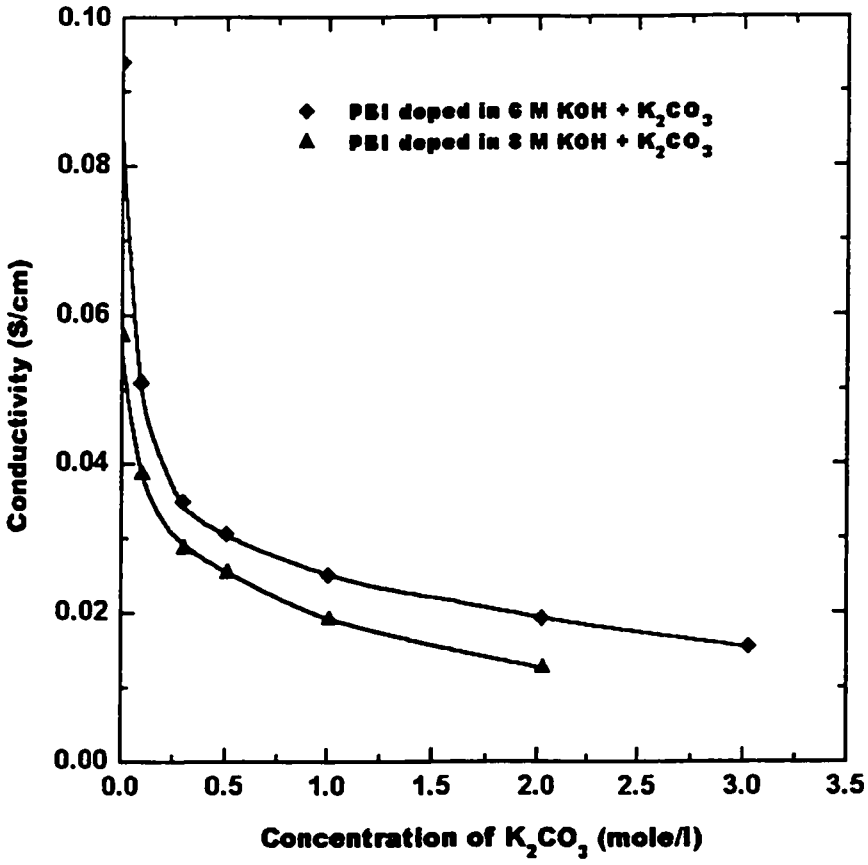

Figure 3.3. Variation of the alkaline + K_2CO_3 doped PBI conductivity with the doping electrolyte concentration for various concentrations of K_2CO_3.

concentration). No optimum conductivity value was observed for the variation of the conductivity with LiOH concentration.

Table 3.1. Variation of the alkaline concentration corresponding to the maximum conductivity with the doping time

Time, day	0.1	10	100
Concentration of NaOH, M	8	10	12
Conductivity, S/cm	0.00637	0.0425	0.0444

3.2. Conductivity in 1 M alkaline solutions

The conductivity of PBI doped with various alkaline solutions was also measured in the corresponding alkaline solution with a concentration of 1 M. The value of the conductivity, as shown in Table 3.2, is lower than that measured directly in the doping solution. The optimum conductivity measured in the 1 M alkaline solution after doping PBI in various concentrations of alkaline also changes with the concentration of doping solution, as shown in Table 3.2. This may be due to the modification of the base functional groups of the doped PBI in the 1 M alkaline measuring solution, since the concentration of the doping solution was generally higher than that of the electrolyte used for the conductivity measurement. These functional groups were sorbed during the process of doping at high alkaline concentration. The conductivities of NaOH doped PBI (0.016 S/cm) and measured in 1 M NaOH are higher than that of Nafion (0.012 S/cm) measured in the same solution.

The changes in conductivity of PBI with the concentration of doping solutions and the conductivity measured in 1 M LiOH, 1 M NaOH or 1 M KOH trends similar to those doped and measured directly in the doping solutions: a) the conductivity of doped PBI are high (~ 4 x 10^{-2} S/cm for PBI doped in 6 M KOH for 10 days); b) the optimum conductivity varies with the doping conditions. This suggests that the improvement in the conductivity of the alkaline doped PBI may be due to the specific modification of PBI by

the alkaline species and OH^-, and not to the cations of the alkaline electrolyte. This result is supported by the determination of the conductivity of PBI doped in NaCl (10^{-9} S/cm) and Na_2CO_3 (10^{-6} S/m). For the same doping electrolyte concentration, the conductivity of NaOH is higher than that of NaCl. This is also supported by the values of the ion transference numbers of K^+, Na^+ and Li^+ in alkali-doped PBI (Table 3.3). The difference between the cation transference numbers is not as large as the difference between the conductivities of PBI doped in the corresponding alkaline solution.

Table 3.2. Variation of maximum conductivity with doping time for various types of alkali. Conductivity is measured in 1 M of the corresponding electrolyte

Electrolyte	LiOH	NaOH	NaOH	KOH
Doping time (days)	10	10	100	10
Alkaline concentration (M)	4	20	15	6
Optimum conductivity ($S.cm^{-2}$)	2.5×10^{-5}	1×10^{-2}	3×10^{-2}	4×10^{-2}

Another factor in support of the important contribution of OH^- ions in the variation of the conductivity is the increase in conductivity with the strength of the alkaline solution (Table 3.3).

Table 3.3. Conductivity of PBI doped over ten days in various alkali-type solutions and that measured in the same electrolyte

Solution (3 M)	KOH	NaOH	LiOH
Conductivity S/cm	6.5×10^{-2}	8×10^{-4}	4×10^{-5}
Transference number	0.45	0.36	0.42

3.3. Effect of carbonate

Figure 3.3 shows the variation between the conductivity of PBI doped in KOH + K_2CO_3 and that measured in the electrolyte containing K_2CO_3. The conductivity of PBI doped in

the binary solution of KOH and K_2CO_3 decreases from 0.095 S/cm to 0.016 S/cm when the K_2CO_3 concentration increases from 0 to 3M. The conductivity of PBI doped in the solution decreases very rapidly when the concentration of K_2CO_3 is less than 0.3 M. Above 0.3 M K_2CO_3, it decreases slowly. Even at a very high K_2CO_3 concentration, e.g. 3 M, which is almost the saturated concentration of K_2CO_3 in 6 M KOH, the PBI doped in the solution still has a high conductivity, 0.016 S/cm, that is higher than that of Nafion® 117 (without K_2CO_3), (0.012 S/cm).

These results show a decrease in the conductivity of the PBI doped with KOH + K_2CO_3. This may affect the characteristics of fuel cells based on such membrane. By contrast, carbonates would block electrolyte pathways and electrode pores on platinum-based electrodes. In the case of Ni or Ag fuel cell electrodes we find that the carbonates do not block the electrode pores [29]. This is in agreement with the results of other investigations [30, 31].

Figure 3.4 shows the variation between the conductivity of PBI doped at various times in KOH + K_2CO_3 and that measured in the same electrolyte. The conductivity of PBI doped over a 10-minute-period is lower than that of PBI doped over 20 days. This is related to the doping effect of the membrane with the hydroxide ions when the doping time increases. The quantity of OH^- ions inserted in the membranes during the doping increases and leads to a higher conductivity with time.

3.4. Temperature effect

The effect of the doping temperature on the conductivity of PBI doped and measured in KOH or KOH + K_2CO_3 solution is shown in Figures 3.5 and 3.6, respectively. The conductivity of PBI doped only in KOH solution increases with the doping temperature as shown in Figure 3.5. The conductivity increases with temperature from 0.02 to 0.095 S/cm for temperature ranging from 25 to 70°C. For the same temperature range, the temperature dependency of the conductivity of the H_3PO_4-doped PBI (2×10^{-3}~4×10^{-3}

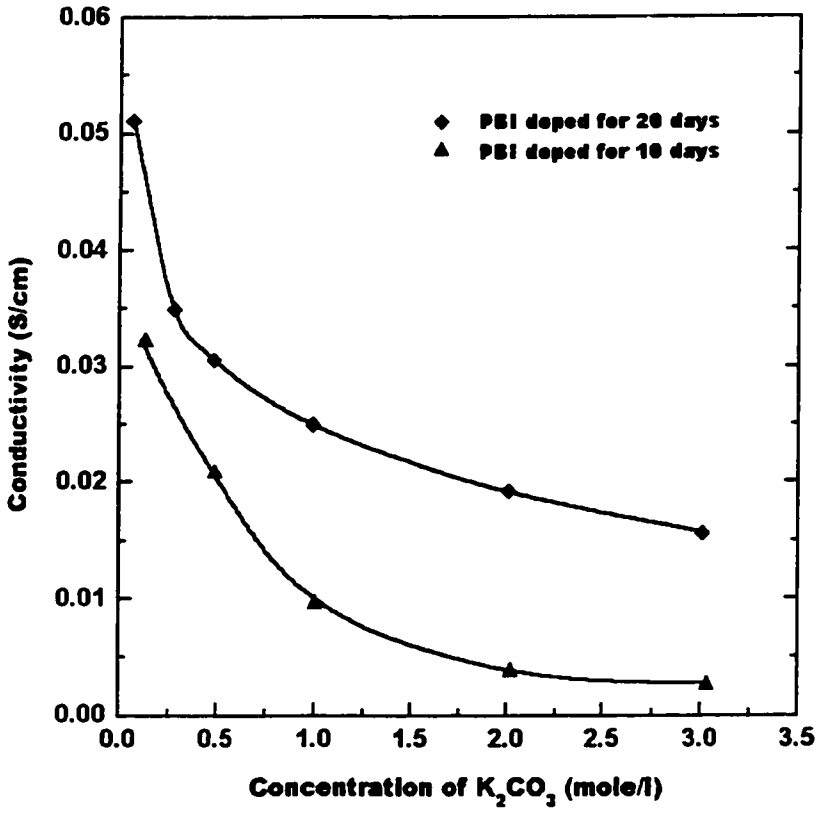

Figure 3.4. Variation of the conductivity of alkaline doped PBI in KOH + K_2CO_3 with the concentration of K_2CO_3 and measured in the same electrolyte for two doping times.

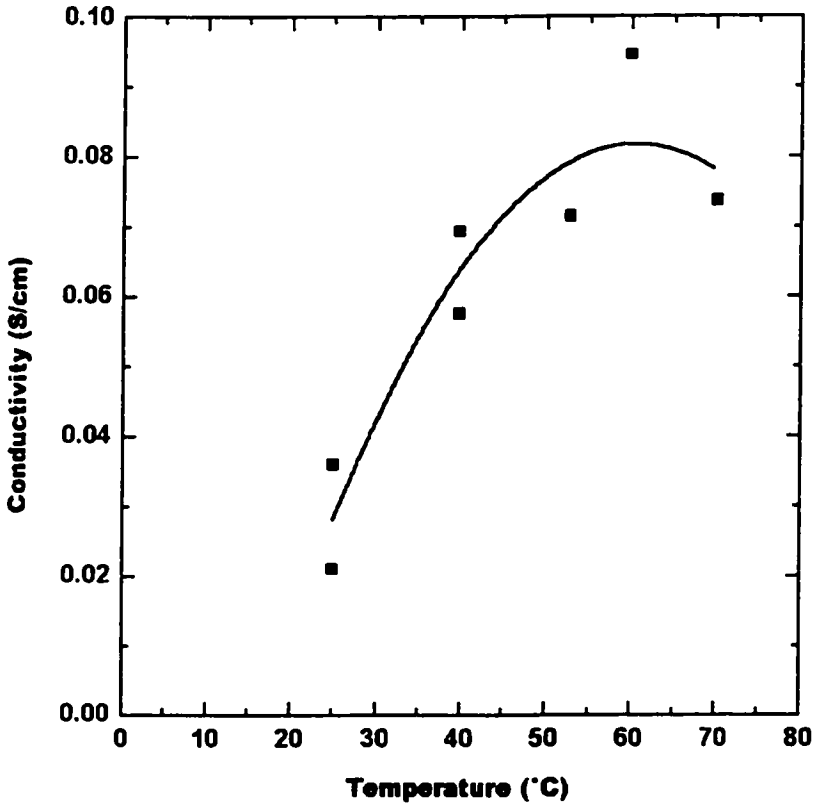

Figure 3.5. Variation of the conductivity of KOH doped PBI with the temperature.

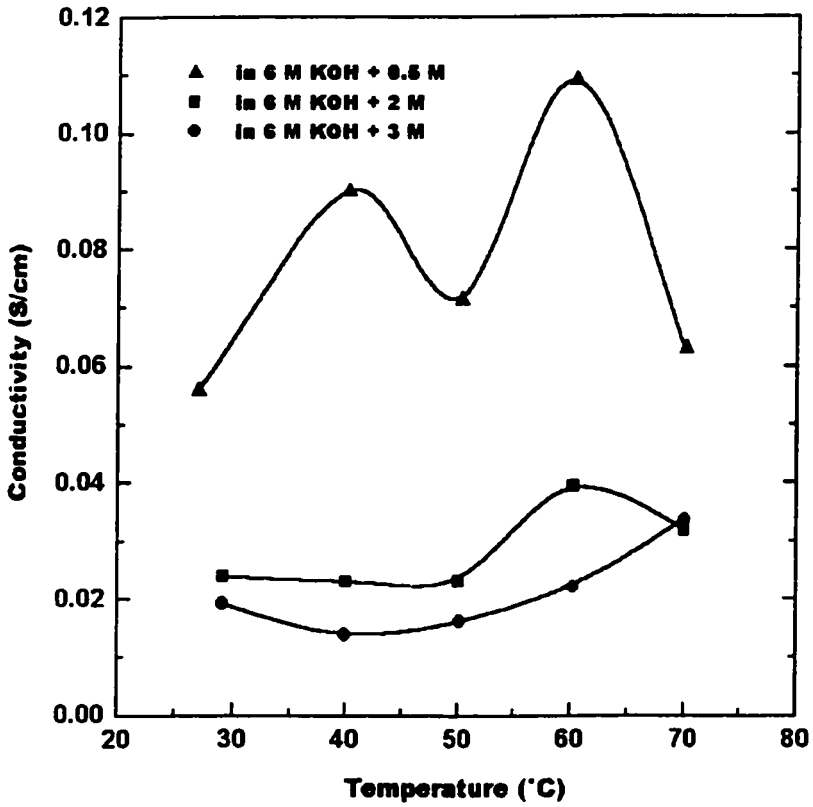

Figure 3.6. The variation of the conductivity of KOH + K_2CO_3 doped PBI with the temperature.

S/cm) over time is less than that observed for KOH-doped PBI. Similar results were obtained in the case of PBI doped in KOH + K_2CO_3 (Figure 3.6) where the conductivity is almost independent of temperature in the range of 30~70°C. This may indicate that the conduction mechanism in KOH doped PBI is different from that in KOH + K_2CO_3 .doped PBI and in H_3PO_4-doped PBI. Determination of the conduction mechanisms is currently being pursued.

3.5. Fuel-cell parameters

Figure 3.7 shows the potential-current polarisation curves of 6.25 cm^2 membrane electrode assemblies (MEA) obtained using a Globe station. The H_2 and O_2 gases were not humidified, the H_2/O_2 pressure ratio was 3/5 and the polarization curves were carried out at 50°C. As may be seen in Figure 3.7, the fuel cell based on the KOH doped PBI membrane exhibited 0.62 $A.cm^{-2}$ at 0.6 V. This value is similar to what we obtained on H_2/O_2 PEMFC based on the Nafion® 117 membrane [25]. Thus, H_2/O_2 PEMFC based on the KOH-doped PBI membrane performs as well as H_2/O_2 PEMFC based on the Nafion® 117 membranes.

4. Conclusion

Alkali-doped PBI exhibited high ionic conductivity (10^{-5}~9.5×10^{-2} S/cm). The highest conductivity was obtained on 6 M KOH-doped PBI. This conductivity is better than that previously obtained on acid doped PBI. In the presence of potassium carbonate, the conductivity of alkaline-doped PBI decreases. The performance of H_2/O_2 PEMFC based on the KOH-doped PBI was similar to that of H_2/O_2 PEMFC on Nafion® 117.

5. Future work

This work opens the way to a new approach to the modification of PBI for PEM fuel-cell application based on alkali-doped PBI, which will necessitate the development of these related aspects:

- Determination of the mechanism of ionic conductivity in alkali-doped PBI.

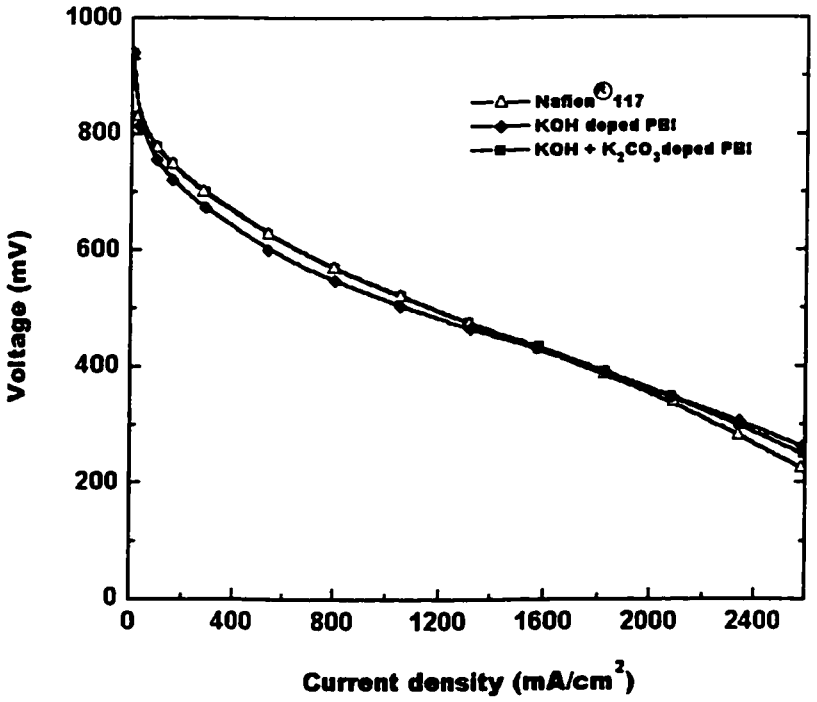

Figure 3.7. Potential-current polarization curves of H_2/O_2 fuel cells using KOH doped PBI (thickness = 40 μm) membrane, anode and cathode based on 0.35 mg Pt/cm^2 from 20% Pt/C catalysts, pressure cation H_2/O_2 = 3/5, gas flow rates O_2 = 0.8 L/min. H_2 = 1.2 L/min. For comparison the polarisation curves of H_2/O_2 fuel cells using Nafion® 117 membrane and KOH + K_2CO_3 doped PBI membrane.

Determination of the effect of alkali concentration on membrane water uptake.

- Determination of the chemical composition of alkali-doped PBI in various experimental conditions.
- Determination of the effect of modification of the doped membrane on water uptake.
- Development of PEMFCs based on these membranes.
- Application of this approach to the preparation of low-cost polymer electrolyte membranes.

6. References

[1] G.P. Schulman and W. Lochte, *J. Macromol. Sci. Chem.*, 1 (1967) 413.

[2] Y. Tsurm Y.L. Freilich and M. Levy, *J. Polym. Sci.*, 12 (1974) 1531.

[3] D.N. Gray, G.P. Schulman and R.T. Conley, *J. Macromol. Sci. Chem.*, 1 (1967) 395.

[4] Dale A. Chatfieleld, *J. Polym. Sci. Chem.*, 19 (1981) 601.

[5] M.B. Gieselman and J.R. Reynolds, *Macomolecules*, 26 (1993) 5633.

[6] P. Musto, F.E. Karasz and W.J. Macknight, *Polymer*, 34 (1993) 2934.

[7] D. Weng, J.S. Wainright, U. Landau and R.F. Savinell, *J. Electrochem. Soc.*, 143 (1996) 1260.

[8] O. Savadogo, *J. New Mat. Electrochem. Systems.*, 1 (1998) 47.

[9] H.A. Pohl and R.P. Chartoff, *J. Polym. Sci. Part A*, 2 (1964) 2787.

[10] S.M. Aharoni and M.H. Litt, *J. Polym. Sci. Polym. Chem. Ed.*, 12 (1974) 639.

[11] D. Hoel and E. Grunwald, *J. Phys. Chem.* 81 (1977) 2135.

[12] S.M. Aharoni and A.J. Signoreli, *J. Appl. Polym. Sci.*, 23 (1979) 2653.

[13] X. Glipa, M.E. Haddad, D.J. Jones, J. Rozière, *Solid State Ionics*, 97 (1997) 323.

[14] J.S. Wainright, J.T. Wang, D. Weng, R.F. Savinell, M. Litt, *J. Electrochem. Soc.*, 142 (1995) L121.

[15] S.R. Samms, S. Wasums and R.F. Savinell, J. *Electrochem. Soc.*, 143 (1996) 1225.

[16] D. Weng, J.S. Wainright, U. Landau and R.F. Savinell, *J. Electrochem. Soc.*, 143 (996) 1260.

[17] W.F. Lin, J.T. Wang and R.F. Savinell, *J. Electrochem. Soc.*, 144 (1997) 1917.

[18] J.S. Wainright, R.F. Savinell and M.H. Litt, in *"Proceedings of the Second International Symposium on New Materials for Fuel Cell and Modern Battery System"*, Eds. P. Savadogo and P.R. Roberge, Montreal, Canada, July 6-7, 1997, p. 808.

[19] J.T. Wang, J.S. Wainright, R.F. Savinell, M. Litt, *J. Appl. Electrochem.*, 26 (1996) 751.

[20] J.T. Wang, S. Wasmus and R.F. Savinell, *J. Electrochem. Soc.*, 143 (1996) 1233.

[21] S. Wasmus, J.T. Wang and R.F. Savinell, *J. Electrochem. Soc.*, 142 (1996) 3825.

[22] J. Wang, S. Wasmus and R.F. Savinell, *J. Electrochem. Soc.*, 142 (1995) 4218.

[23] J.T. Wang, R.F. Savinell, J. Wainright, M. Litt and H. Yu, *Electrochimica Acta*, 41 (1996) 193.

[24] B. Xing, O. Savadogo, J. New Mat. Electrochem. Syst., 2 (1999) 95.

[25] O. Savadogo and B. Xing, *J. New Mat. Electrochem. Syst.*, in press.

[26] R.S. Bogner, Electron Dyn. Div., Hughes Aicr. Co., Proc. Intersoc.

[27] CT, USA, Avail.NTIS, Nada [Contract. Rep.] CR (1978), NASA-CR-159653, FCR-1017, 73 pp. From: *Sci. Tech. Aerosp. Rep.* 1979, 17(24), Abstr. No. N79-33581. CODEN: NSCRAQ ISSN: 0565-7059.

[28] R.E. Martin, Power Syst. Div., United Technol. Corp., South Windsor, CT, USA, Avail. NTIS, NASA [Contract. Rep,] CR (1979), (NASA-CR-159807, FCR-1657), 52 pp. From: *Sci. Tech. Aerosp. Rep.* 1980, 18(10), Abstr. No. N80-19615. CODEN: NSCRAQ ISSN: 0565-7059.

[29] U.S. Pat. 5,71,038, B. Vyas, (Bell Telephone Laboratories) (Sept. 11, 1984).

[30] E. Gülzow, M. Schulze, G. Steinhilber, K. Bolwin, 1994, "*Fuel Cell Seminar*", San-Diego (CA), p. 319

[31] A. Al-Saleh, et al., in "*Alkaline Fuel Cell in the Presence of Carbon Dioxide Impurity in the Feed Gases*", Paper from the Chemical Engineering Department, King Fahd University of Petroleum and Minerals, Dhahran 31261, Saudi Arabia, 1992.

CHAPTER 4

HYDROGEN/OXYGEN POLYMER ELECTROLYTE MEMBRANE FUEL CELL (PEMFC) BASED ON ACID-DOPED POLYBENZIMIDAZOLE (PBI)

O. Savadogo and B. Xing

Laboratoire d'électrochimie et de matériaux énergétiques

École Polytechnique de Montréal

C.P. 6079, Succ. Centre-Ville

Montréal, Qc, H3C 3A7

Canada

(Published in *J. New Mat. Electochem. Syst.* 3, 2000, p343-347)

Abstract

The potential-current characteristics of a H_2/O_2 polymer electrolyte membrane fuel cell using H_2SO_4 or H_3PO_4 doped PBI were studied for the first time. The conditions involved in the doping of PBI with sulphuric acid or phosphoric acid and the preparation of a membrane electrode assembly (MEA) using these membranes were determined. The potential-current fuel-cell characteristics of MEAs using H_2SO_4-doped PBI were compared to those of MEAs using Nafion® 117. The effects of membrane doping and of drying times on the fuel-cell performances of MEAs based on PBI doped with sulphuric acid in various conditions were determined. It was shown that MEAs based on H_2SO_4 doped PBI and non-humidified exhibited higher fuel-cell characteristics than MEAs based on Nafion® 17. The fuel-cell characteristics of MEAs based on phosphoric-acid-doped PBI exhibited high performances at 185 °C even with fuelled with hydrogen containing 3% CO.

Key words: Sulphuric-acid-doped PBI, phosphoric-acid-doped PBI, non-humidified PBI membrane, improved H_2/O_2 PEMFC, resistance to 3%CO poisoning.

1. Introduction

During recent years, a great deal of efforts has been expended in the development of perfluorinated [1-5], partially perfluorinated [2-10] and non-perfluorinated [2, 4, 11-18] membranes for solid polymer electrolyte fuel cell. The long-term stability of Nafion®, Asahi® and Dow® perfluorinated membranes have proven to more than 20 000 hours but their high cost (~ 700$/m^2), worse performance at high temperatures (≥ 100°C) in H_2/O_2 or methanol/O_2 fuel cells may limit their use in the mass production of fuel cells. From the various partially-perfluorinated membranes, e.g. styrene-grafted and sulphonated membranes based on partially fluorinated poly(tetra-fluoroethyene-co-hexafluoropropylene) or poly(ethylene-alt-tetrafluoro-ethylene) [19-26] and sulphonated copolymers incorporating α, β, β-trifluorostyrene [2-4] (referred to a BAM3G), it was shown that in fuel cells, the BAM3G membrane exhibited performances superior to those of both the Nafion® and the Dow® membranes at currents above 600 A/ft^2.

Several non-fluorinated ionomer membranes have also been studied [2-4, 11-18,27,28]. As a result, membranes based on poly(phenylquinoxaline) [2-4], poly (2,6 diphenyl-4-phenulene oxide) polymers [2-4], acid-doped polybenzimidazole [12, 28] , polyimides [13], the styrene/ethylene-butadiene/styrene triblock copolymer [14] and the polyether ether ketone [16] are all under active investigation by groups worldwide. Up to now, no membranes based on non-fluorinated polymers have been used in practical fuel cell systems designed for long-term operation. Very recently, we have developed synthesised Nafion® with silicotungstic-based membranes for fuel cell applications. We have also developed a polybenzimidazole membrane doped with various acid electrolytes for fuel cell applications [28]. The aim of this paper is to present the study of polymer electrolyte membrane fuel cells based on H_2SO_4 or H_3PO_4 doped PBI.

2. Experimental

2.1. PBI membrane preparation

PBI film of 40μm thick was purchased from Hoechst Celanese. The film was cut into small square samples measuring 3×3 cm^2. The samples were washed in boiling deioned water for more than 6 hours to remove the LiCl impurities. These blank samples were kept in water. The samples were doped with sulphuric acid or phosphoric acid by immersing them into the acid solution in a glass beaker for varying number of days. The concentration of sulphuric acid or phosphoric acid was in the 8-16 M range for sulphuric acid and the 1-16 M range for phosphoric acid.

2.2. Fuel cell performance evaluation

For the solid polymer electrolyte fuel cell performance evaluation, an anode, a cathode and a reference electrode of 10% Pt/C from E-Tech were hot-pressed onto each PBI (sulphuric-acid- or phosphoric-acid-doped) membrane at 80°C under 4.8×10^3 kPa of pressure for 4 minutes. The total Pt catalyst loading was 0.4 $mg.cm^{-2}$. The electrode (anode and cathode) surface area was 6.25 cm^2. The resulting membrane electrode assembly (MEA) was incorporated into a single test fixture. The cell was then installed in a BC-60 fuel cell station from Globe Teck. The single-cell test was run at a H_2/O_2 pressure ratio of 1/1 atm at various cell temperatures. No specific hydration of the membranes was achieved before polarisation. The cell voltage versus current density curves of the fuel-cell-based on H_2SO_4-PBI or H_3PO_4-doped PBI then recorded.

3. Results and discussion

3.1. Sulphuric acid doped PBI membrane

Figure 4.1 shows the potential-current polarisation curves of 6.25 cm^2 membrane electrode assemblies (MEAs) obtained using the BC-60 Globe Teck station. The MEAs were based on a 0.40 mg Pt/cm^{-2} catalyst and various concentrations of H_2SO_4-doped PBI membranes. The reproducibility of the potential-current curve of the MEAs prepared in this laboratory is better than 15 mV at cell voltages of 0.6 V. Each PBI membrane was

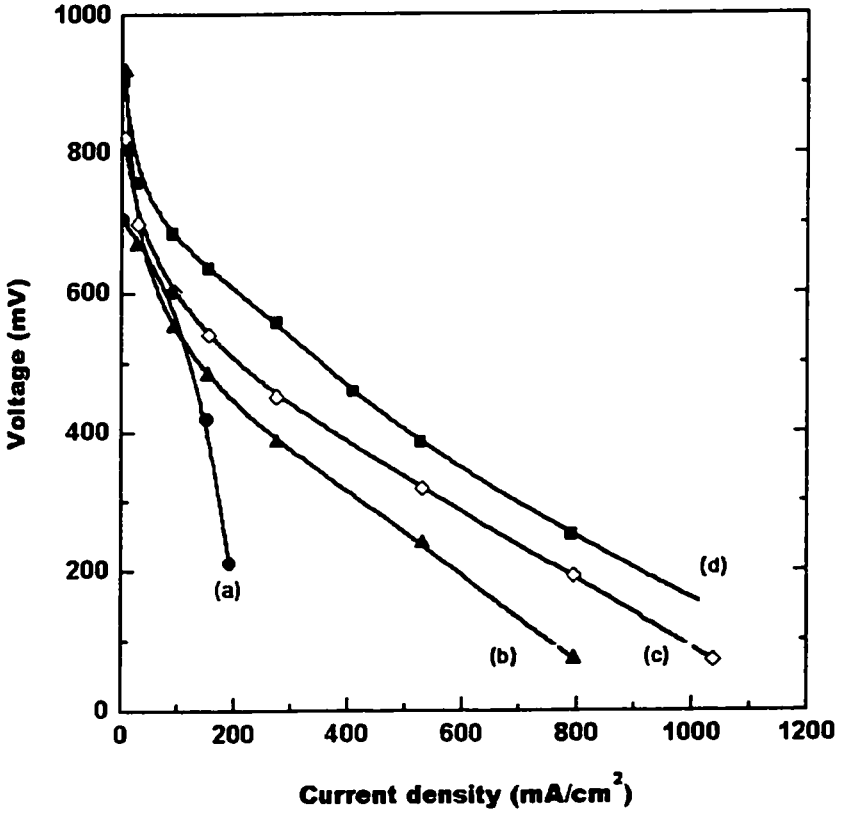

Figure 4.1. Fuel cell polarisation curves of MEAs at 50 °C based on PBI doped in different concentrations of sulphuric acids and dried in air for less than one week: (a) PBI doped in 16M H_2SO_4 and dried in air for one week; (b) PBI doped in 8M H_2SO_4 and dried in air for one day; (c) PBI doped in 10M H_2SO_4 and dried in air for one day; (d) PBI doped in 12M H_2SO_4 and dried in air for one day.

doped in the sulphuric acid solution for seven days and dried in air for one day. As may be seen in Figure 4.1, the potential-current polarization curves were improved when the doping acid concentration increased from 8 M to 12 M. For MEAs based on higher concentration of H_2SO_4-doped PBI (16 M H_2SO_4) and dried in the same conditions, the polarisation curves are not shown since it was not possible to obtain reliable data from them. However their curves were lower than those obtained using MEAs based on PBI doped with 8M to 12M of H_2SO_4. Figure 4.1 shows that, even for MEAs based on PBI doped with 16 M H_2SO_4 and dried for seven days (named MEA0), the polarisation curves were less efficient than those of MEAs based on PBI doped with 8M to 12M of H_2SO_4. This indicates that the change in the difference in the polarization curve characteristics observed in Figure 4.1 may not be related only to the variation in the conductivity of H_2SO_4-doped PBI since the best characteristics are not obtained with H_2SO_4-doped PBI membranes which exhibited the highest ionic conductivity. We have shown previously that the highest bulk ionic conductivity (0.06 S/cm) of H_2SO_4-doped PBI was obtained with 16M H_2SO_4-doped PBI, whereas the conductivity of H_2SO_4-doped PBI changes slightly from 3.6×10^{-3} to 8×10^{-3} when the acid concentration ranges from 8M to 12M [28]. The better polarisation curves obtained with 8M to 12M sulphuric-acid-doped PBI may be related to a synergetic effect between the membrane's bulk conductivity and the drying conditions. This is supported by the fuel cell polarisation curve of MEA based on PBI doped with 16M H_2SO_4 for more than seven days and dried in air for a long time (more than seven days) (Figure 4.2). For comparison, the fuel cell polarisation curves of MEA based on Nafion® 117 membrane and 16M H_2SO_4-doped PBI dried in air for seven days are also indicated. As may be seen, the polarisation curve of the fuel cells based on the 16M H_2SO_4-doped PBI membrane and dried for a long period of time (named MEA1) exhibited better characteristics than the MEA based on Nafion® 117 (named MEA2). With the same open-circuit potential and in the same activation regions of the polarisation curve, MEA1 and MEA2 exhibited almost the same characteristics. This is not the case for the region of high current density (mass transport region), where MEA1 exhibited better characteristics than MEA2. This might be due to better water

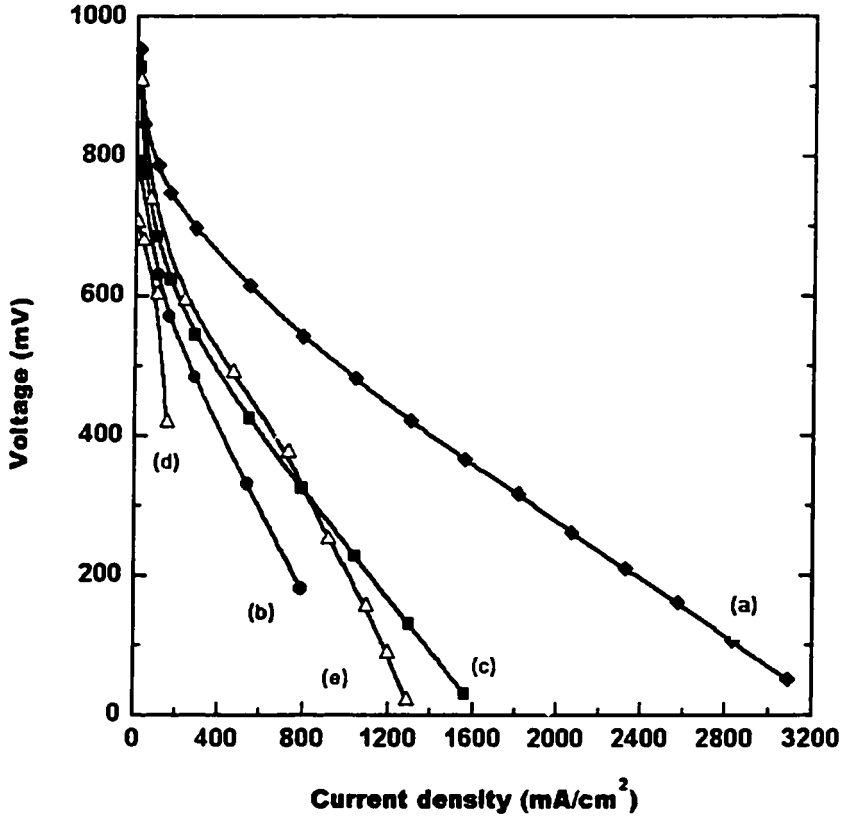

Figure 4.2. Fuel Cell polarization curves of MEAs at various operating temperatures based on 16M H_2SO_4 doped PBI: (a) 50 °C with 16M H_2SO_4 doped PBI and dried in air for a long period of time (more than seven days); (b) 50 °C with 16M H_2SO_4-doped PBI and dried in air for seven days; (c) 30 °C with 16M H_2SO_4 doped PBI and dried in air for seven days; (d) 70 °C with 16M H_2SO_4 doped PBI and dried in air for seven days; (e) 70 °C with 16M H_2SO_4 doped PBI and dried in air for a long time (more than seven days).

management in MEA1 based on a sulphuric-acid-doped PBI membrane dried over a longer period of time. These results indicate that the membrane and the MEA preparation conditions are key factors in fuel cell performance. This is supported by the following results. The characteristics of fuel cells recorded at various temperatures using PBI doped with 16 M H_2SO_4 and dried for seven days (MEA0) increase in the order 70°C < 50°C < 30°C (Figure 4.2). The best characteristics obtained at lower temperature may indicate that the rate of dehydration of the membrane increases with cell temperature. However MEAs based on long doping and drying times (MEA1) exhibited better fuel cell characteristics than those based on short doping and drying times (MEA0). On the other hand, Figure 4.3 shows that the fuel cell characteristics using MEA1 change with the conditioning time of the MEA. The MEA was conditioned by applying a constant current density of 6.4 mA/cm^2 for different periods of times before the potential-current polarisation curves were recorded. It was found that the fuel cell characteristics did not change when the current density of 6.4 mA/cm^2 was applied to the MEA for less than 30 minutes before fuel cell characteristic curves were recorded. We can see in Figure 4.3 that, when the current density of 6.4 mA/cm^2 applied to the MEA 125 minutes before the fuel cell characteristics were recorded, the polarisation curve decreases significantly. When the fuel cell was operated with a MEA which had not previously been conditioned at 6.4 mA/cm^2, no significant decrease in its characteristics was observed after several polarisation curves had been recorded over a period of more than two hours (Figure 4.4).

3.2. Phosphoric –acid-doped PBI membrane

Figure 4.5 shows the polarisation curves of MEAs based on PBI doped with H_3PO_4 at between 50 and 185°C for more than 7 days and dried for a long period time (more than 7 days). The curves show for the first time that phosphoric-acid-doped PBI can also be used in hydrogen/oxygen fuel cell at high temperatures. It can be seen that the characteristic performances increase with the temperature. We can also see in Figure 4.6 that, at 185°C, the presence of 3% CO has no effect on the fuel cell polarisation curves. The suppression of the carbon monoxide poisoning effect at high temperatures (>150°C)

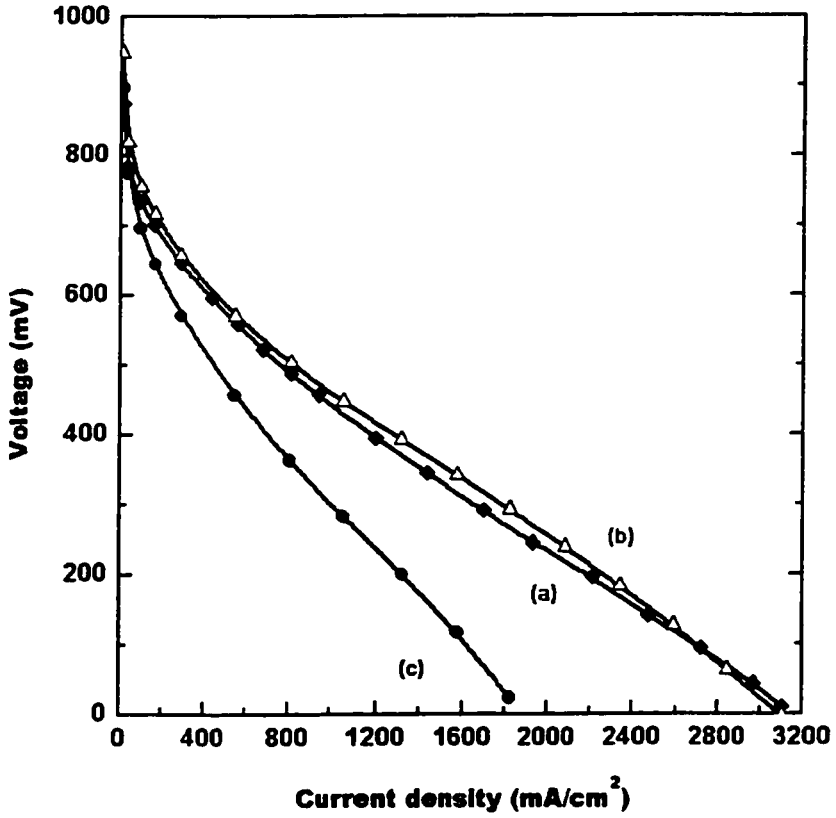

Figure 4.3. Change in fuel cell polarisation curves with the conditioning* time of the MEAs at 50 °C based on 16M H_2SO_4-doped PBI and dried in air for a long period of time more than seven days): (a) without conditioning; (b) after conditioning for 32 minutes; (c) after conditioning for 125 minutes. *The MEAs conditioning consisted applying a current density of 6.4 mA/cm^2 before recording the fuel cell polarization curves.

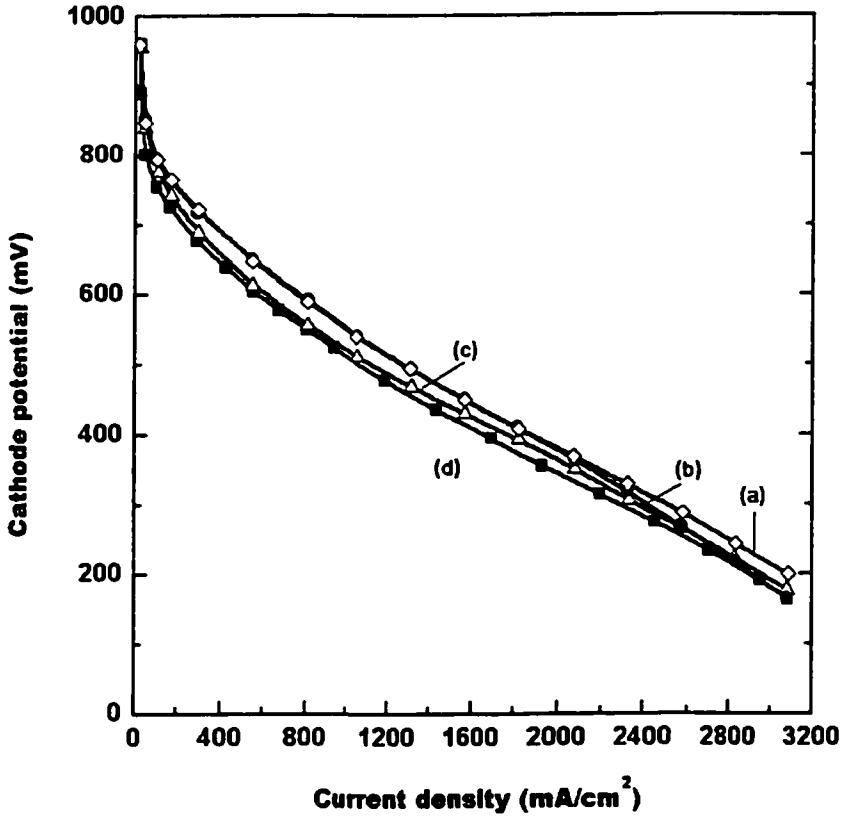

Figure 4.4. Change in fuel cell polarisation curves of MEAs at 50°C without conditioning and based on 16M H_2SO_4 doped PBI and dried in air for a long period of time (more than seven days): (a) first curve; (b) After 30 min; (c) After 1 hr; (d) after 1 h and 30 min.

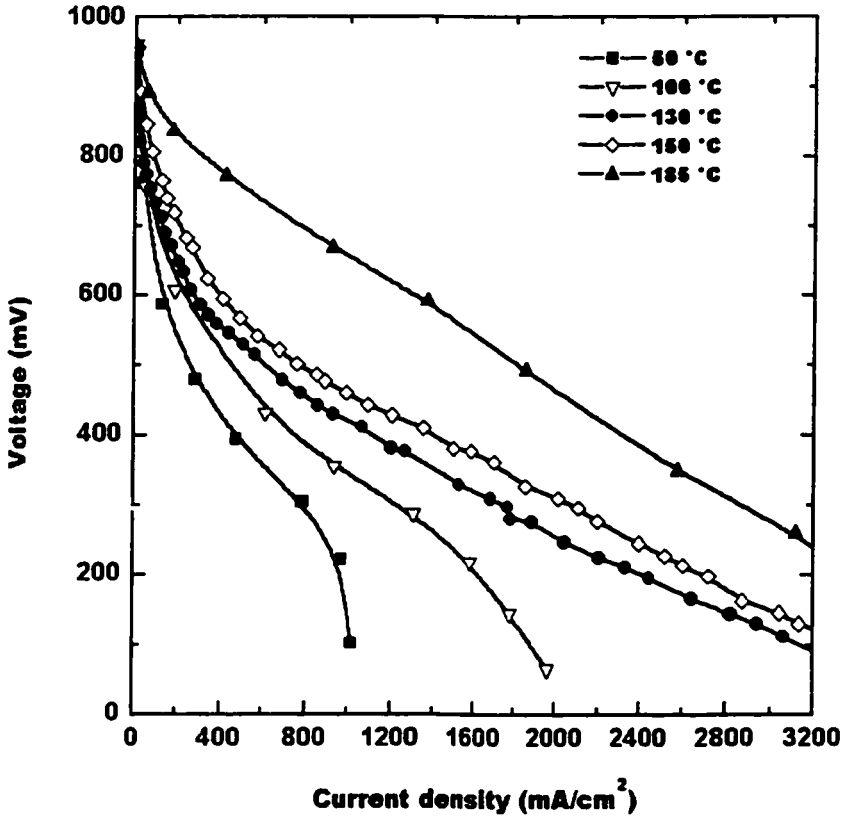

Figure 4.5. Fuel cell polarisation curves of MEAs based on phosphoric-acid-doped PBI and dried in air for a long period of time (more than seven days) at various temperatures. The fuel cell was fed with hydrogen/oxygen with a gas flow rate of 0.8L/min for oxygen and 1.2 L/min for hydrogen and at atmospheric pressure.

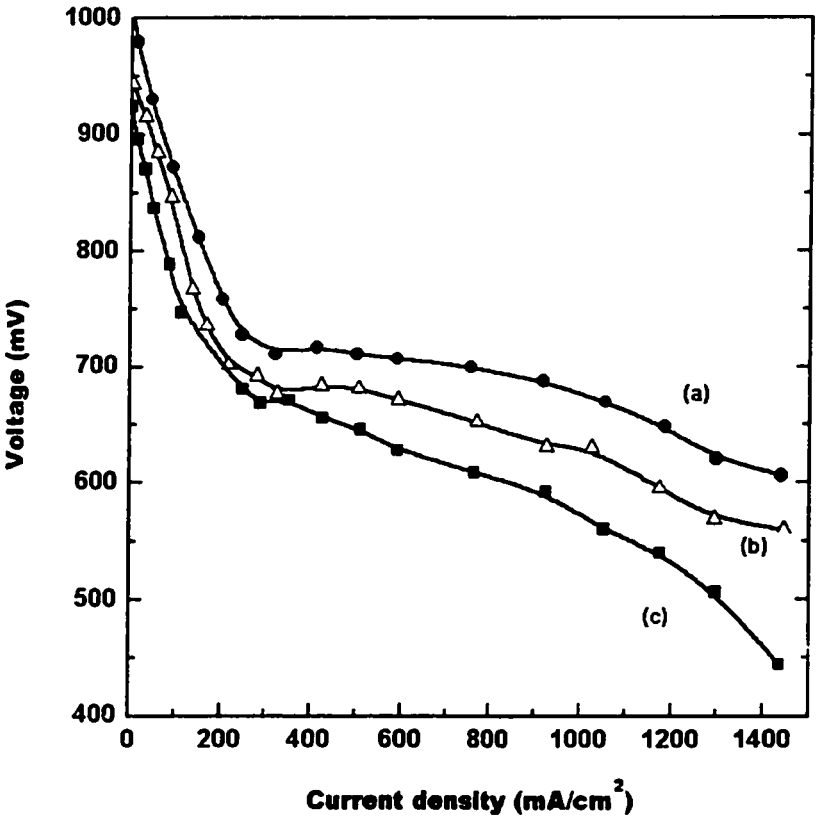

Figure 4.6. Fuel cell polarisation curves of MEAs at 185°C based on phosphoric-acid-doped PBI. The fuel cell was fed with H_2/O_2 at a gas flow rate of 0.8 L/min for O_2 and 1.2 L/min for H_2 and at atmospheric pressure. The hydrogen contained between 100 ppm and 3% by volume of CO: (a) 100% H_2; (b) H_2+100 ppm CO; (c) H_2+3%CO.

indicates that this effect is related to competition between the CO and the H_2 for surface active sites. At lower temperatures (< 150°C), CO may block the surface active sites for the hydrogen oxidation. This is an indication that acid-doped PBI membranes can be used in impure hydrogen containing CO.

4. Conclusions

The aims of this work were: i) to modify PBI films by doping them in acid solutions (sulphuric acid or phosphoric acid); ii) to determine the fuel cell polarisation curves of MEAs based on sulphuric-acid-doped and phosphoric-acid-doped PBI membranes; and iii) to determine the poisoning effect of CO on fuel cell based on a phosphoric-acid-doped PBI membrane operating at a temperature higher than 150 °C. From the results reported here, it may be concluded that:

- The experimental conditions of acid concentration and doping time for the modification of PBI membranes for PEMFCs have been determined.
- The fuel cell polarisation curves obtained on MEAs based on sulphuric-acid-doped PBI are better than those obtained on Nafion® 117.
- The increase in operating temperature from 50 °C to 185 °C significantly improves the polarisation curves of fuel cells based on phosphoric-acid-doped PBI. At atmospheric pressure and 185 °C, the optimum power output of 650 mW/cm^2 was obtained at 1500 mA/cm^2.
- At 185°C and atmospheric pressure the hydrogen/oxygen fuel cell polarisation curves based on phosphoric-acid-doped PBI are not affected by hydrogen fuel containing 100 ppm and 3% CO.

5. Future work

This work opens the way to a new approach to the modification of PBI membranes for PEM fuel cell fuelled with impure hydrogen for use in portable electrical vehicles and in stationary applications, which will necessitate the development of the following related aspects:

- Determination of the relation between membrane doping conditions, water uptake, conductivity, mechanical strength, electro-osmotic drag coefficient and fuel cell performances;
- Determination of the optimum concentration of CO in hydrogen that will not trigger the CO poisoning effect on fuel cell characteristics;
- Determination of the long-term stability of fuel cell characteristics;
- Use of this approach to develop new low-cost polymer electrolyte membranes.

6. References

[1] W. G. Grot, *Macromolecular Symposium*, 82, 161 (1994)

[2] A. E. Steck, in *"Proceedings of the First International Symposium on New Materials for Fuel-Cell Systems"*, Eds. O. Savadogo, P. R. Roberge and T. N. Veziroglu, Montréal, Canada, July 9-13, 1995, p. 74.

[3] A. E. Steck, in *"Proceedings of the Second International Symposium on New Materials for Fuel-Cell and Modern Battery Systems"*, Eds. O. Savadogo and P. R. Roberge, Montréal, Canada, July 6-10, 1997, p. 792.

[4] O. Savadogo, *J. New Mat. Electrochem. Systems*, 1, 47 (1998)

[5] B.Tazi and O. Savadogo, *Electrochim. Acta*, (in press, 2000)

[6] R. B. Hodgdon, J. F. Enos, E. J. Aiken, US Patent 3,341,366 (1967)

[7] J. Wei, C. Stone and A. E. Steck, U.S. Patent No. 5,422,411 (1995).

[8] D. Agostino, U.S. Patent No. 4,012,303 (1977).

[9] O. Hass, H. P. Brack, F. N. Buchi, B. Gupta and G. G. Scherer in *"Proceedings of the Second International Symposium on New Materials for Fuel-Cell and Modern Battery Systems"*, Eds. O. Savadogo and P. R. Roberge, Montréal, Canada, July 6-10, 1997, p. 836.

[10] S. Hietala, M. Koel, E. Skou, M. Elomaa and F. Sundholm, *J. Mater. Chem.* 8, (1998) 1127.

[11] J. Kerres, W. Cui, G. Eigenberger, D. Bevers, W. Schnurnberger, A. Fisher and H. Wendt, in *"Proceedings of the 11th Hydrogen Conference"*, Eds. T. N.

Veziroglu, C. J. Winter, J. P. Baselt and G. Kreysa, Stuttgart, Germany, June 23-28, 1996, p. 1951.

[12] J. S. Wainright, R. F. Savinell and M. H. Litt, in *"Proceedings of the Second International Symposium on New Materials for Fuel Cell and Modern Battery Systems"*, Eds. O. Savadogo and P. R. Roberge, Montréal, Canada, July 6-10, 1997, p. 808.

[13] S. Faure, N. Cornet, G. Gebel, R. Mercier, M. Pineri and B. Sillon, in *"Proceedings of the Second International Symposium on New Materials for Fuel Cell and Modern Battery Systems"*, Eds. O. Savadogo and P. R. Roberge, Montréal, Canada, July 6-10, 1997, p. 818.

[14] E. Zador and G. E. Wnek, in *"Proceedings of the Second International Symposium on New Materials for Fuel Cell and Modern Battery Systems"*, Eds. O. Savadogo and P. R. Roberge, Montréal, Canada, July 6-10, 1997, p. 828.

[15] J. Kerres, W. Cui, W. Neubrand, S. Springer, S. Reichle, B. Striegel, G. Eigenberger, W. Schnurnberger, D. Bevers, N. Wagner and K. Bolwin, in *"Proceedings Book, Euromembrane 92 Congress"*, Bath, UK, Sept. 18-20, 1995, p. 1.284.

[16] A. Schmeller, H. Ritter, K. Ledjeff, R. Nolte and R. Thorwirth, EP. 0574791 A2 (1993).

[17] C. Poinsignon, presented at the *"First International Symposium on New Materials for Fuel Cell Systems"*, Montréal, Canada, July 9-13, 1995, Poster No 29.

[18] W. Wieczorek, Z. Florjanczyk and J. R. Stevens, *Eletrochim. Acta*, 40, (1995) 2327.

[19] Burnett, U.S. Patent No 4,506,035 (1985).

[20] G. Scherer, Ber. Bunsenges, *Phys. Chem.*, 94, (1990) 1008.

[21] G. Scherer, F. N. Buchi and B. Gupta, *Polym. Mater. Sci. Eng.*, 68, (1993) 114.

[22] B. Gupta, F. N. Buchi and G. G. Scherer, *Solid State Ionics*, 61, (1993) 213.

[23] T. Lehtinen, G. Sundholm, S. Holmberg, F. Sundholm, P. Björnbom and M. Bursell, *Electrochim. Acta*, 43, (1998) 1991.

[24] M. Paranen, F. Sundholm, E. Ranhala, T. Lehtinen and S. Heitala, *J. Mat. Chem.*, 7, (1997) 2401.

[25] D. I. Ostrovskü, L. M. Torell, M. Paronen, S. Heitala and F. Sundholm, *Solid State Ionics*, 97, (1997) 315.

[26] S. Heitala, S. Holmberg, M. Karjalainen, J. Näsman, M. Paronen, R. Senmaa, F. Sundholm and S. Vahvaselka, *J. Mat. Chem.*, 7, (1997) 721.

[27] H. A. Liebhabsky, E. J. Cairns, *Fuel-Cells and Fuel Batteries*, New York, 1968.

[28] B. Xing and O. Savadogo, J. New Mat. Electrochem. Systems, 2, 95(1999)

CHAPTER 5

THE MASS TRANSPORT PROPERTIES OF POLYBENZIMIDAZOLE (PBI) IN ALKALINE SOLUTION

Baozhong Xing and O. Savadogo

Laboratoire d'Électrochimie et de Matériaux Énergétiques

École Polytechnique de Montréal

C.P. 6079, Succ. Centre-Ville

Montréal, Québec, H3C 3A7

Canada

(To be published)

Abstract

To establish the ionic conductivity mechanism in alkali doped PBI the mass transport properties of PBI in alkaline solution were studied. The transference number of ions, the permeability of the alkalis and water, and the water electro-osmotic drag coefficient are determined in different kinds of alkali solutions. The effects of alkaline type and concentration on the above parameters are discussed.

1. Introduction

Electrolyte plays an important role in electrochemical systems because electrolyte has significant effect on the system performance. Different electrolytes provide various environments for electrode reactions. In fuel cells and batteries, solid polymer electrolyte has many advantages. For example, it is solid, compact and simple; it provides high current density; it can run at low temperature (<-40 °C). These advantages make solid polymer electrolyte suitable for portable power source and for driving cars or buses.

The most successful acid type solid polymer electrolyte is Nafion® membrane, a sulphonated perfluoropolyethylene polymer. However, the high price limits its use. PBI is much cheaper than Nafion® and has many superior properties. It has excellent mechanical properties, and excellent thermo and chemical stability [2-7]. Hydrogen has lower permeability in PBI than Nafion® [8-9]. Pure PBI is not ionic and electric conductive [10-14]. After doped with acid and alkali, PBI becomes a good ionic conductor and still remains to be electric insulator [1, 10, 15-24]. The acid doped PBI exhibits the same ionic conductivity as Nafion® [1, 10].

PBI has been used as solid electrolyte in alkaline fuel cells and alkaline batteries. They have high power output and long life [25, 26, 27, 28]. Experimental results on alkali doped PBI showed that it exhibits performance in fuel cell as good as both Nafion® and acid doped PBI [1]. Base type solid polymer electrolytes are more preferred than acid type under some conditions. Therefore, alkali doped PBI is a hopeful candidate for solid polymer electrolyte used in electrochemical systems. The knowledge in the conductivity mechanism, mass transport properties, ion transference numbers, diffusion coefficients and water electro-osmotic drag coefficient in alkali doped PBI membrane is essential to optimize the doping conditions and to increase the conductivity of alkali doped PBI.

The objective of this work is to study the mass transport properties of alkali doped PBI. Accordingly the ion transference number, water electro-drag coefficient, alkali and water diffusion coefficients will be measured in alkaline solution under different conditions.

2. Fundamentals

2.1. Diffusion coefficient and permeability coefficient

Different molecules or ions have different diffusion coefficients in a polymer, which render the polymer the selective permeation to different molecules or ions. The diffusion coefficient of a substance changes with its concentration sorbed in the polymer. Therefore, the selectivity of the polymer membrane is concentration dependent.

The diffusion of molecules or ions through polymers follows the first Fick's law. At steady state, first Fick's law is expressed as

$$J = -D\frac{dC}{dx} = consant \quad (1)$$

where J is the flux (transport current); D is diffusion coefficient; C is the concentration of diffusion species in the polymer; x is the distance of diffusion. If the flux and concentration gradient are known, the diffusion coefficient can be evaluated directly.

In liquid (gas)-solid diffusion system, the concentration of the penetrant (ions or molecules) in the solid phase is difficult to measure. In liquid-solid sorption system, Nernst distribution law is used to relate the concentration of penetrant inside the solid phase to the concentration in liquid. According to Nernst distribution law, the concentration of penetrant in polymer (C_{poly}) is proportional to the concentration of penetrant in solution (C) under equilibrium condition, $C_{poly}=k_DC$. Therefore, Fick's law at steady state can be written as:

$$J = Dk_D\frac{\Delta C}{l} \quad (2)$$

where l is the thickness of polymer membrane; k_D is distribution constant; ΔC is concentration difference on the two sides of the membrane. One constant P can be used to substitute Dk_D, $P=Dk_D$. P is defined as permeability coefficient.

P has the similar physical meaning as D. P is affected by k_D. Distribution constant k_D is a thermodynamic parameter that measures the amount of penetrant sorbed by the membrane under equilibrium conditions. In high concentration solution k_D is almost always concentration-dependent as in Langmuir's sorption and dual-mode sorption [29]. In contrast, the diffusion coefficient D is a kinetic parameter that measures the rate of a penetrant being transported through the membrane. Diffusivity is dependent on the geometry of the penetrant. As the molecular size increases the diffusion coefficient decreases. The diffusivity also increases with the increase of penetrant concentration in

membrane. The concentration of penetrant in the membrane can be measured from sorption isotherms.

Diffusion coefficient of an ideal system can be measured by time-lag method. The membrane is located between two chambers. One of chambers is empty or in vacuum. Another one is filled with the penetrant. The membrane is free of penetrant at the start of the experiment. The amount of penetrant (Q_t) passing through the membrane increases with the time t. At beginning the increasing rate increase with time. After a certain period of time the increasing rate becomes constant, e.g., the amount of penetrant passed through the membrane increases linearly with time. By extrapolating the linear part, the intersection on time axis is obtained. The intersection is defined as time-lag which is the time needed for the penetrant to pass through the membrane. The slope is the permeation rate.

The classical lag-time method cannot be used for measuring diffusion coefficients in the case of Langmuir or dual mode sorption. The lag-time method measurement results in a longer diffusion lag time due to the occurrence of the Langmuir sorption. Paul [30] modified the lag-time method and developed a model based on total immobilization of the sorbed penetrant. Later Petropoulos [31] and Paul [32-33] developed models that assume only partial immobilization of the sorbed penetrant in Langmuir mode. Paul assumed that D (diffusion coefficient of total mobile penetrant) is constant. The Paul model is mathematically identical to the diffusion concentration dependency approach when D_{eff} is considered [33]. For the case of partly mobile Langmuir sorption, the concentration dependence of the permeability coefficients in the Paul model can be expressed as:

$$P = Dk_D(1+\frac{FK}{1+bC}) \tag{3}$$

where $K=C'_Hb/k_D$, $F=D_H/D_D$, k_D is Nernst partition coefficient.

Applying transport law, this model led to a D_{eff} [32] that is concentration dependent:

$$D_{eff} = D\frac{1+\dfrac{FK}{(1+\alpha C_D)^2}}{1+\dfrac{K}{(1+\alpha C_D)^2}} \tag{4}$$

where $\alpha=b/k_D$.

The dependence of permeability coefficient on the concentration of penetrants is determined by measuring the average permeability coefficient with two solutions composed of same substances and different concentrations for certain time. The permeability coefficient is calculated from mass balance and equation 2.

2.2. Transference number

When an electric current passes through a solution of an electrolyte, the various ions present carry different proportions of the current. These proportions are called transference numbers of the ions. The transference number, t_+, of the positive ion of a binary electrolyte is expressed as:

$$t_+ = \frac{\text{The charge transfered by cation}}{\text{The total charge transfered}} = \frac{z_+U_+}{z_+U_+ + z_-U_-} \tag{6}$$

where z_+, z_- are charge numbers of the ions, U_+, and U_- are the mobility of ions. If there are only two species of ions in the alkali doped PBI membrane with the same absolute number of charges (OH^- and K^+, Na^+ or Li^+), the transference number of cation, t_+, is expected to be:

$$t_+ = \frac{U_+}{U_+ + U_-}$$

From the transference number the conductivity mechanism can be understood.

The transference number can be measured by mass balance when a constant current is passed through the membrane for a certain time.

2.3. Osmotic drag and electro-osmotic drag coefficient

When ions move they usually drag some water molecules with them. Different ion drags different amount of water. If the drag is due to pure diffusion, the phenomenon is an osmotic drag. When current is passing through the membrane the process is electro-osmotic drag. From the mass balance in permeability and transference number measurement process the osmotic and electro-osmotic drag coefficient can be determined.

3. Experimental

The PBI film with a thickness of 40 μm was purchased from Hoechest Celanese. The film was cut into small square samples of 3×3 cm^2. The samples were washed in deionized boiling water to remove the LiCl impurities. These blank samples were kept in water. The samples were doped by immersing them into the alkaline solution in a conductivity measurement cell for a controlled period of time. The conductivity was measured at different doping times. The measurement was achieved in doping solution using classical two-point probe with home made conductivity measurement cell as shown in Figure 5.1 [34].

The transference number, permeability, and water osmotic and electro-osmotic drag coefficient were measured in the cell as shown in Figure 5.1. When measuring the transference number and electro-osmotic drag coefficient there were electrodes and current passing through them. When measuring permeability and water osmotic drag coefficient there was no electrode.

When measuring the permeability of alkali and water the concentrations of the solutions in the two sides of the membrane are different. The concentration of the solution will change with time. The concentration change is measured by titration. The permeability coefficient of alkali and water can be determined from these concentration changes using equation 3.

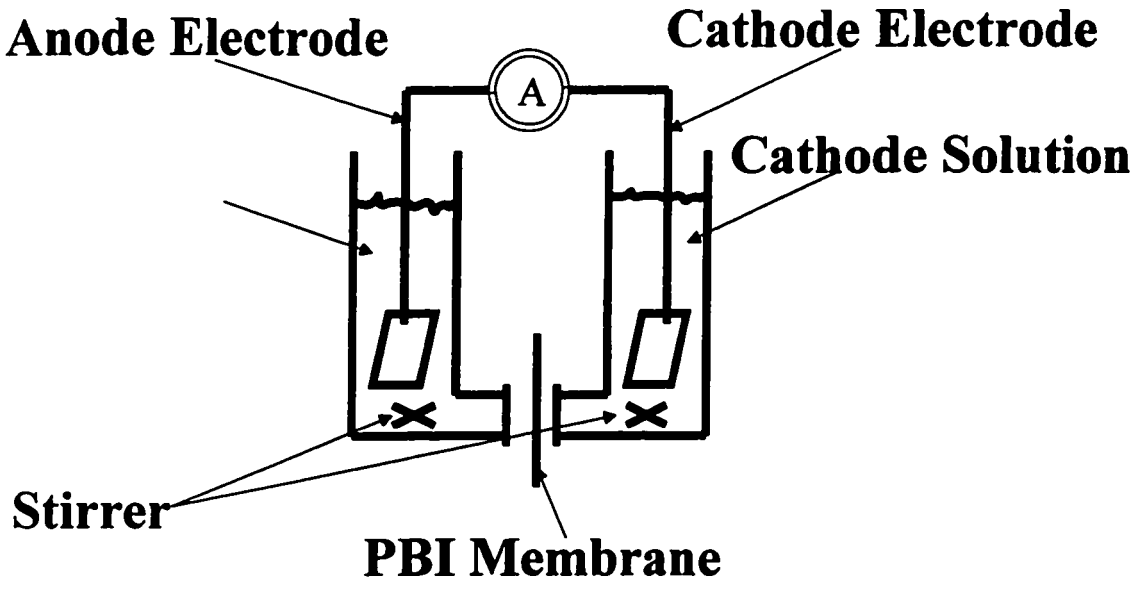

Figure 5.1. Transference number and permeability measurement cell

When measuring the ion transference number and water electro-osmotic drag coefficient, a constant current passes the membrane between the electrodes. The solutions on both sides of the membrane have same concentration. The concentration change is measured by titration. The transference number of ions and the water drag coefficient are determined according to equation 6 and the mass balance from these changes after considering the diffusion effects.

4. Results and discussion

4.1. Permeability coefficient of alkali and water in PBI

The permeability coefficient of alkali and water is calculated from the mass balance at the beginning of the experiment and after some time of diffusion. To calculate the permeability coefficient of water, the concentration of water in alkaline solution must be determined. The concentration of water (in KOH, NaOH, or LiOH solution) can be calculated from the specific density of the solution and the alkali concentration [35]. The concentration relationships between water and KOH, NaOH or LiOH are shown in Figure 5.2-5.4.

4.1.1 KOH

The permeability coefficient of KOH and water is shown in Figure 5.5. The concentration in Figure 5.5 is the average of the two concentrations on both sides of the membrane (the same applies to the case of NaOH and LiOH). The permeability coefficient of KOH is concentration dependent. It has a maximum of 6.2×10^{-11} m^2/s between 2.5 to 7 M. Below 2.5 M the permeability coefficient is a little bit lower than the maximum. Above 7 M it decreases significantly. At 13 M the permeability coefficient is only one sixth of the maximum. The shape of the curve is similar to the curve of conductivity vs. concentration [1]. The conductivity has a maximum at 6 M. However the curve of conductivity is shaper around the maximum point. This is because the concentration in Figure 5.6 is an average concentration. The permeability coefficient of water is also concentration dependent either. It has a small plateau (4.5×10^{-10} m^2/s) at low concentration. Above this

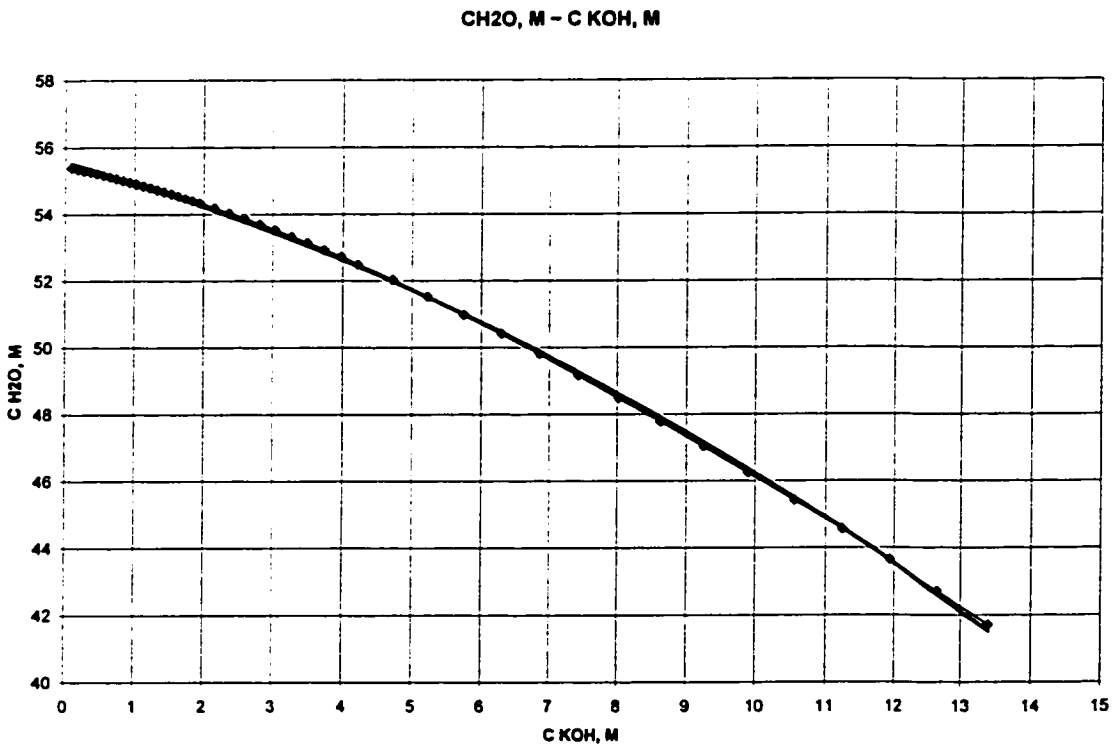

Figure 5.2. The concentration relationship of water and KOH in KOH solution

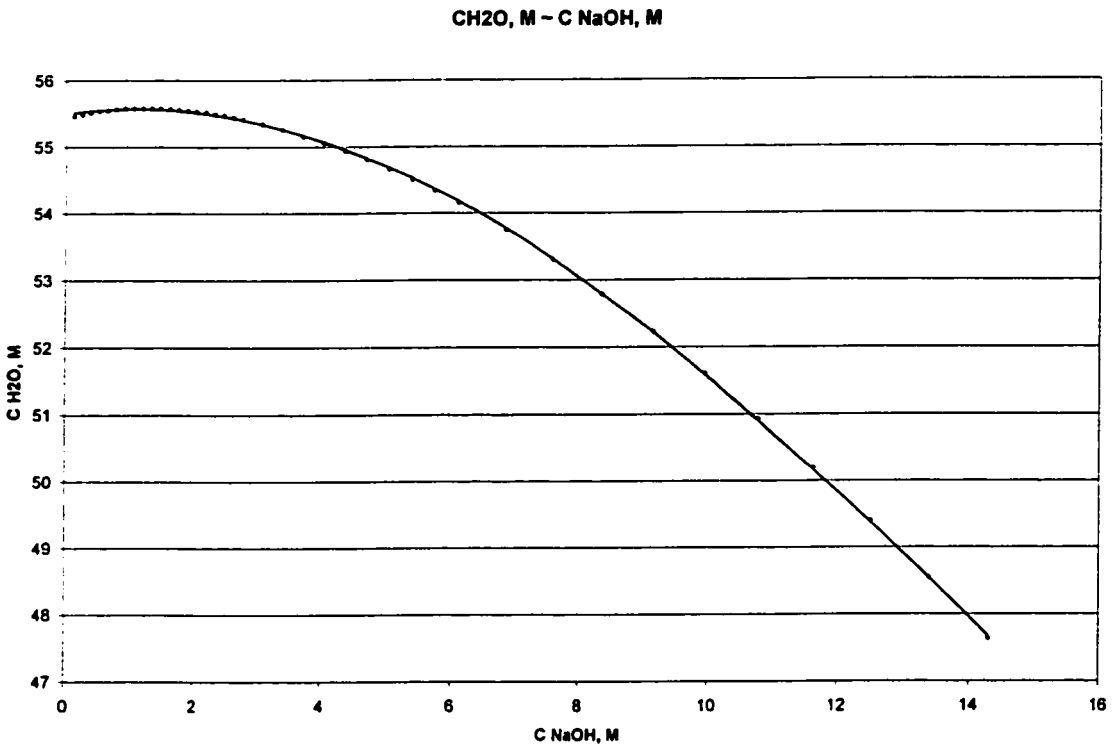

Figure 5.3. The concentration relationship of water and NaOH in NaOH solution

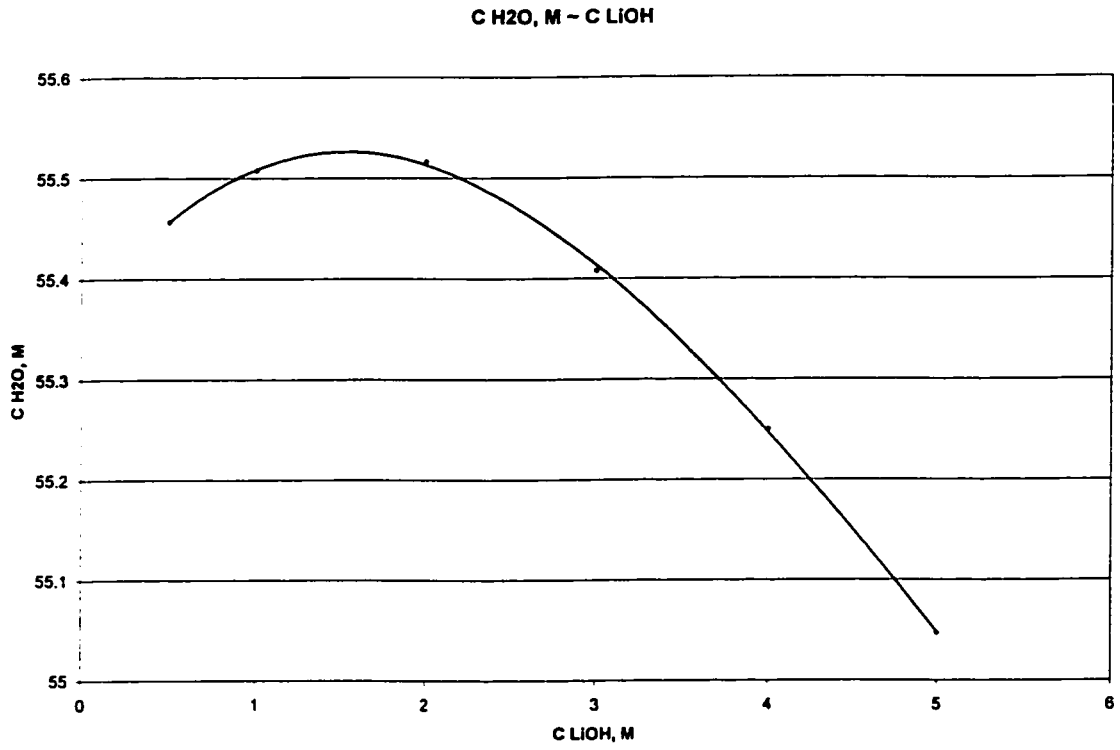

Figure 5.4. The concentration relationship of water and LiOH in LiOH solution

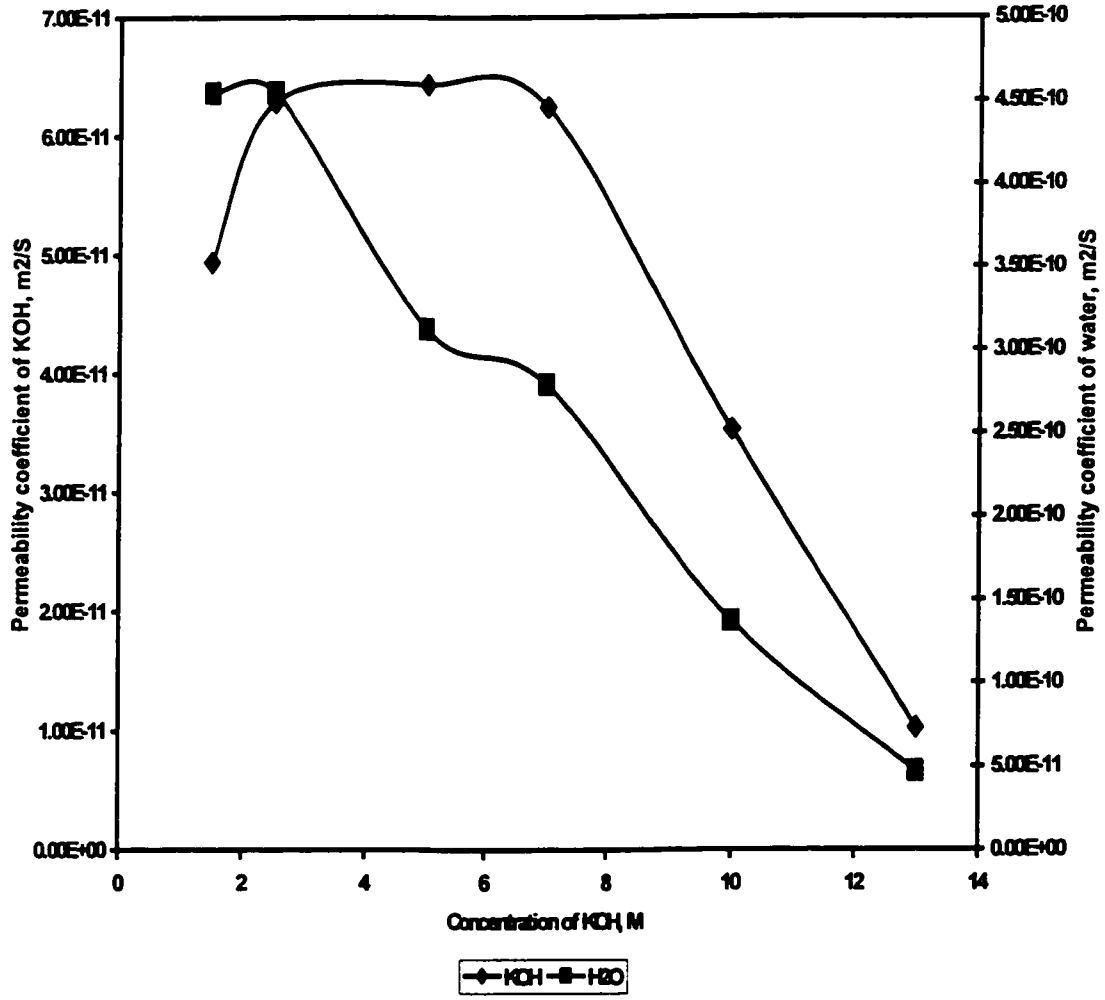

Figure 5.5. The permeability coefficient of KOH and water

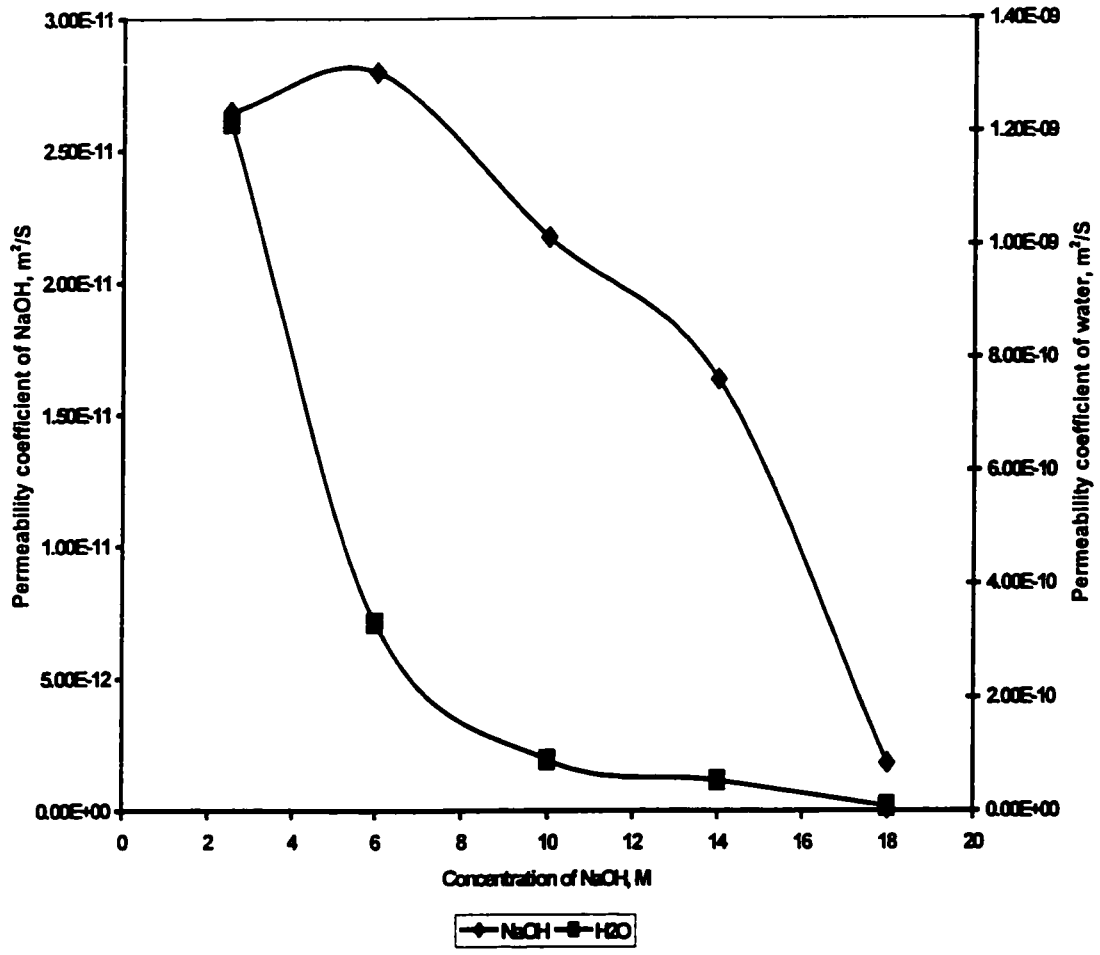

Figure 5.6. The permeability coefficient of NaOH and water

2.5 M it decreases constantly. The permeability of water is about 10 times higher than KOH at the concentration of 2.5 M. At 13 M the permeability of water is still 5 times that of KOH.

4.1.2 NaOH

The permeability coefficient of NaOH and water are as shown in Figure 5.6. The permeability coefficient of NaOH has a maximum of 2.8×10^{-11} m^2/s at 6 M. The effect of concentration is much weaker compared to the case of KOH. The shape of the curve of permeability coefficient vs. concentration also shows similarity to the curve of conductivity vs. concentration [1]. The conductivity has a maximum at 8 M. It is also noticed that the curve of conductivity is shaper around the maximum point because of the average concentration in Figure 5.6. The permeability coefficient of water decreases constantly with the concentration. The permeability coefficient of water is about 50 times higher than NaOH at 2.5 M. At 14 M the permeability of water is only 3.2 times higher than NaOH. The permeability of NaOH is of the same order with that of KOH. The permeability of water in NaOH is much higher than in KOH.

4.1.3 LiOH

The permeability coefficients of LiOH and water are shown in Figure 5.7. The permeability coefficient of LiOH constantly increases with concentration. This shape is also similar to the curve of conductivity vs. concentration [1]. The conductivity increases with concentration constantly. However the curve of conductivity is flatter at high concentration than the permeability of LiOH. The permeability coefficient of water increases slightly with the concentration. The change is much smaller than in KOH and NaOH. The permeability of water is about twice the permeability of LiOH at 2.5 M. At 3.5 M the permeability of water is only one tenth of the permeability coefficient of LiOH. The permeability of LiOH is at the same level with the permeability coefficient of KOH and NaOH. The permeability of water in LiOH is much lower than in KOH and NaOH. The comparison of permeability of alkali and water is shown in Figure 5.8 and 5.9.

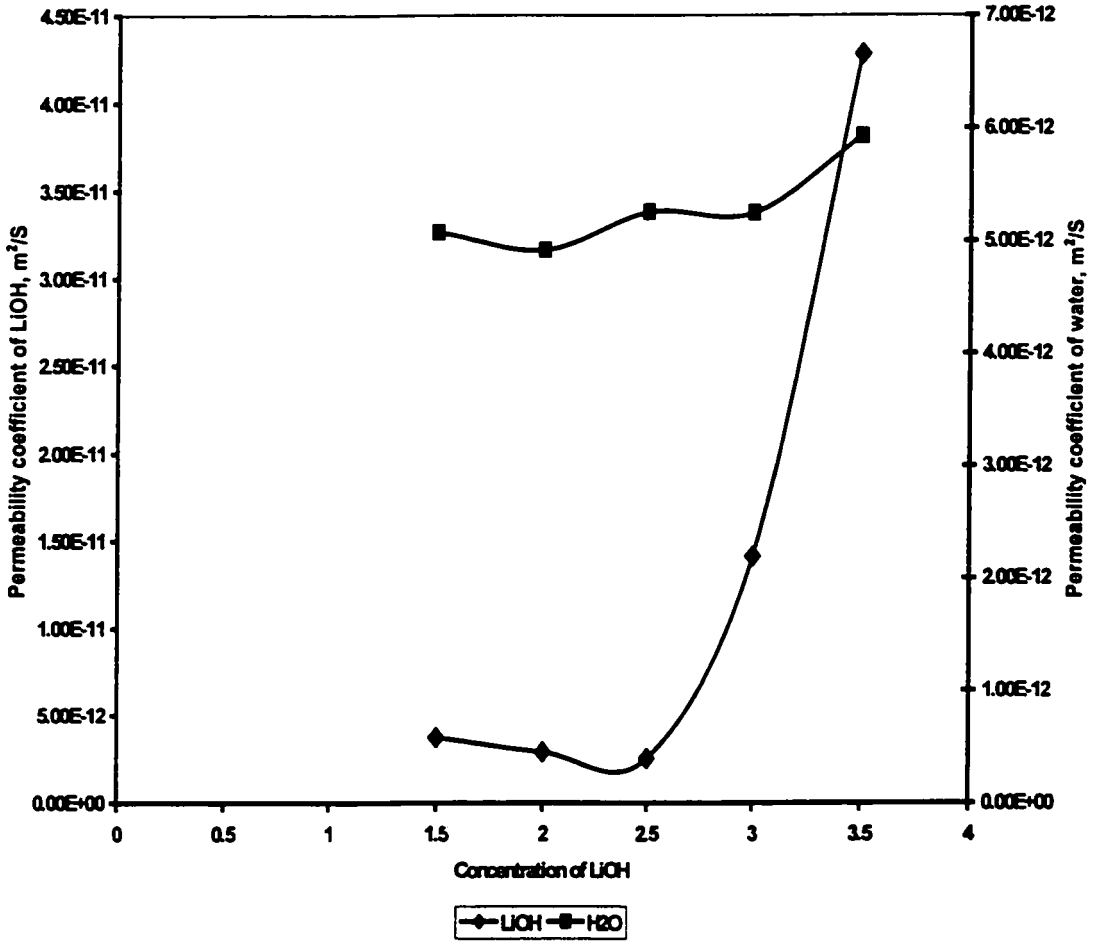

Figure 5.7. The permeability coefficient of LiOH and water

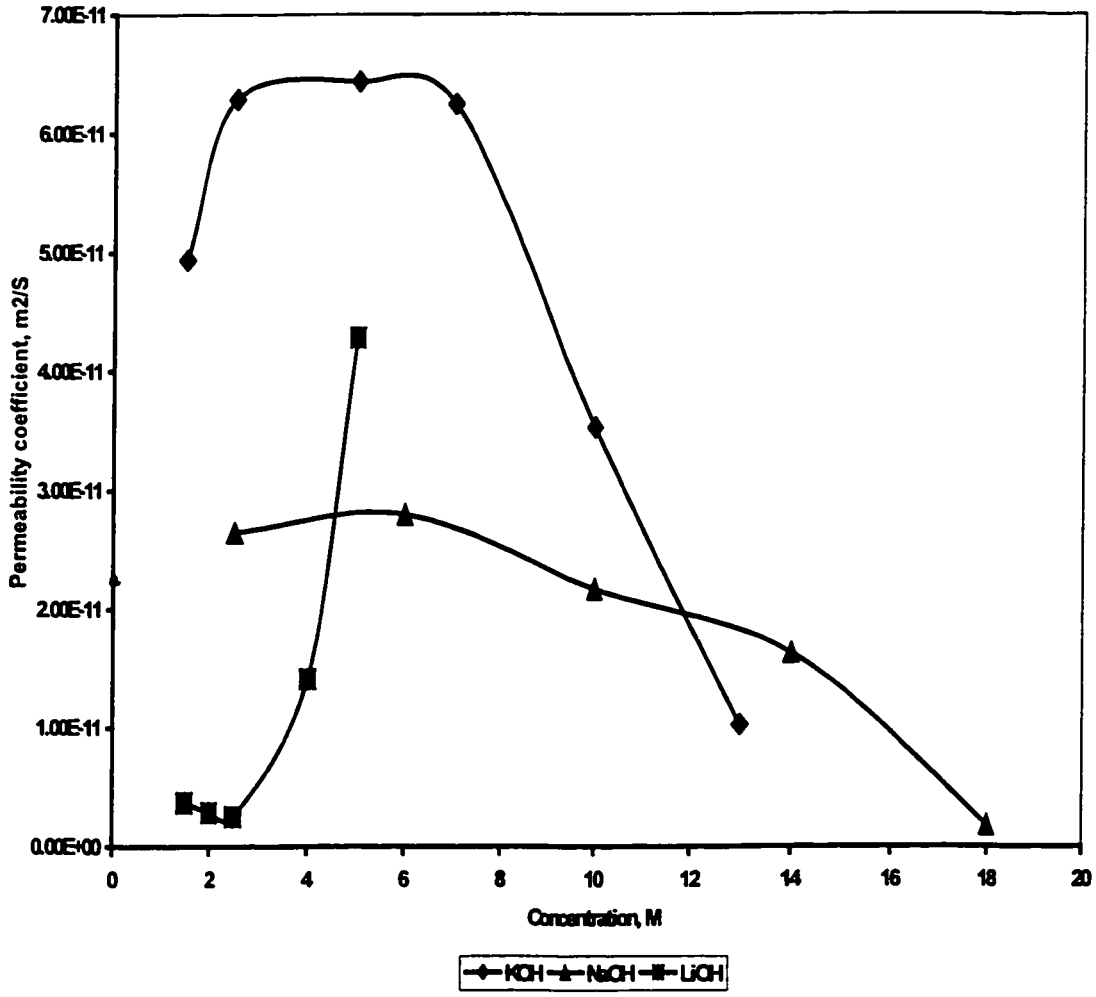

Figure 5.8. The comparison of permeability coefficient of alkali

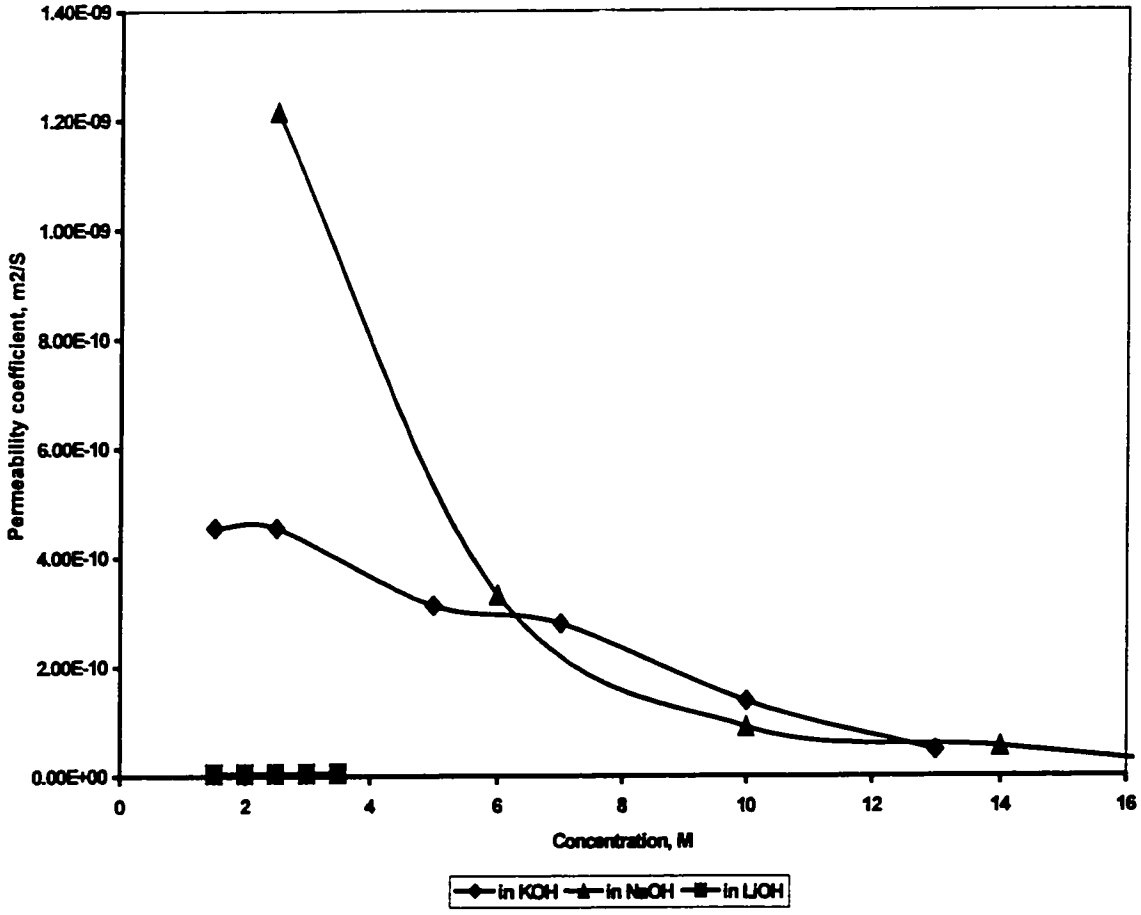

Figure 5.9. The comparison of permeability coefficient of water

The similar trends between the concentration effect on the permeability of alkalis in PBI membrane and the ionic conductivity indicate that the ionic conductivity of PBI membrane in alkaline solution is determined by the permeability of alkali in the membrane. The water permeability basically decreases when the concentration increases. This indicates that the water permeability in the membrane does not affect the ionic conductivity significantly.

4.2. Transference number of cations in PBI

The transference number and water electro-osmotic drag coefficient are calculated from mass balance.

The transference numbers of cations in alkaline solution change with the type of the alkali and its concentration, as shown in Figure 5.10. The shapes of the curve of the transference number vs. concentration are very similar for K^+ and Na^+. The overall trend is that the transference number decreases with concentration. However there is a maximum point at certain concentration for each of them. The concentration corresponding to the maximum transference number changes with the type of the alkali. The low transference number at high concentration implies that the transference number in dry membrane, as used in fuel cell, could be very low.

The differences in transference number between K^+, Na^+ and Li^+ are small and the transference numbers of the cations in PBI membrane are relatively high, which indicates that the cations are not the determinant of the conductivity. (Because the differences in the conductivity of the doped PBI in NaOH, KOH, and LiOH are relatively large [1].) Both cations and OH^- participates in the conduction of the current. The permeability of the alkali in PBI membrane is the main factor that determines the ionic conductivity of PBI in alkaline solution.

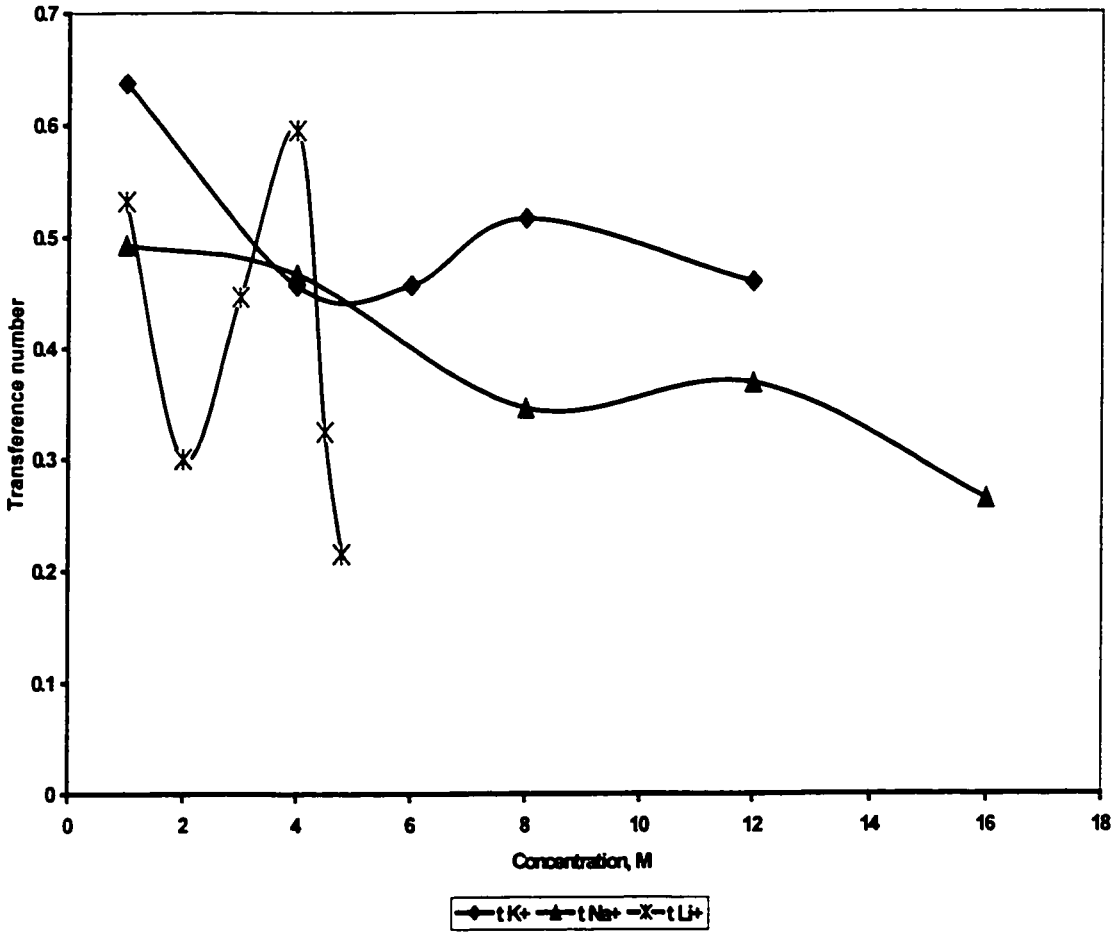

Figure 5.10. Transference number of alkali in PBI

4.3. Electro-osmotic drag coefficient

The electro-osmotic drag coefficient decreases with the concentration of alkalis as shown in Figure 5.11. It indicates that in dry alkali doped PBI the electro-osmotic drag coefficient will be low, which is favorable for fuel cell applications. The type of the alkalis has little effect on the electro-osmotic drag coefficient.

5. Conclusions

The permeability of alkali in PBI membrane changes with the type of the alkalis. For KOH and NaOH the permeability has a maximum at certain concentration. When the concentration increases the permeability change has the similar trend with the ionic conductivity change. The water permeability in PBI decreases when the alkali concentration increases. The ionic conductivity of PBI membrane in alkaline solution is determined by the permeability of alkali in the membrane. The water permeability in the membrane has little effect on the ionic conductivity.

The transference number of cations has high value and small difference between different cations, which indicates that the cations and OH^- all participate in the conduction of the current. The strength of alkali and concentration of OH^- are the main factors that determine the ionic conductivity of the PBI membrane in alkaline solution. The transference number of cations decreases with concentration. In dry membrane as in fuel cells, the transference number may be very low.

The different transportation behavior in LiOH might be attributed to some of the characteristics of LiOH solution. It needs further investigation

The type of the alkalis has little effect on the electro-osmotic drag coefficient. The electro-osmotic drag coefficient decreases with the concentration of alkalis. The low in dry alkali doped PBI the electro-osmotic drag coefficient is low. It is good for fuel cell applications.

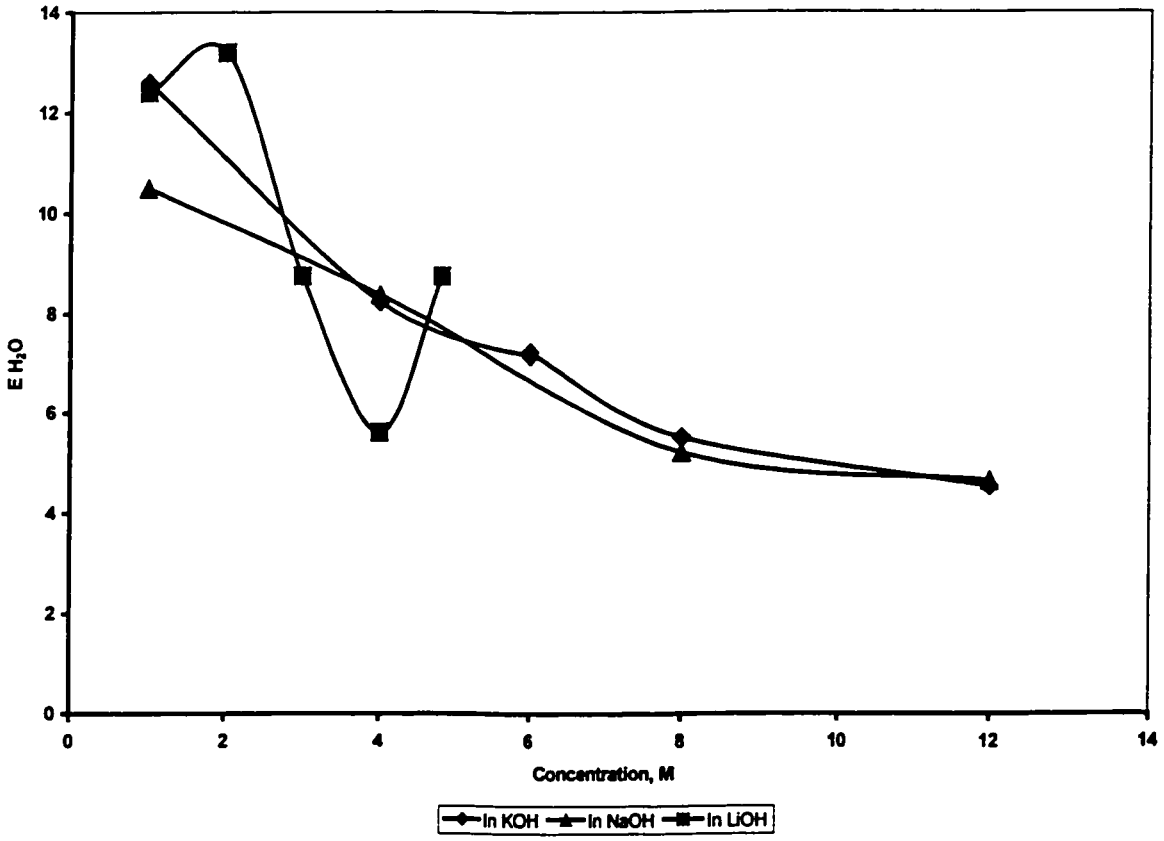

Figure 5.11. The electro-osmotic drag coefficient of water with cations

6. References

[1] B. Xing and O. Savadogo, *Electrochemical communication*, **2**, 697 (2000)

[2] G. P. Schulman and W. Lochte, *J. Macromol. Sci. Chem.*, **1**, 413 (1967).

[3] Y. Tsur, Y. L. Freilich, and M. Levy, *J. Polym. Sci.*, **12**, 1531 (1974).

[4] D. N. Gray, G. P. Schulman, and R. T. Conley, *J Macromol. Sci. Chem.*, **1**, 395 (1967).

[5] Dale A. Chatfieleld, *J. Polym. Sci. Chem.*, **19**, 601 (1981).

[6] M. B. Gieselman, and J. R. Reynolds, *Macromolecules*, **26**, 5633 (1993).

[7] P. Musto, F. E. Karasz and W. J. Macknight, *polymer*, **34**, 2934 (1993).

[8] D. Weng, J. S. Wainright, U. Landau, and R. F. Savinell, *J. Electrochem. Soc.*, **143**, 1260 (1996).

[9] D. WENG, J. S. Wainright, U. Landau, and R. F. Savinell, p. 201, in *Electrode Materials and Processes for Energy Conversion and Storage*, S. Srinivasan, D. D. Macdonald, and A. C. Khandkar, Editors, PV 94-23, p. 201 *The Electrochemical Society Proceedings Series*, Pennington, NJ (1994)

[10] B. Xing, O. Savadogo, *J. New Mat. Electrochem. Syst.*, **2** (1999) 95.

[11] H. A. Pohl and R. P. Chartoff, *J. Polym. Sci. Part A*, **2**, 2787 (1964).

[12] S. M. Aharoni and M. H. Litt, *J. Polym. Sci. Polym. Chem. Ed.*, **12**, 639 (1974).

[13] D. Hoel and E. Grunwald, *J. Phys. Chem.*, **81**, 2135 (1977).

[14] S. M. Aharoni and A. J. Signoreli, *J. Appl. Polym. Sci.*, **23**, 2653 (1979).

[15] J. S. Wainright, J. T. Wang, D. Weng, R.F. Savinell, M. Litt, *J. Electrochem. Soc.*, **142**, L121 (1995).

[16] S. R. Samms, S. Wasums, and R. F. Savinell, *J. Electrochem. Soc.*, **143**, 1225 (1996).

[17] D. Weng, J. S. Wainright, U. Landau, and R. F. Savinell, *J. Electrochem. Soc.*, **143**, 1260 (1996).

[18] W. F. Lin, J. T. Wang, and R. F. Savinell, *J. Electrochem. Soc.*, **144**, 1917 (1997).

[19] J. S. Wainright, R. F. Savinell and M. H. Litt, in *"Proceeding of the second International Symposium on New Materials for Fuel Cell and Modern Battery*

system", Eds. O. Savadogo and P. R. Roberge, Montreal, Canada, July 6-7, (1997), p. 808.

[20] J. T. Wang, J. S. Wainright, R. F. Savinell, M. Litt, *J. Appl. Electrochem.*, **26,** 751 (1996).

[21] J. T. Wang, S. Wasmus, and R. F. Savinell, *J. Electrochem. Soc.*, **143,** 1233 (1996).

[22] S. Wasmus, J. T. Wang, and R. F. Savinell, *J. Electrochem. Soc.*, **142,** 3825 (1995).

[23] Jiangtao Wang, S. Wasmus, and R. F. Savinell, *J. Electrochem. Soc.*, **142,** 4218 (1995).

[24] J. T. Wang, R. F. Savinell, J. Wainright, M. Litt, and H. Yu, *Electrochimica Acta,* **41,** 193 (1996).

[25] R.S. Bogner, Electron Dyn. Div., Hughes Aicr. Co., Proc. Intersoc.

[26] CT, USA, Avail.NTIS, Nada [Contract. Rep.] CR (1978), NASA-CR-159653, FCR-1017, 73 pp. From: Sci. Tech. Aerosp. Rep. 1979, 17(24), Abstr. No. N79-33581. CODEN: NSCRAQ ISSN: 0565-7059.

[27] R.E. Martin, Power Syst. Div., United Technol. Corp., South Windsor, CT, USA, Avail. NTIS, NASA [Contract. Rep,] CR (1979), (NASA-CR-159807, FCR-1657), 52 pp. From: Sci. Tech. Aerosp. Rep. 1980, 18(10), Abstr. No. N80-19615. CODEN: NSCRAQ ISSN: 0565-7059.

[28] U.S. Pat. 5,71,038, B. Vyas, (Bell Telephone Laboratories) (Sept. 11, 1984).

[29] G. M. Barrow, *Physical chemistry,* McGraw-Hill Inc., New York, p217, 1988.

[30] D. R. Paul, *J. Polymer Physics*, **A2, 8,** 1811 (1970).

[31] J. H. Petropoulos, *J. Polymer Physics*, **A2, 8,** 1797 (1970).

[32] D. R. Paul, W. J. Koros, *J. Polymer Science, Polymer Physics*, 14,675 (1976).

[33] W. J. Koros, D. R. Paul, A. A. Rocha, *J. Polymer Science, Polymer Physics*, 14,687 (1976).

[34] B. Tazi and O. Savadogo, *in "Proceedings of the Second International Symposium on New Materials for Fuel Cell and Modern Battery Systems" Eds, O. Savadogo and P. R. Roberge, Montreal Canada,* July 6-10, 1997, p864.

[35] *61th Handbook of Chemistry and Physics*, D-228 - D-276, 1981.

CHAPTER 6

THE DOPING PROCESS OF POLYBENZIMIDAZOLE (PBI) IN ALKALINE SOLUTION

Baozhong Xing and O. Savadogo

Laboratoire d'Électrochimie et de Matériaux Énergétiques

École Polytechnique de Montréal

C.P. 6079, Succ. Centre-Ville

Montréal, Québec, H3C 3A7

Canada

(To be published)

Abstract

A new dynamic method for studying the doping process of PBI in alkaline solution is developed. The concept of different roles of diffusion and interaction at different stages was introduced. The two-step sorption model was proposed for the PBI sorption process in alkaline solution. The effect of the alkali type and concentration on doping process was studied. The conductivity mechanism in alkali doped PBI was established.

1. Introduction

Base-type solid polymer electrolyte is the most desired polymer electrolyte in fuel cells as well as some other electrochemical systems. However, the available base-type solid polymer electrolytes are not as many as the acid-type. Alkali doped polybenzimidazole (PBI) is a hopeful candidate because of its excellent thermo and chemical stability [2-7], superior mechanical properties, and lower permeability coefficient for hydrogen than Nafion® [8-9]. It has been studied in alkaline batteries and fuel cell as separators or matrix materials [25-28]. Alkali doped PBI has high ionic conductivity and exhibits encouraging results in fuel cells [1]. The pure PBI is neither ionic nor electric conductive

[10-14]. After doping with alkali, especially doping with KOH PBI becomes an outstanding ionic conductor and still remains as a good electric insulator. The PBI doped with 6 M KOH showed good performance in fuel cell [1].

The objective of this work is to establish the conductivity mechanism in alkali doped PBI membrane through the study on the dynamic doping process.

2. Theory and fundamentals

Doping process of PBI membrane in alkaline solution is a sorption process of alkalis in PBI membrane. In the sorption process in high concentration solution the permeability coefficient is almost always concentration dependent like in Langmuir's sorption and dual-mode sorption [29]. The classical time-lag method cannot be used to measure the permeability coefficient in these situations. Some modifications on the method have been made [30-33] in order to make it applicable to Langmuir's sorption and dual-mode sorption. However, the modified method is not suitable for two-step sorption process.

In doping process of PBI membrane in alkaline solution the penetrants are ions. When ions penetrate into the membrane the ionic conductivity of the membrane will change. From the ionic conductivity change vs. time, the time lag can be determined.

During the doping process the two sides of the membrane contact with the same solution. Therefore the permeation thickness is half the thickness of the membrane. Since the doping process begins with blank PBI, the concentrations of the penetrants are 0 in the membrane at the beginning. In a period of time they will remain 0 in the middle of the membrane.

To determine the dependence of the permeation on the concentration of penetrants, the average permeability coefficient of alkalis was measured with two solutions of different concentration for certain time [35]. The permeability coefficient was calculated from

mass balance and the First Fick's law as documented in [35]. Previous work shows that PBI membrane changes from ionic insulator to conductor after doping in alkaline solutions [1]. It is indicated that the alkalis interact with PBI membrane and the OH^- and cations can move in the membrane [35]. The permeation process of alkalis in blank PBI membrane) has two mechanisms, diffusion process of the alkalis and interaction process between the alkali and PBI molecules. To dope into the membrane the alkalis must first transfer into the membrane from the solution, and then interact with PBI. If the diffusion process is slower than the interaction process the conductivity change during the doping process is controlled by diffusion. Therefore, the diffusion coefficient can be determined from the conductivity change during doping process. If the diffusion process is faster than the interaction process, the conductivity change during the doping process is controlled by interaction. Therefore, the interaction rate can be determined from the conductivity change during doping process.

The structure of the membrane affects the motion of the ions. Hence it will affect the conductivity of the doped membrane. The study on the kinetics of the doping process will reveal some information on the structure change during the doping process. The doping kinetics is usually studied by the means of weight, pressure or concentration measurement. In this work the conductivity change during the doping process will be used as a parameter to monitor the kinetics of the sorption process; the experimental data of the conductivity change during the doping process will be presented; a model on the sorption process and the conductivity mechanism will be proposed.

3. Experimental

The conductivity change in doping process vs. time was measured in the cell shown in Figure 6.1. The PBI film with a thickness of 40 μm was purchased from Hoechest Celanese. The film was cut into small square samples of 3 ×3 cm^2. The samples were washed in deionized boiling water for more than 6 hours to remove the LiCl impurities. These blank samples were then kept in water. The samples were doped by immersing

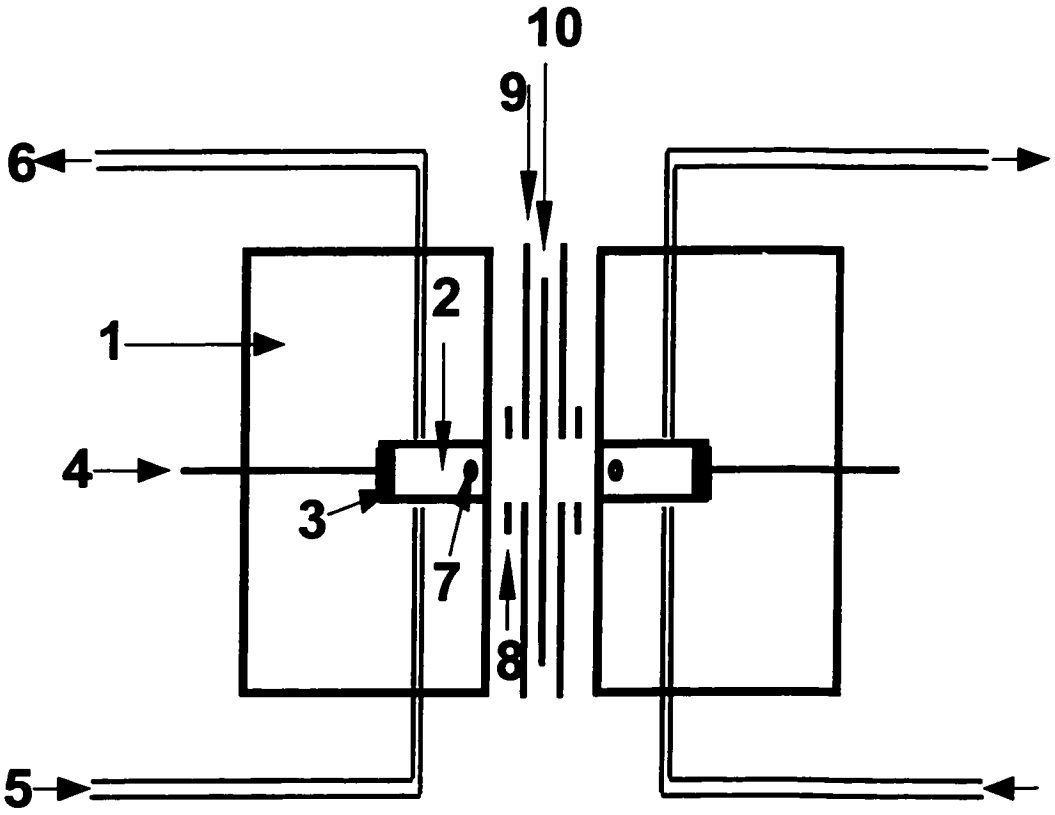

Figure 6.1. The structure of measurement cell

1. Cell body
2. Measurement Chamber
3. Pt electrode
4. Pt electrode
5. Measurement medium solution input from pump
6. Measurement medium solution output
7. Measurement hole connected with calomel measurement electrode
8. Teflon O ring gasket
9. Teflon film gasket
10. PBI membrane

them into the alkaline solution in the conductivity measurement cell. The conductivity was measured at different doping times. The measurement was achieved in doping solution using classical two-point probe with homemade conductivity measurement cell [34].

4. Results and discussion

4.1. Conductivity change with time

The conductivity of the PBI membrane changes with time during doping process in alkaline solution as shown in Figure 6.2. The conductivity of PBI membrane increases with time. The membrane changes from ionic insulator to ionic conductor. This confirmed the results of the previous work in two-stage experiment [1].

In Figure 6.2 it is shown that the conductivity change has two steps in 1 M KOH and 1 M NaOH. In 1 M NaOH the second step is not as sharp as in 1 M KOH. In 1 M LiOH only one step is observed. as LiOH concentration increases, the second step of the conductivity increase appears as shown in Figure 6.5.

The type of the alkaline solution affects the rate of doping process (Figure 6.2). The doping rate is in the order of KOH>NaOH>LiOH. The concentration of the alkaline solution also affects the rate of doping process, as shown in Figure 6.3-6.5 and Figure 6.7-6.18.

In a typical conductivity vs. time curve with two steps there are 6 special points that divide the curve into 7 sections as shown in Figure 6.6. Generally, at low concentration the first step starts late and second step is not obvious. In KOH and NaOH solution, the start time of the first step, t_1, decrease as the concentration increases; the first and the second step become steeper and steeper and their heights increase with concentration. If the concentration is above a certain value, further increase of the concentration can

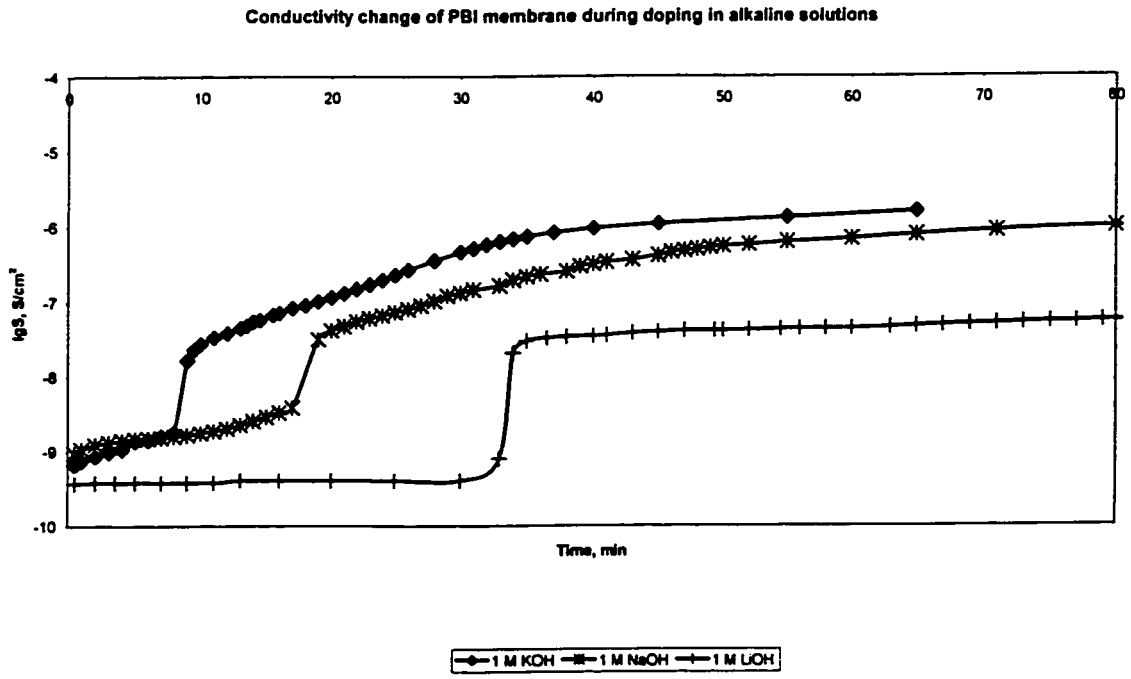

Figure 6.2. Conductivity change of PBI membrane with time during doping process

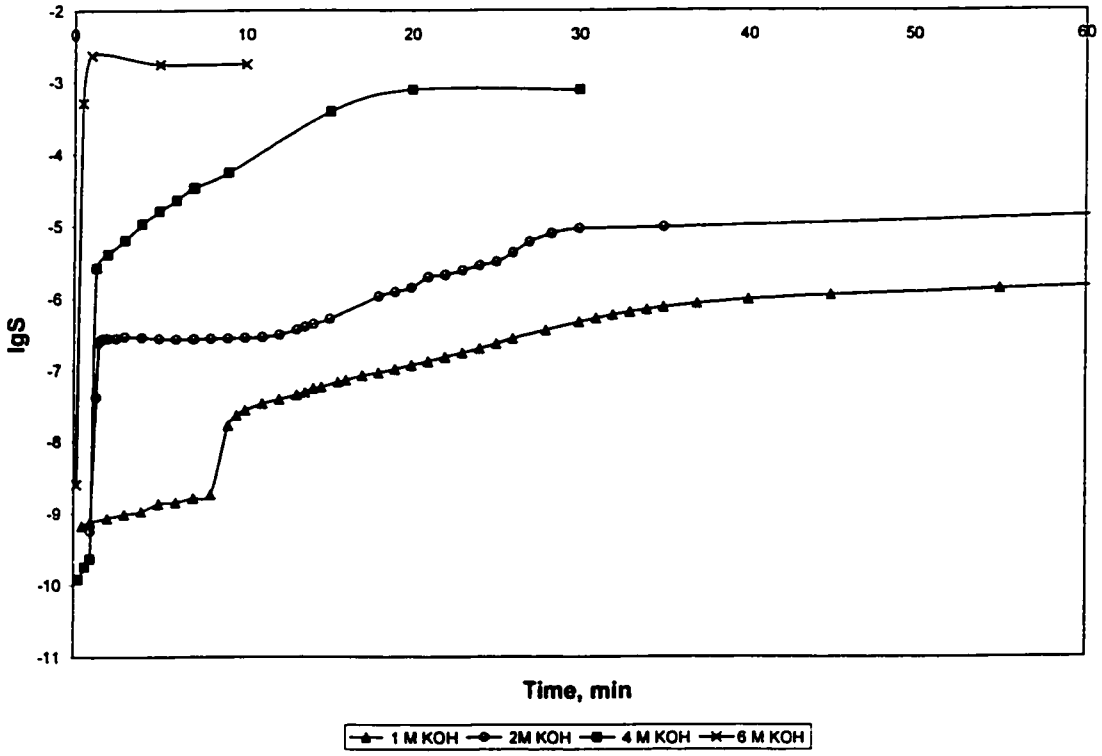

Figure 6.3. Concentration effect of KOH solution on conductivity change of PBI membrane

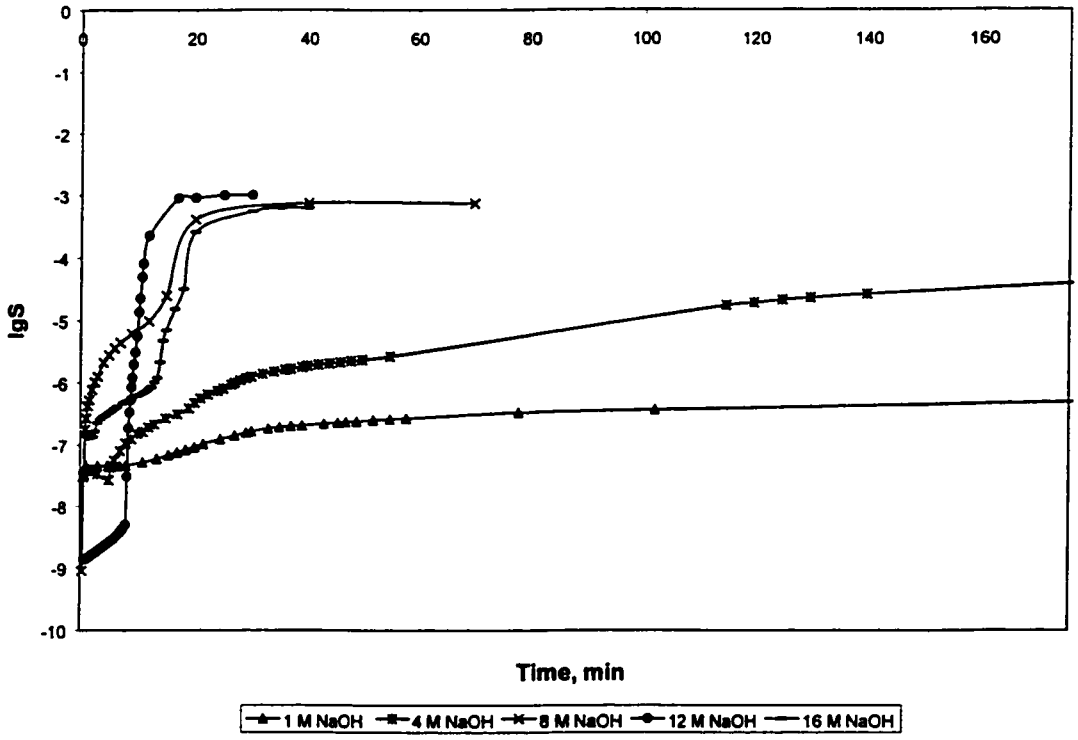

Figure 6.4. Concentration effect of NaOH solution on conductivity change of PBI membrane

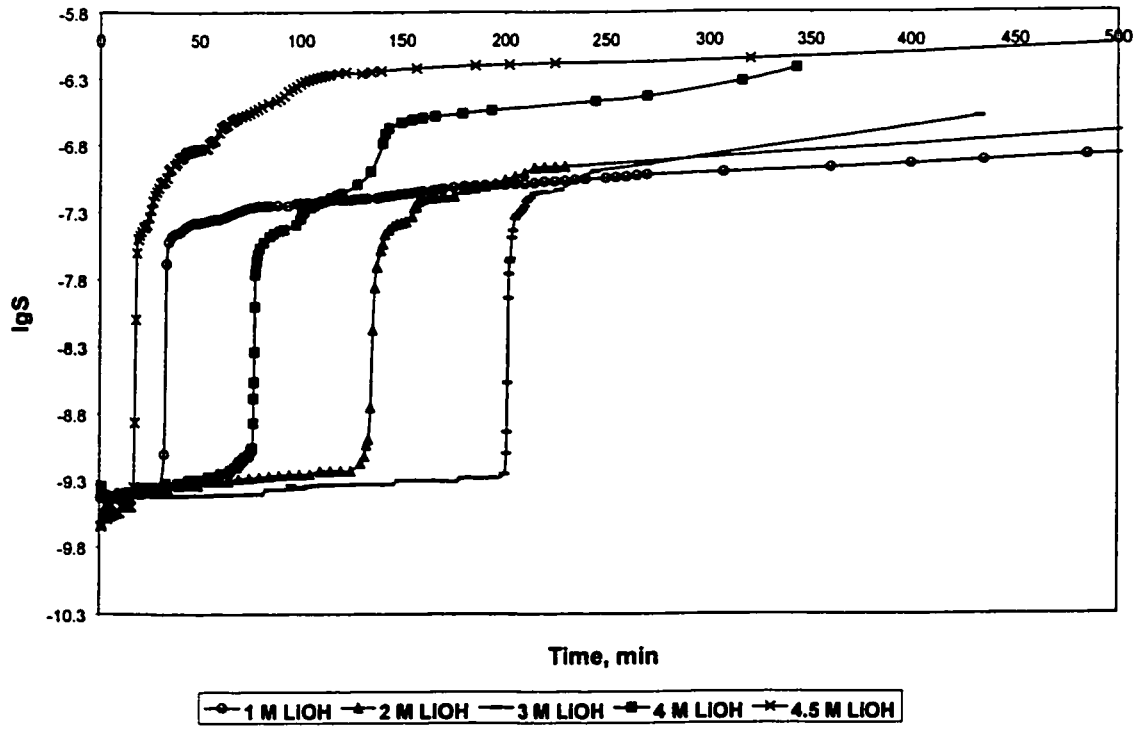

Figure 6.5. Concentration effect of LiOH solution on conductivity change of PBI membrane

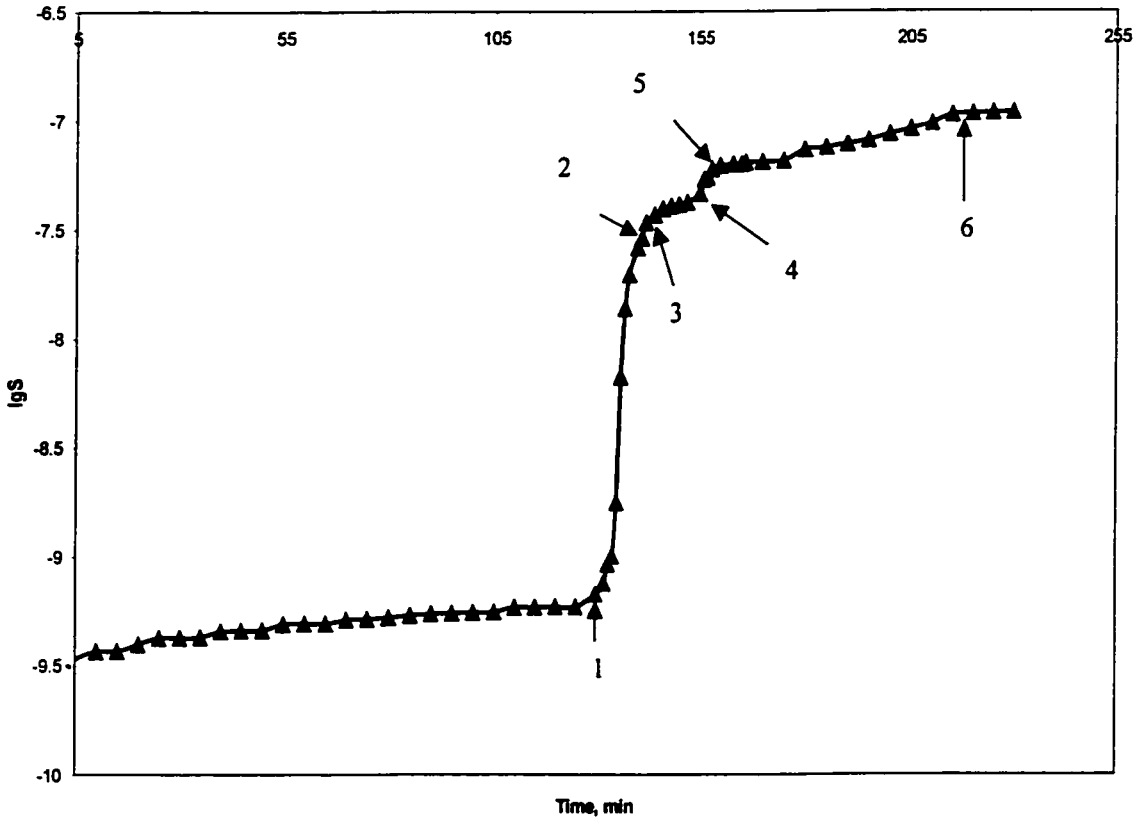

Figure 6.6. The special points of the doping process

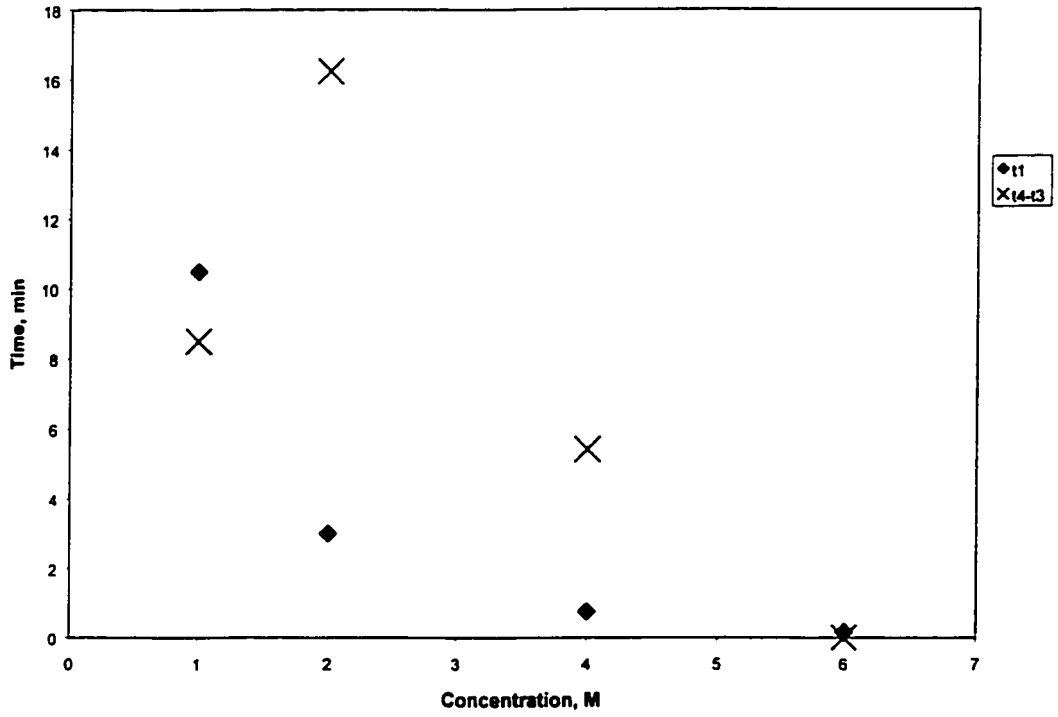

Figure 6.7. The t_1 and t_4-t_3 change with concentration in KOH

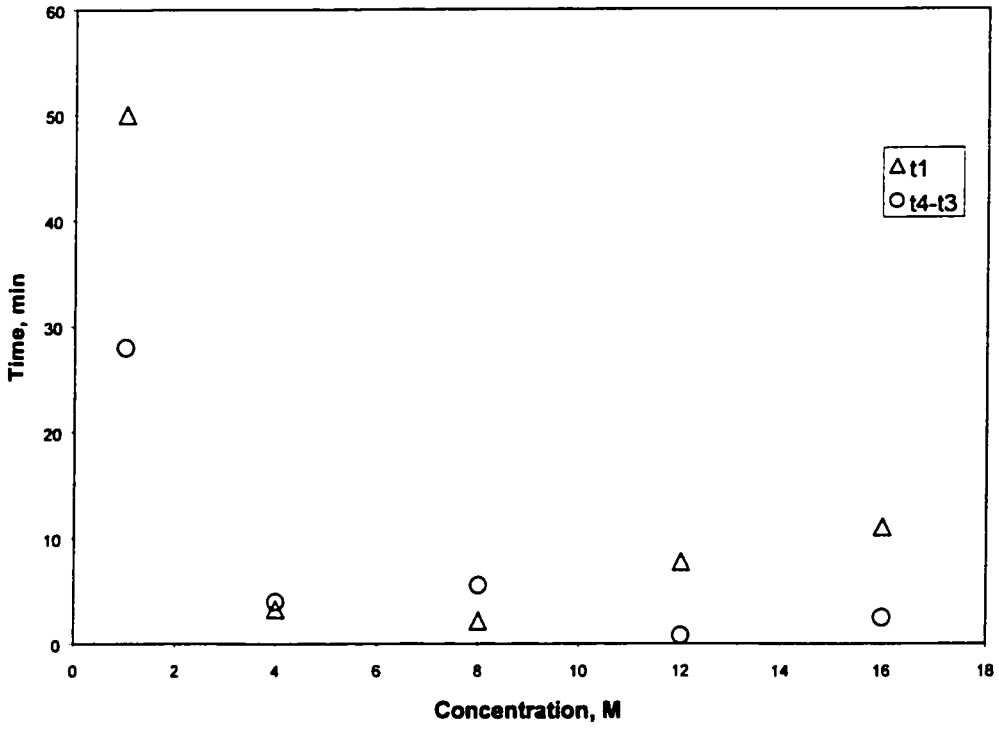

Figure 6.8. The t_1 and t_4-t_3 change with concentration in NaOH

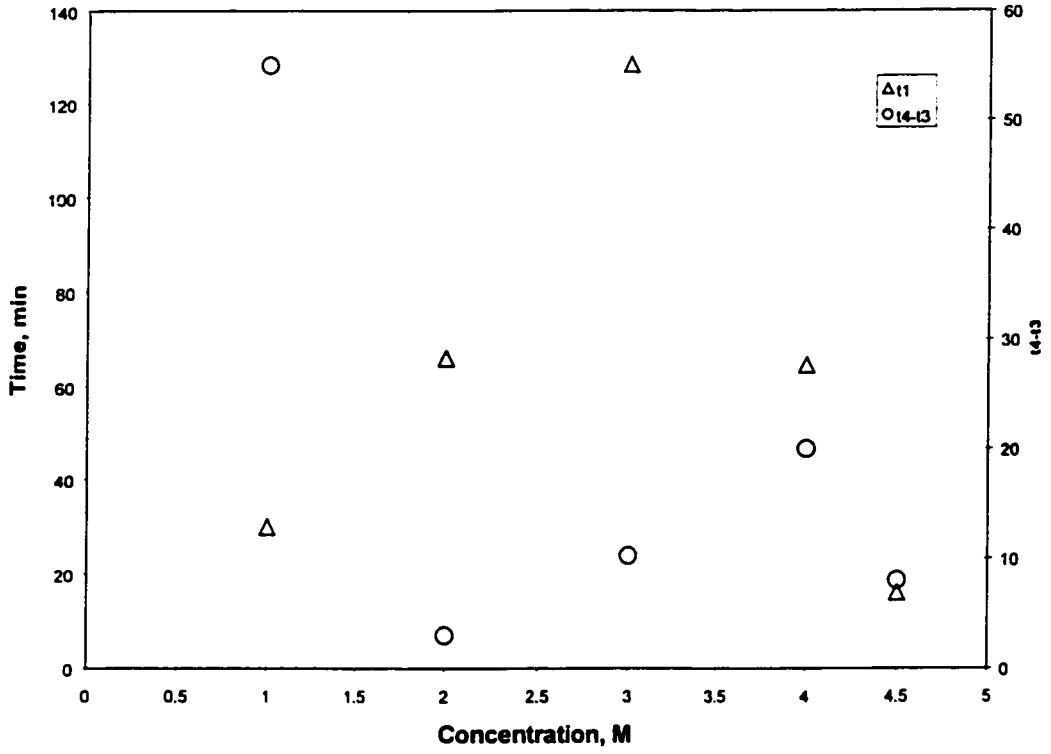

Figure 6.9. The t_1 and t_4-t_3 change with concentration in LiOH

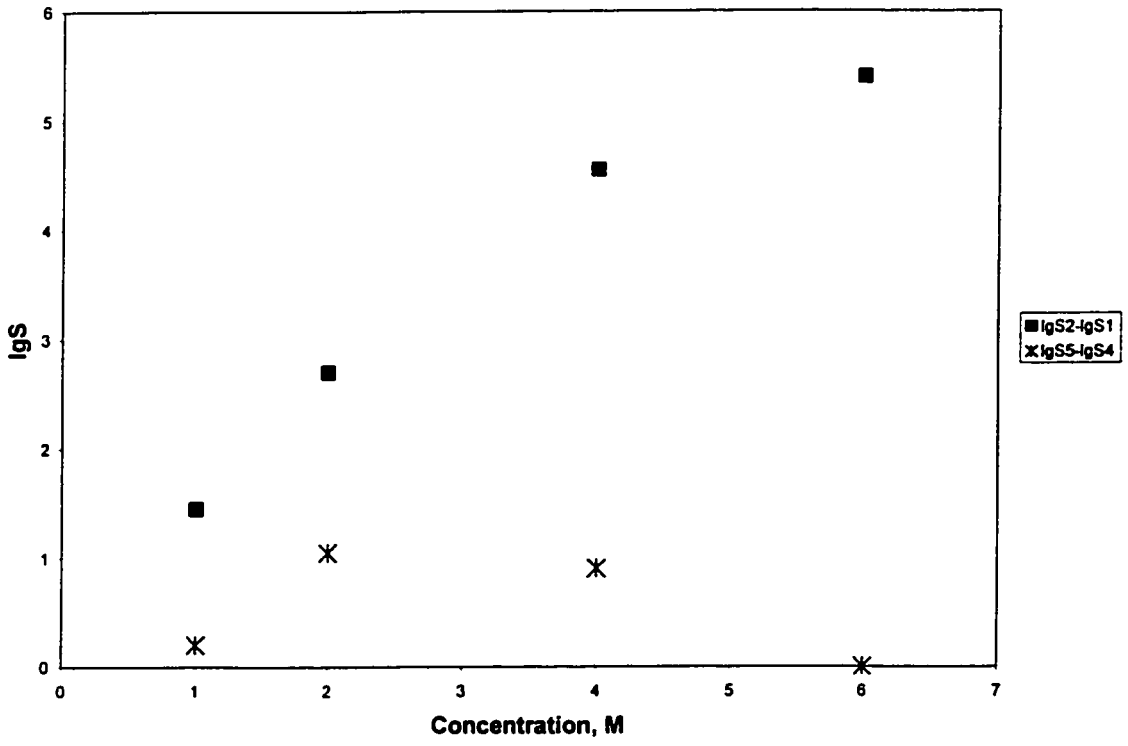

Figure 6.10. The conductivity change at the two steps in KOH solution

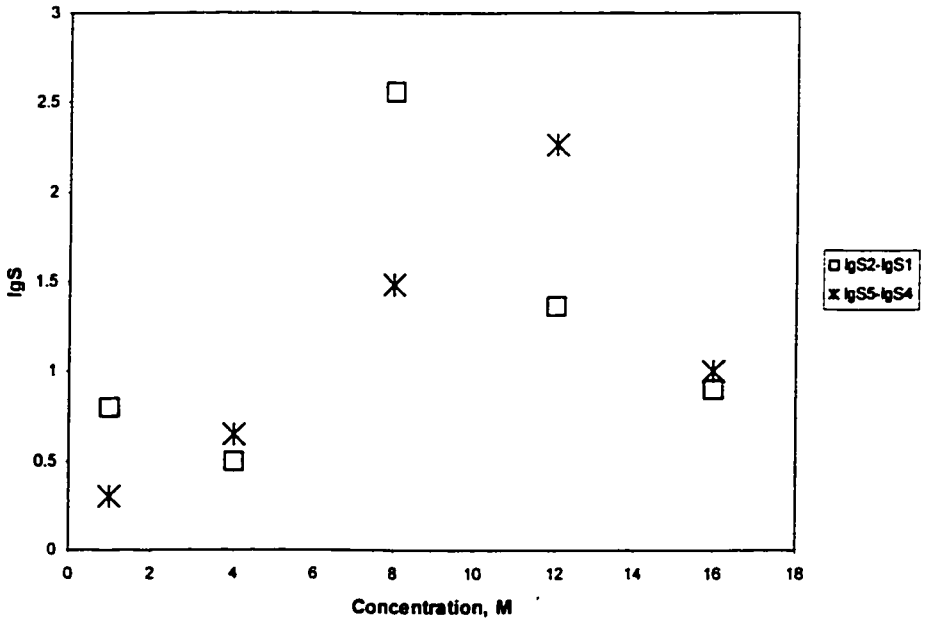

Figure 6.11. The conductivity change at the two steps in NaOH solution

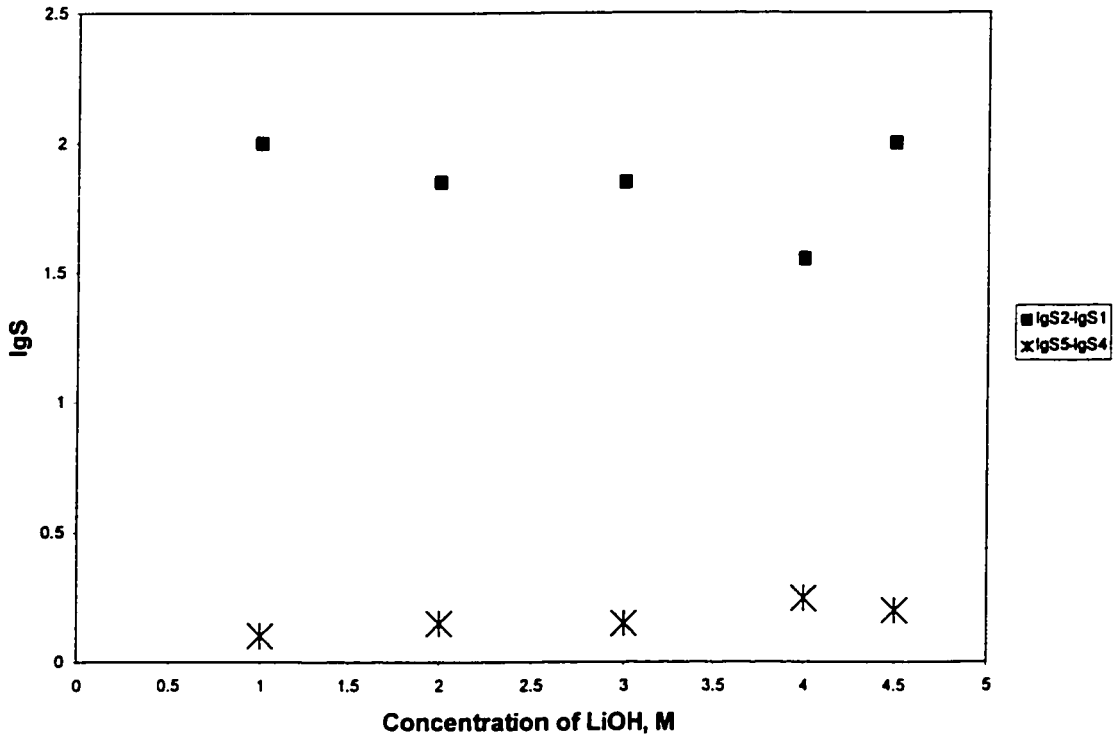

Figure 6.12. The two steps in LiOH solution

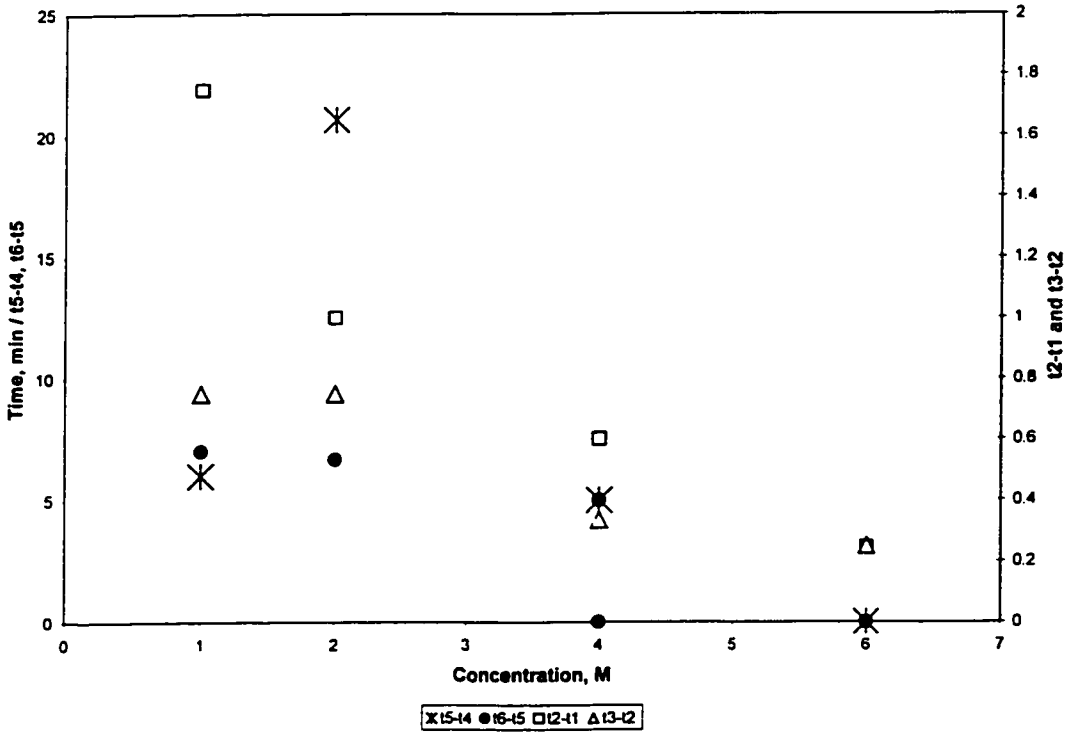

Figure 6.13. The time needed for the stages in the doping process in KOH solution

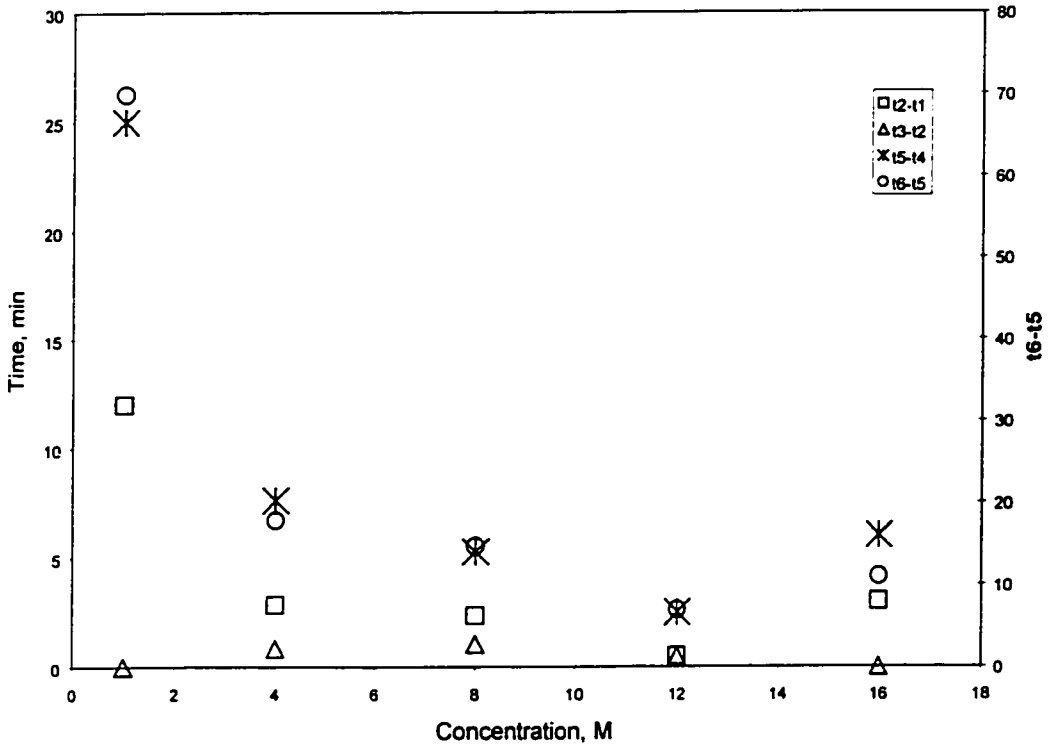

Figure 6.14. The time needed for the stages in the doping process in NaOH solution

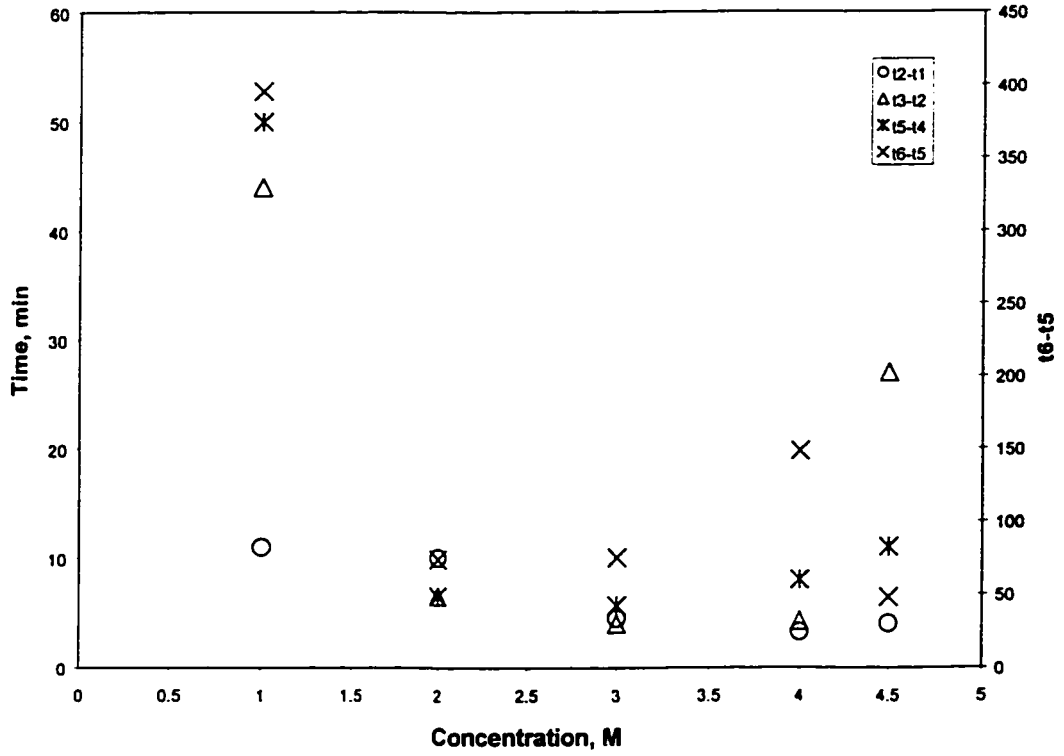

Figure 6.15. The time needed for the stages in the doping process in LiOH solution

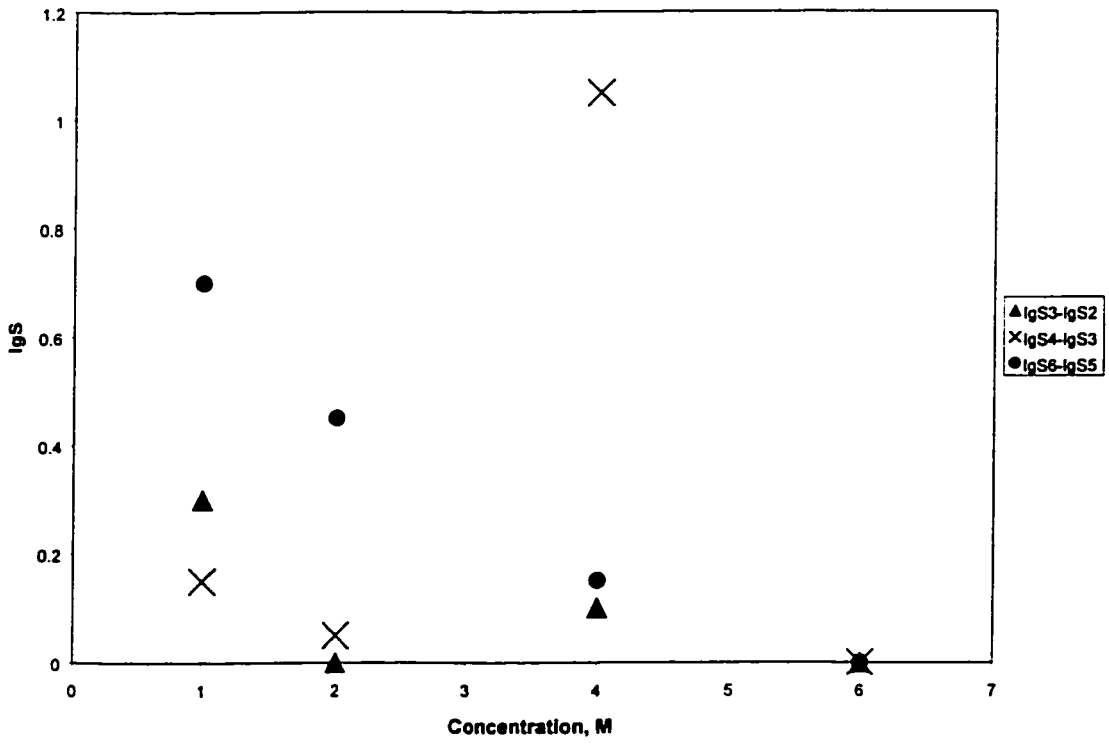

Figure 6.16. The conductivity changes of the steps in KOH solution

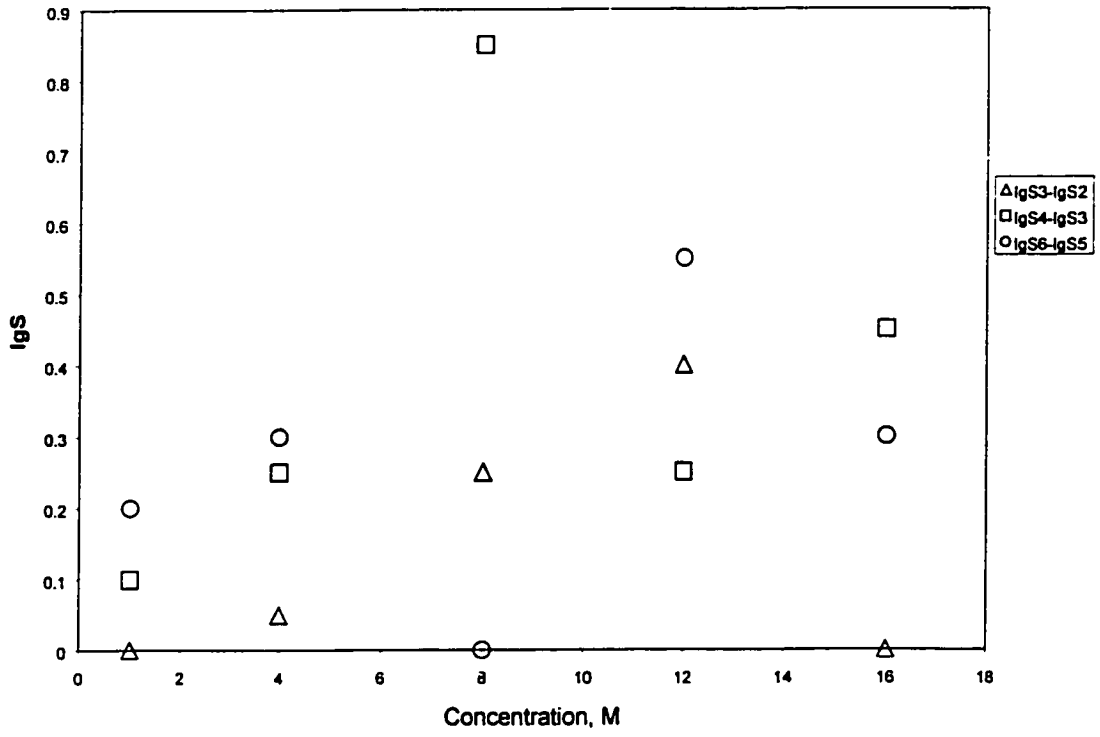

Figure 6.17. The conductivity change in different stages of doping in NaOH solution

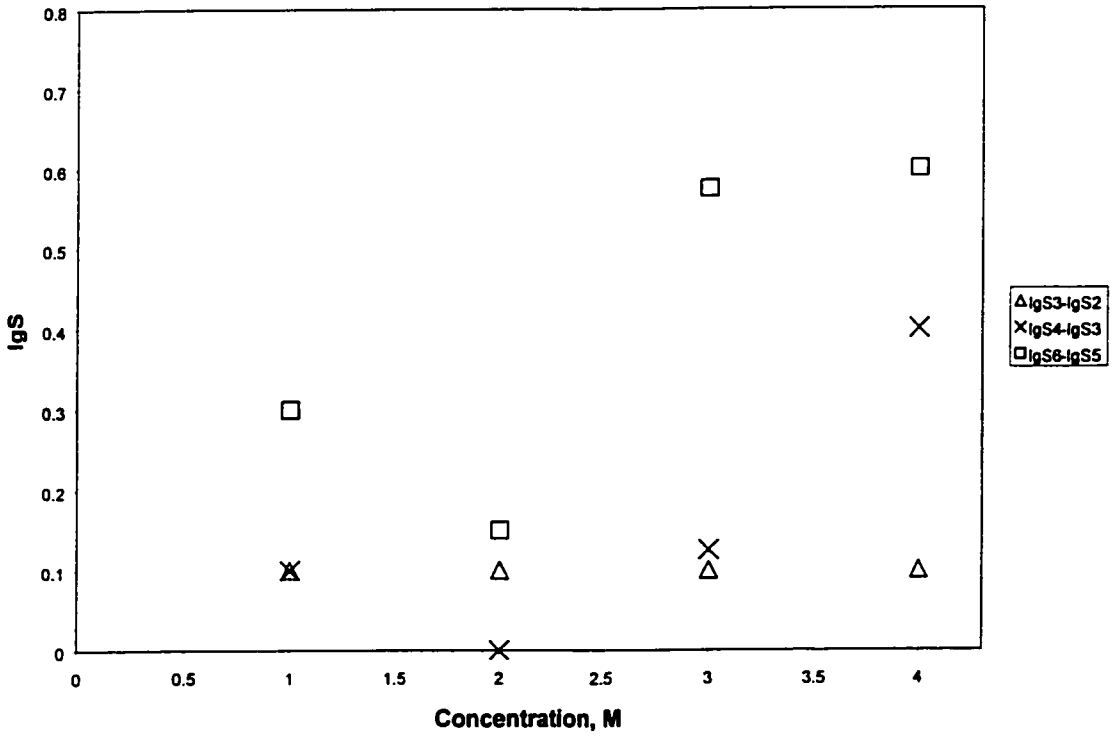

Figure 6.18. The conductivity change in different stages of doping in LiOH solution

produce opposite effect to the trend described above. There is a minimum for t_1 in KOH or NaOH solution. In LiOH solution t_1 has a maximum.

In KOH solution, the concentration effects on the doping process are shown in Figure 6.3, 6.7, 6.10, 6.13, and 6.16. The starting time of the first step, t_1, decreases with concentration (2-6M). The lasting time of the plateau, t_4-t_3, has a maximum at 2 M. At 6 M, the two steps cannot be distinguished any more. The height of the first step, lgS_2-lgS_1, increases with the concentration of KOH. The height of the second step, lgS_5-lgS_4, changes less than the first step. It has a maximum at 2 M. The change rate in the first step increases with concentration. The parameters t_2-t_1, t_3-t_2 and lgS_3-lgS_2 decrease with concentration, as indicated in Figure 6.13 and 6.16. The conductivity change in the plateau, lgS_4-lgS_3 has a minimum at 2 M (Figure 6.16). This indicates that the plateau at this concentration is flatter than the plateau at other concentrations. The second step takes more time (t_5-t_4) at 2 M than at other concentrations, which shows a maximum point in Figure 6.13. Both the time needed to reach the equilibrium after the second step, t_6-t_5, and the amplitude of conductivity change, lgS_6-lgS_5, decrease with the concentration as shown in Figure 6.13 and 6.16. This indicates that at high concentration, the process is faster to reach equilibrium. The rate of doping process in KOH increases with concentration, which corresponds to the results on the conductivity tendency after long time doping in KOH obtained in previous work [1].

In NaOH solution, the concentration effects on the doping process are shown in Figure 6.4, 6.8, 6.11, 6.14, and 6.17. The starting time of the first step, t_1 has a minimum around 8 M (Figure 6.8). It decreases sharply from 1 M to 4 M. Above 8 M t_1 increases slightly with concentration. The lasting time of the plateau, t_4-t_3, has a minimum at 12 M (Figure 6.8). The height of the first step, lgS_2-lgS_1, has a maximum at 8 M (Figure 6.11), which corresponds to the conductivity maximum of PBI membrane after doping to a stable state in NaOH solution [1]. The height of the second step, lgS_5-lgS_4, is almost the same with the first step, except the maximum appears at 12 M (Figure 6.17). At 12 M, the rate of

process in the first step is fastest (t_2-t_1 being minimum, Figure 6.14). For the section between 2 and 3, t_3-t_2 does not change with concentration (Figure 6.14); while lgS_3-lgS_2 has a maximum at 12 M (Figure 6.17). The conductivity change in the plateau, lgS_4-lgS_3 has a maximum at 12 M. This indicates that the plateau at this concentration becomes narrower than at other concentrations. The two steps are too close to separate. The second step takes less time at 12 M than at other concentrations, (the minimum of t_5-t_4 in Figure 6.14). The rate to reach the equilibrium after the second step has a maximum at 12 M as shown in Figure 6.14 and 6.17 (t_6-t_5 and lgS_6-lgS_5).

It can be concluded that the doping process has most clear two steps at 8 M. The doping process in NaOH is fastest at 12 M. This corresponds to the results of conductivity tendency after long time doping in NaOH reported in previous work [1].

In LiOH solution, the concentration effects on the doping process are shown in Figure 6.5, 6.9, 6.12, 6.15, and 6.18. The starting time of the first step, t_1, has a maximum around 3 M as shown in Figure 6.9. The lasting time of the plateau, t_4-t_3, has a minimum at 2M. The height of the first step, lgS_2-lgS_1, has no obvious change with concentration. The height of the second step, lgS_5-lgS_4, is much smaller than the first step, and doesn't change much with concentration. The rate of the process in the first step is highest at 4 M (t_2-t_1 and t_3-t_2 being minimum at 4 M, Figure 6.15). lgS_3-lgS_2 is constant in the concentration range (1-4M, Figure 6.18). The conductivity change in the plateau, lgS_4-lgS_3 has a minimum at 2 M. The second step takes less time at around 3 M than at other concentrations (minimum t_5-t_4 in Figure 6.15). The rate to reach the equilibrium after the second step is fastest at 3 M (minimum t_6-t_5 in Figure 6.15). lgS_6-lgS_5 has no obvious change with concentration.

Therefore, the doping process has most clear two steps at around 2 M. The rate of doping process in LiOH has a maximum at around 3 M. The trend of process rate corresponds to the conductivity change tendency after long time doping in LiOH as shown in previous work [1].

The results show that the conductivity at the last stage of the doping process (S_6), where doping reached equilibrium state, conforms to the results from the previous work [1]. The conductivity of the PBI membrane increases with the concentration of alkaline solution, as shown in Figure 6.19. The conductivity increases in alkaline solutions in the order of KOH≥NaOH>>LiOH.

4.2. Sorption process and the conductivity

Alkalis can penetrate into PBI membrane in the doping process. The sorption of Alkalis includes diffusion of alkali within PBI and the interaction between alkali and the membrane. The interaction changes the structure of PBI membrane and results in an increase in conductivity. The conductivity increases in the doping process in alkaline solution, and has two steps as shown from the results of last section and previous work [10]. It is intuitive that the two steps in conductivity change correspond to the two steps in sorption process. An analysis based on the theoretical fundamental and the experimental results is conducted.

The rate of the sorption is determined by the control step among diffusion and interaction between the polymer and the alkali. For diffusion controlled process the fractional mass uptake (with respect to the equilibrium value) is a square root function of time, e.g., $\frac{M_t}{M_\infty} = \frac{8}{\pi^{1/2}}\sqrt{\frac{Dt}{L^2}}$ [38]. The conductivity of the membrane is the integral result of the sorption in the whole membrane. First the resistance of the whole membrane can be treated as a set of parallel resistance from many small areas on the membrane. The conductivity of the whole membrane is the sum of the conductivities from these small areas on the membrane. Assume that the concentration of the alkalis or ions is uniform in the membrane and the alkalis or ions form an ion-conducting cluster from one side of the membrane to another. When the area becoming smaller and smaller to a limit that there is only one conducting cluster in it, the conductivity of the membrane is proportional to the

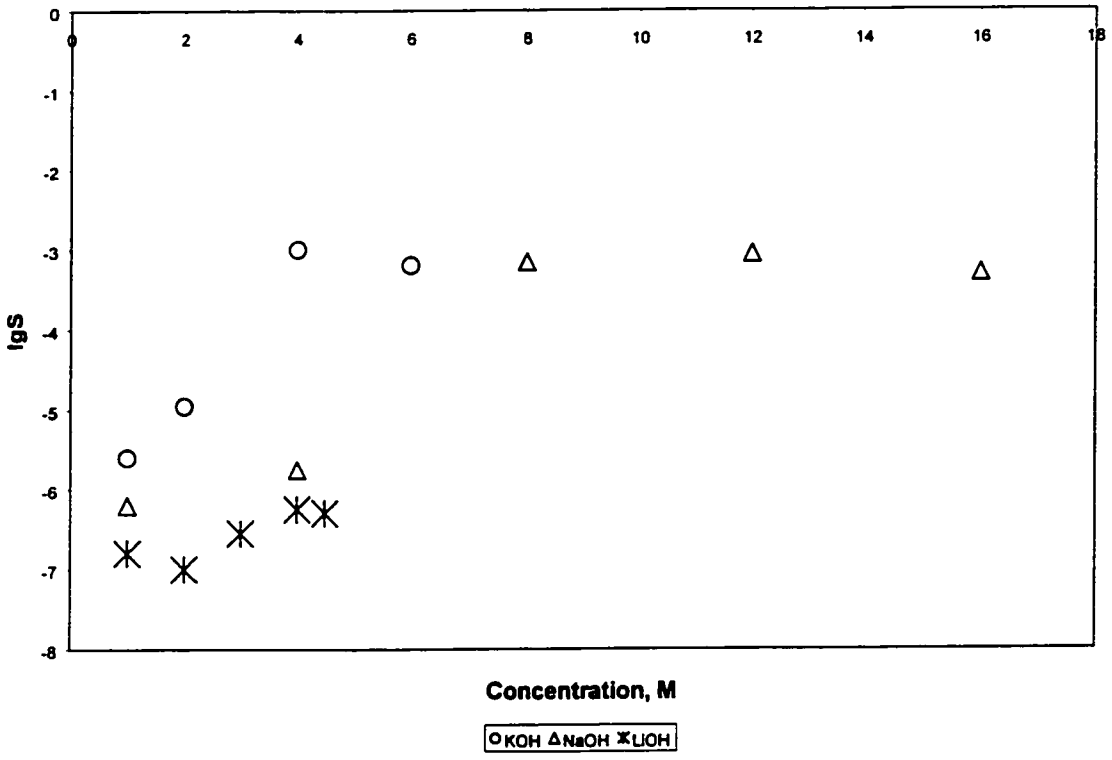

Figure 6.19. The conductivity of PBI membrane after doping process reaching stable state in different alkaline solution

concentration of the alkalis or ions, e.g., $S = \sum S_i = \sum kC_i = kC$. However the concentration of the alkali or ions in the membrane during the doping process is not uniform. There is a distribution along the thickness of the membrane. The series connection model can be used.

Divide the membrane into unlimited thin layers along the thickness of the membrane. The resistance of the whole membrane can be treated as a series of resistance of the many thin parts of the membrane. The resistance of the whole membrane is the sum of these series resistance. For each thin layer the concentration can be treated as uniform and its conductivity is proportional to the concentration or the amount of the alkalis or ions in the thin layer. Therefore

$$R = \sum R_i = \int \frac{dx}{kC}$$

C changes with time and the position in the membrane during the doping process. Before the lag time the concentration of the alkali or ions in the center of the membrane is zero. After lag time the concentration in the center increases with time. At certain point the concentration change with time is shown in Figure 6.20 [37]. The concentration change along the thickness at different time is shown in Figure 6.21 [37]. From the tendency of the concentration change with time and distance, the conductivity increase should not have sharp steps. This inference indicates that the doping process is not controlled by diffusion.

The first step should be due to the permeation of the alkali in pure PBI membrane. It is controlled by the interaction between the polymer and the alkali. It is supposed that the diffusion rate is much faster than the interaction rate. The concentration of the alkali on the permeation edge is the same as that in the completely doped bulk of the polymer. When the permeation process is completed, the two edges merge at the center of the membrane or the permeation reaches the lag time, and the concentration of the alkali is uniform in the whole membrane. Before this time there is always a thin layer of pure PBI

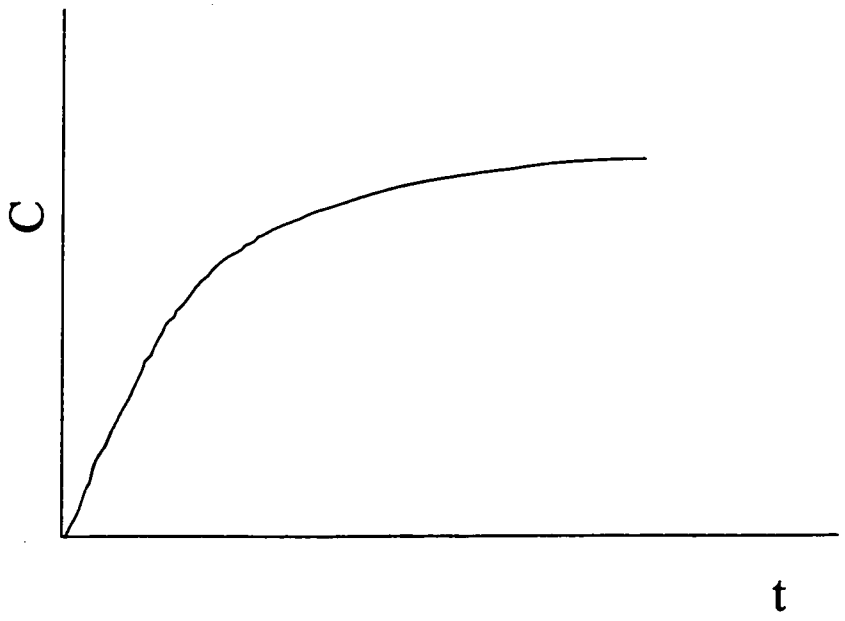

Figure 6.20. The concentration change with time during diffusion process in polymer at a positive position

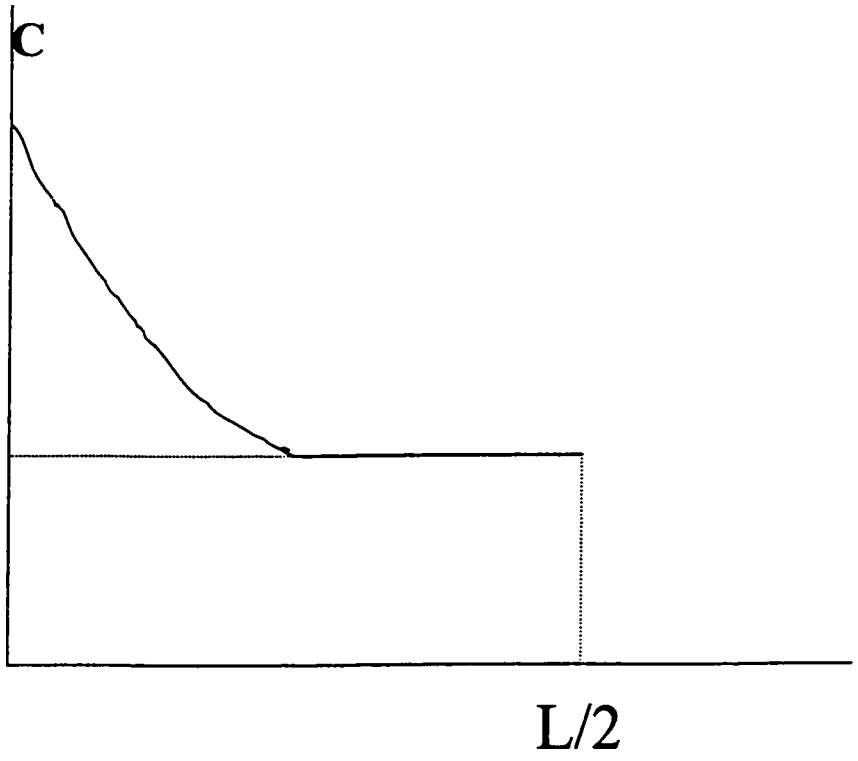

Figure 6.21. The concentration distribution of alkali in polymer at certain time before lag time

polymer as an ionic insulator. As a result the ionic conductivity of the membrane is in the ionic insulator range. At the lag time the whole membrane becomes an ionic conductor and its conductivity has a jump because of the jump of concentration in the middle of the membrane at the moment. This behavior is different from that if the diffusion process is rate control step. The type and concentration of the alkali affect the relative rate of the diffusion and interaction. In KOH the relative rate of the interaction with respect to diffusion is faster than in both NaOH and LiOH. This makes the conductivity change in KOH greater after the first step than in NaOH and LiOH as shown in Figure 6.3, 6.4 and 6.5. In LiOH the relative rate of the interaction to diffusion is the slowest so that the conductivity change in LiOH is completed after the first step. The results indicate that interaction dominates in the first step in the doping process in KOH. Diffusion has limited contribution to the doping rate in the first step. In LiOH the diffusion effect on the first step rate is even smaller than in KOH.

Concentration affects the diffusion and the interaction rate. Because the concentration at the center of the membrane is zero, the diffusion rate is proportional to the concentration. The ratio of lgS_3-lgS_2 to t_3-t_2 could be an indicator. However the ratio distributes widely because the second step process affects the accuracy of the data reading.

4.3. Permeability of Alkalis in pure PBI

The absolute value of the permeability coefficient of alkalis in pure PBI membrane cannot be directly determined because the absolute concentration of the alkalis in the membrane at t_l is unknown. However the tendency and the factors can be shown with t_l. The relative permeability, t_l, is shown in Figure 6.22. The permeability of different kind of alkalis is in the order KOH≥NaOH>>LiOH. The permeability coefficient has a maximum at around 8 M in NaOH, at 6 M in KOH. These results confirm the result of the two-stage experiment [36]. In LiOH the concentration effect on permeability is different.

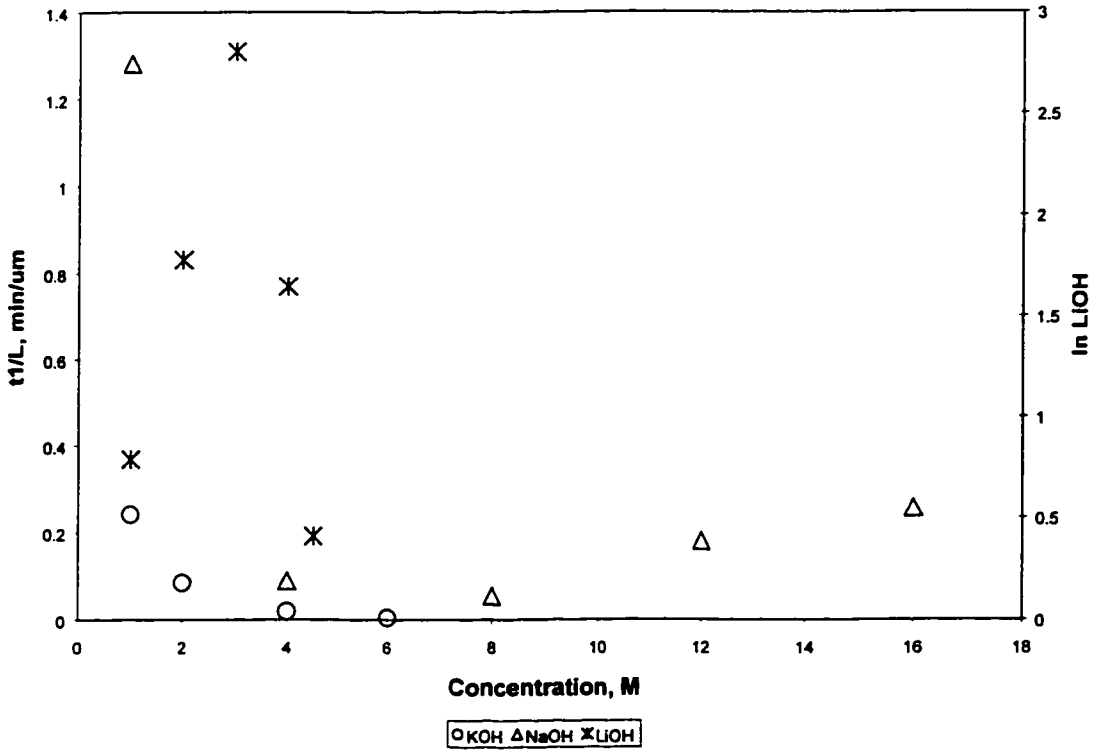

Figure 6.22. The permeation rate of alkalis in pure PBI membrane

The existence of other ions affects the permeability of alkalis in pure PBI membrane. The CO_3^{2-} in 6 M KOH can decrease the permeability of KOH, and delay the first step. The results in Figure 6.23 clearly show the delay. The effect of CO_3^{2-} increases with the concentration. This indicates that the permeability of KOH is determined by both K^+ and OH^-, not only K^+ or OH^-. The existence of CO_3^{2-} dilutes the effective concentration of KOH in the polymer. This indicates that OH^- is more effective than CO_3^{2-}. The existence of CO_3^{2-} also affects the conductivity of KOH in doped PBI. Figure 6.24 shows the conductivity decreases with CO_3^{2-} concentration in PBI doped in KOH + K_2CO_3 solution for 10 minutes. Even after long time doping the tendency is still the same as reported in the previous work [1].

The permeability coefficient of alkalis in blank PBI were also measured by time-lag method as a reference with the two-chamber cell used in previous work [35]. On one side of the blank PBI membrane the solution is 2 M NaCl, on the other side 16 M NaOH. The OH^- concentration change in the NaCl chamber in a time period of 400 minutes is shown in Figure 6.25a-6.25b. The lag time is 5 minutes from Figure 6.25b. At lag time point the change of the OH^- concentration is sharp. This indicates that the sorption process is not diffusion control and confirms the results from the kinetic study by conductivity. The curve bends to time axis at large time region, which shows that the permeability coefficient becomes smaller and smaller as time and thus concentration increases. The data support the results from the average concentration experiment [36]. However the time-lag method cannot be used for the second step, where the conductivity method for the kinetic study shows its advantage.

4.4. The relaxation of the PBI membrane

The second step is due to the membrane relaxation [38]. The relaxation time can be determined in the second step. The contribution of the two states of the polymer to its conductivity can be evaluated. The relaxation time per unit membrane thickness, $(t_4-t_3)/l$, is shown in Figure 6.26. In NaOH the relaxation time has a minimum at around 12 M. At

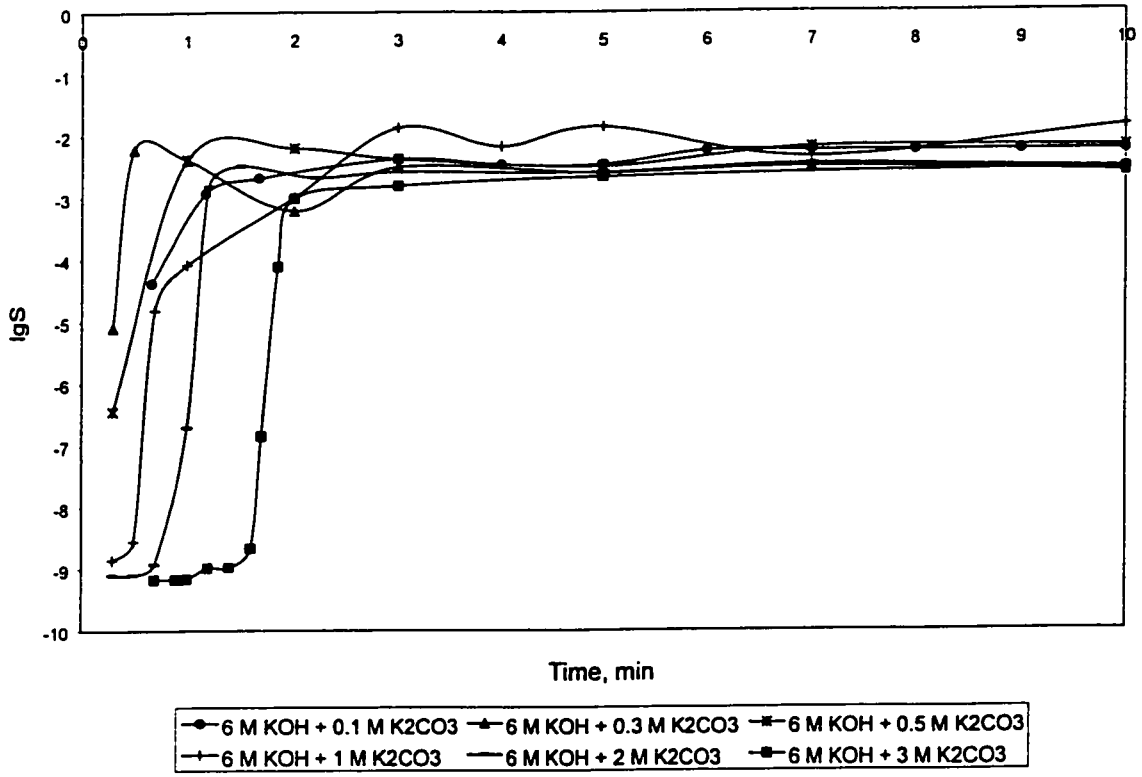

Figure 6.23. The effect of CO_3^{2-} on the conductivity of alkalis in pure PBI membrane

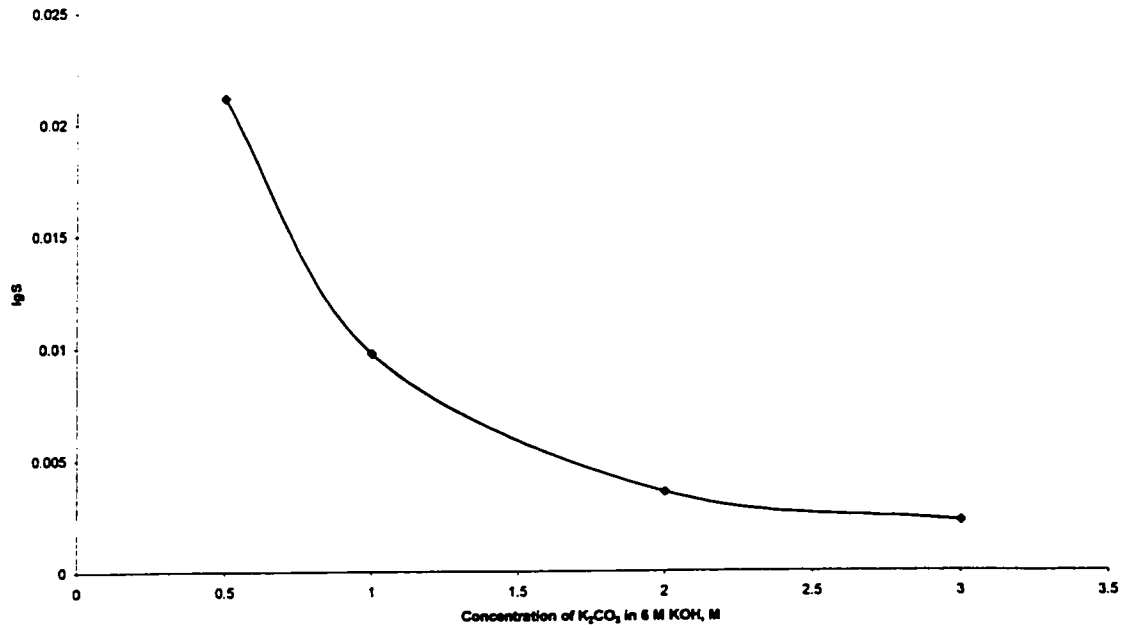

Figure 6.24. The effect of CO_3^{2-} on the conductivity of PBI membrane after doping 10 min in KOH solution

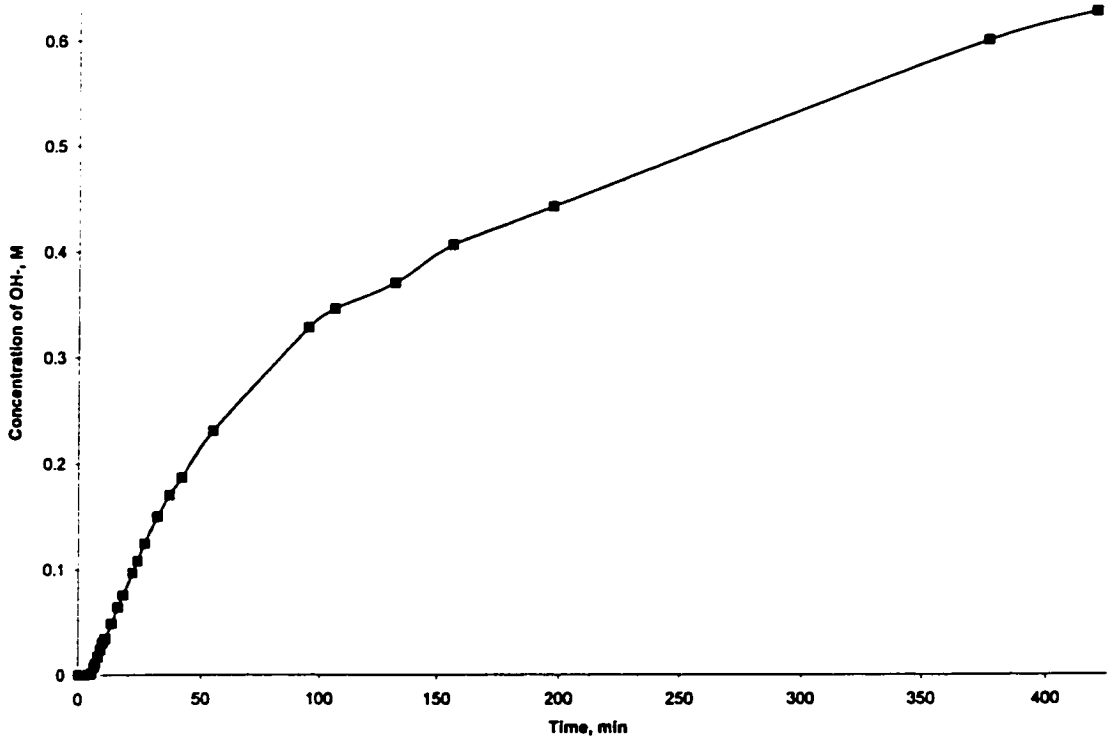

Figure 6.25-a. The NaOH concentration change in measuring permeability coefficient by time-lag method

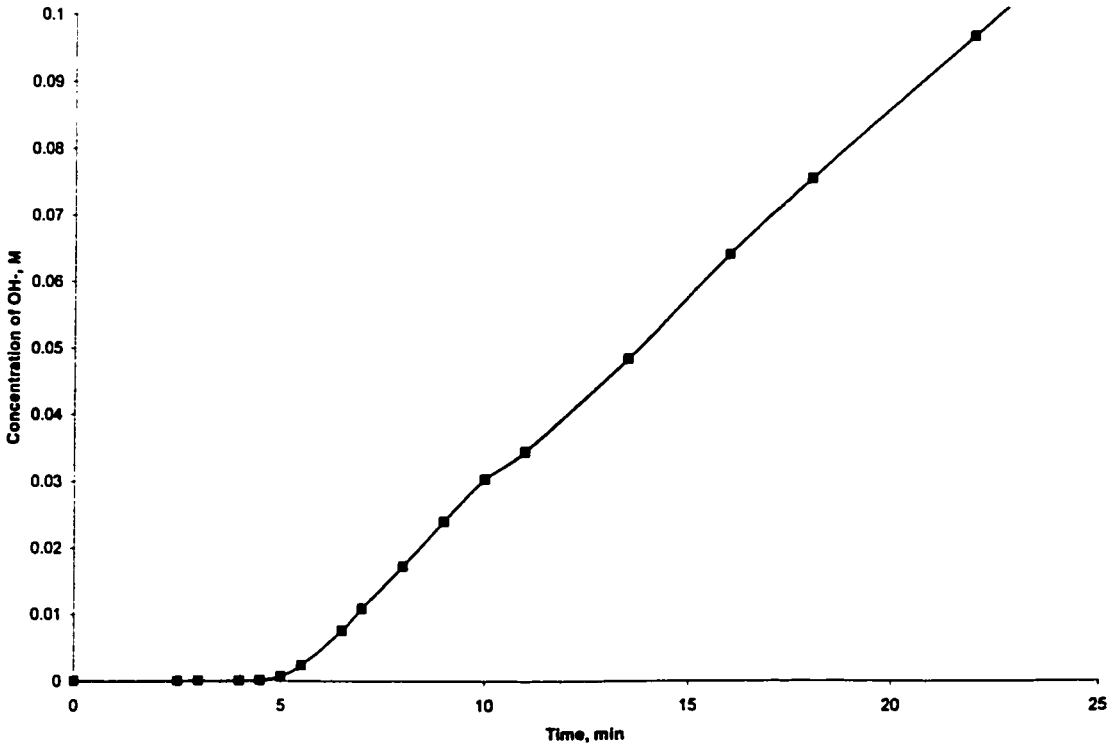

Figure 6.25-b. The NaOH concentration change in measuring permeability coefficient by time-lag method during the beginning of the measurement

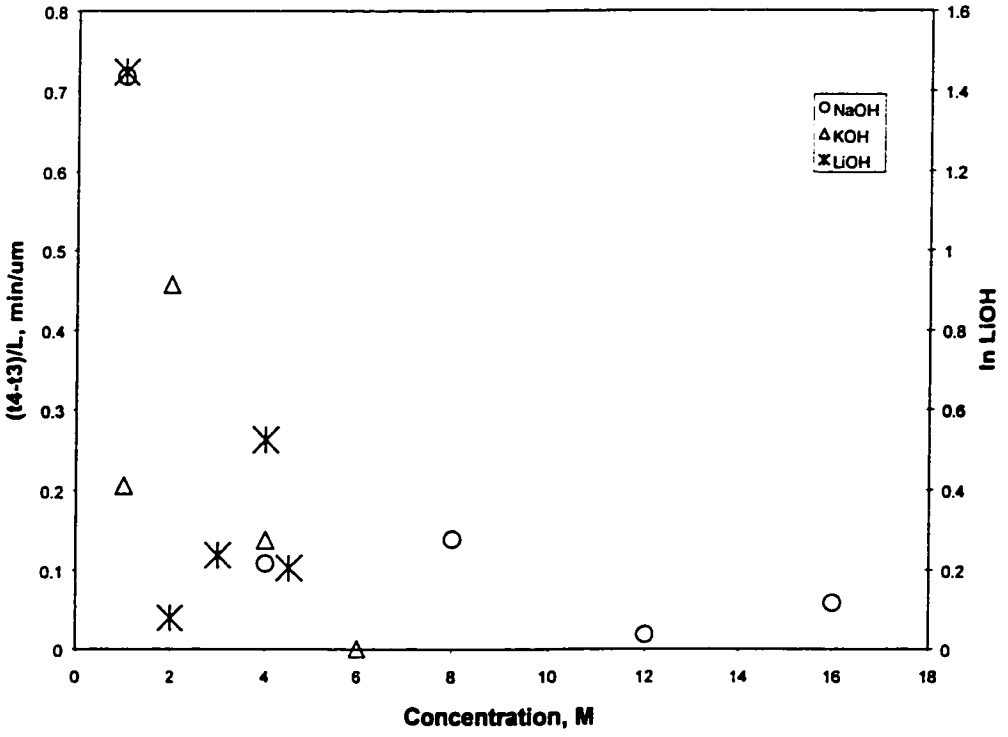

Figure 6.26. The relaxation time of PBI membrane during alkali sorption in alkaline solution

1 M the relaxation time is much longer than at other concentrations. In KOH it has a maximum at 2 M. In LiOH there is a minimum at 2 M. PBI has longer relaxation time in LiOH than in KOH and NaOH because LiOH is a relatively weaker alkali.

The relative contribution of the two steps to the conductivity of the PBI membrane in different alkaline solutions can be measured by $(lgS_2\text{-}lgS_1)/(lgS_5\text{-}lgS_4)$ as shown in Figure 6.27. The contribution of the first step in LiOH and KOH is larger than the second step. In NaOH at low concentration the contribution of the first step is larger than the second step in the scale of lgS (increased ratio). At high concentration, >12 M, the contribution of the second step is larger than the first one. This is because in LiOH the second step is slow to reach the equilibrium. The data taken here are not at equilibrium. In KOH (>6 M) the two steps are too close to distinguish. The second step is always more important than the first one in absolutely value of the conductivity. This shows that the structure of the membrane after doping is important to its conductivity. It can be explained as that the movement of the ions in the membrane after the second step is much easier than before that. The CO_3^{2-} does not affect the second step in the doping process in 6 M KOH solution.

The thickness of the PBI membrane increases during the doping process while the surface area does not change obviously. The increase in thickness depends on the type and concentration of the alkali as shown in Figure 6.28-6.30. High alkaline concentration causes larger increase in the thickness. There is a maximum in KOH or NaOH at 6 or 10 M. The high concentration part rises up with doping time increase. The low concentration part can reach equilibrium state in a shorter time. However the conductivity of the membrane just achieving the second step is 40 times lower than that of the long time doping at the maximum point in KOH and 50 times lower than that in NaOH, as shown in Figure 6.31 and 6.32. This shows that the relaxation is slow to reach the equilibrium after the second step. In LiOH the thickness and the conductivity increase with the concentration of LiOH and doping time, as shown in Figure 6.30 and 6.33. The time

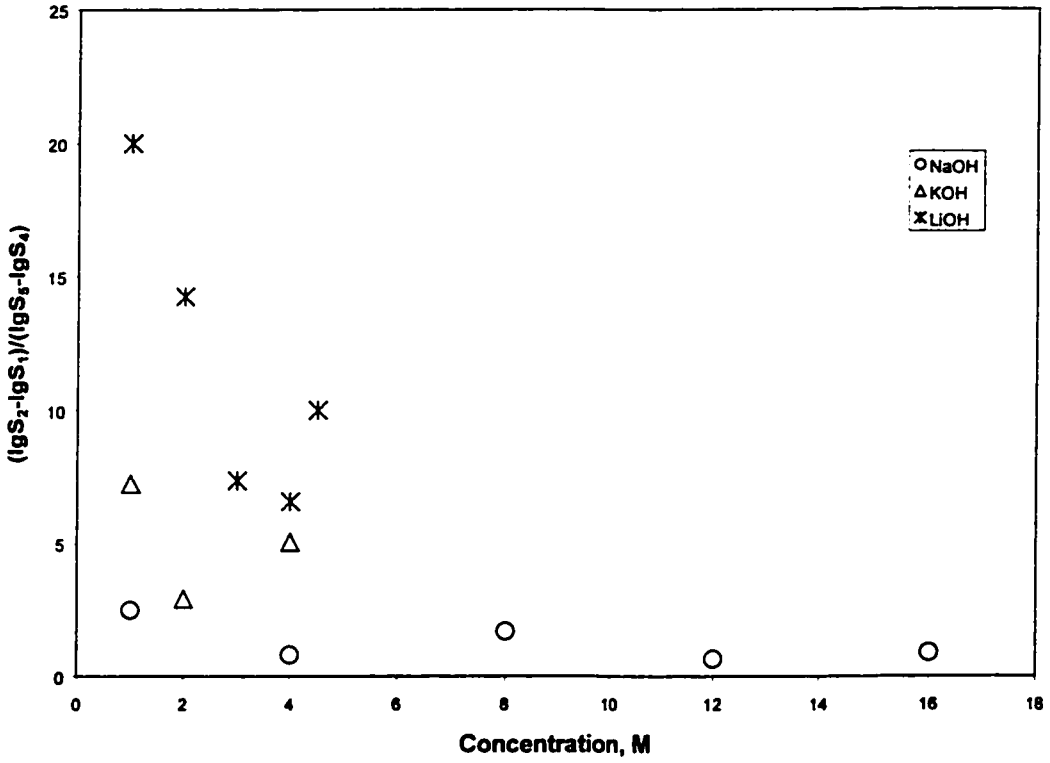

Figure 6.27. The contribution of the two steps to the conductivity of the PBI membrane

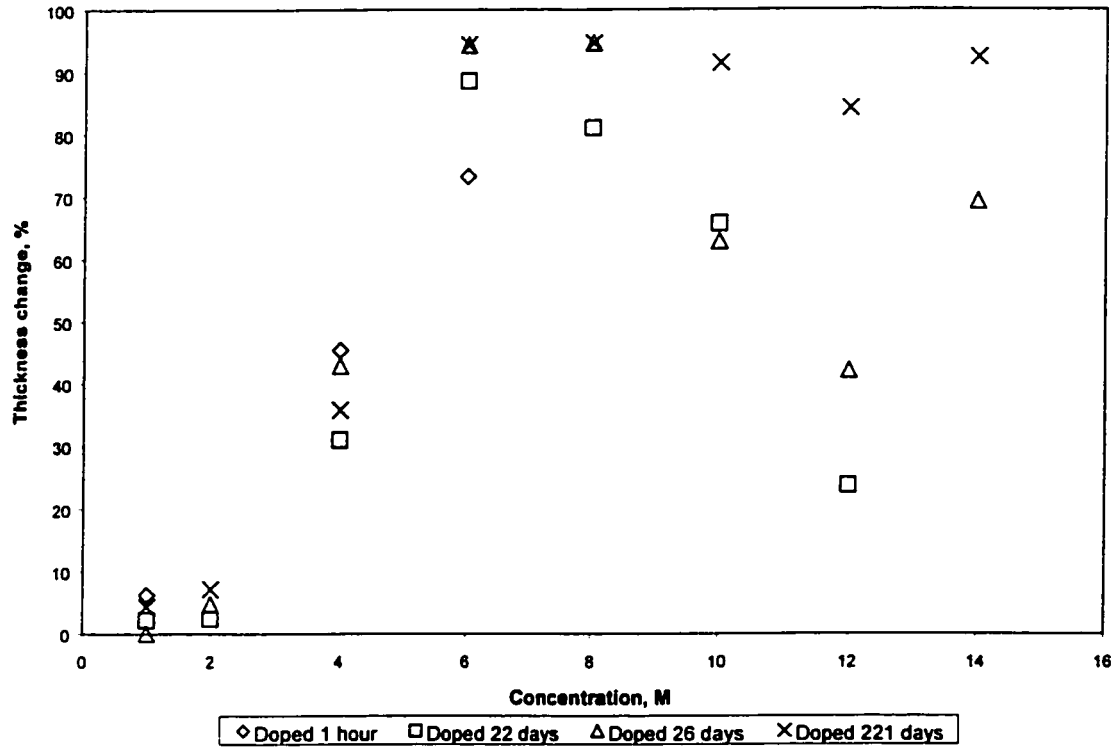

Figure 6.28. The thickness change of PBI membrane with time and concentration during doping process in KOH

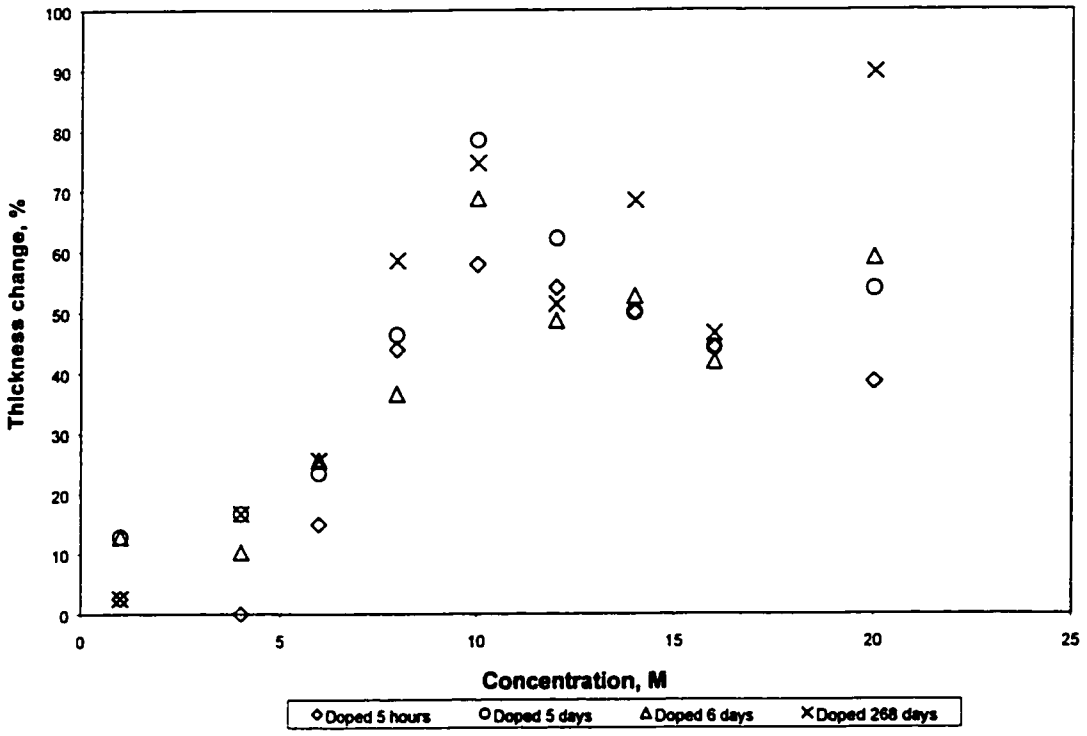

Figure 6.29. The thickness change of PBI membrane with time and concentration during doping process in NaOH

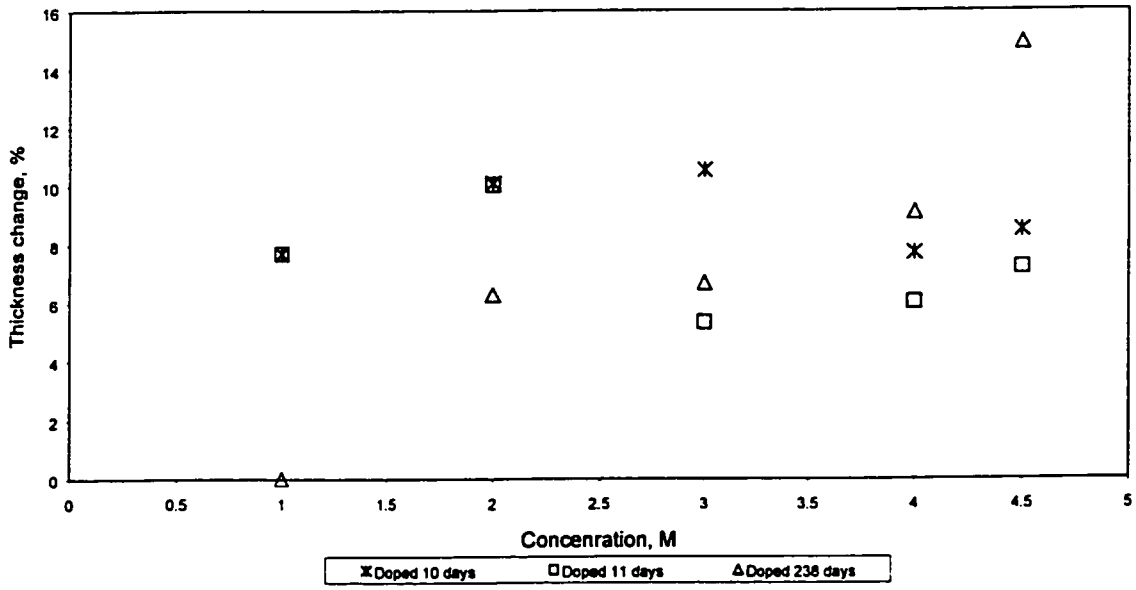

Figure 6.30. The thickness change of PBI membrane with time and concentration during doping in LiOH

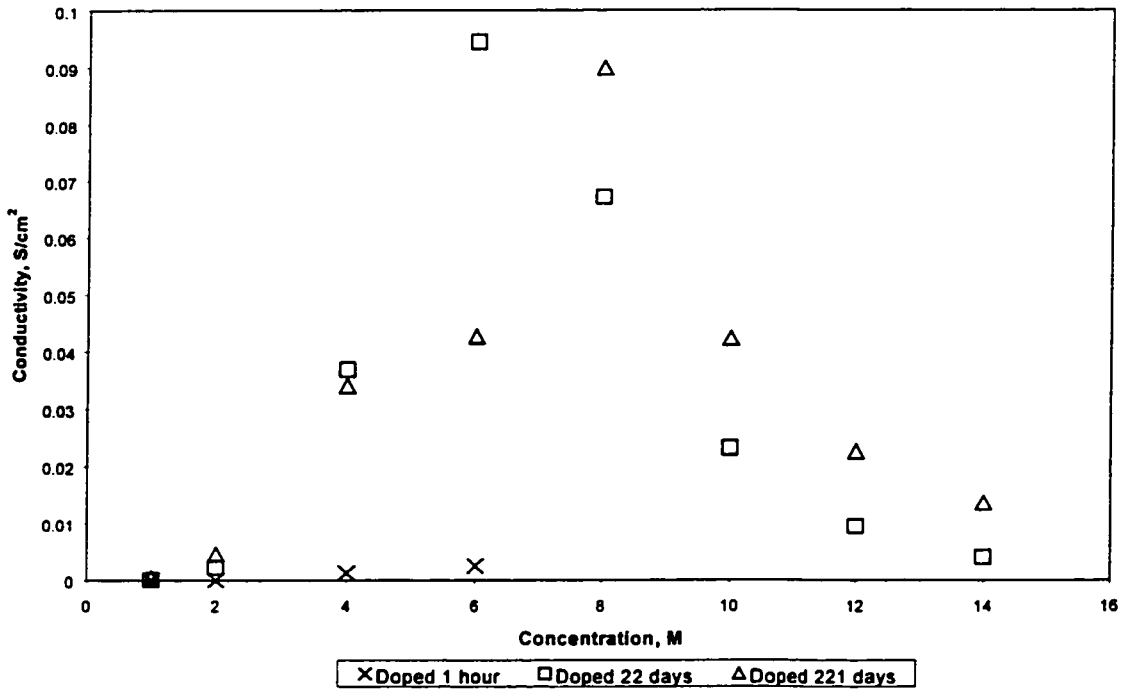

Figure 6.31. The conductivity change of KOH doped PBI membrane with concentration of KOH at different doing time

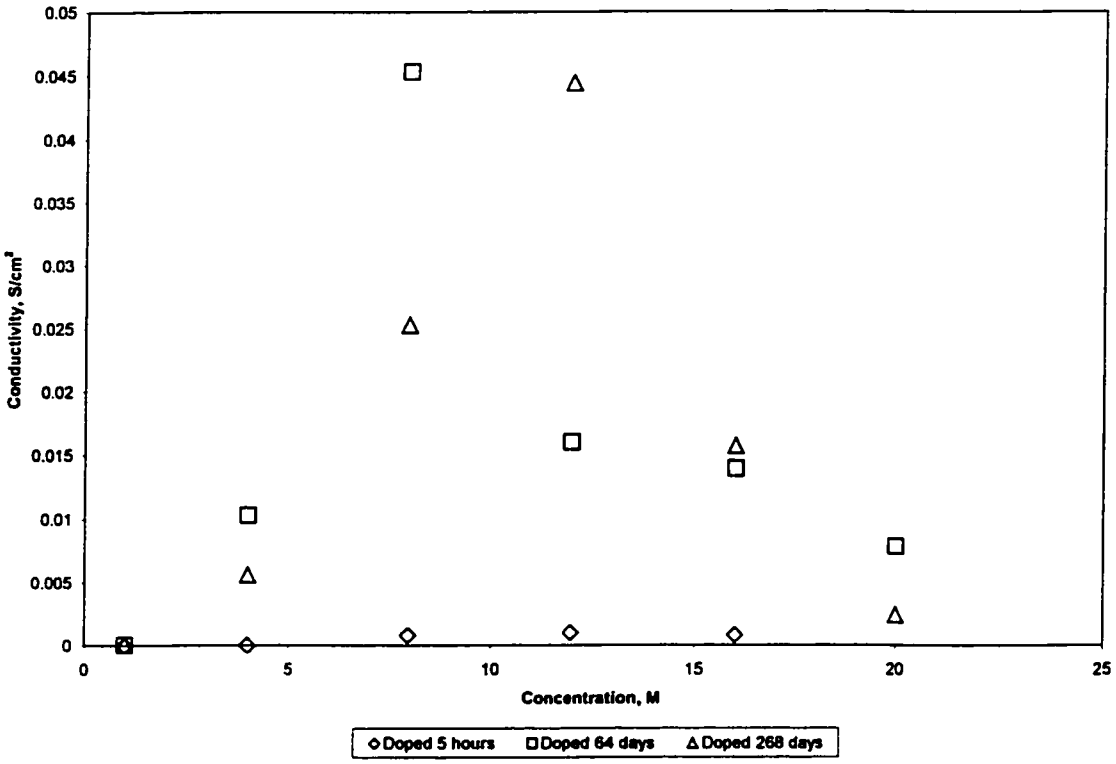

Figure 6.32. The conductivity change of NaOH doped PBI membrane with the concentration of NaOH and doping time

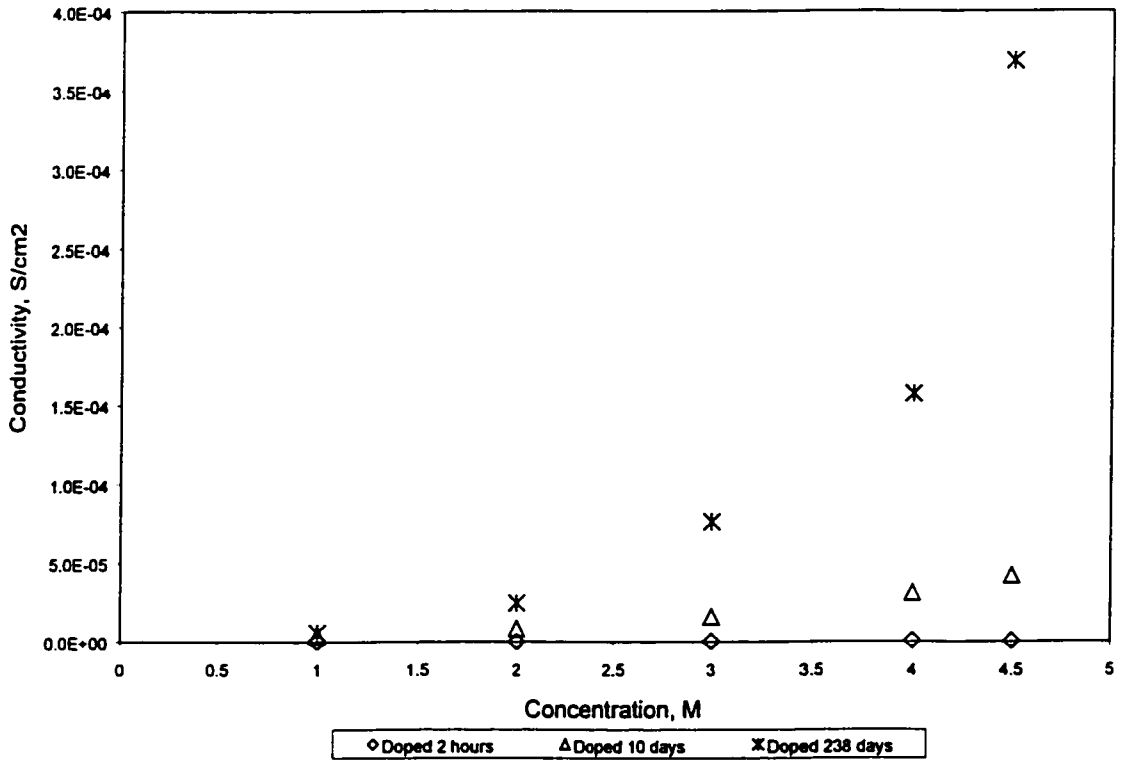

Figure 6.33. The conductivity change of LiOH doped PBI membrane with concentration of LiOH and doping time

effect on thickness increase is stronger than in KOH and NaOH. The time effect order is LiOH>>NaOH>KOH. The thickness increase is in the order KOH>NaOH>>LiOH. The thickness and conductivity change with the concentration of the alkalis and the doping time indicates that water concentration in the solution is an important factor because it affects the activity of the alkalis. The structure change of the membrane after the second step continues. It can be found from the S-time curve, not lgS-time curve, because the conductivity increases with time continually. This part is the main contribution to the conductivity.

To find out the structure effect on the conductivity the structure study on the PBI membrane after the first step and the second is needed.

5. Conclusions

The doping process is a two-step sorption process. The second step contributes more to the conductivity increase of the PBI membrane. The structure of the membrane affects the conductivity. The type and the concentration of the alkali affect the doping process. In KOH the doping process is the fastest and the resulted PBI membrane has the highest conductivity. The doping process is the slowest in LiOH solution.

The comparison of the results obtained in this work with the results from conventional research methods shows that the conductivity change during doping process can be used as a means for the kinetic study of the polymer sorption process in electrolyte solution. In the doping process two types of sorption mechanism exit, the diffusion of the species in polymer and the interaction between polymer and the species. It is proposed that the two types of sorption play different roles in different stages of the doping process. The results on conductivity change with time during the doping process proved that the proposed model represents the physical process.

6. References

[1] B. Xing and O. Savadogo, *Electrochemical communication*, **2,** 697 (2000)

[2] G. P. Schulman and W. Lochte, *J. Macromol. Sci. Chem.*, **1,** 413 (1967).

[3] Y. Tsur, Y. L. Freilich, and M. Levy, *J. Polym. Sci.*, **12,** 1531 (1974).

[4] D. N. Gray, G. P. Schulman, and R. T. Conley, *J Macromol. Sci. Chem.*, **1,** 395 (1967).

[5] Dale A. Chatfieleld, *J. Polym. Sci. Chem.*, **19,** 601 (1981).

[6] M. B. Gieselman, and J. R. Reynolds, *Macromolecules*, **26,** 5633 (1993).

[7] P. Musto, F. E. Karasz and W. J. Macknight, *polymer*, **34,** 2934 (1993).

[8] D. Weng, J. S. Wainright, U. Landau, and R. F. Savinell, *J. Electrochem. Soc.*, **143,** 1260 (1996).

[9] D. WENG, J. S. Wainright, U. Landau, and R. F. Savinell, p. 201, in *Electrode Materials and Processes for Energy Conversion and Storage*, S. Srinivasan, D. D. Macdonald, and A. C. Khandkar, Editors, PV 94-23, p. 201 *The Electrochemical Society Proceedings Series*, Pennington, NJ (1994)

[10] B. Xing, O. Savadogo, *J. New Mat. Electrochem. Syst.*, 2 (1999) 95.

[11] H. A. Pohl and R. P. Chartoff, *J. Polym. Sci. Part A*, **2,** 2787 (1964).

[12] S. M. Aharoni and M. H. Litt, *J. Polym. Sci. Polym. Chem. Ed.*, **12,** 639 (1974).

[13] D. Hoel and E. Grunwald, *J. Phys. Chem.*, **81,** 2135 (1977).

[14] S. M. Aharoni and A. J. Signoreli, *J. Appl. Polym. Sci.*, **23,** 2653 (1979).

[15] J. S. Wainright, J. T. Wang, D. Weng, R.F. Savinell, M. Litt, *J. Electrochem. Soc.*, **142,** L121 (1995).

[16] S. R. Samms, S. Wasums, and R. F. Savinell, *J. Electrochem. Soc.*, **143,** 1225 (1996).

[17] D. Weng, J. S. Wainright, U. Landau, and R. F. Savinell, *J. Electrochem. Soc.*, **143,** 1260 (1996).

[18] W. F. Lin, J. T. Wang, and R. F. Savinell, *J. Electrochem. Soc.*, **144,** 1917 (1997).

[19] J. S. Wainright, R. F. Savinell and M. H. Litt, in *"Proceeding of the second International Symposium on New Materials for Fuel Cell and Modern Battery*

system", Eds. O. Savadogo and P. R. Roberge, Montreal, Canada, July 6-7, (1997), p. 808.

[20] J. T. Wang, J. S. Wainright, R. F. Savinell, M. Litt, *J. Appl. Electrochem.*, **26,** 751 (1996).

[21] J. T. Wang, S. Wasmus, and R. F. Savinell, *J. Electrochem. Soc.*, **143,** 1233 (1996).

[22] S. Wasmus, J. T. Wang, and R. F. Savinell, *J. Electrochem. Soc.*, **142,** 3825 (1995).

[23] Jiangtao Wang, S. Wasmus, and R. F. Savinell, *J. Electrochem. Soc.*, **142,** 4218 (1995).

[24] J. T. Wang, R. F. Savinell, J. Wainright, M. Litt, and H. Yu, *Electrochimica Acta,* **41,** 193 (1996).

[25] R.S. Bogner, Electron Dyn. Div., Hughes Aicr. Co., Proc. Intersoc.

[26] CT, USA, Avail.NTIS, Nada [Contract. Rep.] CR (1978), NASA-CR-159653, FCR-1017, 73 pp. From: Sci. Tech. Aerosp. Rep. 1979, 17(24), Abstr. No. N79-33581. CODEN: NSCRAQ ISSN: 0565-7059.

[27] R.E. Martin, Power Syst. Div., United Technol. Corp., South Windsor, CT, USA, Avail. NTIS, NASA [Contract. Rep,] CR (1979), (NASA-CR-159807, FCR-1657), 52 pp. From: Sci. Tech. Aerosp. Rep. 1980, 18(10), Abstr. No. N80-19615. CODEN: NSCRAQ ISSN: 0565-7059.

[28] U.S. Pat. 5,71,038, B. Vyas, (Bell Telephone Laboratories) (Sept. 11, 1984).

[29] G. M. Barrow, *Physical chemistry,* McGraw-Hill Inc., New York, p217, 1988.

[30] D. R. Paul, *J. Polymer Physics*, **A2, 8,** 1811 (1970).

[31] J. H. Petropoulos, *J. Polymer Physics*, **A2, 8,** 1797 (1970).

[32] D. R. Paul, W. J. Koros, *J. Polymer Science, Polymer Physics*, 14,675 (1976).

[33] W. J. Koros, D. R. Paul, A. A. Rocha, *J. Polymer Science, Polymer Physics*, 14,687 (1976).

[34] B. Tazi and O. Savadogo, *in "Proceedings of the Second International Symposium on New Materials for Fuel Cell and Modern Battery Systems" Eds, O. Savadogo and P. R. Roberge, Montreal Canada,* July 6-10, 1997, p864.

[35] B. Xing and O. Savadogo, "The mass transport properties of PBI in alkaline solutions" To be published

[36] B. Xing and O. Savadogo, "The sorption process of acid in PBI membrane" To be published

[37] R. McGregor, "Diffusion and Sorption in Fibers and Films", Volume1, "An Introduction with particular reference to dyes", Academic Press Inc., London and New York, 1974.

[38] P. Neogi, "Diffusion in polymers", Marcel Dekker inc, New York, Basel and Hong Kong, 1996.

Chapter 7

CONCLUSIONS, CONTRIBUTIONS AND SUGGESTIONS

1. Conclusions

The study on the conducting behavior of PBI under various conditions is vital to the understanding of the mechanism of the doping process and the mechanism on the conductivity of blank and doped PBI, and to the development of solid electrolyte for fuel cells. The thesis has established the experimental and theoretical foundation for a new approach to the study of sorption kinetics in electrolyte solution. For the first time the experimental methodology on the study of the sorption process of membrane in electrolyte solution by monitoring the conductivity change with time was established. The confusion regarding the electrochemical property on PBI membrane is resolved. The mechanism of the doping process and mechanism on conductivity were proposed. The behavior of the PBI in alkaline solution and alkaline doping process were investigated. The highlights of the work are listed.

1.1 Experiments

- The conductivity of PBI membrane changes with the testing environment and with time. The measurement should be done in a dynamic mode that is to measure the conductivity change with time.

1.2. Blank PBI

- Blank PBI is ionic and electronic insulator in HCl, HNO_3, $HClO_4$, H_2SO_4 and H_3PO_4 solutions.

- The conductivity and concentration dependency.

- The conductivity decreases when the acid concentration increases in the case of HCl or H_3PO_4.
- The conductivity increases with the acid concentration in $HClO_4$.
- The acid concentration has no effect on conductivity in HNO_3 and H_2SO_4

- The conductivity and acid type dependency
  - In 2M acid solutions, the conductivity increases with electrolytes in the order of H_3PO_4>HCl>$HClO_4$>HNO_3>H_2SO_4.
  - In ≥ 8M acid solutions, the conductivity increases in the order of $HClO_4$> HNO_3> H_2SO_4>HCl.>H_3PO_4.

1.3. Acid-doped PBI

- Acid doping process is a two-step sorption process.
- The conductivity of PBI doped with high concentration acids (≥8M) increases with the type of the doping acids in the order: H_2SO_4 > H_3PO_4 > $HClO_4$> HNO_3>HCl.
- The conductivity of PBI doped with low concentration acids (≤2M) increases with the type of the acids in the order: H_3PO_4> H_2SO_4>HCl >HNO_3>$HClO_4$.
  - The weaker proton in multiproton acid is loosely bounded with PBI and is freer to conduct ions.
- Conductivity and acid concentration dependency
  - The conductivity increases with the concentration of the acid monotonously.

- The conductivity is related to the amount of the acid sorbed in PBI, not the crystallinity.

- The conductivity increasing rate with the concentration is higher at high concentration range than at low concentration. This indicates that the extra acid sorbed at high concentration, having a looser combination with the PBI molecules, attributes more to the conductivity.

- The morphology effect by annealing

  - The conductivity of PBI doped in 16 M H_2SO_4 is 0.06 S/cm. After being dried in air (annealing) for more than seven days it is 0.1 S/cm in the same testing solution.

  - Drying the PBI membrane doped in 16 M H_2SO_4, (e.g. annealing), can significantly improve the performance in H_2/O_2 fuel cell.

- The performance of H_2SO_4-doped PBI membrane in H_2/O_2 fuel cell changes with temperature in the order 70°C < 50°C < 30°C. It indicates the effect of dehydration process in the membrane.

- The PBI membrane doped with 85% H_3PO_4 has improved performance in H_2/O_2 fuel cell at 185°C, even using H_2 with 3% CO.

1.4. Alkali-doped PBI

- The PBI membrane becomes ionic conductor from insulator after doped in alkaline solution.

- The alkaline-doped-PBI conductivity changes with the type of alkaline electrolyte. The conductivity increases with the strength of the alkaline agent in the order of, KOH>NaOH>LiOH.

- In NaOH and KOH, there is a maximum in the curve of conductivity vs. concentration. In the case of LiOH, no maximum was observed on the curve of conductivity vs. concentration up to the saturation concentration (4M)

- The highest conductivity of KOH-doped PBI at 25°C is higher than the optimum values of both H_2SO_4 or H_3PO_4-doped PBI and Nafion® 117.

- The presence of carbonate in the alkaline solution decreases the conductivity of the doped PBI membrane. However, PBI doped in the solution at high K_2CO_3 concentration (even saturate) still has a higher conductivity than that of Nafion

- The dependencies of conductivity on temperature for KOH-doped PBI and KOH + K_2CO_3-doped PBI are different. The conductivity of KOH-doped PBI is more temperature sensitive. This may indicate that the conduction mechanisms are different in the two systems.

- The improvement in the conductivity of the alkali-doped PBI might be attributed to the specific modification of PBI by the whole alkali molecule and OH^-, but not to the isolated cations of the alkaline electrolyte. OH^- breaks the hydrogen bounds between the PBI molecules. It makes the ions easy to pass through the membrane. When CO_3^{2-} exists in the membrane it replace some OH^- and decreases the conductivity.

- The permeability of KOH, NaOH, and LiOH in alkali-doped PBI membrane is concentration dependent. The permeability dependence on concentration is similar to the conductivity dependence on the concentration of alkaline solution, but at lower extent.

- The conductivity of the alkali-doped PBI depends on the strength of the alkaline solution and the structure of alkali-doped PBI, not simply on the permeability.

- The permeability of water in alkali-doped PBI membrane depends on the type (strength) and concentration of the alkaline solution.
- The ion transference numbers of K^+, Na^+ and Li^+ in alkali-doped PBI membrane decrease while the concentration of alkaline solution increases.
- Both the cations and OH^- participate in the current transport and contribute to the ionic conductivity.
- The doping process in alkaline solution is also a two-step sorption process.
- The permeability of the alkali in pure PBI can be calculated from the first step.
- The relaxation time of PBI membrane in alkaline solution can be calculated from the second step.
- The relaxation time decreases in alkali in the order KOH < NaOH < LiOH.
- The permeability of alkali increases in the order KOH > NaOH > LiOH.
- These facts indicate that the concentration of OH^- determines the structure of the doped membrane; in turn the morphology determines the conductivity.
- In H_2/O_2 fuel cell the KOH-doped PBI membrane performs as well as Nafion® 117.

2. Contributions to knowledge

- Experimentally proved that blank PBI is an ionic insulator for the first time. The doping process in acid and alkali changes the PBI membrane into ionic conductor.
- The methodology on the study of the sorption process of membrane in electrolyte solution was established.

- The two-step sorption process of PBI in acid or alkaline solution was discovered.
- The ionic conducting mechanism was proposed.
- The fuel cell performance of high concentration acid or alkali doped PBI membrane in H_2/O_2 fuel cell has been conducted for the first time.
- A new field for alkaline type PEM in fuel cell is introduced.

3. Suggestions for future work

- Establish the relationship on the morphology structure and the conductivity of acid or alkali doped PBI.
- Construct new solid polymer electrolyte system applying the mechanism established in this work.

Bibliography

[1] G. M. Barrow, *Physical chemistry,* McGraw-Hill Inc., New York, 1988.

[2] L. J. M. J. Blomen and M. N. Mugerwa, *Fuel Cell Systems*, Plenum Press, New York and London, 1993.

[3] G. H. J. Broers and J. A. A. Ketelaar, *Fuel cells,* ed. G. J. Young, Reinhold Pub. Corp., New York, 1960.

[4] D. P. Wilkinson and D. Thompsett, in *"Proceeding of the second International Symposium on New Materials for Fuel Cell and Modern Battery system"*, Eds. O. Savadogo and P. R. Roberge, Montreal, Canada, July 6-7, (1997), p. 266.

[5] H. Wendt, in *"Proceeding of the second International Symposium on New Materials for Fuel Cell and Modern Battery system"*, Eds. O. Savadogo and P. R. Roberge, Montreal, Canada, July 9-13, (1995), p. 532.

[6] L. Giorgi, E. Antolini, A. Pozio and E. Passalacqua, *Proceedings of Fuel Cell Seminar,* November 17-20, 1996, Orlando.

[7] V. A. Paganin, E. A. Ticianelli and E. R. Gonzalez, *J. Appl. Electrochem.* 23, 1107 (1993)

[8] O. Savadogo and M. Lacroix, in *"Proceeding of the second International Symposium on New Materials for Fuel Cell and Modern Battery system"*, Eds. O. Savadogo and P. R. Roberge, Montreal, Canada, July 6-7, (1997), p873.

[9] L. Giorgi, E. Antolini, A. Pozio and E. Passalacqua, *Electrochimica Acta,* 43 (24), 3675 (1998).

[10] D. Raistrick, U.S. Patent No. 4876115 (1989).

[11] M. S. Wilson and S. Gottesfeld, *J. of Appl. Electrochem.*, 22, 1 (1992).

[12] Z. Poltarzewski; P. Staiti; V. Alderucci; W. Wieczorek; N. Giordano, *J. Electrochem. Soc.* 139(3), 761 (1992).

[13] J. Appleby, *Fuel Cell Handbook*, New York: Van Nostrand Reinhold, 1989.

[14] O. Savadogo, *Journal of New Materials for Electrochemical Systems*, 1(1), 47 (1998).

[15] S. Escribano, S. Miachon and P. Aldebert, in *"Proceeding of the first International Symposium on New Materials for Fuel Cell and Modern Battery system"*, Eds. O. Savadogo, P. R. Roberge, and T. N. Veziroglu, Montreal, Canada, July 9-13, (1995), p. 135.

[16] S. Besse, G. Bronoel, N. Tassin, Y. Naimi, A. Tounsi, in *"Proceeding of the first International Symposium on New Materials for Fuel Cell and Modern Battery system"*, Eds. O. Savadogo, P. R. Roberge, and T. N. Veziroglu, Montreal, Canada, July 9-13, (1995), p. 144.

[17] M. S. Wilson, C. R. Derouin, J. A. Valerio and S. Gottesfeld, in *"28th intersociety Energy Conversion Engineering Conference Proceedings Atlanta, August, (1993) (American Institue of Aeronautics and Astronautics, Washington, DC (USA), 1994)*, p. 1.1203.

[18] R. Kumer and S. Ahmed, in *"Proceeding of the first International Symposium on New Materials for Fuel Cell and Modern Battery system"*, Eds. O. Savadogo, P. R. Roberge, and T. N. Veziroglu, Montreal, Canada, July 9-13, (1995), p. 224.

[19] M. Kahlich, M. M. Schubert, M. Huttner, M. Noeske, H. A. Gasteiger and R. J. Behm, in *"Proceeding of the second International Symposium on New Materials for Fuel Cell and Modern Battery system"*, Eds. O. Savadogo and P. R. Roberge, Montreal, Canada, July 6-10, (1997), p. 642.

[20] G. P. Schulman and W. Lochte, *J. Macromol. Sci. Chem.*, 1, 413 (1967).

[21] Y. Tsur, Y. L. Freilich, and M. Levy, *J. Polym. Sci.*, 12, 1531 (1974).

[22] D. N. Gray, G. P. Schulman, and R. T. Conley, *J Macromol. Sci. Chem.*, 1, 395 (1967).

[23] Dale A. Chatfieleld, *J. Polym. Sci. Chem.*, 19, 601 (1981).

[24] M. B. Gieselman, and J. R. Reynolds, *Macromolecules*, 26, 5633 (1993).

[25] P. Musto, F. E. Karasz and W. J. Macknight, *polymer*, 34, 2934 (1993).

[26] D. Weng, J. S. Wainright, U. Landau, and R. F. Savinell, *J. Electrochem. Soc.*, 143, 1260 (1996).

[27] D. Weng, J. S. Wainright, U. Landau, and R. F. Savinell, p. 201, in *Electrode Materials and Processes for Energy Conversion and Storage*, S. Srinivasan, D. D. Macdonald, and A. C. Khandkar, Editors, PV 94-23, p. 201 *The Electrochemical Society Proceedings Series*, Pennington, NJ (1994)

[28] H. A. Pohl and R. P. Chartoff, *J. Polym. Sci. Part A*, 2, 2787 (1964).

[29] S. M. Aharoni and M. H. Litt, *J. Polym. Sci. Polym. Chem. Ed.*, 12, 639 (1974).

[30] D. Hoel and E. Grunwald, *J. Phys. Chem.*, 81, 2135 (1977).

[31] S. M. Aharoni and A. J. Signoreli, *J. Appl. Polym. Sci.*, 23, 2653 (1979).

[32] J. S. Wainright, J. T. Wang, D. Weng, R.F. Savinell and M. Litt, *J. Electrochem. Soc.*, 142, L121 (1995).

[33] S. R. Samms, S. Wasums, and R. F. Savinell, *J. Electrochem. Soc.*, 143, 1225 (1996).

[34] W. F. Lin, J. T. Wang, and R. F. Savinell, *J. Electrochem. Soc.*, 144, 1917 (1997).

[35] J. S. Wainright, R. F. Savinell and M. H. Litt, in *"Proceeding of the second International Symposium on New Materials for Fuel Cell and Modern Battery system"*, Eds. O. Savadogo and P. R. Roberge, Montreal, Canada, July 6-7, (1997), p. 808.

[36] J. T. Wang, J. S. Wainright, R. F. Savinell and M. Litt, *J. Appl. Electrochem.*, 26, 751 (1996).

[37] J. T. Wang, S. Wasmus, and R. F. Savinell, *J. Electrochem. Soc.*, 143, 1233 (1996).

[38] S. Wasmus, J. T. Wang, and R. F. Savinell, *J. Electrochem. Soc.*, 142, 3825 (1995).

[39] Jiangtao Wang, S. Wasmus, and R. F. Savinell, *J. Electrochem. Soc.*, 142, 4218 (1995).

[40] J. T. Wang, R. F. Savinell, J. Wainright, M. Litt, and H. Yu, *Electrochimica Acta*, 41, 193 (1996).

[41] B. Xing, and O. Savadogo, *J. New Mat. Electrochem. Syst.*, 2 (1999) 95.

[42] E. J. Powers and G. A. Serad, *Proceedings of the Symposium on the History of High Performance Polymer* at the American Chemical Society Meeting, April 15-18, New York, 1986.

[43] A. K. Engel, T. Yoden, K.Sanui and N. Ogata, *Polymeric Materials Science and Engineering, Proceedings of the ACS Division of Polymeric Materials: Science and Engineering,* Vol. 54, p. 119, ACS, New York, Spring 1986.

[44] J. K. Gillham, *Critical Review of Macromolecular Science*, Vol. 1, p. 83, 1972.

[45] R. T. Conley, J. J. Kane and S. Ghosh, *Hoechst Celanese Corp. Technical Report AFML-TR-71-219 (November 1971)*

[46] J. R. Bron and N. Mc M. Browne, *Australian Def. Scient. Serv. Mtl. Res. Lab. Report MRL-R-674, Maribyrnong Victoria (August 1976)*, p. 4

[47] P. Hautojarvi, ed., "Positrons in Solids", Springer-Verlag, Berlin, Heidelerg (1979).

[48] Y. Kobayashi, W. Zheng, E. F. Meyer, J. D. McGervey, A. M. Jamieson, and R. Simha *Macromolecules,* 22, 2302 (1989).

[49] S. Tao *J. Chem. Phys.* 56, 5499 (1972).

[50] J. R.Steven, *Methods of Experimental Physics*, 16A, 371 (1980).

[51] D. M. Schrader and Y. C. Jean, eds., *Positron and Positronium Chemistry,* Elssevier, New York (1988).

[52] Q. Deng, F. Zandiehndem and Y. C. Jean, *Macromolecules*. 25, 1090 (1992).

[53] Q. Deng and Y. C. Jean, *Macromolecules*. 26, 30 (1993).

[54] H. Nakanishi, Y. C. Jean, E. G. Smith and T. C. Sandreczki, *J. Polym. Sci., B:* 27, 1419 (1989)

[55] Z. Yu, U. Yahsi, J. D. McGervey, A. M. Jamieson and R. Simha, *J. Polym. Sci., B: Polymer Physic,* 32, 2637 (1994).

[56] M. Y. Ruan, H. Moaddel, A. M. Jamieson, R. Simha and J. D. McGervey, *Macromolecules*. 25, 2407 (1992).

[57] O. A. Hasan, M. C. Boyce, X. S. Li and S. Berko, *J. Polym. Sci., B: Polymer Physic,* 31, 185 (1993).

[58] L. Xie, D. W. Gidley, H. A. Hristov and A. F. Yee, *J. Polym. Sci., B: Polymer Physic,* 33, 77 (1995).

[59] L. B. Liu, D. Gidley and A. F. Yee, *J. Polym. Sci., B: Polymer Physic,* 30, 231 (1992).

[60] J. E. Kluin, Z. Yu, S. S. Cleeshouwers, J. D. McGervey, A. M. Jamieson, R. Simha and K. Sommer, *Macromolecules.* 26, 1853 (1993).

[61] T. Suzuki, Y. Oki, M. Numajiri, T. Miura, K. Kondo and Y. Ito, *Polymer,* 34, 1361 (1993).

[62] J. A. Hinkley, A. Efrekhari, R. A. Crook, B. J. Jensen and J. J. Singh, *J. Polym. Sci., B: Polymer Physic,* 30, 1195 (1992).

[63] H. S. Sodaye, P. K. Pujari, A. Goswami and S. B. Manohar, *J. Polym. Sci., B: Polymer Physic,* 35, 771 (1997).

[64] H. Moaddel *Ph. D. thesis,* "Development and Characterization of Polybenzimidazole as a Solid Polymer Electrolyte", CWRU, (1996).

[65] R. F. Savinell and M. H. Litt, United States Patent, 5,716,727, (1998).

[66] H. A. Vogel and C. S. Marvel, *J. Polym. Sci.*, 50, 511 (1961).

[67] D. P. Griswald Jr., A. E. Casey, E. K. Weisberger and J. H. Weisburger, *Cancer Research,* 28, 924 (May 1968)

[68] K. C. B.Dangayach, K. A. Karim and D. C. Bonner, *J. Appl. Polym. Sci.,* 26, 559 (1981)

[69] M. Hu, E. M. Pearce and T. K. Kwei, *J. Polym. Sci., A: Polymer Chemistry,* 31, 553 (1993).

[70] Y. Iwakura, K. Uno and Y. Imai, *J. Polym. Sci., Part A, 2,* 2605 (1964).

[71] A. B. Conciatori, E. C. Chenevey, T. C. Bohrer and A. E. Prince, Jr., *J. Polym. Sci., C: Polymer Symposia,* 19, 49 (1967).

[72] R. Ameri, *Ph. D. thesis,* "Polybenzimidazole film containing phosphoric acid as proton exchange membrane (PEM)", CWRU, 1997.

[73] D. E. Steutz, A. E. DiEdwards, F. Zitomer and B. P. Barnes, *J. Polymer Science, Polymer Chemistry Edition,* 18, 987 (1980).

[74] S., Wasmus, B. A. Daunch, H. Moaddel, P. L. Rinaldi, M. H. Litt, C. Rogers, A. Veleriu, G. D. Mateescu, D. A. Tryk, and R. F. Savinell, *Abstract 466, p. 716, The Electrochemical Society Extended Abstracts,* 95-1, Reno, NV, May 21-26 (1995).

[75] R. W. Singleton, H. D. Noether and J. F. Tracy, *J. Polymer Science, Part C,* 19, 65 (1967).

[76] J. T. Wang, *Ph. D. thesis, "High temperature proton conducting polymer fuel cell)"*, CWRU, 1996.

[77] R.S. Bogner, Electron Dyn. Div., Hughes Aicr. Co., Proc. Intersoc.

[78] CT, USA, Avail.NTIS, Nada [Contract. Rep.] CR (1978), NASA-CR-159653, FCR-1017, 73 pp. From: Sci. Tech. Aerosp. Rep. 1979, 17(24), Abstr. No. N79-33581. CODEN: NSCRAQ ISSN: 0565-7059.

[79] R.E. Martin, Power Syst. Div., United Technol. Corp., South Windsor, CT, USA, Avail. NTIS, NASA [Contract. Rep,] CR (1979), (NASA-CR-159807, FCR-1657), 52 pp. From: Sci. Tech. Aerosp. Rep. 1980, 18(10), Abstr. No. N80-19615. CODEN: NSCRAQ ISSN: 0565-7059.

[80] U.S. Pat. 5,71,038, B. Vyas, (Bell Telephone Laboratories) (Sept. 11, 1984).

[81] X. Glipa, M. E. Haddad, D. J. Jones, J. Roziere, *Solid State Ionics,* 97, 323 (1997).

[82] O. Savadogo, *J. New Mat. Electrochem. Syst.* 1, 47 (1998).

[83] S. Mukerjee, and J. McBreen, *in "Proceedings of the Second International Symposium on New Materials for Fuel Cell and Modern Battery Systems" Eds, O. Savadogo and P. R. Roberge, Montreal Canada,* July 6-10, 1997, p. 548.

[84] B. Tazi and O. Savadogo, *in "Proceedings of the Second International Symposium on New Materials for Fuel Cell and Modern Battery Systems" Eds, O. Savadogo and P. R. Roberge, Montreal Canada,* July 6-10, 1997, p864.

[85] B. Tazi, and O. Savadogo, *J. New Mat. Electrochem. Syst.* (submitted).

[86] Hong Wang and G. A. Capuano, *J. Electrochem. Soc.*, 145, 780 (1998).

[87] C. A. Linkous and D. K. Slattery, *Frontiers Science (New Eeergy system and Conversions)*, 7, 257 (1993).

[88] Malhotra Sanjiv, Datta Ravindra, *J. Electrochem. Soc.*, 144, L23 (1997).

[89] O. Savadogo and B. Xing, *J. New Mat. Electrochem. Syst.*, in press.

[90] E. Gülzow, M. Schulze, G. Steinhilber, K. Bolwin, 1994, "*Fuel Cell Seminar*", San-Diego (CA), p. 319

[91] A. Al-Saleh, et al., in ``*Alkaline Fuel Cell in the Presence of Carbon Dioxide Impurity in the Feed Gases*", Paper from the Chemical Engineering Department, King Fahd University of Petroleum and Minerals, Dhahran 31261, Saudi Arabia, 1992.

[92] W. G. Grot, *Macromolecular Symposium*, 82, 161 (1994)

[93] A. E. Steck, in *"Proceedings of the First International Symposium on New Materials for Fuel-Cell Systems"*, Eds. O. Savadogo, P. R. Roberge and T. N. Veziroglu, Montréal, Canada, July 9-13, 1995, p. 74.

[94] A. E. Steck, in *"Proceedings of the Second International Symposium on New Materials for Fuel-Cell and Modern Battery Systems"*, Eds. O. Savadogo and P. R. Roberge, Montréal, Canada, July 6-10, 1997, p. 792.

[95] B.Tazi and O. Savadogo, *Electrochim. Acta*, (in press, 2000)

[96] R. B. Hodgdon, J. F. Enos, E. J. Aiken, US Patent 3,341,366 (1967)

[97] J. Wei, C. Stone and A. E. Steck, U.S. Patent No. 5,422,411 (1995).

[98] D. Agostino, U.S. Patent No. 4,012,303 (1977).

[99] O. Hass, H. P. Brack, F. N. Buchi, B. Gupta and G. G. Scherer in *"Proceedings of the Second International Symposium on New Materials for Fuel-Cell and Modern Battery Systems"*, Eds. O. Savadogo and P. R. Roberge, Montréal, Canada, July 6-10, 1997, p. 836.

[100] S. Hietala, M. Koel, E. Skou, M. Elomaa and F. Sundholm, *J. Mater. Chem.* 8, (1998) p. 1127.

[101] J. Kerres, W. Cui, G. Eigenberger, D. Bevers, W. Schnurnberger, A. Fisher and H. Wendt, in *"Proceedings of the 11th Hydrogen Conference"*, Eds. T. N. Veziroglu, C. J. Winter, J. P. Baselt and G. Kreysa, Stuttgart, Germany, June 23-28, 1996, p. 1951.

[102] S. Faure, N. Cornet, G. Gebel, R. Mercier, M. Pineri and B. Sillon, in *"Proceedings of the Second International Symposium on New Materials for Fuel Cell and Modern Battery Systems"*, Eds. O. Savadogo and P. R. Roberge, Montréal, Canada, July 6-10, 1997, p. 818.

[103] E. Zador and G. E. Wnek, in *"Proceedings of the Second International Symposium on New Materials for Fuel Cell and Modern Battery Systems"*, Eds. O. Savadogo and P. R. Roberge, Montréal, Canada, July 6-10, 1997, p. 828.

[104] J. Kerres, W. Cui, W. Neubrand, S. Springer, S. Reichle, B. Striegel, G. Eigenberger, W. Schnurnberger, D. Bevers, N. Wagner and K. Bolwin, in *"Proceedings Book, Euromembrane 92 Congress"*, Bath, UK, Sept. 18-20, 1995, p. 1.284.

[105] A. Schmeller, H. Ritter, K. Ledjeff, R. Nolte and R. Thorwirth, EP. 0574791 A2 (1993).

[106] C. Poinsignon, presented at the *"First International Symposium on New Materials for Fuel Cell Systems"*, Montréal, Canada, July 9-13, 1995, Poster No 29.

[107] W. Wieczorek, Z. Florjanczyk and J. R. Stevens, *Eletrochim. Acta*, 40, (1995) 2327.

[108] Burnett, U.S. Patent No 4,506,035 (1985).

[109] G. Scherer, Ber. Bunsenges, *Phys. Chem.*, 94, (1990) 1008.

[110] G. Scherer, F. N. Buchi and B. Gupta, *Polym. Mater. Sci. Eng.*, 68, (1993) 114.

[111] B. Gupta, F. N. Buchi and G. G. Scherer, *Solid State Ionics*, 61, (1993) 213.

[112] T. Lehtinen, G. Sundholm, S. Holmberg, F. Sundholm, P. Björnbom and M. Bursell, *Electrochim. Acta*, 43, (1998) 1991.

[113] M. Paranen, F. Sundholm, E. Ranhala, T. Lehtinen and S. Heitala, *J. Mat. Chem.*, 7, (1997) 2401.

[114] D. I. Ostrovskü, L. M. Torell, M. Paronen, S. Heitala and F. Sundholm, *Solid State Ionics*, 97, (1997) 315.

[115] S. Heitala, S. Holmberg, M. Karjalainen, J. Näsman, M. Paronen, R. Senmaa, F. Sundholm and S. Vahvaselka, *J. Mat. Chem.*, 7, (1997) 721.

[116] H. A. Liebhabsky, E. J. Cairns, *Fuel-Cells and Fuel Batteries*, New York, 1968.

[117] B. Xing and O. Savadogo, *Electrochemical communication*, 2, 697 (2000)

[118] D. R. Paul, *J. Polymer Physics*, A2, 8, 1811 (1970).

[119] J. H. Petropoulos, *J. Polymer Physics*, A2, 8, 1797 (1970).

[120] D. R. Paul, W. J. Koros, *J. Polymer Science, Polymer Physics*, 14,675 (1976).

[121] W. J. Koros, D. R. Paul, A. A. Rocha, *J. Polymer Science, Polymer Physics*, 14,687 (1976).

[122] *61th Handbook of Chemistry and Physics*, D-228 - D-276, 1981.

[123] B. Xing and O. Savadogo, "The mass transport properties of PBI in alkaline solutions" To be published

[124] B. Xing and O. Savadogo, "The sorption process of acid in PBI membrane" To be published

[125] R. McGregor, "Diffusion and Sorption in Fibers and Films", Volume1, "An Introduction with particular reference to dyes", Academic Press Inc., London and New York, 1974.

[126] P. Neogi, "Diffusion in polymers", Marcel Dekker inc., New York, Basel and Hong Kong, 1996.